TÉCNICO LISBOA

UNIVERSIDADE DE LISBOA
INSTITUTO SUPERIOR TÉCNICO

Unlocking the Potential of Umbilical Cord Blood by Improving *Ex vivo* Expansion of Hematopoietic Stem/Progenitor Cells

André Dargen de Matos Branco

Supervisor: Doctor Ana Margarida Pires Fernandes-Platzgummer
Co-Supervisor: Doctor Cláudia Alexandra Martins Lobato da Silva

Thesis approved in public session to obtain the PhD Degree in
Bioengineering

Jury Final Classification: **Pass with Distinction**

2023

UNIVERSIDADE DE LISBOA
INSTITUTO SUPERIOR TÉCNICO

Unlocking the Potential of Umbilical Cord Blood by Improving *Ex vivo* Expansion of Hematopoietic Stem/Progenitor Cells

André Dargen de Matos Branco

Supervisor: Doctor Ana Margarida Pires Fernandes-Platzgummer
Co-Supervisor: Doctor Cláudia Alexandra Martins Lobato da Silva

Thesis approved in public session to obtain the PhD Degree in **Bioengineering**

Jury Final Classification: **Pass with Distinction**

Jury

Chairperson: Doctor João Pedro Estrela Rodrigues Conde, Instituto Superior Técnico, Universidade de Lisboa

Members of the Committee:

Doctor José Eduardo Marques Bragança, Faculdade de Medicina e Ciências Biomédicas, Universidade do Algarve
Doctor Gabriel António Amaro Monteiro, Instituto Superior Técnico, Universidade de Lisboa
Doctor Cecília Ribeiro da Cruz Calado, Laboratório de Engenharia e Saúde, Instituto Superior de Engenharia de Lisboa
Doctor Ana Margarida Pires Fernandes-Platzgummer, Instituto Superior Técnico, Universidade de Lisboa
Doctor Thomas Brieva, Cell Therapy Process and Analytical Development, Pennsylvania, USA

Funding Institution: Fundação para a Ciência e a Tecnologia

2023

ABSTRACT

Umbilical cord blood (CB) is a clinically relevant source of hematopoietic stem/progenitor cells (HSPC) for cell and gene therapies (CGT). As a by-product of childbirth, CB can be easily procured and has a primitive cellular compartment. Although with a finite volume, *ex vivo* expansion has unsealed considerable potential, allowing CB to respond to any cell dose requirement. Still, CB use in HCT is decreasing and only a single approved CGT based on CB-derived expanded HSPC exists (i.e. Omisirge). Several attempts were made to progress HSPC expansion, hoping to improve its attractiveness.

After development of HSPC expansion media, exogenous cytokines, ubiquitous in expansion strategies, were targeted for optimization. Optimal concentrations of stem cell factor (SCF), fms-related tyrosine kinase 3 ligand (Flt-3L) and thrombopoietin (TPO) were determined for HSPC expanded with two different strategies, liquid culture and mesenchymal stromal cell (MSC) co-culture. An optimal cytokine cocktail was calculated and validated, displaying improved cell yield.

As a contributor to the bone marrow niche, MSC provide hematopoietic support during co-culture expansion. Consequently, MSC have to be integrated in the manufacturing pipeline. Cryopreservation remains the standard method to store and transport cells but also has detrimental effects. Hypothermic alginate beads were evaluated for MSC. Successfully encapsulation was verified up to 12 days, retaining cell fitness and function (including hematopoietic support capabilities).

Cell potency is crucial for assuring quality, with assays being alarmingly underdeveloped. Transcriptomics and Fourier-transform infrared spectroscopy (FTIR) were explored as novel techniques for quality monitoring during *ex vivo* HSPC expansion. Both were able to discriminate between different expansion systems, with systematic dissimilarities being uncovered in expanded HSPC.

These advances in CB-based HSPC expansion aim at promoting a continuous improvement environment, which is deemed crucial for healthy development of CGT. Value of *ex vivo* expansion of HSPC was significantly enhanced, benefitting future CB use.

Keywords: Umbilical cord blood, hematopoietic stem and progenitor cells, cell and gene therapies, *ex vivo* expansion, mesenchymal stromal cell co-culture.

RESUMO

O sangue do cordão umbilical (CB) representa uma fonte relevante de células hematopoiéticas estaminais e progenitoras (HSPC) para terapias celulares e génicas (CGT). O CB é facilmente obtido e contém células bastante primitivas. Apesar do seu volume finito, a expansão celular *ex vivo* veio desbloquear enorme potencial, permitindo que o CB responda a qualquer dose necessária. Contudo, o seu uso está em decréscimo e existe somente uma CGT baseada em HPSC expandidas de CB (Omisirge). Aqui, várias abordagens foram exploradas para aperfeiçoar a expansão de HSPC, incluindo a otimização de citocinas, usadas na maioria das estratégias de expansão. Determinaram-se as concentrações ótimas de SCF, Flt-3L e TPO em dois sistemas de expansão: cultura líquida e co-cultura com células estromais mesenquimais (MSC). Cocktails de citocinas otimizados foram calculados e validados, e demonstraram um melhor rendimento de expansão celular.

As MSC pertencem ao nicho da medula óssea e dão suporte hematopoiético na expansão em co-cultura. Por conseguinte, deverão ser integradas no processo de manufatura. A criopreservação é o método principal de armazenamento e transporte celular, apesar dos efeitos negativos. Esferas de alginato hipotérmicas foram avaliadas para MSC. Conseguiu-se um encapsulamento até 12 dias, preservando a viabilidade celular e função, bem como as capacidades de suporte hematopoiético.

A potência celular é crucial para assegurar a qualidade das CGT, apesar dos ensaios estarem subdesenvolvidos. A transcriptómica e espectroscopia FTIR foram exploradas como novas ferramentas para controlo de qualidade durante a expansão *ex vivo* de HSPC. Ambas conseguiram discriminar entre sistemas de expansão, apresentando diferenças sistemáticas em HSPC expandidas.

Estes avanços na expansão *ex vivo* de HSPC do CB pretendem promover um ambiente de aperfeiçoamento contínuo, recomendado para um desenvolvimento sustentável das CGT. Aumentou-se o valor global da expansão *ex vivo* de HSPC, beneficiando o seu futuro uso.

Palavras-chave: Sangue do cordão umbilical, células hematopoiéticas estaminais e progenitoras, terapias celulares e génicas, expansão *ex vivo*, co-cultura com células estromais mesenquimais.

ACKNOWLEDGMENTS

Although my path to tread, this PhD journey was very much supported with helping hands which I, hopefully, will now properly acknowledge.

Merely after recalling my first legitimate day at my workplace, I am already massively thankful. It was on that day that I met you, Sara. Little did I know, you would come as whirlwind and change my whole life. You are latched onto this accomplishment almost as if it were yours, to which I publicly offer my heartfelt recognition.

Behind me, as I walked and tried to navigate through the chasms of scientific hurdles, two main figures are also responsible for me reaching my destination.
Ana Fernandes Platzgummer trusted me, out of the blue, with her PhD proposal, for which I cannot thank her enough. The way we built this PhD and our relationship couldn't have been more favorable for my scientific and personal growth. She knew exactly how to push, pull, incentivize, give space, recognize and so many other actions that sustained my sails. Her manner of contribution towards our laboratorial community and her concern with colleagues, new or old, was very much aligned with mine. I am fully aware of my luck of having been selected to have her at my side during these years.
As my co-supervisor, Cláudia Lobato da Silva was an exciting presence for a Biological Engineer such as myself. Having heard of her qualities and achievements as an established scientist and professor and witnessed her impressive communication skills with charismatic aura, I truthfully thank her for accepting her supervisor role. Exchanging ideas and having scientific discussion with her during meetings were some of the best parts of my PhD.
Very much complementing each other, I thank this great team for investing their time in helping me finish what I started. I learned from both as much and as fast as I could. They also kindly offered me insight into the intricacies of research and development, as well as, how to maintain and manage a lab, from securing funding and collaborations to ordering pipette tips.

Luckily, I had several generations of colleagues and friends pass by my PhD journey. Each were important for me and had their own distinct impact.
The first batch include other PhD students about to finish theirs, giving me a glimpse of my, at that time, distant future. Although our time together was short, they welcomed me in and taught me everything they knew, always in a good mood and with refreshing humor. Also, they were an example of companionship between themselves that definitely served them when times were bleak but also to celebrate their own

achievements. A big thank you to António Soure, Marta Costa, Sara Rosa, Diogo Pinto, Joana Serra and Francisco Moreira.
The next group of people were probably the ones I spent the most time with during this PhD, which means I am full of good memories and long hours spent working, goofing off, having those highly populated lunches, whining and having deep conversations about almost any topic. You were always there, Sara, from the beginning to the end, my most important companion. A wild Mary Lee appeared shortly after, and our office became ours. We took our baby steps in our PhD together and an inner circle was formed. Those first months were so dense and full of emotion, I have to thank both of you for opening my eyes and my heart. You have left a permanent mark. At that time there were only a few of us in Lab III, but we prevailed together. We joined our friends in the neighboring lab and filled our days with good company and, for some time, the wall that separated both labs seemed not to exist. An honest thank you to Ana Rita Gomes, Teresa Silva, André Rodrigues, João Cotovio, Mariana Branco, Diogo Nogueira, Margarida Alves, Sara Morini and Cláudia Miranda. I cannot not mention (and she wouldn't let me) Carina Manjua, who gracefully entered our lives. After overcoming her fear of a certain person, she became part of our circle. Albeit being inspirational, she quickly became my preferred target. So much laughter between everyone followed, almost forcing fresh air into our chest, making even the hardest days a bit lighter.
A bit later, I had the privilege of reencountering Miguel Fuzeta in our lab. Although from the same Integrated Master's course, I only had few chances to work directly with him. In a rather poetic way, he was one of my first group work colleagues, where we tackled our difficult Programming project. We closed that circle by ending up in the same lab working in complementing fields, which culminated with a fruitful collaboration of a book chapter. I am very grateful to have shared time with him in the lab and am proud to call him my good friend.
After officially starting my PhD, I had the great opportunity of entering a PhD program with other fantastic PhD candidates of other institutions. We quickly became a group and were each other's company for a few months of classes. We shared experiences and most were important to me during a darker period. Although life circumstances did not allow more frequent encounters, I know that I made good friends. A sincere thank you to Filipa Raimundo, Sofia Moreira, João Mendes, Andreia Ferreira and Ana Fradinho. Carina Maranga also was part of this group and eventually joined me at iBB after choosing her PhD project. I was very happy for her decision and was able to count with her important company during most of my PhD.
Mary Lee was the first to receive her own students, and boy, did she receive a bunch of them. Out of that lot of peculiar people that put Mary Lee to the test, came Cristiana Ulpiano. I saw her grow from her Master student internship until today. Her simultaneous savagery and sensitivity are impressive (and I take some credit for unlocking it). With

time, I ended up trusting her above most (entrusting her one of my most important assignments) and cannot thank her enough for everything. I know our great friendship has largely outgrown our workspace.

It is with a warm feeling that I must mention João Carreira, a beacon of scientific spirit. With him, I could spend hours having spirited and mind-defying scientific discussion. He always demonstrated his excitement for science, which was inspirational. I truly thank him for our time shared wherever our paths crossed.

Gradually, a new challenge during my PhD gave me the wonderful experience of mentoring and supervising my own Master students. I hope they learned as much as I did from them. Each were different, leading to different approaches and cemented my enthusiasm for teaching. I am proud of each one and all of them are now walking their own paths. I cannot thank them enough for contributing to my personal growth. Ana Lúcia Tiago came first, having had her labwork condensed into a few months due to the COVID-19 pandemic. She endured long hours of intensive workload and came through without (m)any bruises. Her quality is obvious, although she herself doubts it sometimes. Catalina Cepeleaga followed, showing exemplar professionalism and lack of fear when confronted with her scientific obstacles. Her laughs and open-spirit to learn marked her stay at the lab. João Henriques continued Catalina's project after some initial hiccups in his own project. His good spirit spread throughout the lab and his interest in other scientific projects was noted. Finally, Catarina Carreira came to us in the lab showing authentic interest in science, which can be sometimes rare to find. She immediately dove deep into her project and has grown very much as a scientist. Her enthusiasm is hard to miss.

Although having spent less time with them during my PhD, a new generation of PhD students in our lab also deserve my recognition in this thesis. They have been a window into my own first years and I thank Isabel Doutor and Helder Tavares for our great scientific and non-scientific conversations. I have no doubt you both have success waiting for you.

A thankful mention to João Silva, Paola Alberte and Marta Carvalho. They were great models of successful and respectful scientists who continue their path in science against great odds and obstacles. They were always kind to me and we had fantastic conversations. I appreciate my time spent sharing the lab with them.

In the last months of my PhD, two more presences came to be that also deserve my gratitude. Miguel Casanova joined iBB due to a group merger and we met directly through his initiative of looking for potential collaborations. We connected as collaborators after that initial meeting, and I looked up to his wit during labmeetings and his respectful career track. I very much thank him for his stimulating scientific discussions and his precious help in our collaboration. Teresa Mendes was already an acquaintance of mine, since she was Sara's colleague and friend from her own PhD

program. Ironically, she eventually came to work at iBB and I got to know her even better. Her kindness and good intentions are obvious, although she doesn't admit it. I truly thank her for allowing me to spend time with her, contributing towards a great daily dynamic which I very much cherish.

To Professor Joaquim Cabral, whom I thank as the creator of my course, PhD program, department and institution. Without his contributions, it wouldn't have been possible for me to reach this point in my journey.

I also need to mention my family, starting with Dad and Mom. They have always been there to support me and I can only imagine the effort and sacrifice that was put into raising me. I recognize and strive to honor that sacrifice every day. I thank them for showing me that there is no limit to what I can do, and this thesis is just another milestone to prove that. My brother Sam really deserves every good word I can write about him. He is one of the best humans I will ever know and I am conscious that even at the most gloomiest of times I can always count on him. That feeling made it so much easier going through my PhD and also made me very very proud and grateful to be his brother. I cannot thank him enough (although he will always ask for more). Finally, to my sister-in-law Daniela, whom I esteem a lot. Her immediate support was very warm and she was always available to listen to vents. I hope to be there for her accomplishments as she has been for mine.

Now to us, Sara. Anything I write here will never be enough to adequately describe everything that happened and how immensely grateful I am to you. It has been one hell of a ride. I swear these won't be my vows. Our PhDs have gone parallel to what we have lived, until now. We will leave our PhDs behind, but we will continue. I still remember as if it were yesterday sitting two desks away from you in our office. I will never forget how expensive ice is, our written notes between us and our midnight testing (to name just a few of our adventures). I am not the same person that started this PhD and that is due to you. You are the person I most admire. You have taught me endless lessons. You are my best support. Everything in this thesis can be traced back to you. We went through so much sweat, tears, frustration, desperation, and lethargy that this PhD has transcended its pure scientific purpose. We are both the best witnesses to each other and only you truly know everything we went through. I have grown stronger and wiser because of it. You have seen me at my best and also at my worst. Even with your own extremely challenging difficulties, you always had the generosity to help me. As we evolved from co-workers to friends to partners, I also evolved during this thesis. You have made me feel that no goal was beyond my reach and no obstacle could stop me from reaching it. You have made me a much better man and scientist. With you by my

side, my faults diminish and my qualities stand out, which spread into my PhD. You brought endless laughter, true happiness, limitless effort, a clear mind and so many other blessings that made my PhD days fly by. I had never worked with anyone quite like you and now I live with you. I still cannot believe it. I hope you know how thankful I am for everything, yet I relay it here where my acknowledgment belongs.

Thank you for unlocking me. I Love You. Us.

To my beautiful daughter Liv. You are the one PhD-derived experiment that will take a lifetime to complete. Thank you for choosing me as your father. Daddy loves you.

TABLE OF CONTENTS

LIST OF FIGURES

LIST OF TABLES

LIST OF EQUATIONS

LIST OF ABBREVIATIONS AND ACRONYMS

#

2D – Two-dimensional
3D – Three-dimensional
α-MEM – Minimum essential Eagle medium - alpha modification

A

A/A – Antibiotic-Antimycotic
AGM – Aorta-gonad-mesonephros
ANOVA – Analysis of variance
APC – Antigen presenting cells
AT – Adipose tissue
ATMP – Advanced therapy medicinal products

B

BACS – Buoyancy-activated cell sorting
BET – bromodomain and extra-terminal domain
bFGF – Basic fibroblast growth factor
BFU-E – Erythroid burst-forming unit
BM – Bone marrow
bp – Base pairs
BSA – Bovine serum albumin

C

CAFC – Cobblestone area-forming cells
CAR – Chimeric antigen receptor
CB – Umbilical cord blood
CCF – Face-centered central composite
CFD – Computational fluid dynamics
CFU – Colony-forming unit
CFU-GM – Colony-forming unit granulocyte-monocyte
CFU-Mix – Multilineage colony-forming unit
cGMP – Current good manufacturing practices
CGT – Cell and gene therapies
CLP – Common lymphoid progenitor
CMP – Common myeloid progenitor
COG – Cost of goods
CPP – Critical process parameters
CQA – Critical quality atributes
CV – Coefficient of variance

D

D – Diversity
dECM – Decellularized extracellular matrix
DEG – Differentially expressed genes
DLI – Donor lymphocyte infusions
DLL1 – Delta-like ligand 1
DMEM – Dulbecco's modified Eagle's medium
DMSO – Dimethyl sulfoxide
DO – Dissolved oxygen
DoE – Design of experiments
DUCBT – Double unit cord blood transplant

E

EC – Endothelial cells
ECM – Extracellular matrix
EDTA – Ethylenediamine tetraacetic acid
EHT – Endothelial-to-hematopoietic transition
EMA – European medicines agency
EU – Europe
EV – Extracellular vesicles

F

Fab – Antigen-binding fragments
FACS – Fluorescence-activated cell sorting
FBS – Fetal bovine serum
FC – Fold change
FDA – U.S. Food and Drug Administration
FL – Feeder layer
Flt-3L – fms-like tyrosine kinase 3 ligand
FSC – Forward side scatter
FTIR – Fourier-transform infrared spectroscopy

G

G-CSF – Granulocyte-colony stimulating factor
GMP – Good manufacturing practices
GO – Gene ontology
GSEA – Gene set enrichment analysis
GVHD – Graft-*vs*-host disease
GVL – Graft vs. leukemia

H

HCT – Hematopoietic cell transplantation
HLA – Human leukocyte antigen
HPL – Human platelet lysate

HSC – Hematopoietic stem cells
HSPC – Hematopoietic stem and progenitor cells
HSPC(CB) – Cord blood-derived hematopoietic stem and progenitor cells
HSPC(M) – Bone marrow-derived hematopoietic stem and progenitor cells
HSPC(PB) – Peripheral blood-derived hematopoietic stem and progenitor cells
HUVEC – Human umbilical vein endothelial cells

I

iBB – Institute for Bioengineering and Biosciences
IFN-**γ** – Interferon-**γ**
IL-3 – Interleukin-3
IL-6 – Interleukin-6
IMDM – Iscove's modified Dulbecco's medium
iPSC – Induced pluripotent stem cells
IR – Infrared
ISCT – International Society for Cell & Gene Therapy
ISEL – Instituto Superior de Engenharia de Lisboa
IV – Intravenous

J

J – Joining

L

LepR – leptin receptor
LT-HSC – Long-tern hematopoietic stem cells
LTC-IC – Long-term culture-initiating cells

M

MACS – Magnetic-activated cell sorting
MFI – Median fluorescence intensity
MNC – Mononuclear cells
MNC(CB) – Cord blood-derived mononuclear cells
MNC(M) – Bone marrow-derived mononuclear cells
MNC(PB) – Peripheral blood-derived mononuclear cells
MoA – Mechanism of action
mPB – Mobilized peripheral blood
MSC – Mesenchymal stromal cells
MSC(AT) – Adipose tissue-derived mesenchymal stromal cells
MSC(M) – Bone marrow-derived mesenchymal stromal cells

O

OD – Optical density

P

PAT – Process analytical technology
PB – Peripheral blood
PBS – Phosphate buffered saline
PCA – Principal component analysis
PCL – Polycaprolactone
PEG – Polyethylene glycol
PID – Proportional-integral-derivative

Q

Qbd – Quality by design
QTPP – Quality target product profile

R

R^2 – Coefficient of determination
RGD – Arginylglycylaspartic acid
RTL – Relative telomere length
RMA – Raw material attributes
RMSE – Root mean square error
RT – Room temperature

S

SCERG – Stem Cell Engineering Research Group
SCF – Stem cell factor
SCID – Severe combined immunodeficiency
SEM – Standard error of the mean
SFEM – Serum-free expansion medium
SR-1 – StemRegenin-1
SSC – Side scatter
ST-HSC – Short-term hematopoietic stem cells
SUB – Single-use bioreactors

T

TCR – T cell receptor
TEPA – Tetraethylenepentamine
TERT – Telomerase
TFF – Tangential flow filtration
TNC – Total nucleated cells
TPO – Thrombopoietin
T_{reg} – Regulatory T cells

U

USA – United States of America
UV – Ultraviolet

V

V – Variable

VPA – Valproic acid

W

WBMT – Worldwide Network of Blood and Marrow Transplantation

I. Introduction

This chapter is partly published as:

*de Almeida Fuzeta, M.; *Branco, A. *et al*. Addressing the Manufacturing Challenges of Cell-based Therapies. In *Advances in Biochemical Engineering/Biotechnology*, *Springer: Cham, Germany*, 171, 225-278 (2019). ISBN 978-3-030-40463-5
*These authors contributed equally.

I.1. Hematopoiesis - A Lifelong Commitment

The human body is a structure made up of multiple systems that intricately interact and assure daily functions. When reaching such complexity, a network of channels is required to guarantee inter- and intra-system connectivity. Comparable to urban network development, where roads and avenues tie a city together bringing supplies and people to their functions, the circulatory system connects every element of the body. While the circulatory framework is composed of endothelial, smooth muscle cells and pericytes, an ever in motion fluid (i.e. blood) is transported throughout the network assuring vital functions, such as nutrient, oxygen and signal transport, immune surveillance, waste removal, wound healing, hydration and thermoregulation[1]. To guarantee such diverse tasks, several types of different blood cells are needed, stemming from the same hematopoietic master lineage.

Erythrocytes, enucleated cells that represent 94,1% of the total peripheral blood cell count, have the important task of gas transport, supplying oxygen to and removing carbon dioxide from tissue where gas diffusion would never reach[2]. Their ability for gas transport is due to their harboring of hemoglobin, a protein with high affinity for oxygen. With a mean lifespan of 120 days, a turnover of 2.15×10^{11} cells per day is required to replenish the erythrocyte population[3]. Of note, humans cannot normally survive for more than a few minutes without oxygen, highlighting the importance of stable erythrocyte production.

With nutrients and oxygen being safely distributed, other threats to human life exist. Whether against exterior-originated infiltration of harmful substances, pathogens and infectious disease or self-inflicting genetic disorders or cancer, body immunity is essential and is based on specialized hematopoietic cells present in the blood. Depending on the type of immunity (i.e. innate or adaptive), different protagonists are responsible for triggering a proportional response. The innate immune system is the first layer of defense, comprised of physical, chemical, humoral and cell-based elements[4]. Granulocytes (i.e. neutrophils, eosinophils and basophils), macrophages and natural killer (NK) cells are responsible for the cellular response of the innate immune system[2]. Being chemoattracted by inflammation, granulocytes and macrophages phagocytose threatening pathogens, particles and apoptotic cells. After engulfing them and forming a phagosome, existing granules that characterize these cells and are filled with bactericidal molecules fuse with the phagosome, leading to pathogen digestion[4]. Neutrophils represent the majority of granulocytes, with eosinophils and basophils having a residual contribution, being responsible for a turnover rate of 5.94×10^{10} cells per day[3]. On the other hand, NK cells act through a different mechanism. Either through interferon-**γ** (IFN-**γ**) production or direct cytotoxic activity, these lymphocytes help bolster the response of other immune players and are able to recognize and clear virus-

infected cells and tumor cells[5]. From circulating lymphocytes, 4% to 29% are NK cells, resulting in a turnover rate of up to 2.11 x 10^9 cells per day[3]. Overall, this type of immunity is based on pattern-recognition receptors that detect conserved pathogen-associated molecular patterns. As a generic defensive line, innate immunity is an immediate reaction towards pathogens, while also signaling (when necessary) reinforcements from the adaptive immunity[6]. Contrarily to the innate immune system, adaptive immunity exists to tackle ever-changing pathogens. When facing a novel threat that is not detected nor is resolved by the innate immunity, adaptive immunity steps in and mounts an appropriate response. B and T lymphocytes are responsible for implementing adaptive immunity[2]. Their versatility is due to their very diverse repertoire of surface receptors, that originate from recombination of Variable (V), Diversity (D) and Joining (J) genes[7]. With such extreme diversity, nearly any antigen is eventually covered by a respective receptor. While B cells directly detect the presence of a foreign antigen, T cells require antigen presenting cells (APC) to become activated. B cells also differ from T cells regarding their mode of action. Whereas T cells fight pathogens through cytotoxic granules containing granzyme and perforin, B cells can differentiate into plasma cells and produce neutralizing antibodies. Turnover rates for these two cell types are similar, around 4.00 x 10^9 cells per day[3].

As such an important piece of the human puzzle, blood requires its own safeguarding mechanism to act whenever the circulatory network is compromised. Being pressurized to reach every corner of the body, blood would be drained completely if capillary ruptures could occur without any protective measures. Platelets, another enucleated cell type, hold the essential task of ensuring rapid repair of injured vessel walls, through hemostasis[2]. After sensing subendothelial matrix proteins from the vessel exterior, platelets rapidly adhere to the wound site and aggregate with more platelets to form a temporary plug, keeping blood in[8]. Then, a coagulation cascade is activated by platelets that eventually leads to polymerized insoluble fibrin formation, providing structural stability to the platelet plug. These cellular fragments that originate from megakaryocytes, have a turnover of 1.85 x 10^{10} cells per day[3].

The immense daily cell demand is characteristic of the hematopoietic system, since 86% of total cell turnover are blood cells[3]. To keep blood cell production continuous over several decades, primitive cells that can give rise to the different hematopoietic lineages (multipotency) and are able to self-renew are required. Hematopoietic stem and progenitor cells (HSPC), that encompass long-term (LT-), short-term (ST-) hematopoietic stem cell (HSC) and progenitor populations, define the apex of the hematopoietic tree by having these two properties in different degrees. This hierarchical structure of hematopoiesis was originally designed with consecutive branching between discrete cell states characterized by a unique set of surface marker, beginning with HSC[9].

Advances in cell marker identification have been made, reaching an ever more distinct combination for each hematopoietic cell category. LT-HSC are until now defined by their co-expression of $CD34^{+}CD45RA^{-}CD38^{-}CD90^{+}CD49f^{+}ITGA3^{+}$, linking this subset with the highest long-term engraftment and reconstitution potential[10]. Either by tracking the ratio of active X-chromosomes of paternal and maternal origin in women or by inferring HSC clonal dynamics from somatic mutations, a limited HSC pool of between 3000 and 200 000 HSC has been proposed to maintain steady-state hematopoiesis[11,12]. As multipotency is gradually lost (transitioning to ST-HSC and further into myeloid and lymphoid progenitors) expression of ITGA3, CD49f, CD90 is lost, while CD38 expression increases. Additional markers then appear as hematopoietic progenitors split between the two main hematopoietic lineages (i.e. myeloid and lymphoid). Common myeloid progenitors (CMP) begin to express CD135, while common lymphoid progenitors (CLP) see an upregulation of CD7 and CD10, as well as abovementioned CD45RA[13]. Expression of CD34, a historical HSPC marker that remains the gold standard for HSPC enrichment and also serves as a transplantation criterion, accompanies the different stages of hematopoietic tree, except in fully differentiated progeny[14]. Interestingly, for such a notorious transmembrane protein, much remains to be uncovered concerning the actual function of CD34. As a sialomucin, CD34 has demonstrated ability to bind to selectins and other adhesion molecules, having a role in cell-cell contact and cell migration[14,15].

With such defined and extensive surface marker combinations attributed to the different hematopoietic populations, individual positions in the hematopoietic tree were regarded as homogenous populations. However, following the development of OMICS techniques (e.g. transcriptomics) with single-cell resolution, hematopoietic populations are now known to be heterogenous[16,17]. Functional heterogeneity has also been proven, with single HSC transplanted in a mouse model being unable to reconstitute all the different lineages, indicating marker-independent lineage priming[18]. Consequently, hierarchical hematopoietic representation has evolved, being depicted as a continuum from primitive HSC down to fully differentiated cells (Fig. I-1).

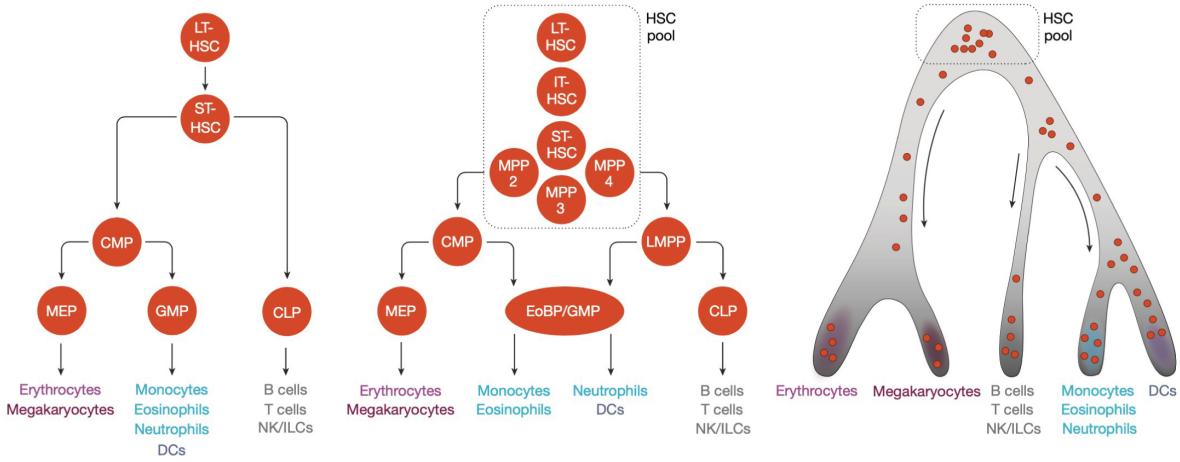

Figure I-1. *Hierarchical models of the hematopoietic system. Initially, a defined state was attributed to each hematopoietic cell type, with an ever-reducing range of precursors until reaching the pinnacle of the hematopoietic tree, the long-term hematopoietic stem cell (HSC) (left). As our understanding of hematopoietic biology increased, the existing pool of HSC was discovered to be heterogenous, with several multipotent progenitor subpopulations with different differentiation and reconstitution potential (middle). Currently, the concept of well-defined and discrete cell states has been overtaken. Lineage priming, which is normally hidden when looking for typical surface markers, is now known to occur even at the more primitive HSC level. Now, hematopoiesis is being described as a continuous flow of malleable cell states that go down well-defined avenues of differentiation (right). Adapted from [16].*

I.2. Bone Marrow – Steady-State Hematopoietic Command Post

Given its importance and high turnover rates, a secure location for *in vivo* blood production by HSPC is needed. Interestingly, sites of hematopoiesis have a spatiotemporal distribution, changing throughout embryonic development to the adult body (Fig. I-2).

Primitive hematopoiesis begins in extraembryonic tissue, namely the yolk sac. When the vascular system begins to form, mesodermal cells adhered to the recently formed endothelium form the first hematopoietic structures (i.e. blood islands)[19]. Right away, shared mesodermal ontogeny, embodied by hemangioblasts, reveal a close relationship between hematopoietic and endothelial lineages that will eventually define the origin of definitive HSC[20]. This primitive hematopoiesis serves to guarantee oxygen supply to the highly proliferative embryo and assist in tissue remodeling, with formation of erythroid, macrophage and megakaryocyte progenitors[21]. After relying on the transient nature of primitive hematopoiesis, definitive hematopoiesis commences once more in the yolk sac, with formation of erythromyeloid progenitors that possess more adult-like phenotype[22]. With time secured by these two initial hematopoietic

phenomena, hematopoiesis can now begin in the embryo itself. So far, no primitive HSC have been formed. In the aorta-gonad-mesonephros (AGM) region, the stem cell pool that will eventually be responsible for decades of blood production starts to emerge. Similarly to the hematopoietic genesis in the yolk sac, HSC are generated from another endothelium, namely the hemogenic endothelium, located in the dorsal aorta, through a process called endothelial-to-hematopoietic transition (EHT). Recently, EHT has also been shown to give rise to hematopoietic progenitor populations, with different transcriptomic signatures compared to HSC[23]. Immense self-renewal capacity of human EHT-derived HSC was experimentally validated in a xenotransplantation model (specifically, the NOD.Cg-Prkdc^{scid} Il2rg^{tm1Wjl}/Sz mouse species)[24].

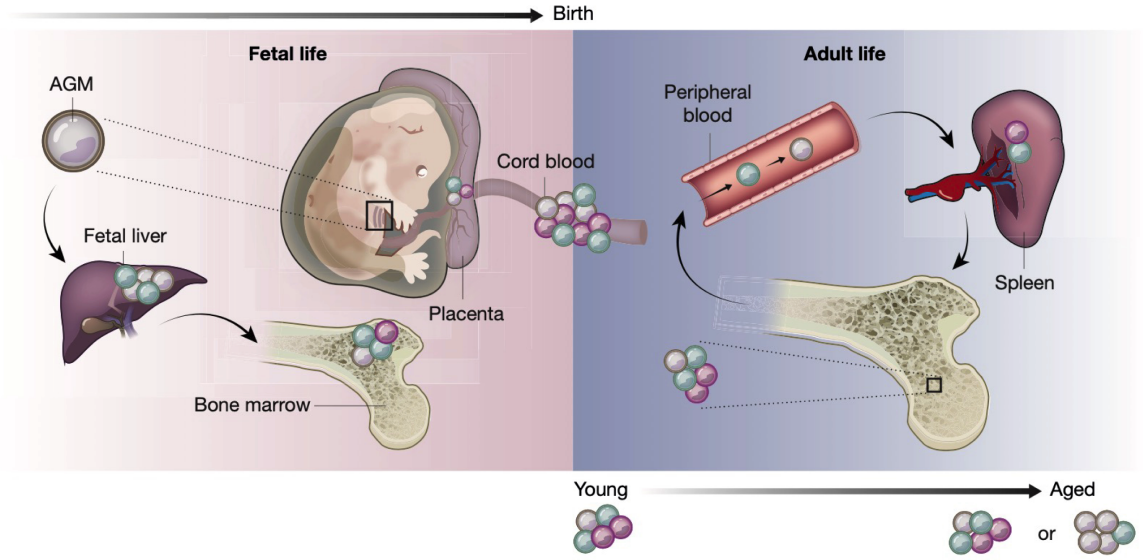

Figure I-2. *Spatial evolution of hematopoiesis from development to adult life. Briefly, after primitive hematopoiesis occurs in the aorta-gonad-mesonephros (AGM) region, hematopoietic stem cells (HSC) migrate to the fetal liver, allowing their significant expansion. Connected to the fetal liver, blood enriched in HSC and hematopoietic progenitor cells (HPC) fills the umbilical cord. Before birth, the HSC pool travels to the bone marrow, where it will assure lifelong hematopoiesis. During adult life, hematopoietic cells produced from the bone marrow move to the peripheral blood to guarantee their cellular functions. After completing their purpose, the spleen takes care of removing cellular waste and damaged or aged cells. Adapted from [16].*

After their generation, as embryo development continues, HSC migrate to the fetal liver (of endoderm origin), serving as its main niche during pre-natal development[25]. Here, HSC suffer significant expansion (around 38-fold), in order to reach enough cells to guarantee lifelong hematopoiesis[26]. Niche signals responsible for inducing expansion are poorly understood, but stromal support through cell-cell contact or paracrine signaling has been implicated. Perivascular Nestin^{+}NG2^{+}cells, endothelial cells (EC) and hepatic progenitors have all been shown to be involved, as well as hematopoietic

cytokines such as stem cell factor (SCF), thrombopoietin (TPO), angiopoietin-like 2 and 3, and insulin-like growth factor 2[27–29]. Since the fetal liver still possesses underdeveloped vasculature at the time of hematopoietic colonization, HSC are found in a dense liver parenchyma, a rich environment that facilitates cell-cell interactions[30]. Simultaneous expansion of the hepatic vascular tree itself may also be a driver of HSC expansion. Difficulties in studying fetal liver hematopoietic expansion can be partially attributed to an ever-changing niche environment, opposed to adult hematopoietic niches (e.g. bone marrow) that have more temporal stability[25]. HSC present in the fetal liver also need to care for the developing embryo, with early fetal-stage HSC showing priming for the erythroid lineage to assure proficient oxygen transport, while late fetal-stage becomes more focused on producing a balanced and complete hematopoietic system[30].

Before the fetus fully develops, hematopoiesis wanders again, from the fetal liver to the fetal spleen and the newly formed fetal bone marrow. The role of the fetal spleen in fetal hematopoiesis is still largely unknown, although studies have hinted towards being a site of hematopoietic differentiation, complementing the fetal bone marrow[31]. Its occupation by HSC from the fetal liver might just be to prepare the spleen for its adult role of supporting the immune system (white pulp) and removing damaged erythrocytes and pathogens (red pulp), as well as adult extramedullary hematopoiesis during stress[32]. Fetal bone marrow, after ossification and bone vascularization, is finally ready to fulfill its function as the ultimate site of hematopoiesis[33]. Although colonized during the later stage of development, HSC numbers also increase after birth, when the umbilical cord is disconnected from liver portal vessels, and these suffer a remodeling that results in the loss of periportal pericytes and remaining HSC[27]. Remarkably, tissues that support fetal development (i.e. placenta) have also been shown to harbor some HSPC during several stages of gestation[34]. As expected, placental stromal cell lines generated from various developmental stages were also capable of supporting HSPC through co-culture[34].

Besides suffering from a final spatial relocalization, HSC also begin to change their behavior after birth. After three initial weeks with a proliferative phenotype, HSC also change their wiring, gaining their more quiescent state[35]. This transition has been transcriptomically shown to be gradual and uncoordinated[36]. Largely protected inside bone, the adult bone marrow ends up harboring a heterogenous but spatially coordinated niche for hematopoiesis (Fig. I-3). Its shielding function accoupled to the critical role of hematopoiesis makes it hard to investigate the bone marrow environment. Unlike most organs, bone marrow lacks physical references aside from its dense vasculature and circulating bone[37]. Still, the hematopoietic bone marrow niche has been described having two main subniches that have radial distribution.

Closer to the bone lining, an endosteal niche has been described associated with

promoting HSC dormancy and genomic protection from proliferation-based stress[38]. Small arterioles, more present next to the bone surface have also been implicated in contributing toward the endosteal niche[39]. Osteoblasts present in the bone surface, responsible for bone formation, have been connected with HSC regulation in the endosteal niche. Osteoblast ablation or increase through genetically altered models caused interference or enhancement in BM hematopoiesis, respectively[40]. With such consistent phenotypical changes, osteoblasts were the first cellular elements of the bone marrow niche to be identified. In addition to their niche-promoting effect, secretion of osteopontin has been proven to promote HSC quiescence, which is coherent with increased presence of more primitive HSC in the endosteal niche[41]. Enveloping arterioles in the endosteal niche are rare Nestin^{high}NG2^{+} pericytes that also promote HSC dormancy[39]. Depletion of these supportive stromal cells caused HSC cycling and disrupted long-term repopulation capacity. However, the endosteal niche remains controversial, since arteriolar contribution as well as the entire endosteal niche has been questioned, as multiple studies have not been able to detect HSC in proximity to arterioles[42].

Sinusoids, unique vessels in the bone marrow that serve as migration avenues for newly formed hematopoietic cells, surrounded by stromal leptin receptor^{+} (LepR^{+}) pericytes are responsible for assuring a sinusoidal niche that harbors much of the HSC population in the BM[42]. More distanced from the bone surface, in addition to sinusoidal EC, these pericytes secrete HSC maintenance and self-renewal factors (e.g. stem cell factor (SCF), CXCL12 and Pleiotrophin)[42]. Perisinusoidal megakaryocytes also have a part in regulating adult hematopoiesis, being able to secrete TGF-ß1 and CXCL4, which are promotors of HSC quiescence[43,44].

With improved imaging techniques as well as more precise cell markers and transcriptomic profiles of cellular populations, more knowledge on the bone marrow niche is continuously being uncovered[45,46]. Although most of our understanding comes from murine bone marrow, fortunately, considerable comparability exists between species. Nevertheless, innovative methods for studying human bone marrow *in vivo* would definitely have impact in the field.

I.3. Hematopoietic Cell Transplantation – The Beginning of Cellular Therapies

Being such a remarkable cell population, HSPC were rapidly exploited therapeutically. The ability of HSPC of creating and sustaining a hematopoietic system was taken advantage of with the establishment of hematopoietic cell transplantation (HCT), marking the onset of cellular therapies. Early work in murine models led to the observation that mice could survive supralethal radiation if animals were infused with a BM graft[47]. BM aspirates containing HSPC were able to migrate to the affected BM after

radiation-derived myeloablative treatment and reconstitute the entire hematopoietic system.

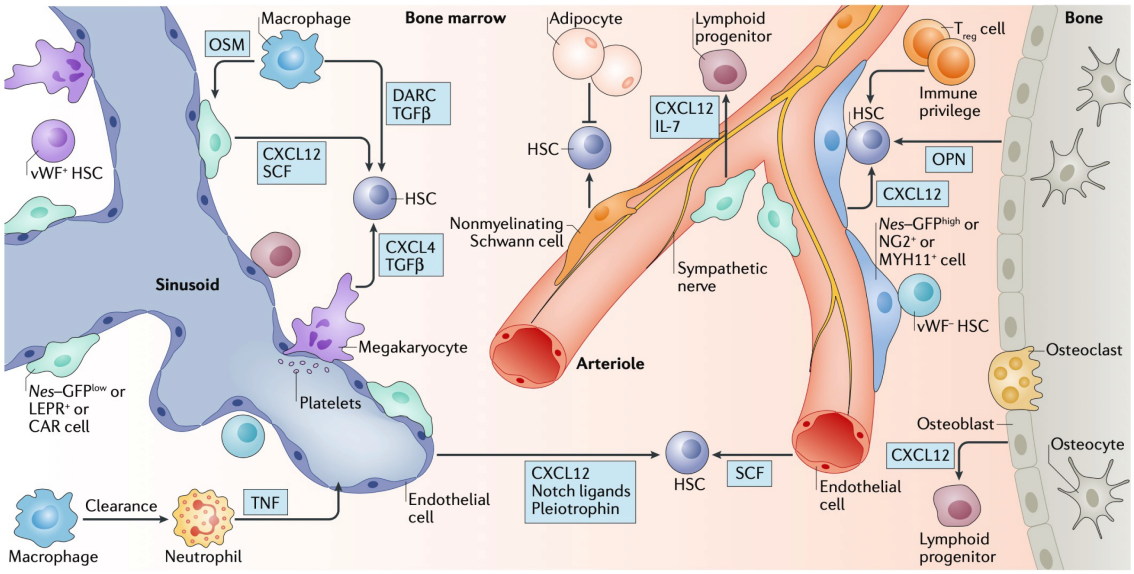

Figure I-3. *The adult bone marrow niche. A complex network of hematopoietic and non-hematopoietic cells make up the controlled environment that regulates medullary hematopoiesis. Whether close to the endosteal bone surface and arterioles or to sinusoids located further away from the bone, hematopoietic stem cells (HSC) are put into contact with a diverse array of signaling factors, that can promote differentiation or self-renewal and quiescence when required. When this network is disrupted, several bone marrow diseases can erupt, causing deficient hematopoiesis. Adapted from* [44].

After proving to treat radiation injury, BM transplantation was considered as a possible treatment for leukemia. In 1956, normal BM grafts were infused into leukemic mice as a proof of concept[48]. Knocking out a murine hematopoietic system also meant eliminating its blood-related malignancies. Transplants of healthy grafts would then repopulate the BM and form a new hematopoietic system. By transposing this knowledge to humans, in 1957, HCT was successfully performed in human leukemia patients, between identical twins (of which one had leukemia and the other served as a matched marrow donor). Although patients did not reach full remission, they did successfully survive HCT, paving the way towards showing the feasibility of cell therapies[49].

HCT development demonstrated that a main and contemporary hurdle of cell therapies, known as rejection, could be overcome. Indeed, early on, rejection was crucially identified as an immunologic response by observing the progressive degradation of skin grafts[50]. In 1953, a breakthrough was described that brought down the inevitability of rejection. The concept of acquired tolerance was described when lack of rejection was seen in mice that were previously infused with donor cells during fetal development,

originating chimeras[51]. HCT was able to surpass rejection through acquired tolerance with elimination of the existing immunological response by radiation pre-conditioning.
Rapidly after the discovery of acquired tolerance, another major concern related with cell therapies arose. Even with spleen or BM cells infused to induce tolerance, skin grafts continued to fail as the age of the recipients increased[52]. The reason behind this adverse reaction was another immunological response, brought upon by the actual graft. Active immune cells from the donor that accompanied the grafts were not tolerant towards the recipient. Consequently, these would launch a hostile immune response mirroring rejection mechanisms. However, this reaction is limited to HCT, not occurring in solid organ transplantation, where the only mechanism of rejection is the attack triggered by the immune system of the recipient against the transplanted organ. Initially termed runt disease, since affected mice would not develop into their adult life, this immune-based effect is presently known as Graft-vs-host disease (GVHD).
Rejection and GVHD possess similar modes of action, being based on an immunologic response. Circumventing these complications in a transplant scenario meant finding the basis of immunological identity, namely genes encoding for the human leukocyte antigens (HLA)[53]. With the development of HLA typing, transplants could be performed between HLA-matched patients, with the hope of avoiding rejection and GVHD. This led to the first successful HLA-matched HCT between two siblings in 1968 to treat severe combined immunodeficiency (SCID), thus demonstrating the potential of HCT to treat illnesses other than cancer[54].
Except for blood transfusions, HCT was the first cell therapy to be adopted in a clinical setting, ultimately gaining widespread acceptance for treatment of genetic or oncological disease with therapeutic success. The implementation of most current cell therapies can be traced back to knowledge gained by the establishment of HCT. For instances, the field of solid organ transplantation, which is very limited by tissue tolerance, has also benefited from HCT experience. Joint transplantation of organs with their respective BM graft was able to cause acquired tolerance towards the solid organ and overcome HLA-mismatch[55]. Gained knowledge of the potential and limits of allogenic and autologous approaches has facilitated therapeutic objective delineation in skin grafts. Using an allogenic source for the production of dermal and composite substitutes (e.g. Dermagraft® and Apligraf®) has limited grafts to serve only as a temporary barrier that promotes wound healing, without any permanent engraftment[56,57]. On the other hand, autologous skin grafts (e.g. EpiCel® and Permaderm®) integrate the skin of the patient while continuously promoting wound closure, reducing scar tissue formation and mitigating an inflammatory microenvironment[58,59].
Besides GVHD, HCT also demonstrate a graft-vs-leukemia (GVL) effect against residual malignant cells that defied conditioning treatments. This behavior has been associated

with lymphoid constituents of the transplant, which has heightened interest in adoptive T cell therapy. Donor lymphocyte infusions (DLI) of specific T cell subsets or, more recently, enhancement of their antitumoral capabilities through chimeric antigen receptor T (CAR-T) cell technology are approaches that have shown great success in both treating cancer and mitigating GVHD in patients[60,61].

Infusion of healthy marrow cells into radiation-treated diseased BM (close to reaching its 70th anniversary) has been able to cure up to 1.5 million patients, according to the Worldwide Network of Blood and Marrow Transplantation (WBMT)[62]. Each year, an average of 84 000 transplants are successfully performed. Interestingly, allogeneic (using cells from a donor) and autologous (using cells from the patient) HCT have each gained their own value and have indications for specific diseases. As of 2019, 53.5% of all HCT were allogeneic, but both have increased between 2006 and 2016 (allogeneic – 89.0%; autologous – 68.9%)[62]. While leukemias and non-malignant hematological disorders (e.g. Hemoglobinopathies or autoimmune disorders) are preferentially treated with allogeneic HCT, patients with lymphoproliferative disorders and solid tumors are mostly subjected to autologous HCT[62].

Although infusion of HSC and their engraftment are the key therapeutic objective in HCT, side objectives, from avoiding thrombocytopenia to accomplishing timely immune reconstitution, are essential for early patient survivability. After myeloablation, the coordinated production pipeline of the hematopoietic system is disrupted. Engrafted HSC can reinstate steady-state hematopoiesis, while more differentiated progenitor cells ensure short-term hematopoietic reconstitution. Therefore, hematopoietic progenitor cells also serve an essential purpose, and their role in the initial success of a HCT might be even more significant than their more undifferentiated progeny (i.e. HSC)[63]. The ideal hematopoietic graft should include a mixture of hematopoietic stem and progenitor cells, safeguarding both long-term and short-term hematopoiesis, respectively, while allowing to reduce transplant-related mortality. Importantly, fully differentiated cells, especially of the immune system, must be avoided to reduce the probability of GVHD and other immune-mediated complications[64].

The success of HCT is multi-factorial, with multiple approaches being explored to continuously improve such an impacting therapy. In what concerns the donor-recipient compatibility, high-resolution HLA-typing has allowed even greater immunological compatibility. Permissive mismatches in HLA-DPB1 have been shown to cause limited alloreactivity (promoting GVL, while shielding from GVHD), which has led to their inclusion in the donor selection criteria[65,66]. Also, the clinical impact of minor histocompatibility antigen mismatching is poorly understood, being a target for research to improve the outcome of allogeneic transplants[67,68]. Concerning pre-HCT patient conditioning, for certain diseases, the development of non-myeloablative and reduced-intensity regimens has significantly reduced toxicity and increased the range

of eligible ages for HCT[69,70]. Patients of age ≥70 years, who did not have access to this treatment option beforehand, are undergoing allogeneic or autologous HCT with steady growth over the years[71]. At the cellular level, improving HSPC homing, and engraftment has been similarly explored as a strategy. Identifying the CXCR4/CXCL12 axis as a primary mechanism for HSPC homing, use of glucocorticoids, stabilization of HIF-1**α** or incorporation of CXCR4 into lipid rafts have contributed towards enhancing this chemotaxis/migration axis[72].

While each of the abovementioned approaches has relevance, graft cell dose is a dominant factor affecting HCT outcome. Patients require a defined number of infused cells to ensure engraftment. For HCT transplants using BM grafts, an optimal dose of 3 x 10^8 total nucleated cells (TNC) per kg is sought[73]. Reaching clinically relevant cell doses may be more complicated depending on the HSPC source and has limited making HCT more widespread.

I.4. Sourcing HSPC – Reaching Hematopoietic Ancestors

For clinical application of HSPC, cell procurement is essential and defines the availability of HSPC and patient's eligibility for HCT. Fortunately, HSPC can be harvested from different locations for later application in HCT and other curative therapies (Fig. I-4). As the homeostatic home of adult HSPC, BM was the sole source of HSPC for many years. While HSPC were also found in peripheral blood, their number is residual and insufficient for clinical application. However, with better knowledge on HSPC regulation and biology, spatial restriction of HSPC in the BM was seen to be tightly regulated. Granulocyte colony-stimulating factor (G-CSF) and, more recently, plerixafor came as disruptors of HSPC retention, through suppression of CXCL12/CXCR4, c-kit/SCF and VCAM-1/VLA-4 axes[74,75]. Consequentially, mobilization of HSPC was made possible, opening another alternative for HSPC harvest[76]. With time, gained knowledge of developmental hematopoiesis pointed out that HSPC might exist in other tissues, leading to the finding of HSPC in umbilical cord blood (CB), drawing enthusiasm towards exploiting a medical waste of easy procurement[77]. Together, BM, mobilized peripheral blood (mPB) and CB provide complementing options for HSPC isolation, with differences between them, impacting their potential as a source for HCT. These HSPC sources, each with distinct properties and advantages, have made it possible for nearly any patient to find a potential donor[78].

As the base of operations of lifelong hematopoiesis, BM is a naturally protective environment for HSPC. Accordingly, HSPC collection involves an invasive procedure under general anesthetic where a needle must pierce bone multiple times in order to retrieve up to 1.5 L of marrow[79]. Although devices have been developed to significantly improve marrow aspiration (e.g. MarrowMiner), BM collection is the most invasive

intervention and has the most relevant harvest risks for the donor[79]. With its historical background, harvesting has had considerable success. Yet, quality of BM grafts has been declining, with a multivariate study showing correlation with diminishing treatment center and physician experience with BM[80]. Depending on donor availability and HLA-matching score, BM aspirates can be sourced for matched sibling, matched unrelated and haploidentical transplants. These transplants have a moderate risk of developing GVHD, since T cell maturation is done in the thymus instead of the BM and many differentiated immune cells are located in secondary hematopoietic organs or in circulation[81]. Unsurprisingly, for matched unrelated and haploidentical transplants BM-derived grafts resulted in lesser incidence of chronic GVHD compared to mPB, with equivalent or improved survival measures[82,83].

When looking to mPB, collection of HSPC from this source has progressively gained popularity, being by far the preferred source in allogeneic HCT for adult patients[84]. Mobilization of HSPC has very practical benefits, with graft procurement becoming similar to a common blood harvest for donation. Although actual recovery of HSPC from mPB has reduced risks compared to BM, donors must follow a stringent and costly mobilization regimen (IV administration) that can last up to 5 days[74]. Furthermore, successful mobilization is not guaranteed, with failure rates reaching up to 40% and affecting donors without any known risk factors (e.g. multiple myeloma, lymphoma or diabetes diagnosis)[85]. When mobilized, BM HSPC gradually migrate into circulation, mixing with normal PB and their native hematopoietic populations. Thus, immunologically active cells are much more present in mPB grafts, increasing the threat of GVHD[86]. This increased alloreactivity also has benefits, especially in allogeneic HCT for malignant diseases. GVL is enhanced in mPB grafts and helps reduce relapse risk[87]. To push the balance between GVHD and GVL towards the latter, increased mobilization of regulatory T cells (Treg) might improve patient protection against GVHD while maintaining a valuable GVL effect[88].

When sourcing HSPC from CB (HSPC(CB)), grafts benefit from inherent neonatal primitiveness. As such, GVHD-contributing populations are rare, providing an important option that can partially circumvent such a transplant-related complication[89]. Its attractiveness is also due to its collection as a source, which involves recovering blood from a severed umbilical cord, existing no risk for the donor. Moreover, such a naïve graft also allows loosening of HLA-matching requirements, with recent selection guidelines for HCT stating at least a 4/6 HLA-match or 4/8 for high-resolution HLA-match[90]. On the other hand, compared to the remaining sources, patients with HCT performed with HSPC(CB) have the longest time to engraftment and hematopoietic reconstitution due to this same graft trait[91]. Without more differentiated progenitors, transplanted HSPC will take longer in replenishing the entire hematopoietic system until steady-state hematopoiesis can be reached. Limited collection volume (around 100 mL,

with a range of 50 – 200 mL) also restrains use of an increased $CD34^+$ cell dose, having pressured the development of *ex vivo* expansion to bypass this obstacle[92,93]. A recent systematic review has confirmed clinical advantages of HCT done with expanded HSPC from cord blood, though alerting towards the need for long-term outcome data[94].

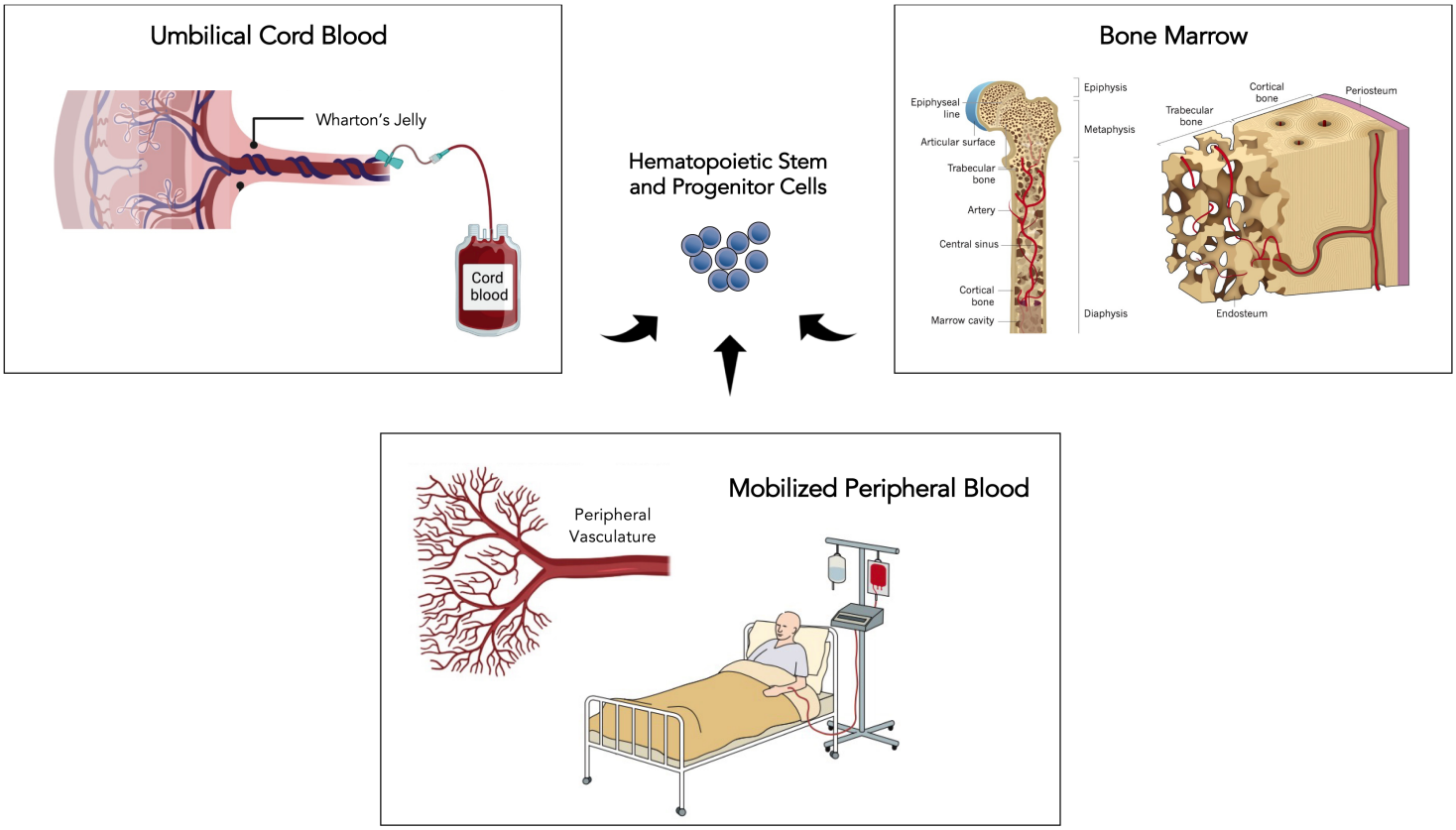

Figure I-4. *Clinically relevant sources of hematopoietic stem and progenitor cells (HSPC). HSPC can be obtained by aspirating the bone marrow several times. With the discovery of stem cell mobilization, HSPC can be collected from peripheral blood, as soon as HSPC have been stimulated to leave the bone marrow. Additionally, HSPC can also be found and successfully harvested from umbilical cord blood, which is considered medical waste. Adapted from* [45,86].

The diversity of available HSPC sources brings forth an array of options that differentially affect HCT measures, such as overall survivability, graft failure, onset of GVHD, HLA-match availability or time to hematopoietic reconstitution[91]. Ideally, depending on the clinical condition of a patient, the best grouping of source – disease should be investigated, taking into account the best prognostic prediction. Nevertheless, the field of HCT has seen trends in source selection that do not necessarily have scientific rationale or are due to over extrapolation of clinical results. Although the benefits of CB transplantation are well described, its use has declined steadily over the last decade[95].

The improvement of haploidentical transplants through depletion of **α**/**β** T cells or use of post-transplant cyclophosphamide can potentially justify this registered drop in CB transplants[96]. Also, in spite of increased incidence of acute and chronic GVHD, mPB has largely overtaken remaining sources in allogeneic transplants (reaching up to 80% in the U.S.)[97]. These decisions should be made with caution and have scientific consensus, since disregard for a certain source will lead to limited experience of the transplant center, compromising source handling. Specifically for CB, when a matched related donor cannot be found, clinical results show that unrelated CB transplants still typically perform better than other transplants when treating metabolic diseases, aggressive acute myeloid leukemia and primary immunodeficiencies that suffer from viral infections[96]. Therefore, results of retrospective and prospective comparative studies should be consulted to back up decisions in source selection for HCT.

I.5. Ex Vivo Expansion of HSPC – More from Less

The ability to generate desired numbers of any cell type *in vitro* is a tremendous feat. Harnessing the expansion potential of HSPC is meaningful since they and their progeny represent such a significant portion of the body cell turnover (86%)[3]. Development and rapid evolution of *ex vivo* expansion of HSPC have been pushed essentially by researchers and clinicians tackling the limited application of CB units as a cell source for HCT. Nevertheless, new fields of study also take advantage of possibly having HSPC as unlimited raw material, such as hematopoietic gene therapy and hematological disease modeling[98,99]. Instead of directly using expanded HSPC, important hematopoietic populations of interest may also be generated, including virus-specific T cells, NK cells, lymphocytes for DLI, CAR-T or CAR-NK production, regulatory T cells (T_{reg}) and erythrocyte production for transfusions[96,100].

Initial protocols for HSPC expansion were solely based on cytokine supplementation, causing a chase for novel ligands or signaling molecules responsible for promoting self-renewal. At that time, along with basal medium formulations and animal serum, the use of cytokines and growth factors became the bedrock of any HSPC expansion system. While a great variety of cytokines were sequentially discovered to promote HSPC expansion, a recurrent core of signaling molecules, including stem cell factor (SCF), fms-related tyrosine kinase 3 ligand (Flt-3L), thrombopoietin (TPO) and interleukin-6 (IL-6), have solidified their almost ubiquitous presence in expansion cultures (extensively reviewed[101–103]). Improvement of cytokine-based expansion then turned to the development of tailored expansion media, specifically tuned to improve HSPC proliferation[104–106]. Beyond personalizing basal formulations, undefined sera were phased out, significantly reducing batch variability during expansions. In the hope of eventually reaching chemically-defined media, remaining animal-derived products still

present have also been slowly substituted, coalescing with recommendations by regulatory agencies for cGMP[107]. As cytokine-based expansion became more widespread, to boost HSPC self-renewal even more, cytokine concentrations were identified as a relevant target for optimization. Through experimental design, fine-tuning cytokine concentrations was achieved, uncovering synergistic relationships and giving rise to multiple optimized cytokine cocktails[108,109]. Although cytokine-based expansion alone was able to expand HSPC enough to originate a clinical trial[110], numerous strategies have now evolved from this initial platform.

I.5.1. *Co-Culture Expansion*

As previously described, the native environment of HSPC is rich in cell diversity, responsible for upholding the complex structure of the BM. Different niches exist inside the BM, regulating HSPC behavior to maintain a healthy steady-state hematopoiesis[111]. In coexistence, EC lining the marrow vasculature, as well as supportive mesenchymal stromal cells (MSC) (i.e. pericytes), are part of the sinusoidal niche, where HSPC are stimulated to increase their proliferative capacity to respond to hematopoietic needs[112]. An expected strategy would be establishing a co-culture system with cell types that promote expansion of HSPC *in vivo*.

Following that rationale, several attempts have been made to expand HSPC using EC. Since primary EC cannot be sustained for many passages *in vitro* without losing their characteristic phenotype or undergoing cell death, an adenovirus gene, *E4ORF1*, has been used to stabilize cultured EC[113]. EC hematopoietic support was initially shown in murine models to be contact-dependent, and their mechanism based on AKT-activated expression of an array of angiocrine factors, including Notch pro-expansion ligands (i.e. Jagged-1, Jagged-2, DLL1, and DLL4)[114]. However, the benefit from EC co-culture has been hypothesized to be tissue-dependent[115]. A recently completed clinical trial exploiting this strategy (i.e. NCT03483324 – Completed: January 2022) successfully uses human umbilical vein EC (HUVEC). Interestingly, *E4ORF1*$^+$-umbilical arterial EC were shown to promote more significant HSPC expansion, namely approximately double fold change (FC) in TNC, CD34$^+$, CD34$^+$CD38$^-$ and CD34$^+$CD38$^-$CD90$^+$ cells, compared to co-cultures with HUVEC after 14 days[116]. On the other hand, kidney-derived EC worsened the fold increase of HSPC compared to EC-free conditions[117]. Thus, vascular niches have been labeled organ-specific with unique angiocrine phenotypes, highlighting the importance of correct EC-procurement for HSPC expansion by co-culture[118].

An alternative adherent cell candidate for co-culture would be BM-derived MSC. Unlike EC, MSC have significant expansion capacity *in vitro* and have proven to be a valuable cell population in cell therapy[119]. Given their diverse therapeutic properties (e.g. anti-

inflammatory, immunomodulatory and anti-apoptotic), MSC manufacturing has witnessed impressive evolution. Numerous scalable expansion platforms have been developed and required reagents improved to uphold ever more stringent regulatory standards (e.g. xeno-free formulations or chemically-defined media)[120–122]. As with EC, MSC can be sourced from various tissues, with most having been studied for their population-specific hematopoietic support capacity[123,124]. Interactions between HSPC and MSC were also seen to be contact-dependent[125–127]. HSPC expansion dynamics during this type of co-culture have been shown to be elaborated. After sedimentation, HSPC that maintain contact with supportive MSC become the main drivers of proliferation[125]. A more differentiated non-adherent population forms as progeny of adherent HSPC, through cell egress[125]. A fraction of adherent HSPC eventually migrate beneath the MSC feeder layer, proliferate slower and become more enriched in $CD34^{+}CD38^{-}$ cells[125]. Interestingly, reported HSPC behavior is comparable to the native BM, with the formation spatially and functionally distinct HSPC populations (i.e. primitive cells under MSC – proliferative cells over MSC – non adherent cells; quiescent HSPC in endosteal niche – proliferative HSPC in contact with MSC in sinusoidal niche – progenitor cells that migrate into sinusoids). By creating such a biomimetic effect with a single supportive cell type, HSPC expansion through MSC co-culture has originated two clinical trials, starting with unselected CB MNC[128]. Enhancement of MSC and their known hematopoietic support capabilities was eloquently pursued by having them express angiopoietin-like-5 or a selection of 5 transcription factors (*Klf7*, *Ostf1*, *Xbp1*, *Irf3* and *Irf7*) that regulate niche factors, leading to improved HSPC expansion[129,130].

I.5.2. *Extracellular vesicles (EV)-mediated expansion*

The discovery of EV, cell-derived particles comprising exosomes and microvesicles, has disrupted our established knowledge of cell biology by uncovering new means of cell communication[131]. Since mechanisms by which the abovementioned co-cultures benefit HSPC expansion are unknown, EV have been proposed as a possible key player. Although cell contact has been implicated, EV may partially explain the advantage brought upon by EC or MSC. Naturally, MSC-derived EV were one of the initial candidates to be tested on HSPC expansion[132,133]. BM-derived MSC (MSC(M)) EV from fetal or adult origin were evaluated side-by-side for their possible hematopoietic supportive capacity[133]. While EV isolated from adult MSC(M) nearly doubled TNC FC and $CD34^{+}$ cell FC compared to an experimental control (i.e. expansion without EV), fetal EV showed no advantage compared to control conditions. Through proteomic profiling, a deeper look into the EV cargo uncovered enrichment of proteins involved in the TGF-**β** receptor pathway in EV from fetal MSC(M). TGF-**β** is described as one of the major inhibitors of HSPC proliferation, and a recent report has also identified the

presence of Smad2, a TGF-β signal transducer, in murine MSC-derived EV [134,135]. Consistently, the addition of a TGFB1 inhibitor to the expansion cocktail, including fetal MSC(M)-derived EV, significantly increased the expansion of TNC, $CD34^+$ and $CD34^+CD38^-CD45RA^-$ expressing cells[133]. Intriguingly, osteoblast-derived EV have been described to have a similar effect on HSPC expansion[136]. Although belonging to a quiescence-promoting microenvironment (i.e. endosteal niche), osteoblast-derived EV led to a 2.4 FC of $CD34^+$ cells relative to increases without EV supplementation. Here, the most abundant elements of the EV cargo, both at the miRNA and protein level, were identified as having the *EGR1* gene as a target, which encodes a transcription factor responsible for HSPC regulation[136].

Improvement of an EV-based benefit for HSPC expansion largely depends on cargo manipulation. A more native approach would explore other cell types as EV producers to find the ideal match between cargo and hematopoietic supportive properties. Another strategy has been, considering EV as a cellular derivative, to apply cell pre-conditioning to have the producing cell alter its own EV composition. By exposing MSC to a hypoxia culture before EV collection, changes in their native EV cargo were observed, which led to improved TNC FC and percentage of $CD133^+$ cells[137]. Still, to harness the full potential of EV as systems of signaling modulation, instead of working with native cargos, bioengineering EV to reach customizable cargos would be the ultimate objective in the field[138,139].

I.5.3. *Ligand Immobilization-based Expansion*

Different methods have been used to tap into signaling pathways that drive HSPC expansion. Although the use of ligands was early explored and simple to incorporate, some were observed to require structural stability to enhance their effect[140,141]. The Notch-mediated expansion system was developed through ligand immobilization. Specifically, Notch ligand delta-like ligand 1 (DLL1) was fused to the Fc portion of human IgG-1 ($Delta1^{ext\text{-}IgG}$) and immobilized onto plastic culture ware, being able to support HSPC expansion[142]. Initial efforts in translating this system led to the development of a clinical trial to evaluate the applicability of expanded HSPC in double unit cord blood transplantation (DUCBT) (NCT00343798)[143]. Although rapid myeloid reconstitution was observed due to the expanded unit, persistent long-term engraftment was mainly assured by the unexpanded graft. In fact, after 16 days of culture, the expression of CD34 was down to 14.5%, indicating the presence of more differentiated populations[143]. This result was not unexpected since the Notch signaling pathway is also highly associated with T cell development and involved in the regulation B cell differentiation[144,145]. Acknowledging the limitations of this particular expanded HSPC-based product in what concerns long-term engraftment and reconstitution, a shift in

therapeutic purpose was admitted. Instead of pursuing long-term reconstitution, requiring more primitive HSC, expanded HSPC deriving from this expansion system could be employed to facilitate/accelerate immune reconstitution after an HCT, a major post-transplant constraint. Multiple clinical trials have explored the applicability of using the Notch system to accelerate immune reconstitution as therapeutic approach, sponsored initially by a Seattle-based spin-off, Nohla Therapeutics[146,147]. In the meantime, as a technological platform, this expansion system has been transferred to the proprietary portfolio of Deverra Therapeutics. Nevertheless, attempts were made to maintain undifferentiated populations by combining Delta1$^{ext\text{-}IgG}$ coatings with hypoxia, limiting ER stress[148]. By using hypoxia (1-2% O_2), long-term HSC experienced a 4.2 FC compared to the same experimental system under normoxia[148].

I.5.4. *Bioreactor-based Expansion*

For cell and gene therapies, translation to bioreactor systems is deeply encouraged[107]. These systems, widely implemented in the pharmaceutical industry for the production of biologicals, facilitate reliable manufacturing since they take advantage of feedback from sophisticated monitoring instruments to monitor and control production. Early application of bioreactor systems in HSPC expansion saw the arrangement of two clinical trials, one using BM MNC for autologous transplants and another evaluating expansion of CB MNC for HCT[149,150]. HSPC were expanded in an AastromReplicell System, where stromal populations (only present in BM MNC) can form an adherent supportive layer *in situ*. A feeding regimen based on perfusion, allows continuous exchange of nutrients and metabolites, while maintaining cells inside. No advantage in reconstitution timeframes was observed, although these trials were pivotal in demonstrating safety of expanded HSPC.

The benefit of active monitoring of secreted factors that negatively affect HSPC expansion (e.g. TGF-**β**1) has been demonstrated. Through computational modeling, a fed-batch routine was hypothesized to increase HSPC expansion levels, due to the dilution of paracrine factors that accumulate over time[151]. Real-time monitoring of individual secreted factors, through quantum dot labeling, allowed for continuous adjustment of dilution rates, improving HSPC proliferation even more[152]. Further development of a proportional-integral-derivative (PID) controller optimized the feedback control system, showcasing the impact monitoring can have on HSPC expansion[153].

Recently, a membrane bioreactor (Quantum® Cell Expansion System) was used as a platform for HSPC expansion[154]. As an automated platform, labor times are significantly reduced and medium changes are performed through a perfusion system. A central chamber lined with a membrane separates it into two different compartments (hollow

fiber membrane module). In this particular study, the dividing membrane was coated with fibronectin and SDF-1, adding an extracellular matrix element and simulating chemotactic homing in the system to support growth of HSPC in the lumen of the bioreactor. An 8-day expansion from a starting inoculum of 2 x10^6 $CD34^+$ cells yielded a 51 FC in the same population, largely overcoming minimal doses for single cord and DUCBT[90]. Concomitant differentiation was seen to be predominantly of the myeloid lineage, namely immature neutrophils and platelets.

I.5.5. *Biomaterial-supported Expansion*

The incorporation of natural or synthetic biomaterials in devising novel strategies for HSPC expansion has been primarily explored[155]. These biomaterials provide structural support by granting cell anchorage for possible 3D assembly and control cell organization depending on their distribution or geometry. Biochemical and mechanical cues are also introduced based on the choice of biomaterial and these might be exploited to stimulate cell behavior.

ECM is an indispensable component of any cell niche, especially in a complex and multilayered environment like the BM. Cell type-specific ECM can now be produced and exploited through decellularization, for different applications. Decellularized ECM (dECM) from HS-5 (a human BM stromal cell line) was tested as a substrate for HSPC expansion. Native dECM from traditional 2D cultures and spin-coated dECM were directly compared with expansions with a HS-5 feeder layer and without dECM nor HS-5 cells[156]. Spin-coated dECM had a more uniform distribution and doubled the roughness of the native dECM. Interestingly, spin-coated dECM had the best performance, with increased FC in every studied HSPC population (i.e. TNC, $CD34^+CD45^{low}$, $CD34^+CD38^-$ and $CD34^+CD133^+$) and CFU colony type. Of note, quality of produced dECM through traditional *in vitro* culture has been questioned. To boost the benefit of dECM, macromolecular crowding during ECM production has been shown to improve ECM organization, better mimicking *in vivo* conditions[157]. A 7-day expansion of HSPC on dECM substrates produced with macromolecular crowding consistently showed better results than traditionally made dECM.

By maintaining a biomimetic perspective, hydrogels have provided an attractive avenue to integrate numerous niche factors (e.g. extracellular mechanics, structure three-dimensionality (3D) or matrix turnover)[158]. As water-swollen materials based on polymeric networks, their hydrophilicity and softer stiffness align with the native environment of HPSC. Additionally, hydrogels also have the advantage of being translucid, therefore highly compatible with multiple microscopic techniques for observation. Polyethylene glycol (PEG)-based macroporous hydrogels functionalized with adhesive motifs (i.e. Arginylglycylaspartic acid (RGD)) successfully harbored HSPC

supported by MSC(M) and led to increased expansion when compared to traditional two-dimensional (2D) culture surfaces[159]. In trying to validate expansion of circulating HSPC, a PuraMatrix™ hydrogel was used as an expansion system[160]. From a starting population of peripheral blood MNC, an impressive 70 FC in $CD34^+$ cells was observed. Of note, while most expansion systems focus on HSPC(CB), this study managed to demonstrate the potential of expanding non-mobilized peripheral blood-derived HSPC. Still, to date, the most thorough and tailored hydrogel development for HSPC expansion was done using a zwitterionic hydrogel[161]. By using a super-hydrophilic zwitterionic polymer, negative culture artifacts linked to their hydrophobic surfaces were avoided, providing an interaction-free scaffold. Polymer links through a polypeptide with metalloproteinase cleavable motifs allowed expanded HSPC to modulate the matrix as desired. After a 24-day period, encapsulated HSPC maintained their primitiveness (94.6% $CD34^+$ expression) and suffered a 322 FC in TNC, showing preservation of long-term repopulating capacity through secondary transplants in mouse models.

Ultimately, the use of biomaterials is allowing the formation of more complex systems for HSPC expansion. The ability to construct hierarchical structures or reach resemblance with organ-like organization might unlock even greater expansion potential. An interleaved lattice-mesh structure made of PCL spiked with hydroxyapatite (lattice) and polyurethane (mesh) was coated with vitronectin and seeded with HPSC(CB)[162]. The HSPC-infused scaffold was then incubated in a vessel capable of applying controlled hydrostatic pressure. Scaffold-adhered HSPC were not indifferent towards the existence of hydrostatic pressure, outperforming the remaining conditions. Taking advantage of extramedullary niches where HSC naturally go through an extensive expansion phase during development, fetal liver has been hypothesized to be an interesting alternative to model. Ferret-derived fetal livers were decellularized and repopulated with human fetal liver-derived stromal cells before infusing HSPC(CB)[163]. This top-down approach produced ECM with native structure to better recreate the fetal liver niche. 3D fetal liver constructs were able to better support HSPC expansion than 2D co-cultures and fetal liver-derived stromal cells outdid other tested cell types for repopulation of decellularized livers, such as hepatoblasts or BM Stro-1^+ progenitor stromal cells. In an attempt to mimic the trabecular bone structure where HSPC reside, a porous ceramic scaffold was populated with MSC(M) that underwent three weeks of osteogenic differentiation[164]. ECM production was promoted, causing the formation of a gel-like film around the ceramic scaffold, renamed engineered niche. After HSPC injection, cells were expanded in a perfusion regimen, reaching a 61 FC in TNC. Differentiated compartments were observed inside the engineered niche, similarly to the several microenvironments found in the BM.

I.5.6. *Small Molecule Expansion*

Recognizing the simplicity of supplementation of recombinant cytokines or EV supplementation in *ex vivo* expansion protocols, small molecules have also penetrated the field. Their simplified manufacture (compared to cytokines and EV) allied with their compatibility with high throughput molecular design and optimization have made them very appealing[165]. While initially tallying only a few molecules, small molecules have become the most rapidly expanding category of HSPC expansion promoters.

Tetraethylenepentamine (TEPA) was an early representative of small molecule-based HSPC expansion. TEPA was able to improve HSPC expansion compared to a cytokine-only control. Re-sorted $CD34^+$ cells derived from the expanded population also showed increased engraftment in xenotransplantation models[166]. As a copper chelator, cytosolic copper seizing in HSPC might be behind the mechanistic effect of TEPA, particularly by promoting histone acetylation[167]. Since copper has been described to induce oxidative stress, a decline of free intracellular copper avoids production of reactive oxygen species, promoting HSPC expansion[168]. Nicotinamide, a form of vitamin B3, was also identified as an enhancer of HSPC expansion and homing properties[169]. Interestingly, nicotinamide demonstrated potent inhibitory activity against sirtuin1, a histone deacetylase. An expansion system using nicotinamide has successfully advanced the clinical trial pipeline, having been recently granted market authorization by the US Food and Drug Administration (FDA)[170]. Specifically, Omisirge is an expanded HSPC product resulting from nicotinamide-based expansion for use in HCT or immune reconstitution after HCT (affected or not with post-transplant viral infection) or chemotherapy[170]. This marks a remarkable achievement, stemming from years of research and clinical development, bringing forth the first expanded HSPC cell product to the market. This overlapping effect of two different small molecules highlighted the impact of epigenetic modification on HSPC self-renewal. Unsurprisingly, more molecules affecting histone acetylation have come forward as candidates for improving HSPC expansion. Valproic acid (VPA) has been shown to increase HSPC self-renewal by upregulating HOXB4[171]. While initially demonstrated using HSPC(CB), adult HSPC (from mPB and BM) were also proven to be susceptible to VPA-based expansion[172]. Currently being evaluated in a clinical trial, a VPA-expanded HSPC product was produced using clinical-grade reagents and its cryopreservation was optimized, contributing towards its translation[173]. These abovementioned molecules were a result of having identified a specific mechanism of action and, consequently, fully exploiting its potential.

Another approach that was especially explored for small molecules was high-throughput screening of compound libraries. Being a simple expansion system, iterative testing of a myriad of molecules was facilitated and led to the identification of more impacting small molecules. StemRegenin-1 (SR-1) (aryl hydrocarbon receptor

antagonist), UM171 (repressor of differentiation through degradation of an epigenetic regulator), P18IN011 and P18IN003 (p18 inhibitors), and CPI-203 (bromodomain and extra-terminal domain (BET) inhibitors) were all flagged after screening[174–177]. Both SR-1 and UM171 have distanced themselves from remaining candidates, with impressive *in vitro* results and their own clinical trials as stand-alone grafts[178,179]. More molecules are being brought up every year, being detailed in a recent review[180]. Notably, a recent chemically defined cytokine-free expansion system (a caprolactam polymer-based culture with a cocktail of UM171, 740Y-P and butyzamide) was developed with stable long-term expansion of HSPC capable of serial engraftment in xenotransplantation assays[181]. Such an approach aligns deeper knowledge of HSPC biology with a translational focus, facilitating the transition towards manufacturing according to current good manufacturing practices (cGMP).

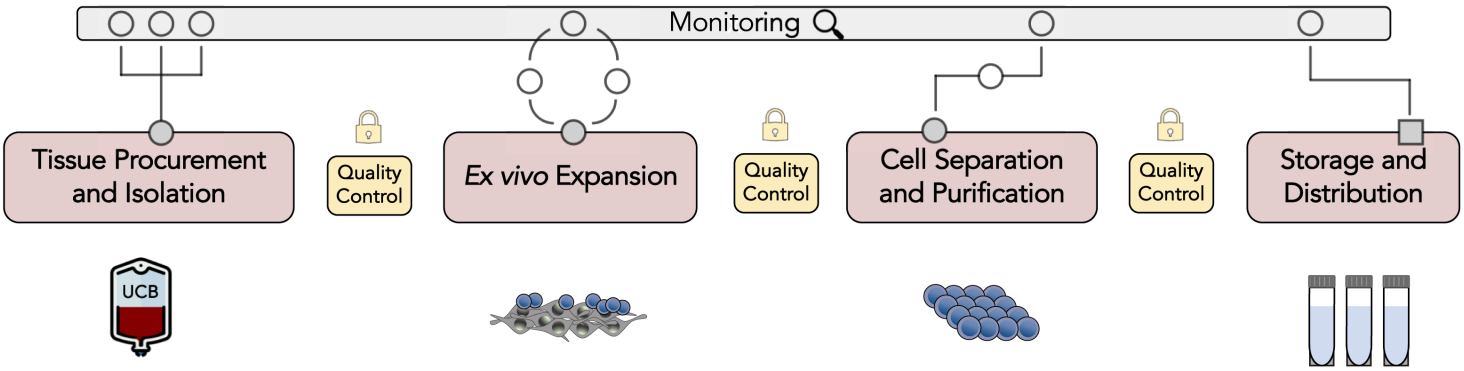

Figure I-5. *Overview of a generic manufacturing pipeline for production of expanded hematopoietic stem and progenitor cell (HSPC) products. Tissue procurement guarantees collection of necessary cells and tissues. When required, defined cell subpopulations can be isolated, through positive or negative selection techniques. In this particular case, isolated cells are then manipulated through ex vivo expansion (e.g. co-culture expansion) until production goals are reached. Expanded HSPC need to be subsequently purified from cellular (e.g. mesenchymal stromal cells) or molecular contaminants (e.g. exhausted expansion medium). Finally, expanded HSPC need to be stored and transported to clinical facilities for final patient infusion. Between each process unit, cell product quality needs to be guaranteed according to stringent guidelines (i.e. cell identity, function and purity). For such a complex production pipeline, continuous monitoring is strongly encouraged.*

I.6. Cell and Gene Therapy Manufacturing – Translating Bench to Bedside

With multiple cell and gene therapies (CGT) already reaching the market, one of the most pressing issues will be addressing the challenges in manufacturing these products. Expanded HSPC are no exception, although expertise in handling of hematopoietic products can be seized from extensive HCT experience. As of January 2023, 36 CGT

have been approved and received marketing authorization in the European Union (EU) and United States of America (USA) combined[182–184]. Omisirge (omidubicel), an expanded HSPC product produced with a nicotinamide-based expansion system by Gamida Cell, has just joined the list of approved CGT[170].

Due to their uniqueness, cell therapies have earned their own category in regulatory agencies with special directives concerning approval candidature. In the EU, CGT are considered advanced therapy medicinal products (ATMP), defined by the European Medicines Agency (EMA) as medicines for human use that are based on genes, tissues or cells, offering groundbreaking new opportunities for the treatment of disease and injury[183]. Although this millennium has been marked with considerate advances, with regulatory victories for multiple CGT, recent success is due to much effort in the past, uncovering and understanding all the obstacles that stood before the establishment of cell-based therapeutic options. HCT was decisive as a vehicle of problem-solving and thus has deserved its recognition as a foundation for cell therapy development[185].

CGT have pushed therapeutic potential to new heights, but therapy costs have followed the same tendency, with never-before-seen prices. Price tag for Omisirge has been set around $338 000, but other CGT have reached up to $3.5M (Hemgenix – a gene therapy for adults with hemophilia B)[186,187]. Additionally, CGT have been targeting medical conditions with increasing population incidence. Hence, implementation of cost-effectiveness measures that facilitate healthy process development, potentially being able to influence end product pricing, are urgently needed.

Robust and scalable cell manufacturing for the cost-effective delivery of safe and potent CGT (either with autologous origin (i.e. cells from the patient) or allogeneic) relies on process engineering tools to track cell product function and performance. The manufacturing process of CGT generally requires tissue collection, cell isolation, culture and expansion (upstream processing), cell manipulation, cell harvest, separation and purification (downstream processing) and, finally, product formulation and cryopreservation (Fig. I-5). Each of these stages presents significant challenges that have been the focus of study over the years, leading to innovative and ground-breaking technological advances. Although HSPC are non-adherent simplifying many bioprocessing stages, co-culture expansion systems also require adherent supportive cell types (e.g. MSC) and their respective manufacturing.

I.6.1. *Isolation of Target Cell Population*

CGT depend primarily on obtaining the appropriate material from which cells with possible therapeutic application can be isolated and manipulated. Depending on the nature of a specific CGT, cell isolation might be complicated due to lower cell frequency (e.g. stem and progenitor cells) or tissue access (e.g. bone marrow). HSPC ($CD34^+$)

frequency in BM aspirates is only 1.1% and MSC frequency in a BM aspirate is only 0.001% to 0.01%[188,189]. A large scale study of 126 341 red blood cell-depleted CB units in the USA inventory revealed that the median frequency of $CD34^+$ cells was 0.34%[190]. Assuring source availability and succeeding in tissue collection may be enough to proceed to the following bioprocessing stage. For minimally manipulated cell products, such as HCT, heterogeneous populations are isolated and directly infused into the patient. However, newer and more advanced cell therapies are becoming ever more population specific. Thus, bulk populations that normally result from harvesting procedures need funneling techniques that isolate a desired cell type.

For adherent cell types (e.g. MSC), the most commonly used method employed for isolation relies solely on the ability of cells to adhere to plastic surfaces[191]. After tissue collection, cells are plated on polysterene-based tissue culture flasks. After adhering to the plastic surface, non-adherent contaminating cells, are washed away after medium change and passaging[192,193]. Before plating MSC that are obtained from tissues such as cord matrix, AT or synovial membrane, they can be either enzymatically digested using collagenase solutions[193–195] or simply plated directly onto plastic surfaces as explants[196–198].

More sophisticated techniques can be used to isolate specific cell populations following tissue collection, typically relying on affinity-based and centrifugation-based separations. Although affinity-based separation has gained significant momentum in cell therapy manufacturing, classical centrifugation techniques are still part of typical bioproduction processes. When CB, BM or mPB samples are used, a first isolation step with density gradient centrifugation, using a polymeric solution (e.g. ficoll or percoll), separates the mononuclear cell (MNC) fraction from other constituents such as plasma and erythrocytes[192]. Considerable percentage of CGT are centered on hematopoietic subpopulations (e.g. CAR-T cells, T_{reg}, monocytes and HSPC), whose mentioned isolation consists on centrifugation approaches for separation and extraction of MNC.

Several Sepax (GE Healthcare) cell processing systems, have brought a fully closed and automated centrifugation unit to cell therapy production pipelines[199]. More advanced centrifugation platforms combine different physical forces to achieve higher isolation recovery and purity. Terumo BCT has established a continuous centrifugation system (Elutra®) that joins centrifugal forces with counterflow[200]. Using blood, initial centrifugation separates the MNC layer from plasma and erythrocytes. Fluid moving in counterflow separates the buffy coat into different fractions. By achieving cell population separation based on size and density, these platforms are able to reach much higher resolution in separation.

Cell isolation through affinity is an ever-growing alternative due to its separation criteria being based on biological instead of physical characteristics. Cell population immunophenotype is commonly used to isolate specific cells from their original sources,

such as HSPC ($CD34^+$ selection)[201,202] and MSC ($Stro\text{-}1^+$ selection)[203,204]. Typically mediated by antibody-antigen interactions, fluorescence activated cell sorting (FACS) and magnetic activated cell sorting (MACS) occupy leading roles in affinity-based separation. Through fluorescent labelled antibodies, FACS is able to separate cell populations based on their surface marker expression. This technology allows for multiple marker selection with high selectivity due to single-cell analysis[205]. In combination with cell separation, multi-parametric studies can be performed simultaneously, allowing for identity and quality control.

MACS shares the same separation criteria as FACS (i.e. immunophenotype) but achieves cell sorting with antibodies coupled to magnetic particles. While these techniques are not novel, direct and thorough comparison have only recently been established[206]. Whereas FACS dominates selectivity and subpopulation purity, the respective cell sorter is not inherently prepared for a clinical setting. An expensive hardware system combined with lack of parallelization, sterility issues and time-consuming protocols are some constraints that contribute against its translation. Due to its column-based system, MACS is able to separate cells at a much faster rate with possibility for parallel operation and is compatible with cGMP guidelines. Closed versions of MACS (e.g. CliniMACS Plus® by Miltenyi Biotec and CTS™ DynaMag™ by ThermoFisher) have been developed for clinical scale cell isolation[207,208]. Nevertheless, lack of bead detachment from cells after isolation is a significant drawback for MACS as a CGT bioprocessing unit. Besides particle contamination during the production process, epitope restrain by antibody-magnetic particle complexes can affect cell performance and undermine therapeutic value.

Interestingly, both techniques are complementary and therefore selection of cell sorting technique is application-dependent. Still, for CGT process development, there is a clear tendency towards MACS due to previously mentioned arguments. Recently, efforts have been made by both sides to overcome their limitations.

New platforms for FACS that include disposable microfluidic cartridges provide optimism for its adaptation into production pipelines. WOLF (NanoCellect Biomedical) and On-chip Sort (On-chip Biotechnologies) are two cell sorters that use this concept to overcome typical FACS limitations. The microfluidic cartridges allow for a closed circuit that includes the optical path and sterile sorting containers, minimizing contamination risks. Still, these systems have intrinsically low sorting rates that combined with demanding clinical cell dose targets make their use unrealistic[205]. Development of the MACSQuant Tyto (Miltenyi Biotec) system has been the latest contribution towards FACS adoption into the cell therapy bioproduction process. With sorting speeds reaching 30 000 cells/sec, MACSQuant Tyto outmaneuvers its microchip competitors by a factor of 100[205]. Although not possessing an established clinical platform, vortex actuated cell sorting (VACS) has come forward as a potential challenger for MACSQuant

Tyto. This technology uses the same principles for cell sorting as FACS but possesses a different sorting mechanism. The valves or deflection plates used to separate distinctive cell populations are substituted by a microfluidic thermal vapor bubble actuator that deflects cells due to the formation of an inertial vortex in the flow. Designed by Cellular Highways, the prototype sorter named Highway 1 is currently being developed, with sorting rates reaching 43 000 cells/sec. It combines full automation with closed circuits, possibility for multiplexing and a respectable sorting speed[209].

On the other hand, strategies for MACS improvement regarding disruption of cell-magnetic particle complexes have also been explored, focusing on the interaction between antibody and magnetic particle. ThermoFisher's Dynabeads® FlowComp™ combine streptavidin coated beads with biotin conjugated antibodies, enabling a post-isolation bead removal mechanism[210]. STEMCELL Technologies established their own product, termed Releasable RapidSpheres™, that possess a tetrameric antibody complex which assures cell and particle interaction[211]. Following cell isolation, a mild dissociation agent cleaves the tetrameric complex, releasing the magnetic particles. Successful particle removal will also help alleviate regulatory issues over end product safety. Consequences of nano and microparticle contaminations are still debatable, with magnetic bead internalization being a validated concern.

Instead of improving existing techniques, novel approaches for affinity-based cell isolation have also been investigated. Since cell therapies possess more stringent safety criteria, delivering cells without any by-products due to bioprocessing is crucial. Therefore, antibody removal after affinity separation is of considerable interest. Traceless affinity cell selection (Fab-TACS®) is an innovative technology that explores a reversible antibody-antigen interaction. Antigen-binding fragments (Fab) are combined with a short peptide tag (Strep-tag®II) with significant affinity towards a derivative of streptavidin (Strep-Tactin®). By having a Strep-Tactin® coated agarose matrix, desired cells are retained in a Fab-TACS® column[212]. Using biotin analogs, cells are eluted from the column due to interaction competition. Since the antibody fragments have low affinity towards the selected antigen, Fab release occurs, leaving the isolated cells without any separation by-product or trace. This technology has been translated into an automated commercial device (FABian® by IBA Lifesciences)[212].

A combinatorial approach for cell isolation has been explored by Akadeum Life Sciences. Instead of improving or developing new techniques, a new method has been devised that brings centrifugation and affinity-based separation together. Buoyancy-activated cell sorting (BACS™) brings several above-mentioned concepts together in a novel manner[213]. Biotinylated antibodies are introduced in a cell suspension to target undesired cells (negative selection). Glass-shelled microbubbles coated with streptavidin are mixed to capture antibody-tagged cells. These microbubbles are separated from the remaining cells populations through centrifugation by flotation.

Isolation of a target cell population can have different impact depending on a specific cell therapy, with products ranging from bulk and heterogeneous populations to very selective subpopulations with a defined phenotype. Adequate selection of a separation method is also dependent on the prioritization of opposing purification concepts, such as purity and recovery.

I.6.2. *Scalable Culture Vessels*

After successful isolation, cell populations of interest need to undergo manipulation, requiring appropriate cell culture vessels and systems. Scalability is of utmost importance in CGT, since patient coverage is ever-growing and costly development needs cost-effective means of increasing production when necessary.

In terms of complexity, at the rear-end of cell culture technology are simple plasticware containers. Petri dishes, T-flasks, roller bottles and multiwell plates all incorporate cell culture plasticware and are typically made of polystyrene that is previously treated either chemically or physically in order to gain hydrophilic functional groups (e.g. ketones, aldehydes, hydroxyl and carboxyl groups)[214]. Indeed, surface treatment has a dramatic impact on adherent and non-adherent cell culture. For HSPC expansion, use of zwitterionic hydrogels was deemed a clean slate for HSPC proliferation, removing adverse side effects of cultureware contact and being partially responsible for the impressive results observed[161]. For adherent cells, unfortunately, when using culture media without animal components, cell adhesion can be compromised due to deficiency in serum-derived adhesion factors[215]. Commercial enhanced plasma treatment plasticware (e.g. CellBIND® by Corning Life Sciences) and xeno-free surface coatings (e.g. CELLstart™ by ThermoFisher Scientific and Synthemax® by Corning Life Sciences) have been developed to address this issue[216,217].

Besides allowing gas exchange through the cap region and having excellent optical clarity, commonly used vessels are seriously limited regarding any type of monitoring and control. Conventional plasticware as culture flasks also lack an agitation mechanism, not being able to assure fully homogenized cell cultures. Since their design was directed mainly towards research purposes, manufacturers quickly identified scalability issues for large-scale production. Advanced and scalable culture systems based on plasticware were created to avoid laborious and unsustainable scale-out.

Although very simplistic, plastic malleable bags have a consolidated place in cell culture. Being integrated in basic plasticware, they offer a simple closed system solution which is critical for manufacturing under cGMP. However, lack of any culture control and poor agitation severely limit their application in optimized processes. Nevertheless, therapies based on hematopoietic cells (e.g. HSPC, Tumor-infiltrating lymphocytes, CAR-T) have relied on these platforms for cell culture, reaching human use in clinical

trials [218–220]. Notably, Omisirge has been described to be produced in these cell culture bags[221].

Roller bottles have also been optimized for large scale manufacturing of cells. Cord blood-derived MNC were isolated and expanded in multiple 500 mL roller bottles with rotation assured by a bottle roller[222]. Further improvement led to the design of RollerCell™ by Cellon, a system capable of simultaneously holding 40 roller bottles with automated robotic processors for cell handling. RollerCell™ comparison with CellCube® (a perfusion-based multi-layered polystyrene plates) for cell line production yielded similar results[223].

Although planar systems have evolved to closed and scalable systems, bioreactors have been the ultimate objective for cell therapy manufacturing, seeing that they incorporate monitoring and control, reduce process footprint and minimize cell handling. Incorporating highlighted challenges of a cell-centered process requires platforms capable of dealing with parameter complexity to deliver a safe and reproducible cell-based product. Innovative bioreactor designs have come forward to challenge more classical versions.

Stirred tank bioreactors maintain widespread use, with their simpler and more standardized geometry. With extensive experience in what concerns the production of traditional biopharmaceuticals, much knowledge regarding these bioreactors has been transposed to cell-based therapies. These systems have mechanical impellers that are responsible for appropriate mixing and assuring dynamic flow. High compatibility with monitoring probes and respective modules has made culture control an intrinsic part of this bioreactor. Internal sparging mechanisms allow for efficient gas transfer, although shear stress associated with bubbling can be an issue to sensitive cells[224]. Exhaustive knowledge on fluid profiles based on computational fluid dynamics (CFD) models have given significant predictive control on culture estimates. While being naturally prone for suspension cultures, adherent cell culture has been adapted through microcarrier development[225]. These spherical particles provide the surface area for cell adhesion to occur. A broad variety of materials, porosity levels and surface coatings have been developed to fulfil specific cell needs. The high variety of microcarriers has been extensively reviewed[226,227]. Clinical-grade expansion of MSC of different human sources (i.e. BM and AT) in scalable microcarrier-based bioreactors using S/XF culture components has been achieved[228]. The scalability potential of stirred tank bioreactors for cell-based therapies has been embodied by development of MSC expansion processes. Sscalability of stirred tank MSC culture was pushed forward by successfully expanding human MSC in a 50-L bioreactor, being able to produce 177 clinical doses (70 million cells/patient assuming a 70 Kg patient) in a single run[229]. Consequently, both adherent and suspension cultures are firmly established for cell culture in stirred tank bioreactors.

Cells are known to be shear sensitive which stimulated efforts to develop non-abrasive environments during cell culture. Packed bed bioreactors provide a fixed chamber where microcarriers or scaffolds are located, being an attractive choice for co-culture systems[230]. Adhered cells that populate the chamber have translational movements restricted, thus being able to better mimic solid tissue presence. Their constrained movement also promotes structured organization and cell-cell interaction, leading to high density cultures. Low velocity fluid flow guarantees dynamic culture without causing shear damage to cells. Culture medium has access to the chamber providing necessary nutrients and removing metabolites. Diffusion limitations or nutrient deficiency can occur due to 3D culture organization. Furthermore, significant cellular organization can result in beneficial biological outcomes, but will normally complicate cell extraction and subsequent downstream processes. Expansion of MSC in a 2,5 L CelliGen® bioreactor (New Brunswick Scientific) with Fibra-Cel® (Eppendorf) disks demonstrated large-scale manufacturing potential for packed bed bioreactors[231]. Co-culture of HSPC with human primary stromal cells immobilized in porous glass carriers was successfully adapted to a packed bed bioreactor[232].

Increasing available area for cell culture while protecting cells from harsh conditions, has inspired innovative bioreactor designs. Hollow fiber bioreactors fulfill those requirements by joining thousands of hollow fibers. These fibers are made of thin and porous material that provide a selective passage of nutrients. Culture medium recirculates through the fibers producing interesting tangential flow, mimicking vasculature to some extent[230]. However, significant quantity of fibers originates successive diffusion barriers that cause concentration gradients for nutrients, signaling factors or gases. Similar to packed bed bioreactors, cell extraction processes are challenging to perform due to high cell interaction and difficulty in reaching cells uniformly inside the bioreactor. These bioreactors have been validated with adherent AT MSC, MSC(M), periosteum-derived MSC and neural stem cells[233–237]. Furthermore, recent application of HSPC expansion in a hollow fiber bioreactor demonstrates its potential to impact CGT that use expanded HSPC[154].

With unprecedented tight regulatory measures, the field of bioreactors has moved towards disposable and single-use versions. In order to avoid clean-in-place (CIP) and steam-in-place (SIP) procedures and assure contamination-free product quality, conventional stainless steel or other reusable bioreactors are being substituted by plastic single-use bioreactors (SUB). They reduce cross-contamination and can be combined with limited monitoring probes. Disposable technology has been able to successfully adapt existing geometries, such as the Mobius series by EMD Millipore for stirred tank bioreactors and the Quantum® bioreactor by Terumo BCT for hollow fiber bioreactors. However, other designs, such as the wave bioreactor and the Vertical-Wheel™ bioreactor, have also shown that there is space for bioreactor innovation that

integrate single-use technology. An overview of SUB and their applicability towards cell therapy has been investigated[238]. Their versatility and single-use nature align with cost reduction and demanding regulatory guidelines associated with cell therapies. However, culture monitoring remains a challenge and long-term bag stability must be assured.

Numerous bioreactor designs exist for performing cell culture, nevertheless selecting the correct culture vessel with an appropriate scalability strategy is the actual challenge for the manufacture of cell therapies. Achieving parallelization of individual units (scale-out) tends to be more associated with autologous therapies, while increasing bioreactor size and maintaining culture conditions (scale-up) is more adequate for an allogeneic production. A compromise between scalability and optimal culture conditions is deemed necessary.

I.6.3. *Downstream Processing*

For traditional biopharmaceuticals, cellular contribution ends after upstream processing, where cells are taken advantage of as miniature factories to produce a desired product. Downstream units from cell-centered bioprocesses have an unprecedented challenge in trying to design purification methods that give special care to cell sensitivity without changing cell identity and potency. Fortunately, cell separation is a common practice in research, thus manufacturing units can try to scale existing technology or develop entirely novel techniques. The same techniques mentioned in the previous cell isolation section are also valid for downstream processing.

After upstream manipulation, cells must be harvested from their respective vessels to proceed to downstream processing. While cells grown in single cell suspensions can be easily recovered, adherent cells require surface detaching techniques. Enzymatic methods disrupt cell-surface interactions by causing proteolytic cleavage of integrins, which are proteins responsible for cell adhesion and contribute to cell signaling by transducing ECM stimuli[239]. While damaging integrins can affect cell phenotype or function, enzymatic detachment of cells is common in cell-related processes[240–243], with possibilities varying between Trypsin-EDTA, TrypLE™ and Accutase™. In order to avoid disrupting cell phenotype, approaches focused on reversible adherence to microcarriers have been pursued.

Considering that many cell therapies will be administered intravenously, the presence of particulates or intact microcarriers into the final cell product represents a major safety risk[244]. In this context, different technologies have emerged that may address this concern. For instances, Advanced Corning® Dissolvable Microcarriers (Corning Life Sciences) have been developed to facilitate adherent cell harvesting. These carriers are comprised of polygalacturonic acid chains cross-linked by calcium ions, which can be

dissolved with exposure to ethylenediamine tetraacetic acid (EDTA) and pectinase. iPSC expanded in a Vertical-Wheel™ bioreactor were successfully extracted from dissolvable microcarriers[245].

Considering their different size and density, cell-carrier separation has been explored by filtration or centrifugation techniques. These selected approaches must be compatible with manufacturing processes of considerate scale, while respecting cell sensitivity. Dead-end filtration represents the scalable version for small scale mesh filters, with commercial versions (Opticap® series by Merck Millipore) being applied for efficient separation of MSC from respective microcarriers after cell expansion and detachment[246]. In order to avoid fouling and membrane clogging associated with normal flow filtration, tangential flow filtration (TFF) might be an improved alternative for such separation. Hollow fibers (developed by Repligen or GE Healthcare) allow for separation with less pressure due to feed flow occurring tangential to the membrane. Being reliant on pressure for separation, filtration methods can cause cellular stress. Therefore, centrifugation techniques are a suitable alternative for such separations. Aforementioned counterflow centrifugation or fluidized bed centrifugation minimize shear stress during cell separation and can also be implemented for downstream purposes[247]. However, the more demanding volume scale might limit application of previously described instruments. kSep systems developed by Sartorius explore the same centrifugation principles, having been designed to be able to process larger volumes and also allow for continuous cell isolation[248].

At this point, both adherent or suspension cells converge in their respective downstream pipeline, requiring concentration and washing units before entering the formulation and filling stage. Fortunately, reducing volume possesses coincident methods with cell-carrier separation. Previously mentioned TFF or counterflow centrifugation are both viable options for concentration. TFF implementation for MSC concentration after microcarrier detachment and clarification was studied with a systematic breakdown of hollow fiber characteristics[246] (i.e. material and pore size) and filtration operation modes[249].

Although downstream stages appear to be dominated by filtration and centrifugation processes, disruptive separation mechanisms are being explored for cell therapy manufacturing applications. FloDesign Sonics has harnessed acoustic waves to influence cell movement[250]. Using acoustophoresis, cells are restrained in produced acoustic waves, which allows for washing and volume reduction without negatively affecting cells. Ekko represents a continuous, closed and scalable platform that has been commercially developed by FloDesign Sonics for cell therapy manufacture.

Downstream flowcharts for cell therapy manufacturing vary between adherent and suspension cultures. Still, the limited amount of approaches for downstream processing is a critical issue for cell therapy manufacturing.

I.6.4. *Formulation and storage*

When purified cells are compliant with quality control objectives, their formulation and filling is required for commercialization. Transport of CGT is much more demanding than conventional biopharmaceuticals. For minimally manipulated therapies, such as transplants, cells are delivered fresh in cold storage. Autologous products can follow similar formulation and filling principles, since their shelf-life is typically low. However, allogeneic cell therapies that serve a one-fit-all business model, depend heavily on cryopreservation methods. Logistically, cryopreserved products are a burden as specialized infrastructure and equipment are necessary for handling and transport.

Moreover, cryopreservation processes are prone to inflict cell damage through multiple mechanisms[251]. These include abrupt temperature changes and unwanted thermal fluctuations. Therefore, appropriate cooling rates and temperature maintenance are important parameters for a successful cryopreservation. Cell injury can be associated with extracellular and intracellular ice formation. In order to prevent ice formation, crypoprotectants are usually added to cryopreserved suspensions. However, cryoprotectants can also be toxic to cells. Finally, cells are also subject to thawing injury, as a result of intracellular recrystallization.

In order to minimize cryopreservation-induced cell damage and enhance product reproducibility, automated and quantitative tools can be used for cryopreservation and thawing[252]. Programmable controlled rate freezers (CRFs) employing liquid nitrogen as a refrigerant offer greater control and customizability of cooling rates. New freezing systems that do not require liquid nitrogen have recently emerged such as the Asymptote VIA Quad, Duo, and Research freezers[252]. These are suitable for GMP cleanroom facilities where the use of liquid nitrogen tanks leads to risks in terms of contamination and air quality.

Automated dry-thawing devices can eliminate the risks associated with manual thawing in a water bath, such as water-borne contaminants and operator variability[252]. Examples of this technology include the Asymptote VIA Thaw SC2 and CB1000, the Biocision ThawSTAR, Medcision ThawCB, and Sarstedt Sahara.

To some extent, it might be desirable to avoid cryopreservation at all, either to prevent cryo-induced cell damage, or to circumvent laborious and expensive freeze and thawing procedures. Storage at 2-8°C can be sufficient, especially in situations that only require short-term storage. Specialized hypothermic storage media such as HypoThermosol (BioLife Solutions) allow an increased product stability at hypothermic temperatures (e.g. 2-8°C), avoiding the need for cryopreservation procedures[253]. In 2012, TiGenix completed the first phase I clinical trial with MSC from AT (MSC(AT)) (i.e. Alofisel) stored and administered in HypoThermosol (NCT01743222)[254].

An innovative technique has been developed that could have major implications on tissue and cell preservation. Osiris Therapeutics has designed a lyophilization technology (Prestige Lyotechnology) to preserve living cells and tissue. A proof-of-concept was performed with placental tissue, which can be used as biological dressings for treatment of burns and deep wounds[255]. Lyophilized tissue was compared directly with cryopreserved samples concerning cell viability, ECM components and tissue organization, showing comparable results. Lyopreservation of cells has major consequences, as lyophilized samples can be stored at room temperature without the need for expensive cryopreservation equipment. For cell therapy manufacturing, this breakthrough might imply considerable cost reductions, with deep structural changes to formulation and filling.

I.7. Improving Therapy Viability – Manufacture, Cost and Quality

With CGT reaching unmatched complexity, heavy investment is required for their development. This allied with abovementioned manufacturing challenges and lack of full control over cells as dynamic systems, exposes many threats to CGT viability[182]. Fortunately, steps can be taken to mitigate those threats and improve therapy viability and sustainability.

I.7.1. *Culture Monitoring*

Monitoring of culture conditions is essential in any cell manufacturing process. An ideal continuous gathering of information from every bioprocess stage would allow for real-time informed decision making, complete control and oversight, extensive knowledge of the whole manufacture process and model estimation with response simulation. Naturally, any cell therapy manufacturing process would hugely benefit from such observational power, especially due to inherent complexity of being based on living organisms. The dynamic nature of cells is a significant source of instability for process control.

Monitoring has been exposed to ever increasing difficulties associated with more advanced processes and products. Cell therapies has turned the spotlight towards cells and monitoring has not been able to fully respond to newfound needs. However, regulatory agencies have implemented guidelines in order to stimulate the improvement of monitoring tools, establishing the process analytical technology (PAT) framework[256,257]. It highly recommends design, incorporation and control of innovative analytical tools for continuous improvement of cell therapy manufacturing. In order to ensure product quality and facilitate monitoring variable selection strategies and prioritization, critical process parameters (CPP) must be identified and closely followed.

As previously mentioned, cell therapies possess conventional physicochemical process parameters (e.g. pH, temperature and agitation speed). Nevertheless, introduction of cells has brought a significant amount of unprecedented process parameters, whose nature revolves around cellular-based concepts. For a cellular product, assurance of cell viability and cellular fitness involves controlling a microenvironment based on complex nutrient formulations and dissolved gas concentrations. Besides parameters related with cellular well-being, complexity in cell therapy production monitoring is associated with information on cell state, including phenotype and functionality. Identity of a cell population during production must meet desired standards and quality control, thus surface marker expression, transcriptomics and metabolic profile are also important monitoring targets. Concisely, having cells as therapeutic products has considerably extended the list of CPP in both length and complexity, forcing PAT to advance and to try to develop novel tools at an unprecedented and unmanageable rate.

With the identification of process parameters present in cell therapy production that can be difficult to measure, versatility in monitoring might facilitate early development of new PAT tools. Measurement of process parameters should preferably be performed *in situ*, avoiding lag phases and delays in information gathering that can endanger the whole bioprocess[258]. By measuring directly inside the manufacturing unit, these sensors provide real-time data and do not compromise the sterility barrier. However, another possibility includes online measurement, which requires sample displacement and return to the unit through a by-pass mechanism, but also maintains vessel sterility.

For techniques that have not been developed for *in situ* integration, off-line and at-line monitoring are possible alternatives. These require destructive sampling accoupled with external sample preparation and analysis. The difference between both is related with the distance of the assay equipment, with at-line having the advantage of close proximity to the respective manufacturing unit. Consequently, any process control with these monitoring strategies will be performed in retrospective with delayed information.

Currently, cell therapy manufacturing possesses process parameters with different kinds of monitoring methods. Nevertheless, advancement of PAT aspires for universal *in situ* monitoring.

Conventional CPP have monitoring techniques that have existed for several decades. The lack of modernization associated with industry resistance in applying PAT advancements has crippled much needed innovation in cell therapy manufacturing. Instead of having monitoring development accompany efforts in making standard bioprocessing units cell-centered, manufacturers have paradoxically opposed it[259]. This is clearly evident for traditional univariable parameters, whose monitoring is based on outdated techniques.

Historically, pH and dissolved oxygen (DO) tracking is performed using electrochemical sensors[260,261]. Fortunately, advancements in optical fibers have made it possible to follow

pH and DO without the need of electrochemical probes. Optical sensors are able to quantify these parameters through the presence of indicator or fluorescent dyes[262]. Continuous optical monitoring of pH in a perfusion bioreactor for a baby hamster kidney (BHK-21) cell culture was achieved using phenol red as an indicator[263]. Additionally, instead of having bulk media constituents as indicators, dye adsorption on a solid matrix combined with patch technology has originated viable products and systems for cell culture during manufacture (e.g. Optical pH and DO sensors by PreSens Precision Sensing GmbH or Ocean Optics). Optical patch sensors were used to monitor pH and DO in a high-throughput system for simultaneous operation of 12 bioreactors[264]. Versatility, easy implementation and miniaturization potential of patch sensors have also been exploited in disposable culture technology. Single-use bioreactors, such as BIOSTAT STR® produced by Sartorius, have integrated patch sensors for both DO and pH. This system has been used for scalability studies on AT MSC expansion using microcarriers in a stirred bioreactor[265]. Although optical sensors exhibit great adaptability and allow for continuous external monitoring, their dyes are vulnerable to photobleaching. Nevertheless, a comparison between electrochemical and optical pH and DO sensors highlighted considerable correlation between parameter measurements, easing concerns regarding lesser robustness of optical sensors[266].

Cell-related CPP demand pioneering approaches and instruments that are capable of following complex and multivariate data. For certain parameters it would be impossible to individually follow each specific component in a parallel manner. Cell OMICS techniques (e.g. transcriptomics) are an interesting option that provide a widespread perspective on cell state. Spectroscopy is an attractive technique to address multi-parametric needs since a broad range of wavelengths can be covered[262]. Additionally, electromagnetic radiation interacts with any type of matter, which makes spectroscopy also applicable to biological parameters[258]. Partition of this wide-reaching field originates multiple techniques, with several being adapted as PAT tools for monitoring. Ultraviolet (UV)/visible spectroscopy focuses on consequences of sample or analyte excitation through a UV or visible light source. Information for cell-based bioprocessing monitoring can be retrieved by observing two different radiation phenomena, namely scattering and absorption. Measurement of light absorption through a specific pathlength is the basis for optical density (OD) and absorbance techniques[258]. Although restricted to suspension cultures, medium turbidity can be correlated with cell concentration. Furthermore, significant absorption targets for this range of the spectrum include aromatic molecules, such as fluorophores, chromophores and aromatic amino acids. The latter can be extremely useful for protein quantification. Quality of cytokines used in medium supplementation can be certified using this technique.

Moving to higher wavelengths in the spectral window leads to infrared (IR) spectroscopy. Lower energy radiation associated with IR spectroscopy affects the

vibrational states of molecules. Fortunately, each molecule after excitation emits its own unique radiation fingerprint[258]. Spectral monitoring of culture media allows for multiple quantification of culture medium components and metabolic by-products in a non-invasive manner. Unfortunately, water molecules present can also interfere with data acquisition. Deconstruction of these measured spectra are necessary to distinguish between individual analytes[267]. Thus, there is a significant dependence on chemometric algorithms to unravel incoming data. An *in situ* near infrared spectroscopy probe was validated in determining analyte concentrations in a CHO-K1 cell culture[268]. Fourier transform infrared (FTIR) spectrometers are a third generation of instruments to reach the field of IR spectroscopy. With a higher signal-to-noise ratio, this technique has also been successfully used to follow MSC osteogenic differentiation and the metabolic profile of MSC expanded on microcarriers in a XF culture system[269,270].

Molecular vibrational interactions are also responsible for originating Raman spectroscopy. This technique is based on sporadic inelastic scattering of incident light. In contrast to IR spectroscopy, it is less affected by water interference and therefore substantial focus is being given to Raman spectroscopy[258]. This method combines possibility for versatile *in situ* probes, continuous and non-invasive real-time monitoring, sensitivity for most culture components and a high signal-to-noise ratio. Cellular events aside from proliferation are also potential targets for Raman spectroscopy, with differentiation of adipose-derived MSC in multiple lineages being followed with an *in situ* probe[271].

Radiation-based monitoring strategies have an extensive application potential and have unquestionably expanded monitoring capabilities. Further spectroscopy techniques that have been explored as PAT tools include fluorescence spectroscopy and dielectric spectroscopy[272]. *In situ* probes based on the latter (e.g. iBiomass by Fogale Biotech and Incyte by Hamilton) have been developed for cell density measurements and are compatible with microcarrier-based cultures[273,274].

With an ever-growing listing of CPP, the demand for techniques or instruments that incorporate multiple culture parameters in an efficient manner is growing. YSI 2950D by YSI is a metabolite analyzer that has been used to simultaneously measure up to 6 different culture parameters using proprietary immobilized enzyme electrodes[275,276]. The leading instrument BioProfile Flex2 by Nova Biomedical has challenged the boundaries of parameter parallelization with monitoring capacity for 16 different parameters, ranging from glucose concentration to cell vialbility[277]. However, these devices do not fulfill in-line monitoring ambitions. In trying to solve this issue, a prototype capsule (PATsule) currently in development has heightened hopes for a real-time multiparametric in-line device[259].

The development of these techniques hopes to give PAT significant observational power, helping assure cell therapy manufacturing needs. The need for PAT

advancement emphasized beforehand has culminated with a momentum in solving this issue. Recently, Raman spectroscopy was employed as a PAT tool in an autologous immunotherapy model for cell therapy bioprocessing[278].

I.7.2. *Cost of Goods*

Feasibility is a key concept concerning cell therapy development. Although possessing great therapeutic potential, cell therapies have inherently complex manufacturing processes that can impact on their commercial viability. The introduction of cells as a therapeutic product has caused a paradigm shift in bioproduction. Every manufacture stage has had difficulties in translating typical manufacturing units to cell-based products. More sophisticated microenvironments during upstream production are necessary when producing cell-based therapies, which can include feeder layers and biomaterial-based scaffolds. During the downstream phase, sensitivity of living cells to typical separation and purification processes demands innovative approaches, which usually are costly. Also, end-stage product transportation cannot yet fully rely on more conventional lyophilization options, since cells still depend either on fresh or cryopreserved storage for transport.

In turn, production has a high risk of becoming exceptionally expensive, leading to an unsustainable commercial product. Even after achieving regulatory approval, recent products have suffered with suspicions against long-term commercial sustainability. CAR-T therapies, such as Yescarta and Kymriah, have battled with health insurers to achieve coverage deals in several countries[279]. In England, its health cost-effectiveness watchdog (NICE) had initially ruled against acceptance of Yescarta into the national healthcare system, claiming £300 000 per patient was an excessive strain on its healthcare budget[280]. However, progress was made when Yescarta-producing Gilead offered a confidential discount on the listed price, leading to the approval of Yescarta for treatment of adult patients with diffuse large B-cell lymphoma[281]. Being potential cures for blood malignancies, their pricing must recognize a less favorable commercial and manufacturing scenario associated with one-time treatments. Additionally, their therapeutic indication has been for cancer patients who have shown resistance to chemotherapy and have ruled out bone marrow transplants. Thus, expected demand for such CGT is relatively low. Every one of these constraints is a threat against reliable commercialization of these potentially life-saving cell therapies.

CAR-T cell therapies are not isolated cases, since approved Alofisel has also suffered from similar concerns. In early 2019, NICE released its final appraisal on this cell-based product, advising against its adoption for treatment of perianal fistulas in adults with non-active or mildly active luminal Crohn's disease[282]. Although possessing very promising clinical trial results with 50% of patients treated with Alofisel during its Phase

3 trial showing fistula remission[283], lack of long-term remission studies has raised suspicions on the durability of its treatment benefit. Consequently, the proposed therapeutic value of Alofisel reflected in its pricing (List price – £13 500/vial with one dose consisting in four vials) cannot be assured, leading to rejection of coverage by NICE.

In order to assure the sustainability of approved therapies, with regulatory consent and adoption by healthcare providers, detection of cost reductions at any stage of a cell therapy bioprocess is crucial[284].

Incorporation of cost of goods (COG) analysis allows for a systemic search for cost drivers and should be included during any decision related with the manufacture process[285]. Assessing COG at a preliminary level facilitates process modifications that would become laborious and critically expensive at a later stage. In the case of cell therapies, there are some inherent characteristics that differentiate their production backbone and are responsible for immediate distinctions in the COG analysis approach. Interestingly, cell origin has a profound impact on manufacture, commercialization and business model choice. Production of allogeneic therapies is an economy of scale, which becomes increasingly cost-effective as the demand increases. Aligned with common concerns regarding the need of high cell doses for most cell therapies, donor to patient treatments have a desired production profile. Scale-up allows for reductions of consumable costs and operating labor. However, allogeneic therapies have yet to fully harness the potential for COG reduction of an economy of scale. The abovementioned lack of automation and closed production pipelines for "off-the-self" allogeneic products have been holding these therapies back. Nevertheless, these concerns have been identified and efforts are being made to overcome them. Decisional tools for the manufacture process based on risk management analysis that incorporate COG breakdown have been developed for allogeneic cell-based therapies[286]. Recently, an open source bioprocess economics tool revealed that the Vertical-Wheel™ bioreactor system would allow cost savings in the manufacturing of MSC for cell therapy purposes[287].

Autologous therapies have their own distinct scenario concerning COG. Being patient-specific, each produced lot is restricted to only one patient. Instead of implementing a scale-up strategy, these therapies require parallelization as their manufacturing dogma. This has clear consequences in COG analysis, with single-use modular options becoming more attractive than traditional larger scale production vessels. Furthermore, autologous cell therapies do not follow conventional demand-supply relationships. In this case, demand is simultaneously supply, since the patient possesses the cellular component for its own cell therapy. This significantly reduces any implementation of cost-effectiveness measures due to demand predictability. Although demand can be tracked, increasing cell therapy stock is not possible for autologous therapies, as they

are not an "off-the-shelf" product. In terms of manufacturing facility policy, autologous therapies require prioritized point-of-care. Since cells from the patient are extracted, altered/expanded and reinfused, proximity to the patient is critical. Accordingly, the concept of decentralized facilities for COG reduction in autologous approaches has been explored[288].

Tailored COG analysis models are necessary to accurately reduce costs in autologous and allogeneic therapies. However, there have been attempts to increase cell therapy versatility by changing its cell source requirement. By removing the endogenous T-cell receptor (TCR) from allogeneic T-cells, advances were made towards the creation of a universal CAR-T product[289]. Consequently, an allogeneic COG model was able to be developed for such a cell therapy[290]. Altering the nature of tissue procurement may be a COG solution when trying to convert an unsustainable cell therapy into a commercially available product. Although cell source is able to deeply condition cost drivers due to different production models, other manufacturing parameters also have impact on commercial sustainability. COG optimization should be pursued through the whole bioprocess, even as development advances.

I.7.3. *Quality by Design*

Having cells taking the central role in a therapy has broaden therapeutic angles to tackle innumerous diseases. However, ensuring high quality products with consistency is more challenging for such CGT. The complexity of the cellular component associated with lack of complete comprehension of its machineries demands even more stringent quality measures during manufacture.

After initial proof-of-concept research, bioprocess development must include product quality guidelines to guarantee cellular therapeutic attributes, avoid manufacturing failure and alleviate regulatory concerns regarding safety. Quality assurance in the biopharmaceutical field was introduced by the FDA to tackle alarming waste rates, nonexistence of predictable models and insufficient production control[291]. cGMP were delineated to renew the pharmaceutical sector to address this issue. Quality management of biopharmaceuticals changed with the creation of the Quality by Design model (QbD)[292]. Due to its increasing impact, the FDA and EMA launched a joint pilot program with parallel application assessments in order to harmonize and integrate QbD guidelines[293]. A holistic view of the bioprocess allied with extensive scientific knowledge of each production component and a systematic and iterative method of improvement serve as the basis of QbD (Fig. I-6).

Cell therapies have followed traditional biopharmaceutical development mistakes regarding manufacturing development. Inability to apply QbD and COG analysis has increased manufacturing failures and unsustainable bioprocesses. Translation of

prominent clinical trial results to a scalable and cost-effective bioprocess has led to several letdowns with development suspension and product withdrawal[294,295]. A logical sequence of steps is delineated by QbD in order to advise manufacturers regarding intelligent production pipeline development for cell therapies. Initial guidelines concern the end product, with the identification of therapeutic objectives. These should describe with great detail cut-off goals for concepts such as identity, potency and purity[107]. High degree of clarity and detail in defining end product properties will facilitate identification of critical production processes and problem localization and solving. By creating a quality target product profile (QTPP), the framework for QbD is established.
With the target profile set, the entire process needs to be broken down to identify critical variables that have a direct effect on the QTPP. Raw material attributes (RMA) need to be controlled for quality with selected checkpoints so that variability and lack of quality cannot compromise the bioprocess from the start[292]. After controlling process inputs, continuous monitoring with PAT throughout the entire process should exist to assure correct transformation or manipulation of raw materials into the final product.
Considering that following every possible variable is unrealistic, critical quality attributes (CQA) should be selected. For CGT, these attributes correspond to cellular features. Since living cells are multi-variate systems, isolating inputs (e.g. signaling factors) and controlling outputs (e.g. cell expansion) is not trivial. Knowledge on cell networks is increasing, but a complete map of cellular machinery is still far from reach. Thus, identification of CQA, which are crucial for QbD, can be difficult.
Throughout the bioprocess, each unit has an impact on cells and is accountable for altering their characteristics to some extent. Controlling CQA will depend on identifying which CPP are responsible for changing those same features. Control strategies should build on CPP discovery, which serve as directives for selection of monitoring techniques[292]. The holistic nature of QbD demands whole process overview, with parallel interventions as the production pipeline moves forward. After definition of individual CQA and respective CPP, studying their interactions should follow. By uncovering and exploring networks, process knowledge increases greatly. In turn, reaction to process variability can be achieved quickly and pragmatically by tweaking CPP. Rapid process correction is particularly relevant for cell therapy manufacturing. Even with RMA tightly controlled, cells have inherent complexity that leads to aberrant and unpredictable behavior. Therefore, discerning connections between CQA and CPP will increase process mapping and improve decision making[296].

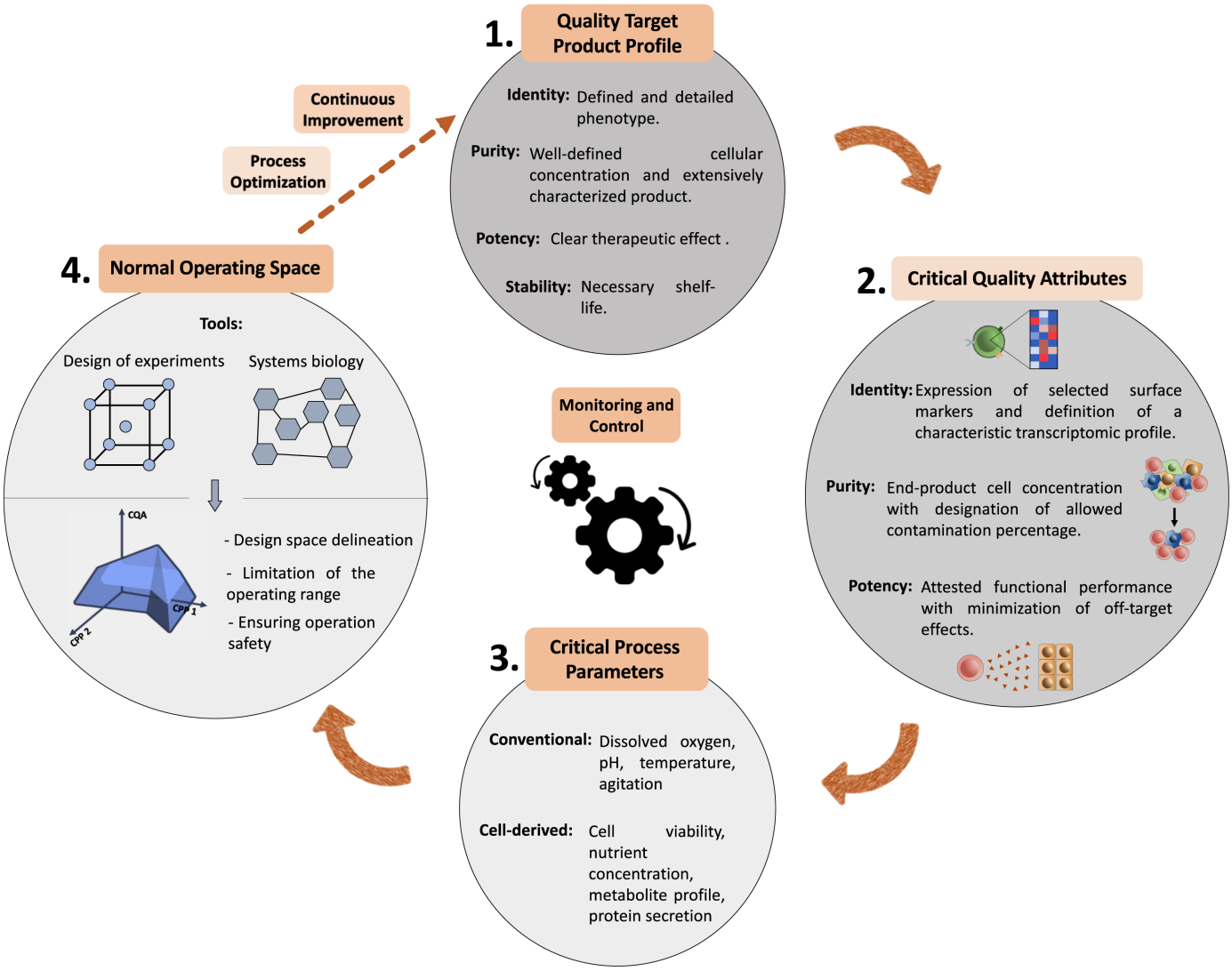

Figure I-6. Quality by design framework. An initial quality target product profile (QTPP) requires defining end product objectives that satisfy therapeutic needs. Translation of these objectives to their cellular features uncovers process critical quality attributes (CQA). In turn, process variables that are responsible for influencing CQA are identified as critical process parameters (CPP). Controlled variation of these parameters originates a normal operating space, which limits process operability. Continuous process monitoring and control facilitates improvement implementation, creating a cycle of process optimization. Adapted from [117].

Interactive effects can be revealed by analyzing a defined design space. The range of variability of CQA caused by fine-tuning of CPP or RMA will define boundaries for a normal operating range in the design space. Working inside the normal operating range admits changes in CPP without compromising end product quality. CQA-CPP connection can be very laborious and difficult to obtain, with a substantial need for

varied experimental data. In order to circumvent excess labor and costly optimizations, design of experiments (DoE) and systems biology are effective tools that originate the same results using up only a fraction of expected time and resources[107,297].

DoE is dedicated to evidencing relationships between input and response variables in an optimized manner. Extensive multivariable exploration inside a selected design window is performed using the least amount of experimental conditions. Factorial design is responsible for generating necessary experimental combinations. Obtained experimental data allows delineation of a response surface for every CPP. These surfaces are described by behavior functions, which model the abovementioned CQA-CPP relationships[298]. Besides enhancing process knowledge, behavior functions enable CPP optimization resulting in CQA improvement. Implementation of DoE has caused process improvements from pluripotent stem cell cultivation to *ex vivo* HSPC expansion[299–301].

Systems biology tools can also contribute to discerning CQA-CPP interactions. OMICS-based techniques, such as gene expression and protein production, can contribute to QTTP review, updating end product identity and potency. Also, metabolic pathways can derive similar information without directly compromising cells. In this context, metabolic by-products were used to construct a fed-batch platform for HSPC expansion in order to avoid inhibitory feedback signaling[151]. Intrinsically, large amounts of generated data can also yield reduced dimension mechanistic models, similar to behavior functions. Overall, the impact of any CPP modifications on CQA can be more easily detected.

Roadmaps for thorough evaluation of cell potency (an important CQA) in CGT are normally lacking. Scarcity of means to measure therapeutic action spreads throughout most CGT, in contrast with traditional pharmaceuticals and biopharmaceuticals[284]. Inherent complexity of living cells as a therapeutic product has made development of functional assays difficult. In many cases, the therapeutic mode of action (MoA), which serves as footing for potency measurements, is partially unknown[302]. In cases where *in vitro* or *in vivo* functional assays are available, they may not be adequate for quality control of cell-based manufacturing. Extensive read-out waiting period, fragile reproducibility or high dependence on operator capability, are some of the concerns that affect these important quality and security checkpoints[302]. Potency assays for CGT are, in general, alarmingly underdeveloped, making manufacturers unable to rigorously track therapeutic cell function.

As QbD requires the combination of extensive fundamental knowledge with engineering principles, applying it to cell therapies is a daunting task. Biological variability is inherent, making standardization and quality control a struggle for any process that includes cells. However, QbD guidelines serve as a backbone for correct cell therapy manufacturing development. Its implementation is critical to any future

bioprocess, assuring quality and robustness throughout each unit. Additionally, continuous improvement associated with QbD brings process evolution to the production pipeline, making it dynamically resistant to unsustainability[107].

I.8. Thesis Aim and Outline

The surge of CGT, with their remarkable level of therapeutic potential, has exposed challenges in their development, clinical approval and manufacturing. Severe therapy funneling during the development lifecycle of CGT and low success rates are vulnerabilities that jeopardize translation of therapeutic value into patient treatment.
Efforts are required to facilitate CGT development, which also suffers from manufacturing inexperience and low compatibility with production knowledge from biologicals. QbD provides a framework to tackle these challenges, pushing for continuous improvement.
Although with extensive experience in the CGT field, approaches based on the manipulation of the hematopoietic system are also crippled by these challenges. While hematological disorders are wide-ranging, providing hematopoietic CGT with more potential targets, few therapy candidates have made the final list of therapeutic products with regulatory approval.
This thesis focuses on the improvement of *ex vivo* expansion of HSPC as a platform for future CGT. Despite being initially developed as a means of increasing coverage of CB-derived HCT, expansion of HSPC can also explore new applications, benefiting from the attractiveness of CB as a source. By aiming for process optimization and innovation, this thesis strives to demonstrate that peak therapeutic potential may still be locked for many CGT.
Chapter I provides setting for the remaining chapters, introducing concepts and offering a comprehensive review of relevant topics. It addresses the presence of the hematopoietic system (its cellular occupants and native environments), development of *ex vivo* expansion of HSPC (including main expansion systems) and CGT manufacturing (with important process units and means to improve).
Chapter II features an optimization of cytokine concentrations used during *ex vivo* expansion of HSPC. With their use being transversal to most expansion systems and similar between them, tailored cytokine cocktails were developed to maximize the capacity of each studied system to promote HSPC expansion.
Chapter III attempts to disrupt the inevitability of cryopreservation for CGT. To avoid cryo-derived cell revitalization, MSC were encapsulated in alginate beads and stored at hypothermic temperatures to test its application for certain CGT storage and distribution scenarios.

Chapter IV tackles the underdeveloped landscape of potency assays and CGT quality control. In order to adequately match the complexity of cells, methods with high dimensionality, namely FTIR and transcriptomics, were explored for discrimination of expanded HSPC populations.

Chapter V identifies the main milestones of each experimental chapter and extrapolates possible avenues of future research that can be built upon results obtained during this thesis.

II. Tailored Cytokine Optimization for *Ex Vivo* Culture Platforms Targeting the Expansion of Human Hematopoietic Stem/Progenitor Cells

This chapter is published as:

Branco, A. *et al*. Tailored Cytokine Optimization fo *Ex Vivo* Culture Platforms Targeting the Expansion of Human Hematopoietic Stem/Progenitor Cells. *Front. Bioeng. Biotechnol.* , **8**, 573282 (2020). https://doi.org/10.3389/fbioe.2020.573282.

II.1. Summary

Umbilical cord blood (CB) has been established as an alternative source for hematopoietic stem/progenitor cells (HSPC) for cell and gene therapies. Limited cell yields of CB units have been tackled with the development of cytokine-based *ex vivo* expansion platforms. To improve the effectiveness of these platforms, namely targeting clinical approval, in this study, we optimized the cytokine cocktails in two clinically relevant expansion platforms for HSPC, a liquid suspension culture system (CS_HSPC) and a co-culture system with MSC(M) (CS_HSPC/MSC). Using a methodology based on experimental design, three different cytokines (stem cell factor (SCF), fms-like tyrosine kinase 3 ligand (Flt-3L) and thrombopoietin (TPO)) were studied in both systems during a 7-day culture under serum-free conditions. Proliferation and colony-forming unit assays, as well as immunophenotypic analysis were performed. Five experimental outputs (fold increase (FI) of total nucleated cells (FC TNC), FC of $CD34^+$ cells, FC of erythroid burst-forming unit (BFU-E), FC of colony-forming unit granulocyte-monocyte (CFU-GM) and FC of multilineage colony-forming unit (CFU-Mix)) were followed as target outputs of the optimization model. The novel optimized cocktails determined herein comprised concentrations of 64, 61 and 80 ng/mL (CS_HSPC) and 90, 82 and 77 ng/mL (CS_HSPC/MSC) for SCF, Flt-3L and TPO, respectively. After cytokine optimization, CS_HSPC and CS_HSPC/MSC were directly compared as platforms. CS_HSPC/MSC outperformed the feeder-free system in 6 of 8 tested experimental measures, displaying superior capability towards increasing the number of hematopoietic cells while maintaining the expression of HSPC markers (i.e. $CD34^+$ and $CD34^+CD90^+$) and multilineage differentiation potential. A tailored approach towards optimization has made it possible to individually maximize cytokine contribution in both studied platforms. Consequently, cocktail optimization has successfully led to an increase in the expansion platform performance, while allowing a rational side-by-side comparison among different platforms and enhancing our knowledge on the impact of cytokine supplementation on the HSPC expansion process.

II.2. Background

Hematopoietic cell transplantation (HCT) continues to be the leading cell therapy for malignant and non-malignant blood-based disorders and advances in this field have expanded the options available for patients concerning graft source. Umbilical cord blood (CB) is an accepted and appealing source of hematopoietic stem/progenitor cells (HSPC) for HCT[303,304]. Compared with bone marrow (BM) or mobilized peripheral blood, CB transplants have shown similar survival outcomes with lower chances of developing graft *vs.* host disease (GVHD) and lesser compatibility issues concerning human

leukocyte antigen (HLA) matching[305,306]. However, low CB volume recovered from births results in an unsatisfactory cell dose for transplants in adults, having initially limited transplants of a single CB unit to pediatric patients[307]. In order to address this problem, *ex vivo* expansion of HSPC has been pursued. By manipulating CB units to increase their cell yield, the drawbacks of single unit transplants (such as increased graft failure and delayed immune reconstitution) can potentially be surpassed[308]. Multiple strategies have been developed towards achieving a successful expansion, with several reaching phase III clinical trial level[309]. Approaches have varied from promoting HSPC expansion with novel small molecules (including StemRegenin-1[310], UM171[175] and nicotinamide[221]), co-culture with mesenchymal stromal cells [128] and induction of Notch signaling pathways[143].

Although different strategies have been explored, HSPC *ex vivo* expansion has always been largely based on the addition of exogenous cytokines[102]. Numerous cytokines have been employed to promote HSPC expansion *ex vivo*, including fms-like tyrosine kinase 3 ligand (Flt-3L), granulocyte colony-stimulating factor (G-CSF), interleukin-3 (IL-3), interleukin-6 (IL-6), stem cell factor (SCF) and thrombopoietin (TPO)[311–313] (reviewed in Costa et al., 2018). However, selection of individual cytokines and their concentrations for an expansion cocktail has differed between existing strategies. Disparity of concentrations can reach 30-fold among similar cytokines included in different expansion protocols[143,314]. Whereas cytokine dosage may vary due to the nature of the expansion approach (e.g. targeted expansion of more primitive self-renewing hematopoietic stem cells compared to expansion of both hematopoietic stem cells and early committed progenitors), a defined and clear optimization rationale concerning cytokine supplementation has been lacking. Ignoring or underestimating optimization opportunities can have a negative impact on existing culture protocols, especially concerning cytokine supplementation. Suboptimal cytokine concentrations can cause underperformance of cell expansion driving misleading conclusions, especially when carrying out comparisons with other competitive strategies. On the other hand, overuse of cytokine supplementation has shown to interfere with HSPC self-renewal and promote unwanted differentiation[315,316]. Moreover, considering their significant cost, these abnormally high cytokine concentrations can also compromise process viability, cost-effectiveness and potential for clinical translation[317,318]. Thus, there is a clear gap in protocol standardization and optimization for current HSPC *ex vivo* expansion platforms.

With the lack of optimized platforms, current evaluation of the performance of various expansion approaches based on their published results might be inaccurate, since these platforms are most likely not performing at their peak production potential. Therefore, improper optimization of cytokine usage can affect decision-making and eventually be responsible for negligent or premature withdrawal of certain expansion approaches

from the clinical approval pipeline. While improving existing expansion platforms, cytokine cocktail optimization will also enable a fair side-by-side comparison of current strategies.

Systematic studies on cytokine use in ex vivo expansion of HSPC will also support platforms towards an effective protocol for clinical applications based on cGMP. Besides highlighting the abovementioned cost reduction opportunities, cytokine optimization will also elucidate on important biological interactions between cytokines and cultured HSPC. The knowledge gathered from this relationship will benefit bioprocess engineering from a future manufacturing line perspective. The understanding of these cytokine requirements will have a direct impact on the feasibility of such a GMP-based expansion protocol, which is a priority for platforms at a clinical trial level[284]. Although an initial focus on the cytokine cocktail existed during the early development of *ex vivo* HSPC expansion protocols, previous attempts to study cytokine influence are mostly based on simple dose-response studies and are outdated[311,316,319–322]. Furthermore, due to major advances in *in vitro* culture of HSPC (e.g. development of serum-free medium formulations), tested culture conditions are inconsistent with expansion strategies presently in clinical trials, making the application of previous optimizations inadequate. With a considerable amount of HSPC expansion strategies in late-stage development, where major changes in the experimental procedure are rare, any cytokine optimization performed at this stage could endure. Thus, existing cytokine variation throughout current CB-based expansion strategies was surveyed (reviewed in [103,323]). Despite some expected variants between strategies, we identified the trio of cytokines SCF, Flt-3L and TPO as the most used cytokine combination in the majority of expansion studies (reviewed in [103]), including those which have progressed to Phase I/II clinical trials (reviewed in [323]). By specifically selecting these three cytokines, we expect to boost the relevance of our study, turning its application more widespread.

Over the last years, we have gathered significant expertise in what concerns the *ex vivo* cultivation of human HSPC by establishing a co-culture system with MSC(M), in order to improve our understanding of the mechanisms underlying the hematopoietic supportive capacity of human MSC[204,324–328]. Having identified the aforementioned gap in the field, we tackled the issue with initial efforts focused on pursuing optimization of our established co-culture platform with MSC(M) using statistical tools, such as design of experiments[301]. Unable to perform feeder-free HSPC expansion with the selected culture conditions, in particular for CB cells[324], our previous optimization study was restricted to a single expansion platform, exclusively performed in a co-culture system with MSC(M).

Using the same statistical approach based on experimental design, in the present study, we have determined unique optimal cytokine cocktails for two different HSPC expansions systems (i.e. HSPC expanded alone in a liquid culture system or co-cultured

with a MSC(M) feeder layer) currently exploited in clinical trials. By enhancing the cytokine contribution for each platform, we were able to level the field and perform a rational and pragmatic comparative study between both systems (liquid suspension culture versus co-culture). By optimizing the established expansion platforms, we have reached a durable optimal cytokine cocktail to hopefully endure and facilitate the road to regulatory approval of a viable cell product based on expanded CB-derived HSPC. Furthermore, by expanding HSPC from cryopreserved CB MNC, we have made our optimization more reliable and applicable to the manufacturing scenario. Indeed, upon collection, CB units are routinely kept cryopreserved in public/private banks worldwide. Also, we have shown that tailored cytokine optimization should be used as a tool to enable unbiased evaluation of existing strategies, rationally impacting the highly competitive field of ex vivo expansion of HSPC, namely (but not limited to) CB-derived.

II.3. Methods

II.3.1. *Human Tissues*

CB units and BM samples were secured through collaboration agreements between Institute for Bioengineering and Biosciences (iBB) at Instituto Superior Técnico (Lisbon), Hospital São Francisco Xavier from Centro Hospitalar de Lisboa Ocidental (Lisbon) and Instituto Português de Oncologia Francisco Gentil (Lisbon), respectively. Both CB and BM samples were obtained from healthy donors and with informed consent following the Directive 2004/23/EC of the European Parliament and of the Council of 31st of March 2004 on setting standards of quality and safety for the donation, procurement, testing, processing, preservation, storage and distribution of human tissues and cells, represented in the legal framework of Portuguese legislation by Law n°22/2007 of 29th of June.

II.3.2. *CB Mononuclear Cell (MNC(CB)) Isolation*

CB was removed from collection bags and diluted with phosphate buffer saline (PBS) (Sigma-Aldrich) supplemented with 2 mM ethylenediamine tetraacetic acid (EDTA) (Sigma-Aldrich). To isolate MNC(CB) by density gradient centrifugation, diluted CB was carefully layered on top of a solution of Ficoll (GE Healthcare) and centrifuged at 500g for 30 minutes without brakes. After phase separation, MNC ring was carefully aspirated and washed with PBS supplemented with 2 mM EDTA. Removal of contaminating erythrocytes was done by incubating MNC(CB) in a cold solution of ammonium chloride (155 mM) (Sigma-Aldrich) for 10 minutes. Isolated MNC(CB) were cryopreserved in low glucose Dulbecco's Modified Eagle's Medium (DMEM) (Thermo Fisher Scientific)

supplemented with 10% (v/v) fetal bovine serum (FBS) (Thermo Fisher Scientific) and 10% (v/v) dimethyl sulfoxide (DMSO) (Sigma-Aldrich) and stored in the liquid phase of a liquid/vapor phase nitrogen tank.

II.3.3. *$CD34^+$-Enrichment from MNC(CB)*

Cryopreserved MNC(CB) were thawed in DMEM supplemented with 10% (v/v) FBS and 1% (v/v) Antibiotic/Antimycotic (A/A) (Thermo Fisher Scientific) and washed with Magnetic Activated Cell Sorting (MACS) buffer (0.5% (v/v) bovine serum albumin (BSA) and 2 mM EDTA in PBS). CD34 positive selection through MACS was done using the Human CD34 MicroBead Kit (Miltenyi Biotec), according to the manufacturer's instructions.

II.3.4. *Enrichment for $CD34^+$ cells*

Cryopreserved MNC from three CB samples were individually thawed in DMEM + 20% (v/v) FBS and washed with magnetic-activated cell sorting (MACS) buffer. $CD34^+$ HSPC were then isolated using the CD34 MicroBead Kit UltraPure (Cat. #130-100-453, Miltenyi Biotec) through MACS, according to the manufacturer's instructions. In order to attain a highly pure $CD34^+$ cell population (i.e., >98%), cells from the positive fraction were subjected to a second LS MACS column.

II.3.5. *Bone Marrow-Derived MSC (MSC(M)) Feeder Layer (FL) Preparation*

Isolated MSC(M) from BM were obtained from the Stem Cell Engineering Research Lab (SCERG) cell bank at iBB, Instituto Superior Técnico, Lisbon. Cell isolation, expansion, characterization according to ISCT standards and preservation were performed through previously established protocols[329]. A single MSC donor was used to isolate HSPC variability in the study and mimic an allogeneic universal MSC donor. Cryopreserved MSC(M) were thawed and seeded at 3000 cells/cm^2 in DMEM supplemented with 10% (v/v) FBS MSC-qualified (Thermo Fisher Scientific) and 1% (v/v) A/A. After a revitalization passage, MSC(M) were passaged into 12-well plates. After reaching confluence, MSC(M) were growth arrested by Mitomycin C (Sigma) treatment. Cells were incubated with their culture medium supplemented with 0.5 µg/mL Mitomycin C for 2-3 hours. After treatment, inactivated FL were washed three times with culture medium to eliminate any residue of the treatment solution and stored in the incubator with fresh culture medium until further use in co-culture experiments.

II.3.6. *Ex Vivo Expansion of HSPC(CB)*

$CD34^+$-enriched cells were seeded on a 12-well plate at 30 000 cells/mL, using 2 mL of StemSpan™ Serum-free Expansion Medium (SFEM) II (STEMCELL Technologies) per well (60 000 cells/well) supplemented with 1% A/A and defined cytokine cocktails composed of SCF, Flt-3L and TPO (PeproTech), with concentrations ranging between 0-100 ng/mL. Basic fibroblast growth factor (bFGF) (PeproTech) was additionally used in all conditions at a concentration of 5 ng/mL to support BM feeder layer cells during the co-culture experiments[301]. HSPC expansion was performed during 7 days at 37°C and 5% CO_2. For co-culture expansion, MSC culture medium was removed from growth arrested FL and $CD34^+$-enriched cells were carefully seeded on top.

II.3.7. *Proliferation Assay*

After 7 days, adherent and non-adherent expanded HSPC were harvested with forced pipetting (with extra care for co-cultures to avoid lifting the MSC(M) feeder layer). Total nucleated cell (TNC) number was determined with the Trypan Blue (Thermo Fisher Scientific) exclusion method. Fold change (FC) in TNC was calculated by dividing the number of expanded cells by those initially seeded (i.e. 60 000 cells).

II.3.8. *Colony-Forming Unit (CFU) Assay*

A clonogenic assay was used to evaluate HPSC potential to originate colonies and differentiate into different myeloid lineages. 1000 $CD34^+$-enriched cells (day 0) or 2500 expanded HSPC (day 7) were suspended in 100 µL PBS and then carefully mixed with 2 mL MethoCult™ Classic medium (STEMCELL Technologies). Prepared cell suspension was split into three wells of a 24-well plate and incubated for 14 days at 37°C and 5% CO_2 in a humidified atmosphere. At the end of the assay, formed colonies were manually classified as multi-lineage colony-forming unit (CFU-Mix), burst-forming unit erythroid (BFU-E) and colony-forming unit granulocyte-macrophage (CFU-GM) and counted with a brightfield microscope (Olympus CK40). Colony number was calculated by dividing colony counts by the number of seeded cells and multiplying by the number freshly isolated (i.e. 60 000 cells) or expanded HSPC(CB). FC in colony number was determined by dividing the colony number after expansion (day 7) by the colony number before expansion (day 0).

II.3.9. *Cobblestone Area Forming-Cells (CAFC) Assay*

As a surrogate for quantification of long-term culture-initiating cells (LTC-IC), a CAFC assay was performed to characterize expanded HSPC(CB). An inactivated murine stromal cell line (MS-5) FL was prepared as described in the abovementioned section for MSC(M). Briefly, MS-5 cells were expanded with DMEM supplemented with 1% A/A

and 10% FBS and seeded in 24-well plates for FL preparation. After reaching confluence, MS-5 cells were treated with 5 µg/mL Mitomycin C for 2-3 hours. 2000 freshly isolated or expanded cells were suspended in MyeloCult™ medium (STEMCELL Technologies) supplemented with 1% A/A and 350 ng/mL of hydrocortisone (STEMCELL Technologies) and seeded on top of inactivated MS-5 FL. Each experimental condition was tested in duplicates and incubated at 37°C and 5% CO_2 in a humidified atmosphere for 14 days. When finished, each well was visually inspected with a phase-contrast microscope (Leica DM3000 B) for the presence of colonies with at least five cells with cobblestone morphology (phase-dim, compact grouped and angular shaped[330]) that migrated beneath the MS-5 FL. Colony number and FC CAFC colonies were calculated similarly to the previous CFU section.

II.3.10. *HSPC(CB) Immunophenotype*

Expression of HSPC identity surface markers was assessed by flow cytometry. Single cell suspensions of HSPC(CB) were washed with PBS and incubated with Far Red Fixable Dead Cell Stain Kit (Thermo Fisher Scientific) at room temperature (RT) for 15 minutes to determine cell viability. Afterwards, cells were surface stained with previously titrated CD90 (5E10) PE (BioLegend) and CD34 (8G12) PerCP-Cy5.5 (BD Biosciences) at RT for 15 minutes. Data acquisition was done on a FACSCalibur™ cytometer (BD Biosciences) and analyzed using FlowJo v10 software (Flowjo LLC).

II.3.11. *Cytokine Experimental Design*

Response surface methodology was applied to optimize cytokine concentrations for *ex vivo* expansion of HSPC [331]. A face-centered central composite (CCF) design was used to select concentrations for three different cytokines (SCF, Flt-3L and TPO), resulting in 17 experimental points. For co-culture expansions, bFGF was present at a constant concentration (5 ng/mL), not being a target for optimization. The tested observational window was limited by a minimum concentration of 0 ng/mL and a maximum of 100 ng/mL, for every cytokine. With defined limits, concentrations were coded to simplify listing of experimental points (lower level (-1) - 0 ng/mL; center level (0) - 50 ng/mL; higher level (1) - 100 ng/mL). The experimental points included three center points in order to gain an estimation of the experimental error. Effect on cytokine variation on FC TNC, FC $CD34^+$ cells, FC BFU-E, FC CFU-GM and FC CFU-Mix was investigated. These outputs were termed response variables (Y_n). Every response variable was measured in a blinded manner, eliminating experimental bias. A second-order polynomial function was suggested to describe and model the experimental data.

Equation II-1. Proposed second-order polynomial function as a behavior function for a specific response variable (Y_n), considering three cytokines (X_1, X_2 and X_3). This model includes an intercept (K), responsible for describing the response variable when no cytokines are present, and three different types of cytokine effects. These include main individual cytokine impact (β_i parameters), interaction between the different cytokines ($\beta_{i\,j}$ parameters) and molecular effects within the same cytokine ($\beta_{i\,i}$ parameters).

$$Y_n = K + \beta_1[X_1] + \beta_2[X_2] + \beta_3[X_3] + \beta_{12}[X_1][X_2] + \beta_{13}[X_1][X_3] + \beta_{23}[X_2][X_3] + \beta_{11}[X_1]^2 + \beta_{22}[X_2]^2 + \beta_{33}[X_3]^2$$

II.3.12. *Optimization Validation*

Determined regressions were validated by comparing predicted values for each response variable with corresponding experimental values of cytokine combinations not included in the original concentration panel. Two different cytokine combinations, the optimized cytokine cocktail and a previously established cocktail (Z9; ([SCF] = 60 ng/mL; [Flt-3L] = 55 ng/mL; [TPO] = 50 ng/mL) from our previous study [301] were chosen to test the applicability of the regressions in its defined experimental design space.

II.3.13. *Statistical Analysis*

Function fitting was performed using a backward stepwise regression. Briefly, all terms were considered in the regression. An iterative F-test on the overall regression was applied. In each step, when the respective p-value was above the stipulated threshold (i.e. 0.05), the least significant parameter was eliminated from the model. This was done repeatedly until the regression itself gained significance. Goodness of fit variables (R-squared, adjusted R-squared and root mean squared error (RMSE) were determined to assess regression quality. Unless stated otherwise, values are presented as the estimated mean and plotted error bars represent the standard error of the mean (SEM).

II.4. Results

Combinations of selected cytokines (SCF, Flt-3L and TPO) were defined using an experimental design approach (Fig. II-1). A CCF design delineated a panel of 17 cytokine combinations, which included three repeated center points to assess intra-donor variability of CB cells (Table 1). Cytokine concentrations were limited to an experimental design window between 0 ng/mL and 100 ng/mL. FC TNC, FC $CD34^+$, FC BFU-E, FC CFU-GM and FC CFU-Mix were chosen as response variables for this

optimization study, acting as measures of cytokine performance. Two different expansion platforms were studied, with HSPC being expanded alone in a liquid culture system (CS_HSCP) or co-cultured with an MSC(M) feeder layer (CS_HSPC/MSC). Response variables were modelled and corresponding regression surfaces were maximized in order to uncover optimized cytokine cocktails for both expansion systems (Fig. II-2). Three independent CB donors of were studied to include biological variability in the model. CB $CD34^{+}$-enriched cells (purity: [82 – 98%]) were expanded in serum-free conditions for 7 days using both expansion strategies.

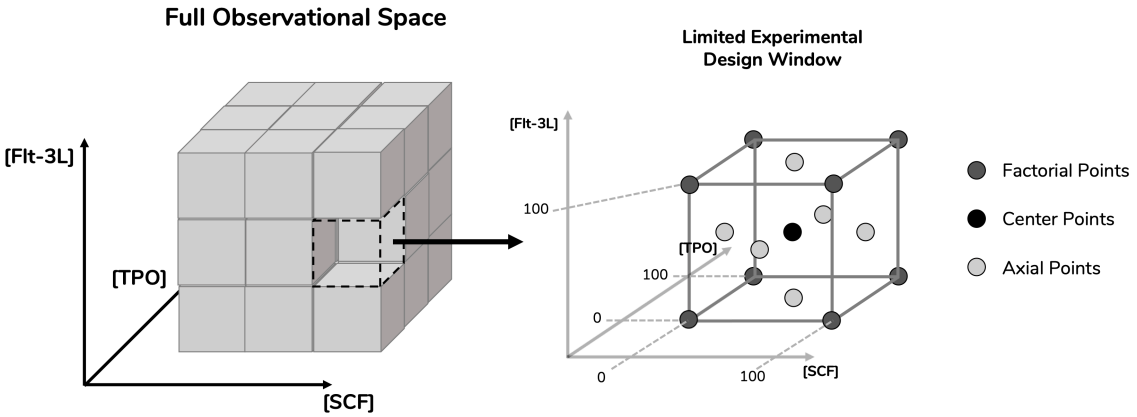

Figure II-1. *Definition of experimental design space for the optimization studies. Surface response methodology requires limitation of parameters in order to study response variables. Concentrations of the cytokines stem cell factor (SCF), fms-related tyrosine kinase 3 ligand (Flt-3L) and thrombopoietin (TPO) were selected as parameters. A limited experimental design window was selected from their full observational space with respective concentration ranges between 0 and 100 ng/mL. By incorporating three levels of dimensionality, the design space gained a cubic geometry. Having defined the design space, a face-centered central composite design was applied, which provided the experimental points necessary in order to reach the response surface. These include center points, axial points (located in the center of the cubic planes) and factorial points (located in the cubic vertices).*

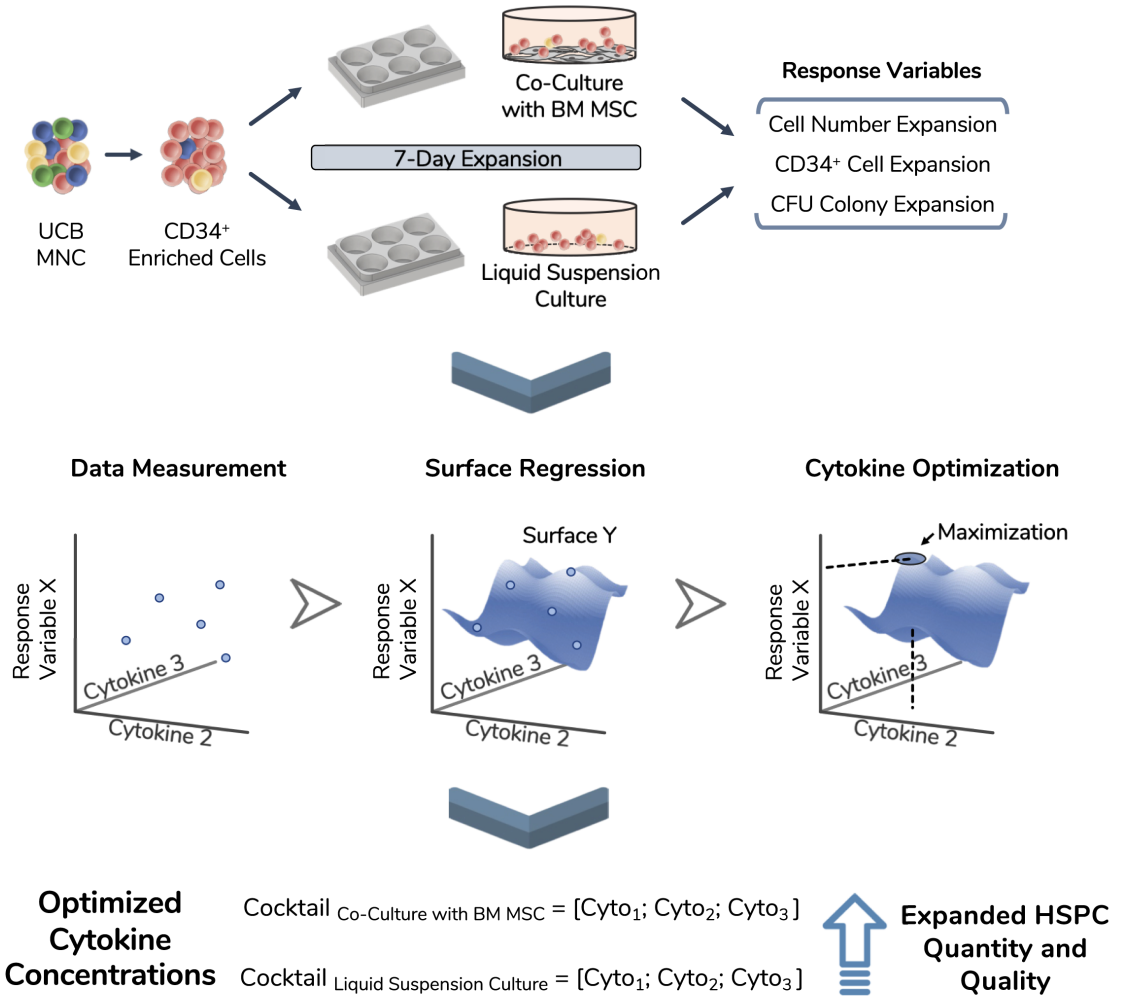

***Figure II-2**. Experimental workflow of the performed optimization. Cord blood (CB) mononuclear cells (MNC) were thawed and enriched for CD34 expression. These isolated cells were used as the starting population in two different expansion systems (i.e. liquid suspension culture and co-culture with bone marrow-derived mesenchymal stromal cells) and expanded during 7 days. Total nucleated cell number, CD34 expressing cell number and CFU readouts were selected for optimization and termed as response variables. Using an experimental design approach, 17 different cytokine combinations were used during expansion runs and response variables were tracked. Experimental data points were modelled, giving rise to unique response surfaces for each expansion system. By locating the surface maximum, each response variable originated an optimized cytokine cocktail, improving the quantity and quality of the expanded cell product.*

Table II-1. *List of cytokine combinations derived from the face-centered central composite (CCF) design. Concentrations values were symbol coded to facilitate identification and combinations were numbered to aid with cocktail recognition. In total, 17 combinations were defined, consisting of 8 factorial points, three repeated center points and 6 axial points. (+) 100 ng/mL; (0) 50 ng/mL; (-) 0 ng/mL.*

Cytokine	Factorial Points								Center Points			Axial Points					
SCF	+	+	+	+	-	-	-	-	0	0	0	0	0	+	-	0	0
Flt-3L	+	+	-	-	+	+	-	-	0	0	0	0	0	0	0	+	-
TPO	+	-	+	-	+	-	+	-	0	0	0	+	-	0	0	0	0
Combination	*1*	*2*	*3*	*4*	*5*	*6*	*7*	*8*	*9*	*10*	*11*	*12*	*13*	*14*	*15*	*16*	*17*

II.4.1. *Response Variable Measurement*

Selected response variables were successfully measured for three independent CB unit donors. FC TNC number fluctuated considerably when expanding cells with the different cytokine combinations of the established panel in both expansion culture systems (coefficient of variation $CV_{CS\_HSPC/MSC}$ = 60 ± 3%; CV_{CS_HSPC} = 76 ± 1%) (Fig. II-3). Taking into account every center point replicate, their low deviation (CV_{Center} = 13 ± 5%) demonstrated reproducibility of the expansion performance, discarding possible experimental error interference. Combinations with an absence of a certain cytokine caused a significant decrease in expansion capabilities, demonstrating the individual importance of the tested cytokines (Fig. II-3). Overall, cell expansion capacity varied to a higher extent at a lower range (0 – 50 ng/mL), while displaying similar culture performance for combinations with concentrations in the higher testing range (50 – 100 ng/ml). Nevertheless, cytokine panel screening resulted in a FC TNC reaction fingerprint that was coherent between donors. Although biological variability was present and the absolute values of measured variables were different, the overall pattern was very coincident. Additionally, this fingerprint was uniquely distinctive between expansion approaches.

The CFU assay contributed with three response variables (Fig. II-3). Since BFU-E formation was always neglectable, it was not possible to progress with the variable FC BFU-E to the regression modelling phase. Without quantifiable BFU-E populations, CFU-GM and CFU-Mix were mirrored in their population percentage in each assay. FC CFU-GM and FC CFU-Mix demonstrated similar sensitivity to cytokine concentration variation as with FC TNC, but they developed their own cytokine fingerprint.

Table II-2. *Parameter estimations after regression determination for each response variable and expansion system. A backward stepwise regression algorithm was used to correlate the experimental data with the proposed model. Quality of determined regressions and degree of correlations was expressed by the coefficient of determination (R^2), root mean squared error (RMSE), adjusted coefficient of determination and statistic regression test and associated p-value.*

	Normalized FC TNC		Normalized FC CD34$^+$ Cells		Normalized FC CFU-GM		Normalized FC CFU-Mix	
Parameter	**Estimate**	**p-value**	**Estimate**	**p-value**	**Estimate**	**p-value**	**Estimate**	**p-value**
CS_HSPC/MSC								
K	-	-	-	-	-	-	-	-
SCF	9.90×10^{-3}	1.05×10^{-9}	9.27×10^{-3}	1.04×10^{-8}	1.00×10^{-2}	2.02×10^{-5}	3.82×10^{-3}	6.09×10^{-6}
Flt-3L	9.89×10^{-3}	4.62×10^{-10}	9.95×10^{-3}	8.47×10^{-10}	6.88×10^{-3}	2.05×10^{-3}	6.70×10^{-3}	1.90×10^{-2}
TPO	5.67×10^{-3}	3.35×10^{-5}	6.66×10^{-3}	4.18×10^{-6}	1.09×10^{-3}	4.98×10^{-2}	1.24×10^{-2}	5.40×10^{-5}
SCF x Flt-3L	2.80×10^{-5}	1.60×10^{-4}	2.82×10^{-5}	2.15×10^{-4}	3.10×10^{-5}	1.48×10^{-2}	-	-
Flt-3L x TPO	-	-	-	-	-	-	-	-
SCF x TPO	1.60×10^{-5}	2.23×10^{-2}	1.51×10^{-5}	3.49×10^{-2}	-	-	-	-
SCF^2	-7.53×10^{-5}	5.49×10^{-8}	-6.95×10^{-5}	5.23×10^{-7}	-7.16×10^{-5}	6.17×10^{-4}	-	-
$Flt\text{-}3L^2$	-7.60×10^{-5}	4.53×10^{-8}	-7.62×10^{-5}	8.10×10^{-8}	-4.89×10^{-5}	1.53×10^{-2}	-6.08×10^{-5}	2.70×10^{-2}
TPO^2	-4.46×10^{-5}	3.19×10^{-4}	-5.35×10^{-5}	4.35×10^{-5}	-	-	-9.48×10^{-5}	8.89×10^{-4}
Regression Quality								
R-squared (R^2)	0.95		0.95		0.79		0.65	
Root Mean Squared Error (RMSE)	0.08		0.08		0.15		0.20	
Adjusted R-squared	0.94		0.94		0.76		0.60	
F-statistic vs constant model	97.8		92.8		26.8		16.0	
p-value	3.23×10^{-24}		8.77×10^{-24}		4.89×10^{-13}		5.87×10^{-9}	
CS_HSPC								
K	-1.65×10^{-1}	9.90×10^{-3}	-1.86×10^{-1}	4.06×10^{-3}	-1.84×10^{-1}	5.52×10^{-3}	-1.38×10^{-1}	3.66×10^{-2}
SCF	1.51×10^{-2}	1.10×10^{-7}	1.47×10^{-2}	1.98×10^{-7}	1.80×10^{-2}	1.75×10^{-10}	1.63×10^{-2}	1.11×10^{-7}
Flt-3L	6.55×10^{-3}	8.85×10^{-3}	6.30×10^{-3}	1.14×10^{-2}	8.56×10^{-3}	3.05×10^{-4}	-	-
TPO	8.02×10^{-3}	1.65×10^{-3}	9.31×10^{-3}	3.26×10^{-4}	2.37×10^{-3}	2.09×10^{-4}	1.15×10^{-2}	5.53×10^{-5}
SCF x Flt-3L	-	-	-	-	-	-	-	-
Flt-3L x TPO	-	-	-	-	-	-	-	-
SCF x TPO	-	-	-	-	-	-	-	-
SCF^2	-1.19×10^{-4}	5.67×10^{-6}	-1.15×10^{-4}	1.02×10^{-5}	-1.49×10^{-4}	7.78×10^{-9}	-1.38×10^{-4}	1.55×10^{-6}
$Flt\text{-}3L^2$	-5.41×10^{-5}	2.40×10^{-2}	-5.12×10^{-5}	3.21×10^{-2}	-6.57×10^{-5}	3.04×10^{-3}	-	-
TPO^2	-5.01×10^{-5}	3.59×10^{-2}	-5.85×10^{-5}	1.50×10^{-2}	-	-	-8.22×10^{-5}	1.86×10^{-3}
Regression Quality								
R-squared (R^2)	0.78		0.79		0.78		0.71	
Root Mean Squared Error (RMSE)	0.16		0.16		0.16		0.19	
Adjusted R-squared	0.75		0.76		0.76		0.69	
F-statistic vs constant model	26.4		27.9		31.5		28.1	
p-value	4.51×10^{-13}		1.77×10^{-13}		1.68×10^{-13}		9.96×10^{-12}	

In contrast with the remaining response variables, CD34 expression did not show the same sensitivity towards different cytokine concentrations (not shown). Since CD34 expression exhibited minor influences by the cytokine panel, its respective response variable (FC $CD34^+$ cells) revealed the same response pattern as the FC TNC number (Fig. II-3).

II.4.2. *Regression Determination and Analysis*

Several steps were taken to prepare and polish the response variables for regression modelling. Data from each donor was normalized to remove the biological variability on cell expansion intensity, highlighting the effects driven by the cytokine panel (Fig. II-4A; Fig. VII-1A; Fig. VII-2A; Fig. VII-3A). Prior to regression determination, outliers were detected through a Z-score method and eliminated (Fig. II-4B; Fig. VII-1B; Fig. VII-2B; Fig. VII-3B). Regressions for each response variable were calculated, reaching significance in every case (Table II-2).

For both expansion systems, the hypothesized model was able to describe cytokine influence on the values of FC TNC to a considerable extent. For CS_HSPC/MSC, every projected term was significantly present, except for interaction effects between Flt-3L and TPO (Table II-2). Negative quadratic effects were determined, leading to the existence of a concavity in the response surface and the existence of a local maximum in the tested range. On the other hand, for CS_HSPC, there were no interaction terms between cytokines. Also, regression fitting determined a negative intercept (K = -0.165), which has no biological translation and was disregarded.

CFU assay response was modelled by a lesser number of significant parameters. FC CFU-GM and FC CFU-Mix had regressions with two particular characteristics. Unlike FC TNC number, some cytokines did not have a negative quadratic effect. Additionally, FC CFU-Mix for CS_HSPC showed total independence towards Flt-3L, lacking every type of cytokine effect considered in the model. In terms of overall regression quality, CFU-Mix originated fittings with lower quality ($R^2_{CS\_HSPC/MSC}$ = 0.65; $R^2_{CS\_HSPC}$ = 0.71) compared to the remaining response variables.

As previously observed, FC $CD34^+$ cells had similar behavior as the FC TNC number. Consequently, parameter estimation led to the same significant parameters and resembling values.

Regression performance was quantitively assessed by the chosen quality measures. Although the regression quality varied, adjusted correlation coefficients maintained above 0.6 and were able to describe the experimental data significantly. Quantitative variables (FC TNC number and FC $CD34^+$ cells) consistently produced higher quality regressions when compared to the semi-quantitative variables (FC CFU-GM and FC

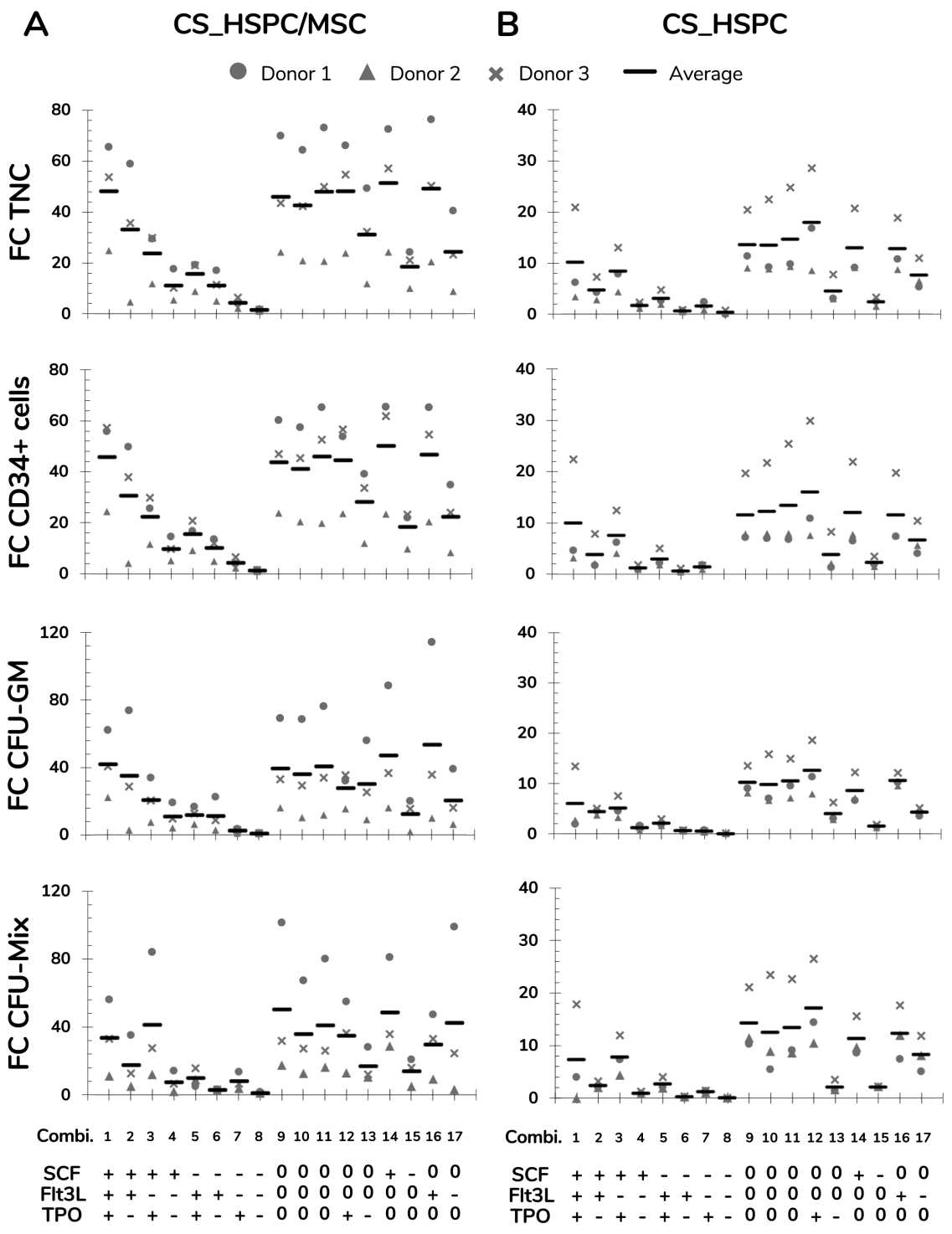

*Figure II-3. Measurements of response variables for two different expansions systems, HSPC suspension culture (CS_HSPC) and co-culture with bone marrow mesenchymal stromal cells (CS_HSPC/MSC). Throughout the entire cytokine panel of 17 combinations, values of fold change (FC) of total nucleated cells (TNC), FC of CD34⁺ expressing cells, FC of colony-forming unit granulocyte-monocyte (CFU-GM) and FC of multilineage colony-forming unit (CFU-Mix) were followed. Cells isolated from three different donors were used for testing the response variables for CS_HSPC/MSC **(A)** and CS_HSPC **(B)**. (+) 100 ng/mL; (0) 50 ng/mL; (-) 0 ng/mL.*

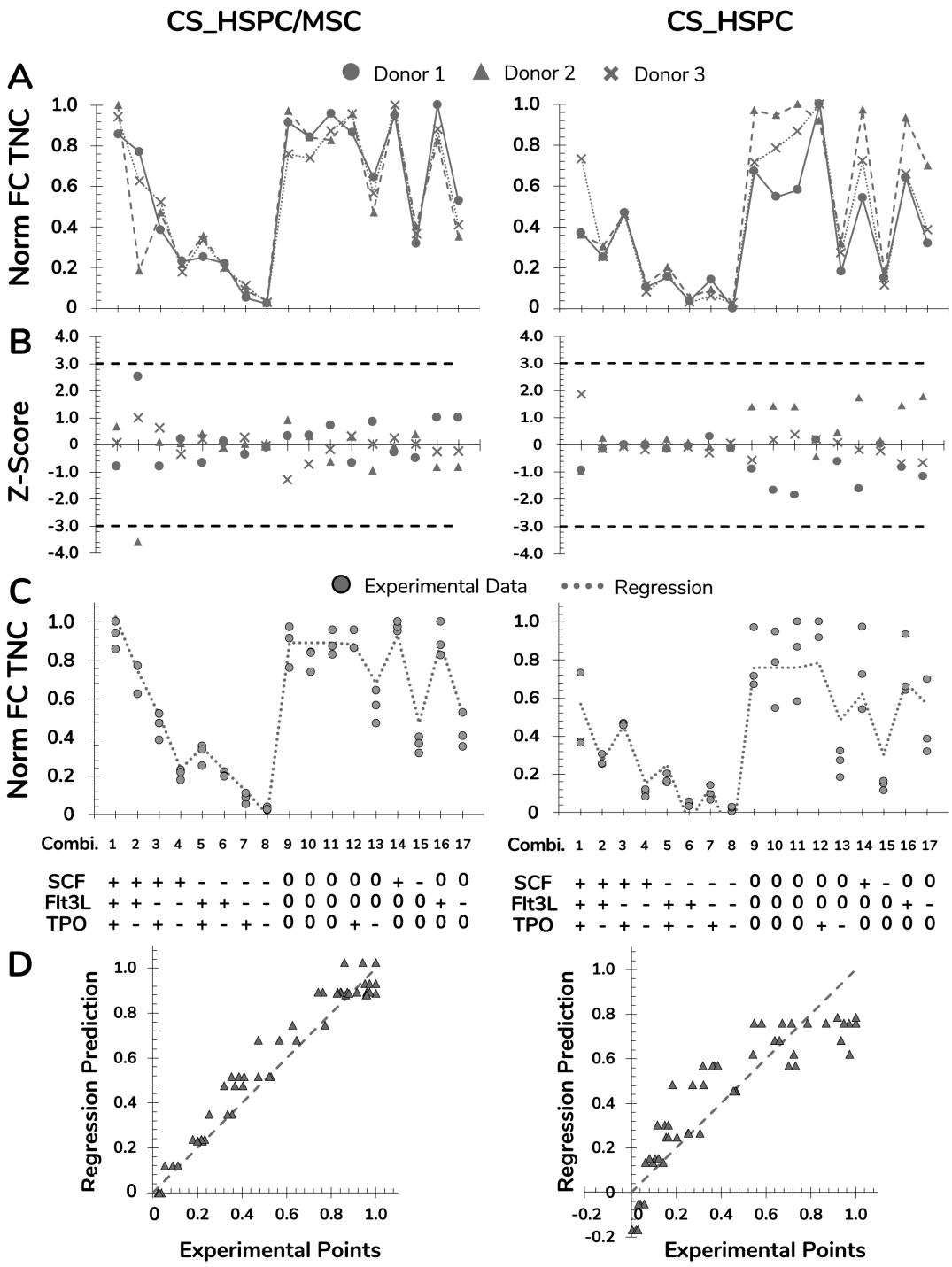

Figure II-4. *Preparation and polishing of experimental data with assessment of regression quality for FC TNC for HSPC suspension culture (CS_HSPC) and co-cultured with MSC(M) (CS_HSPC/MSC).* ***(A)*** *Data from every CB donor was normalized, highlighting variability exclusively due to different cytokine combinations.* ***(B)*** *Outlier screening was performed through Z-score determination. Data points with absolute score values higher than 3 were labelled outliers and were consequently removed from their dataset.* ***(C)*** *After regression determination, experimental data points were compared with calculated regression.* ***(D)*** *Deviations between data points and regressions were visualized. Norm – normalized.*

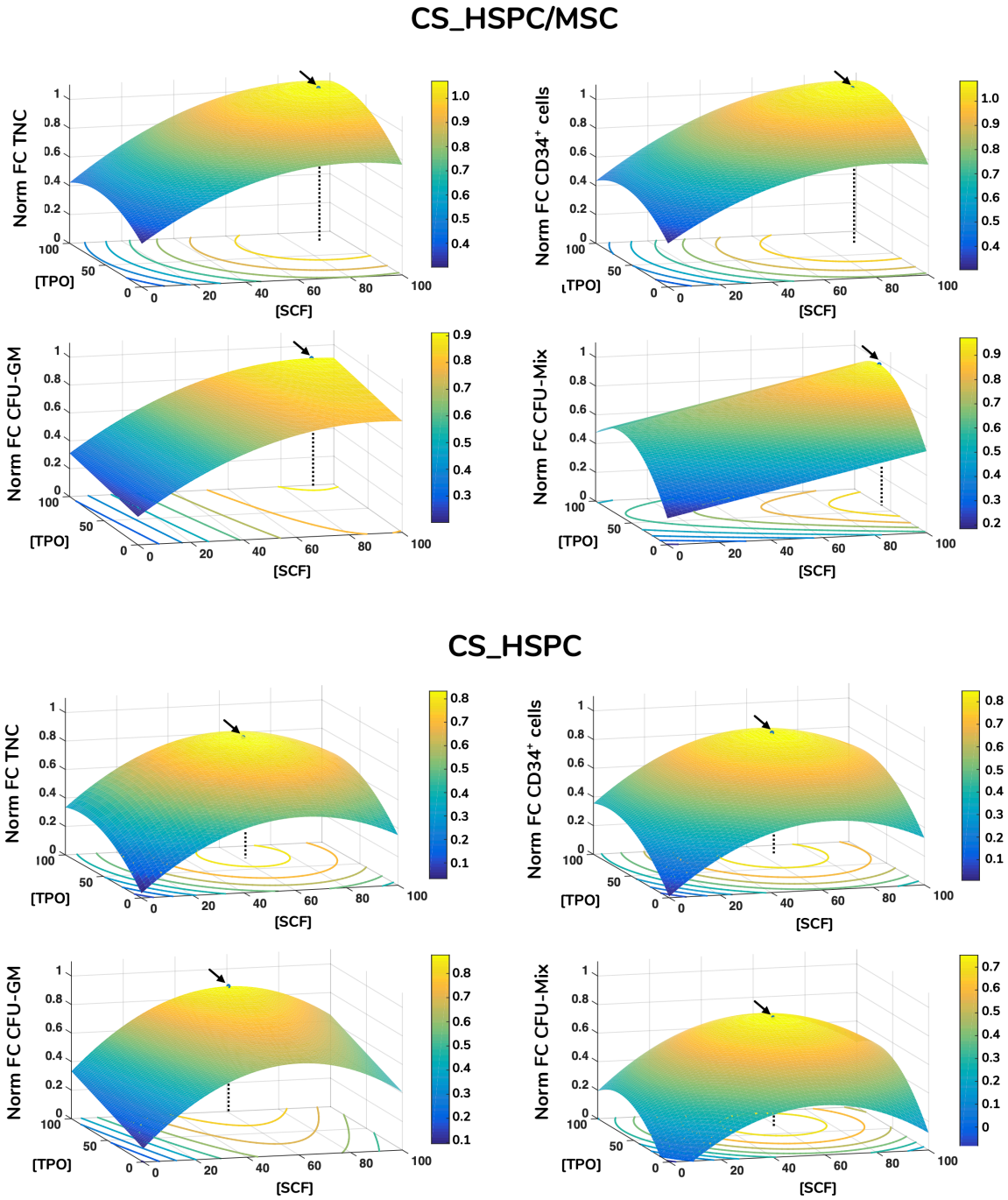

Figure II-5. *Response surface plots of every response variable with localization of optimal cytokine concentrations for HSPC suspension culture (CS_HSPC) and HSPC co-cultured with MSC(M) (CS_HSPC/MSC). Calculated regressions were extrapolated to the whole design window, originating response surfaces. Surface plots containing the response surfaces were observed for the identification of a local optimal response. Regressions were maximized inside the limited design window, giving rise to the optimized cytokine cocktail. These are represented by a black arrow, while a dotted line highlights the corresponding cytokine concentrations that led to the maximum response. Flt-3L concentrations was maintained constant at their respective optimal concentration. Norm – normalized.*

CFU-Mix) of the same expansion system. Quality assured regressions were then used to predict responses for the cytokine panel and were compared with experimental data points (Fig. II-4C; Fig. VII-1C; Fig. VII-2C; Fig. VII-3C). Residual determination was performed to visualize and quantify deviation between the model and data points (Fig. II-4D; Fig. VII-1D; Fig. VII-2D; Fig. VII-3D).
With an average residual of 0.10 ± 0.02, CS_HSPC/MSC consistently showed increased correlation between the experimental data and the determined regressions for every response variable compared to the CS_HSPC with an average residual of 0.13 ± 0.01.

II.4.3. *Cytokine Concentration Optimization*

Each calculated regression gave rise to a distinct response surface, limited by the design space. As predicted by the estimated parameters, every response variable produced a response surface with some degree of concavity, being a direct consequence of negative quadratic effects (Fig. II-5). Maximization of each surface inside the design window was performed. Concentrations corresponding to the maximum were defined as the optimal cytokine combination for that specific response variable (Table II-3). Since the values of FC TNC and FC $CD34^+$ cells possessed coinciding reaction fingerprints, their respective optimal combinations were very similar, which was observed for both expansion systems (Fig. II-6). Variables that did not possess negative quadratic effects for a certain cytokine in their regression caused their optimal concentration to reach the limit of the design space (100 ng/mL). Optimization was done for every response variable, which resulted in 4 optimized cytokine concentrations in each expansion approach. Due to their higher quality regressions and more quantitative nature, optimal concentrations of FC TNC number and FC $CD34^+$ cells were given priority over the CFU output variables. Equal importance was given to the chosen variables and an average of their optimal combinations was performed to reach the final optimal combination (coined as AB20) for each expansion type.

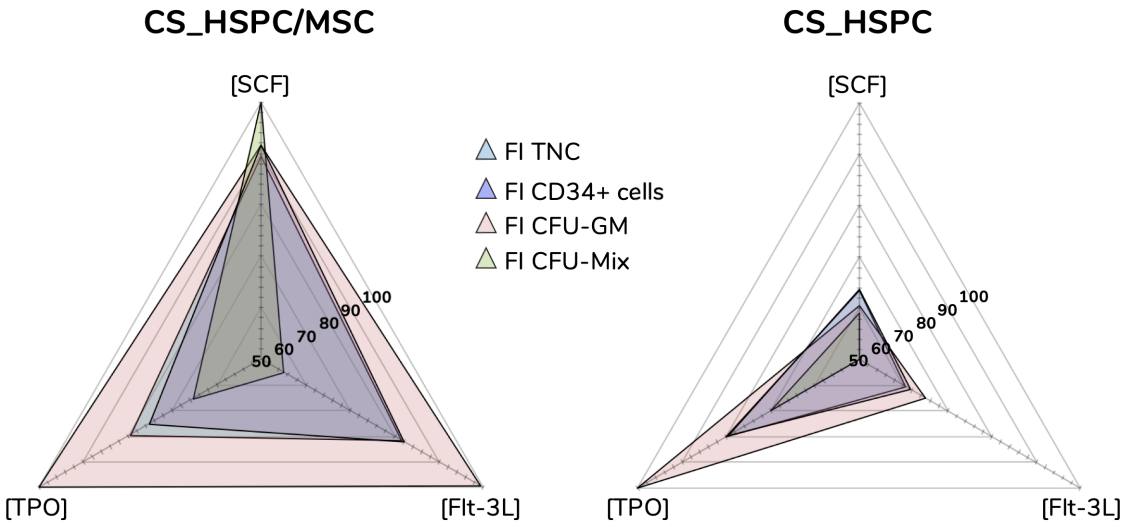

Figure II-6. *Optimal cytokine concentrations for every response variable and expansion system. Maximization of regressions led to optimal cytokine concentrations. Concentration plots displaying the different optimal cocktails observed for each response variable. Sharp differences were detected between both expansion systems, evidencing that cytokine influence is majorly dependent on the expansion approach.*

Table II-3. *List of every optimized cocktail with respective denomination and selection of the final selected combination (ng/mL). A total of 8 different optimal combinations were obtained. Prioritization for FI TNC and FI CD34⁺ cells with an average of their optimal concentrations, originated the selected cocktail for both expansion systems (AB20).*

	CS_HSPC/MSC				CS_HSPC			
Response Variable	Cocktail	[SCF]	[Ftl-3L]	[TPO]	Cocktail	[SCF]	[Flt-3L]	[TPO]
FI TNC	**HM1**	88	82	80	**H1**	63	60	80
FI CD34+ cells	**HM2**	92	82	75	**H2**	64	62	80
FI CFU-GM	**HM3**	92	99	100	**H3**	61	65	100
FI CFU-Mix	**HM4**	100	55	75	**H4**	59	-	70
Selected Cocktail	**AB20**	90	82	77	**AB20**	64	61	80

II.4.4. *Validation*

In order to validate the determined response surfaces for each response variable, their range of applicability was evaluated. Cocktails with concentrations not included in the initial experimental design panel are excellent candidates to assess predictive capabilities of calculated regressions. Besides the optimized cocktails (AB20), the combination of cytokines from our previous study (Z9) [301], determined exclusively for the co-culture expansion system and using a different serum-free culture medium formulation, was also selected for validation studies ([SCF] = 60 ng/mL; [Flt-3L] = 55 ng/mL; [TPO] = 50 ng/mL).

Respective regressions were applied to determine predicted responses of each variable. Also, confidence intervals were determined to define the expected range of prediction variation. HSPC expansion using the selected conditions was performed and resulting experimental data compared. Only 2 out of 32 experimental points (6.25%) were outside the predicted range, FC CFU-GM expanded with Z9 in CS_HSPC/MSC and FC CFU-GM expanded with AB20 in CS_HSPC (Fig. II-7A).

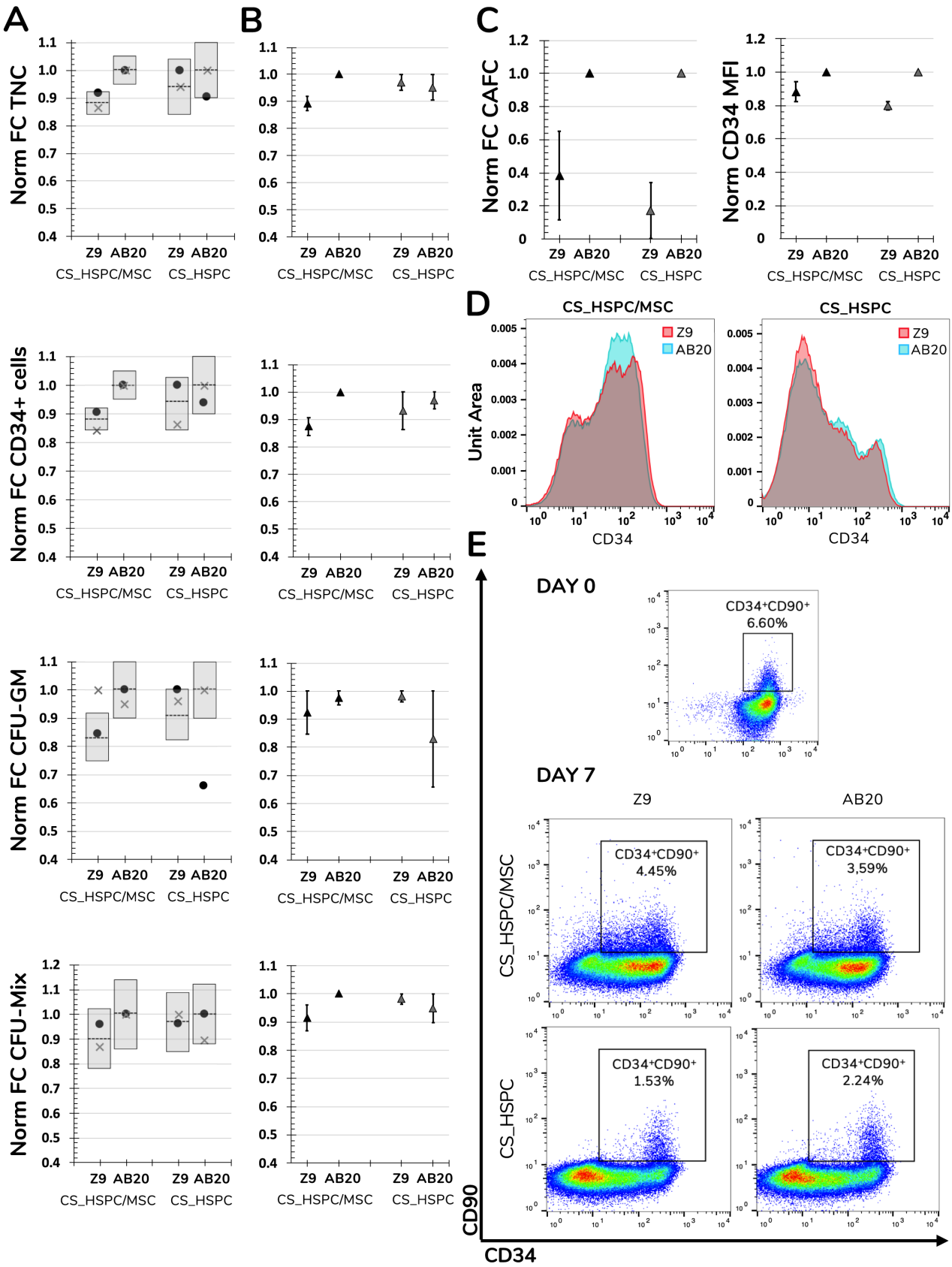
A
B
C
D
E
Norm FC TNC
Norm FC CD34+ cells
Norm FC CFU-GM
Norm FC CFU-Mix
Norm FC CAFC
Norm CD34 MFI
Z9 AB20 Z9 AB20
CS_HSPC/MSC CS_HSPC
CS_HSPC/MSC
CS_HSPC
Z9
AB20
Unit Area
CD34
DAY 0
CD34+CD90+
6.60%
DAY 7
Z9
AB20
CS_HSPC/MSC
CS_HSPC
CD34+CD90+
4.45%
CD34+CD90+
3,59%
CD34+CD90+
1.53%
CD34+CD90+
2.24%
CD90
CD34

Figure II-7. *Validation of determined response surfaces and in-depth analysis of AB20 cocktails.* ***(A)*** *AB20 and Z9 cocktails were used as validation tests for calculated regressions. Predictability of regressions was analyzed by comparing function predictions and respective confidence intervals with experimental confirmation for every response variable and expansion system. Prediction represented by dashed line and confidence intervals by grey columns.* ***(B)*** *Average of two different donors showed that biological variability did not affect the predicted outcomes of comparison between Z9 and AB20. AB20 performed better or similar to Z9 cocktails as anticipated by the prediction and respective 95% confidence intervals.* ***(C)*** *Further comparison highlighted that benefits of AB20 cocktail determination went beyond selected response variables. Expansion using AB20 cocktails led to higher fold increase in CAFC and higher CD34 median fluorescence intensity.* ***(D)*** *Representative histogram of CD34 expression demonstrating that AB20 cocktails are able to delay loss of this marker during expansion.* ***(E)*** *Representative dot plots of CD34 and CD90 expression before and after expansion using both culture systems and cocktails. Initial $CD34^+CD90^+$ population is mostly lost during expansion, although a residual population percentage is observable in every condition. Mixed results were visible concerning maintenance of the more primitive population. Populations were previously gated for live cells using a viability assay. Data is represented by the mean ± standard error of the mean.*

If regressions were to be used as a comparison tool and AB20 and Z9 considered as competitors, every regression would able to successfully predict the outcome between them. FC TNC number and FC $CD34^+$ cells using a AB20 combination in CS_HSPC/MSC were considerably higher when compared to the Z9 cocktail (FC $TNC_{CS\_HSPC/MSC}$: 1.00 ± 0.00 vs. 0.89 ± 0.03; FC TNC_{CS_HSPC}: 0.95 ± 0.05 vs. 0.97 ± 0.03) (FC $CD34^+_{CS\_HSPC/MSC}$: 1.00 ± 0.00 vs. 0.87 ± 0.03; FC $CD34^+_{CS\_HSPC}$: 0.97 ± 0.03 vs. 0.93 ± 0.07) (Fig. II-7B). The remaining comparisons resulted in no substantial difference between tested cytokine cocktails, as predicted by their respective regressions. CD34 median intensity fluorescence (MFI), CAFC assays and levels of expansion of cells with a more primitive phenotype (%$CD34^+CD90^+$) were also analyzed to discern the effects of the AB20 combination on other relevant clinical variables (Fig. II-7C, D, E). Coherent increases of CD34 MFC in both culture systems using the AB20 cocktail were observed when compared to the Z9 cocktail (CD34 $MFI_{CS\_HSPC/MSC}$: 1.00 ± 0.00 vs. 0.88 ± 0.06; CD34 MFI_{CS_HSPC}: 1.00 ± 0.00 vs. 0.80 ± 0.03). In terms of FC CAFC, AB20 cocktails in both expansion systems originated more colonies. Optimized cocktails were responsible for an increase of 2.5 ± 0.3 in CAFC compared to Z9 in the CS_HSPC/MSC, while AB20 also produced 4.7 ± 1.1 more colonies than Z9 in the CS_HSPC. On the other hand, AB20 cocktails had mixed performance concerning expansion of primitive progenitors. Both cocktails maintained a residual population percentage of $CD34^+CD90^+$ cells regardless of the culture system, with AB20 resulting in an average of 2.59 ± 0.68% and Z9 in an average of 2.65 ± 0.74%.

II.4.5. *Differential Cytokine Influence*

This systematic method of achieving optimization provided considerable insight into the relationship between cytokines and cells in both expansion systems (i.e. HSPC culture with/without a MSC(M) feeder layer). Cytokine reaction fingerprints were previously mentioned and were compared to highlight differences in cytokine influence (Fig. II-8).

Normalized FC TNC number (Fig. II-8A) displayed significative differences in several specific combinations, leading to three main observations. Firstly, the total fingerprint area for this variable for CS_HSPC/MSC was higher compared to the CS_HSPC ($Area_{CS\_HSPC/MSC}$ = 1.02 vs. $Area_{CS\_HSPC}$ = 0.59). Thus, the presence of a feeder layer appears to synergize with cytokine benefit during culture, boosting expansion levels closer towards their maximum performance. Moreover, the reaction fingerprints show that CS_HSPC is more vulnerable to the lack of an individual cytokine than CS_HSPC/MSC. Cells expanded in co-culture display an alleviated negative response whenever a combination without the presence of a cytokine was used. Lastly, adverse effects in cell expansion performance due to excess of cytokines are evident in CS_HSPC, shown by the transition between center points (combination 9, 10 and 11) and the combination with highest concentration of each cytokine (combination 1).

Lack of sensitivity of CD34 expression (Fig. II-8B) to the cytokine panel led to a circular-shaped reaction fingerprint. Over the entire cytokine panel, CS_HSPC/MSC displayed a reduced CV of 4.5 ± 3.9% for $CD34^+$ cell percentage, while CS_HSPC exhibited a CV of 12.4 ± 8.8%. Nevertheless, CS_HSPC showed some dependence on TPO, since combinations without TPO had some negative impact on CD34 expression (Fig. II-8B). A decrease in $CD34^+$ cell percentage of 16.4% was observed between combination 1 to 2, 17.3% from combination 3 to 4 and 12.5% from combination 12 to 13.

CFU outputs (Fig. II-8C,D) had complementary reaction fingerprints, due to insignificant BFU-E quantification. Percentage of CFU-GM had low variation due to the cytokine panel, although some differences were visible. Fingerprint area was ubiquitously larger for co-culture system ($Area_{CS\_HSPC/MSC}$ = 17 142 vs. $Area_{CS\_HSPC}$ = 9838), demonstrating that its priming towards the granulocyte-macrophage lineage did not change with different cytokine cocktails. Clear benefits were apparent from Flt-3L supplementation, whereas TPO seemed to influence against CFU-GM development. This was more obvious in CS_HSPC, where combinations with those features (combination 2, 6 and 13) caused the differences in CFU-GM percentage between fingerprints of both systems to narrow.

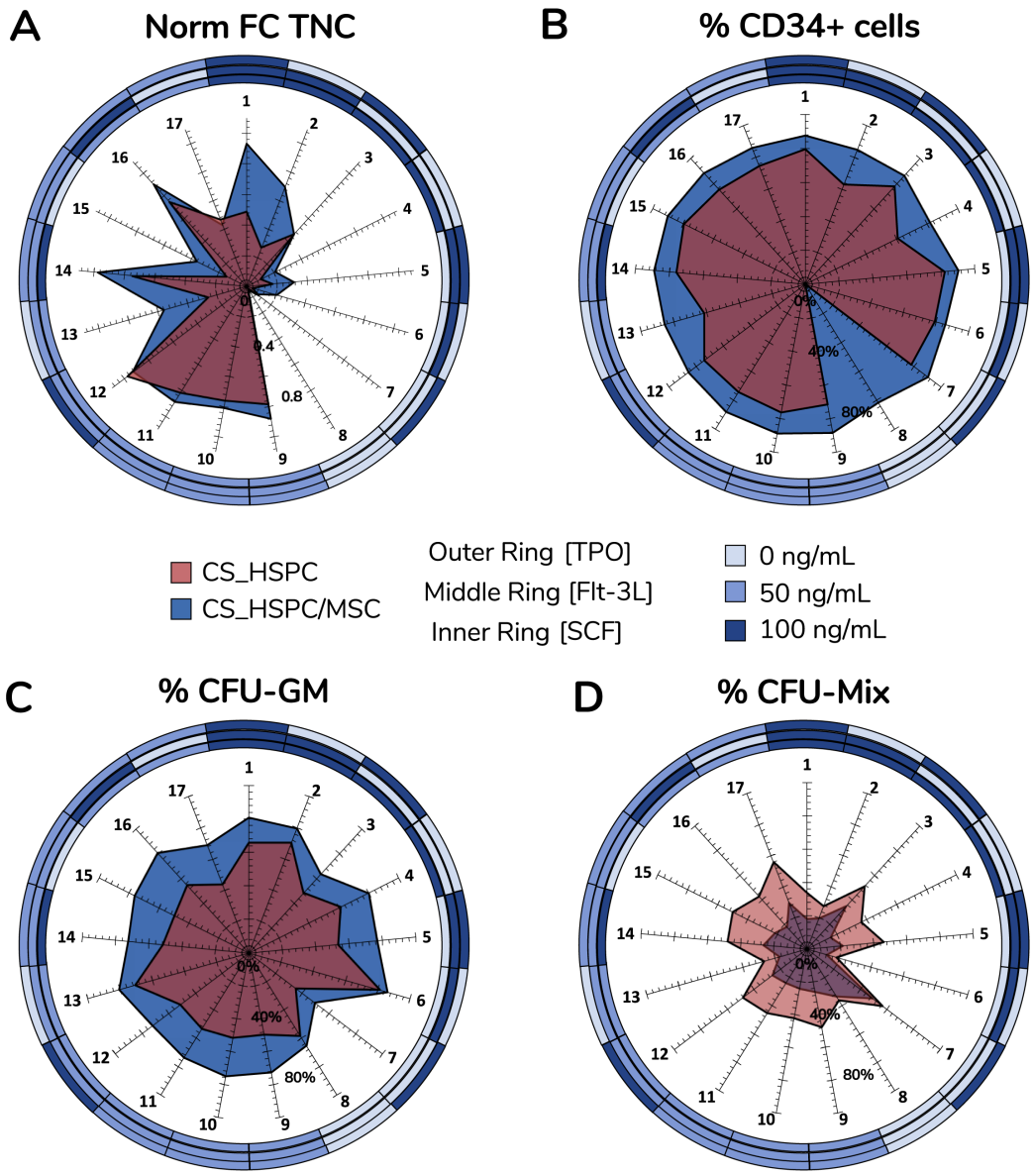

Figure II-8. *Reaction fingerprints obtained out of the 17 cytokine combinations. Information obtained from creating response surfaces can be exploited to further assess the relationship between an expansion system and cytokine use. Unique reaction fingerprints were determined for normalized FC TNC* ***(A)****, percentage of CD34⁺ cells* ***(B)****, percentage of CFU-GM* ***(C)*** *and percentage of CFU-Mix* ***(D)****. Circular rings around plots display respective cytokine concentrations associated with each data point. CS_HSPC/MSC appear to synergize better with cytokines, except for CFU-Mix. Percentage of CD34 expression for cytokine combination 8 in the CS_HSPC was not quantified due to insufficient cell number.*

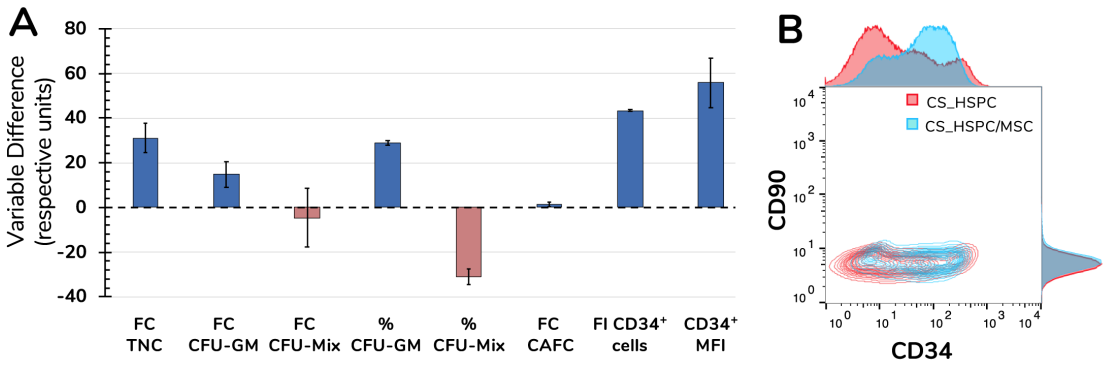

*Figure II-9. Side-by-side comparison between expansion systems with respective optimal cytokine concentrations. **(A)** A number of significant variables concerning HSPC expansion were chosen as comparison criteria between CS_HSPC (red) and CS_HSPC/MSC (blue). Co-culture displayed superior performance in most variables, with the exception of FI CFU-Mix and percentage of CFU-Mix. **(B)** Contour plot of CD34 and CD90 expression after 7 days expansion with AB20 cocktail. At day 7, CS_HSPC/MSC demonstrated a substantially different CD34 expression profile, being able to retain expression of CD34 more effectively when compared to CS_HSPC. Two different CB donors. Data is represented by the mean ± standard error of the mean.*

II.4.6. *Comparison of Expansion Strategies*

Upon completion of the optimization approach, cytokine contribution in each HSPC expansion system was maximized allowing a fair side-by-side comparison of the two studied expansion platforms. Several variables were followed during cell expansion at their maximum cytokine strength. The overall scale was clearly favorable towards the co-culture system, with seven out of nine measures (78%) evidencing a better performance (Fig. II-9A). However, CS_HSPC demonstrated more capability towards promoting mixed colonies in the CFU assay in detriment to granulocyte-macrophage colonies. Although none were able to maintain the initial CD34 phenotype of CB cells after 7 days, CS_HSPC/MSC showed it was able to significantly reduce the loss of this surface marker in cultured cells with a positive CD34 MFC difference compared to the CS_HSPC of 55.8 ± 7.8. When compared, the respective CD34 expression histograms appear almost mirrored (Fig. II-9B). Thus, with their cytokine cocktails optimized, expansion using a co-culture system demonstrated an overall superior potential in generating an expanded a HSPC product with higher retention of CD34 expression and primed for originating more CFU-GM.

II.5. Discussion

With cell therapy manufacturing gaining traction as more advanced cell-based therapies get approved and reach the commercialization stage, efforts have been made in promoting the adoption of "Quality by Design" (QbD) guidelines, including process optimization and experimental design, while encouraging their implementation early on during the research and development phase[107,292].

Experimental design of cytokine cocktails has been previously pursued, especially during initial studies on CB-derived HSPC *ex vivo* expansion[108,301]. However, applicability of the aforementioned studies to current expansion strategies is restricted. Whether due to having been performed in non-human cells[315], used to study *ex vivo* hematopoietic differentiation rather than HSPC expansion[332,333] or to the lack of surface response models and optimizatio[319,334], previous attempts struggle in being transposed to present expansion protocols. This can be justified by a gradual improvement of HSPC expansion protocols, where innovation has eventually led to inconsistencies between culture conditions in current strategies and in abovementioned optimizations. Basal culture media have had their own dynamic evolution over time. Earlier culture media used in *ex vivo* HSPC expansion protocols were typically composed of basic formulations, having been developed for more generic cell culture applications. These usually required supplementation with FBS in order to enrich the formulation to allow for cell expansion, with such basal media varying between Minimum Essential Medium Eagle - Alpha Modification (**α**-MEM)[221,335,336], Iscove's modified Dulbecco's Medium (IMDM) [314,337] and others (reviewed[103]). With the development of culture media specifically for human HSPC expansion, aligned with growing concerns with the use of FBS as an undefined supplement, formulations were developed to be serum-free, with protocols implementing specialized culture media such as X-VIVO™ 10 medium[338], QBSF-60 serum-free medium[104,204], StemLine® stem cell expansion medium[339] and StemSpan™ serum-free expansion medium[143,175,310,340]. This has benefited cell expansion results but ultimately compromised the applicability of previous optimizations described in the literature. Although we have contributed towards the resurgence of optimization of culture conditions targeting the expansion of human HSPC, our own initial study on cytokine supplementation optimization was performed with QBSF-60 medium as the established expansion medium[301]. This proprietary serum-free medium was originally designed to support human $CD34^+$ cells[104].

With StemSpan™ (STEMCELL technologies) medium being more prevalent in latest studies on HSPC *ex vivo* expansion and in most advanced clinical trials testing expanded HSPC[179,310,340–342], we have seized this opportunity to achieve an enduring optimization with direct impact on ongoing late-stage development of cell therapies based on *ex vivo* expanded HSPC from CB. However, the formulation StemSpan™ serum-free

medium used herein still has undisclosed supplements and some animal-derived components in its formulation (i.e. bovine albumin). In the absence of a clearly defined and disclosed formulation, possible extrapolation of our results to different media is limited and any animal-derived components increase the risks of contamination. Nevertheless, with the cell therapy manufacturing field pressing for animal-component free and chemically defined formulations, StemSpan™ medium has currently adapted to those needs. If existing or novel strategies decide to transfer to such formulations through regulatory pressure or due to new GMP guidelines, our optimization study with StemSpan™ stands a considerable chance in maintaining its applicability on clinical-grade *ex vivo* HSPC expansion.

In our work, we have aimed at achieving an enduring optimization of cytokine supplementation for two clinically relevant *ex vivo* HSPC expansion platforms, CS_HSCP and CS_HSPC/MSC (i.e. HSPC being expanded alone in a liquid culture system or co-cultured with a MSC(M) feeder layer, respectively). With cytokines maintaining a significant role in protocols of *ex vivo* expansion of human HSPC[102], namely those from CB, optimization of the used concentrations through experimental design is crucial. When attempted, optimization applied to biological issues with inherent variability is largely determined by the existence of a donor-independent pattern. Once approved as a therapy, CB-derived expanded HSPC will hope to be produced from a single cord unit. Therefore, donor variability is a central issue and must be considered when performing such studies and thus selected response variables were followed for three different donors to increase the robustness of the optimized cocktail[343]. As expected, biological variability was present and may be partly related to differences observed in the initial CD34 expression after enrichment[327]. Interestingly, this variability did not prevent the appearance of a recurring pattern in every response variable (Fig. 4; Fig. S1; Fig. S2; Fig. S3). Although different donors of CB cells originated different absolute values for the selected response variables, cell-cytokine relationship did not change and cytokine optimization was carried out.

Early on, we observed that our response variables displayed greater fluctuations with lower concentrations of the defined cytokine panel (SCF, Flt-3L and TPO). A certain degree of cytokine saturation was apparent from the center points (concentrations of 50 ng/mL) onward (Fig. 3). With many expansion platforms being employed in clinical trials using concentrations of 100 ng/mL or higher[128,143,174,175], there is an observable overuse of cytokine supplementation without a rational justification. Excess amount of these molecules will be responsible for unnecessary costs, which might jeopardize the implementation of the respective potential cell therapies[343]. Eventually, this overload of cytokine molecules can also have a negative impact on the cells themselves, since it largely differs from the levels of cytokines that HSPC experience *in vivo*. With concentrations of cytokines in the BM ranging in the picomolar[344–346], several groups

may be crippling their expansions with HSPC overstimulation. Interestingly, in contrast to the four main response variables (FC TNC, FC $CD34^+$ cells, FC CFU-GM and FC CFU-Mix), CD34 expression observed post-expansion was an exception to the previously described behavior. This surface marker expressed by HSPC did not display any significant variation to the cytokine panel but did vary with other factors, such as cell expansion platform (CS_HSPC vs. CS_HSPC/MSC) and culture duration (Fig. 8B). In general, selected response variables met optimization requirements, such as pattern emergence and fluctuation inside the design space.

As mentioned beforehand, modelling biological behavior with precision can be a challenge, depending on the nature of the selected response variables. Naturally, better quality regressions arose from more quantitative measures, such as FC TNC number (Table 2). Both CFU and CAFC outputs suffer from some subjectivity, inherent to these specific assays, requiring a significant dependence on experimental technique to originate results that make modelling possible[347,348]. The existence of a single outlier proves the quality of the response variable measurements.

Taking each of these regressions into account, CS_HSPC/MSC was able to produce more consistent results than its counterpart system (i.e. without a feeder layer). The presence of a MSC(M) feeder layer (originally anticipated to better recreate the HSPC niche *ex vivo*) appears to create a buffer zone environment which is capable of making responses and expansion performance more uniform. This may be related with the specific cell expansion dynamics of a co-culture setting. During this type of culture, HSPC that adhere directly to the stromal feeder layer and are phase-bright (i.e. do not migrate underneath the feeder layer) become responsible for most of the cell division observed over the culture duration[349]. Although the fraction of non-adherent or suspended cells typically has the highest fold increase in cell number, these cells themselves do not seem to be proliferatively active. Only phase-bright adherent cells were observed to have an active cell cycle with a considerable cell number in the G2/M phase[125]. Thus, attached HSPC, which saturate the entire stromal layer, are responsible for the increase in the non-adherent cell fraction observed by releasing their progeny into suspension[125]. This behavior may justify lower cell expansion variation, since contact area saturation of the stromal layer appears to become the main regulator of proliferation, creating a stable cell expansion mechanism. Of note, CS_HSPC/MSC also has an additional cytokine (i.e. bFGF) in its experimental setting. While its main function is stromal support during HSPC expansion, synergistic or other type of interactions with targeted cytokines may exist and cannot be ruled out. Although co-culture introduces more biological factors, the results obtained for this platform have displayed reduced experimental deviation. Despite this, every response variable in both systems originated a good degree of correlation in their respective regressions, despite the existence of some expected variability.

Regression manipulation gave origin to a total of 8 optimal combinations, resulting from the selection of four response variables (FC TNC, FC $CD34^+$ cells, FC CFU-GM and FC CFU-Mix) for two different expansion systems (Fig. 6). Prioritization of variables was required to appoint a single and representative optimal cytokine combination for each expansion platform. For most clinical trials related with *ex vivo* expansion of HSPC, TNC and number of $CD34^+$ cells are selected as critical parameters[179,310]. Considering their significant clinical relevance allied to their higher regression quality, these two measures (i.e. FC TNC and FC $CD34^+$ cells) were chosen to define the optimal cocktails for each culture system. Following the described rationale, prioritization of variables led to determination of optimal cocktails (AB20) for the CS_HSPC ([SCF] = 90 ng/mL; [Flt-3L] = 82 ng/mL; [TPO] = 77 ng/mL) and for the CS_HSPC/MSC (([SCF] = 64 ng/mL; [Flt-3L] = 61 ng/mL; [TPO] = 80 ng/mL) (Table 3). These cocktails were responsible for expansion results up to 49 FC TNC and 33 FC $CD34^+$ cells for the CS_HSPC and 75 FC TNC and 70 FC $CD34^+$ cells for the CS_HSPC/MSC from a single CB unit. When comparing with clinical trial data using these types of platforms (Median FC TNC = 56, Median FC $CD34^+$ cells = 4 for cytokine-based expansion (i.e. feeder free) and Median FC TNC = 12, Median FC $CD34^+$ cells = 30 for co-culture expansion[102]), cell expansions obtained herein with optimized cocktails demonstrated competitive outcomes, surpassing the performance of most reports of *ex vivo* HSPC expansion in similar platforms. Additionally, with the optimized cytokine cocktails displaying concentrations lower than many current protocols (e.g. [143,174]), we have highlighted avoidable costs and uncovered an opportunity for a cost-effectiveness measure. These results demonstrate the need for tailored optimization in improving the viability and financial feasibility of CB-derived HSPC expansion platforms.

Following optimization, regression-derived response surfaces required validation in order to confirm their donor-independent applicability. Validation was successfully completed using two different cocktails, the determined optimal cocktails (AB20) and a previously established optimized cocktail by our group (Z9)[301]. Expansion outcome and behavior using these cocktails performed as projected by their respective regressions (Fig. 7A). The few out-of-bounds experimental points were associated with the semi-quantitative nature of the CFU assay. When compared, AB20 cocktails outperformed or matched Z9 performance concerning the four response variables. Interestingly, AB20 cocktails were able to overtake Z9 in other important measures that were not included in the initial experimental design, including CD34 mean fluorescence intensity and CAFC formation (Fig. 7C, D). However, since AB20 and Z9 cocktails were located in the higher concentration range, their comparison was challenging, since lower variations of response variables were previously highlighted for that range. As expected, with concentrations differences lower than 30 ng/mL, determined regressions predicted only slight differences between AB20 and Z9 for some response variables. Nevertheless,

solid predictive capacity was demonstrated and optimized cocktails still showed superior expansion performance.

Throughout this study, we have once more confirmed the important role cytokines play in promoting HSPC expansion. Taking advantage of this optimization, we also focused on the cell-cytokine relationship to further complement our comparison between CS_HSPC and CS_HSPC/MSC. By identifying the existence of unique reaction fingerprints, we were able to shed light on the different impact cytokines have on both studied expansion platforms. These fingerprints showed obvious distinctions in cytokine reaction behavior. In agreement with previous observations, the MSC(M) feeder layer seems to develop a protective microenvironment around the HSPCs, resembling their role in the BM niche. In fact, FC TNC reaction fingerprint from CS_HSPC evidenced its higher vulnerability to early culture saturation by excess quantities of cytokines (Fig. 8A). Indeed, the presence of a MSC(M) feeder layer was able to ameliorate negative cytokine inhibition. When adding an interactive feeder layer, the network of individual and synergistic cytokine effects changes and gains complexity[350]. While the exogenous cytokines added to the culture medium in both systems are the same, the environment of endogenous cytokines and their respective quantities change due to feeder cell presence. With a very dynamic secretome, MSC are known to produce other cytokines that promote HSPC expansion[102]. By better mimicking the hematopoietic niche with this stromal component, the microenvironment is able to reach a higher number and level of synergies which can potentially lead to higher cell expansion yields[351,352].

Knowledge from these reaction fingerprints and their regressions may be used for purposes other than the expansion of CB-derived HSPC for HCT. Revived interest in autologous gene therapy has consolidated the application of expanded adult HSPC for treatment of genetic hematological diseases[353,354]. Approval of Strimvelis, a gene therapy product of transduced autologous BM-derived $CD34^+$ cells for treatment of severe combined immunodeficiency due to adenosine deaminase deficiency, was a milestone in the field and represents the considerable potential that expanded HSPC have in gene therapy[355]. Other areas within the hematological field can also potentially take advantage of these regression strategies to tailor HSPC culture for their own needs. There has been interest in using CB-derived HSPC culture platforms for the differentiation of cells towards the lymphoid lineage for use in immunotherapy (e.g. donor lymphocyte infusions, tumor-infiltrating lymphocytes, etc.)[356]. Both culture systems included in this study have been explored for such purposes. CS_HSPC/MSC has been shown to have potential as a system to maintain early lymphoid progenitors (i.e. $CD34^+CD7^+$ cells)[326] and support the generation of functional natural killer and dendritic cells [357]. On the other hand, CS_HSPC in combination with the small molecule StemRegenin-1 has been recently used for generation of progenitor T cells[358]. Exploitation of these expansion systems for such different applications can also largely

benefit from the cytokine optimization strategy established in the present study and the information gathered on the effects of cytokines on cultured cells.

To our knowledge, cytokine optimization has not been used as a tool to enable a correct side-by-side comparison of different strategies. This evaluation is critical for decision-making over which platform should be supported for clinical trial progression or apply for regulatory approval. Criteria for the selection of cytokine concentrations have roughly been the same throughout different types of expansion culture systems, ignoring high specificity of each strategy. Without determining unique cytokine cocktails for each one, direct comparison of published results in an unstandardized manner may cause unrealistic conclusions. By pursuing a tailored cytokine optimization in two expansion approaches, these may be rightfully compared at their full cytokine potential, making their critical steps and parameters more easily identifiable[107].

In the optimized conditions of our study, CS_HSPC/MSC undoubtedly showed better capabilities in promoting HSPC expansion, which explains the progression of ex vivo mesenchymal-cell coculture through the clinical trial pipeline [128]. In our assessment, CS_HSPC/MSC proved to have a superior production capacity as a platform concerning every studied variable except for FC CFU-Mix (Fig. 9). Notably, CD34 expression, which displayed reduced variability due to cytokine effects, was observed to be consistently higher in an HSPC/MSC co-culture setting. This difference was originally observed by comparing cytokine reaction fingerprints of the percentage of $CD34^+$ cells (Fig. 8B) and was quantitively confirmed in optimal conditions by comparison of CD34 median intensity fluorescence (Fig. 9A, B). Indeed, enhanced expansion of HSPC through a co-culture setting with MSC has also been observed in other studies. Beneficial impact compared to traditional liquid suspension has been described concerning cell expansion levels[326,359,360], but also in what concerns the biological features of the cultured cells, for instances, contributing towards an enhanced migration capability of HSPC[349,361]. Overall, our evaluation of each expansion system after cytokine optimization has provided a more reliable and unbiased view over their genuine production capabilities of a potential expanded HSPC product.

To fully assess the viability of these such systems as potential cell therapy platforms, the entire manufacturing process needs to be considered. Importantly, we have used cryopreserved CB HSPC to mimic the CB unit processing in current clinical trials, as these pioneering trials normally lay the groundwork for the manufacturing process of the respective approved product. With source cryopreservation being an important bioprocess step that can have an impact on the characteristics of the cell product (e.g. need for cell revitalization), disregarding it can also affect optimization applicability. Additionally, acquired process knowledge of cytokine interactions will also prove to be very useful in building such a manufacturing pipeline for an expanded HSPC product [107]. Determined regressions will provide critical information on expansion reaction and

a degree of predictability if unavoidable changes in cytokine concentration should happen during production. However, expansion yield by itself is not the only priority in cell therapy development and an overall balance among operational parameters is needed[122]. Although CS_HSPC/MSC was shown to produce a higher number of expanded HSPC with superior quality measures necessary for HCT, it also holds a higher level of complexity as a culture system. Normally, a trade-off between complexity and feasibility has existed in the manufacturing of cell therapies, hindering their translation[362]. In this case, the presence of a feeder layer in the expansion system will require add-ons or modifications to its manufacturing process when compared to the simpler CS_HSPC. An additional upstream source collection and isolation procedure for MSC will be needed, while downstream units will have to be able to separate MSC from expanded HSPC to assure end product purity. Also, preparation of MSC feeder layers inevitably increases the total culture duration and requires culture formats compatible with adherent cell culture. All these issues, which might prove challenging or costly, need to be considered and counterbalanced with the performance increase shown by CS_HSPC/MSC in product quantity and quality. Therefore, bioprocessing studies with economic modelling must accompany this co-culture system to determine if this more complex platform is worthwhile[343,363–365].

Strategies similar to our experimental design should become widespread, as they represent a statistically sound and efficient way to reach optimal experimental conditions[107,366]. The methodology applied in our study, targeting the use of cytokines for *ex vivo* HSPC expansion, can be translated to other culture parameters and applications. Stem cell fate studies (self-renewal *versus* differentiation)[367,368], as well as biomaterial development for tissue engineering[369], are fields that are centered on continuous improvement and optimization of experimental conditions in order to reach a defined differentiated cell type or scaffold, respectively. Filled with possible optimization parameters (e.g. differentiation media, oxygen tension, cell aggregate size, scaffold porosity, stirring speed in bioreactor systems, etc.), studies benefit immensely by using experimental design as they avoid unnecessary iterations of dose-response experiments, reduce reagent and material costs and become more time-efficient[369,370].

III. Hypothermic Preservation of Adipose-Derived Mesenchymal Stromal Cells as a Viable Solution for the Storage and Distribution of Cell Therapy Products

This chapter is published as:

Branco, A. *et al.* Hypothermic Preservation of Adipose-Derived Mesenchymal Stromal Cells as a Viable Solution for the Storage and Distribution of Cell Therapy Products. *Bioengineering* , **9**, 805 (2022). https://doi.org/10.3390/bioengineering9120805.

III.1. Summary

Cell and gene therapies (CGT) have reached new therapeutic targets but have noticeably high prices. Solutions to reduce production costs might be found in CGT storage and transportation, since it typically involves cryopreservation, a heavily burdened process. Encapsulation at hypo-thermic temperatures (e.g. 2-8°C) could be a feasible alternative. Adipose tissue-derived mesenchymal stromal cells (MSC(AT)) expanded using fetal bovine serum (FBS)- (MSC-FBS) or human platelet lysate (HPL)-supplemented medium (MSC-HPL) were encapsulated in alginate beads for 30 minutes, 5 days and 12 days. After bead release, cell recovery and viability were determined to assess encapsulation performance. MSC identity was verified by flow cytometry and a set of assays was performed to evaluate functionality. For a standard transportation period of 5 days, MSC(AT) were able to survive encapsulated, with recovery values of 56 ± 5% for MSC-FBS and 77 ± 6% for MSC-HPL (a negligible drop compared to earlier timepoints). Importantly, MSC function did not suffer from encapsulation, with recovered cells showing robust differentiation potential, expression of immunomodulatory molecules and hematopoietic support capacity. MSC(AT) encapsulation was proven possible for a remarkable 12 day-period. Currently unable to completely replace cryopreservation in CGT logistics and supply chain, encapsulation has shown potential to act as a serious competitor.

III.2. Background

CGT have seen a significant growth in the past decades due to their unmatched potential to improve the treatment landscape of a large variety of diseases[371]. CGT products differ from traditional biopharmaceuticals since they are capable of a much more complex response to disease than small molecules or antibodies. By dynamically reacting to environmental and biological cues, CGT can restore tissues or increase the body's innate ability to fight disease[372].

Among potential CGT products, MSC became the subject of great research interest, spurred mainly by their potential for application in regenerative medicine. Their differentiation potential into different lineages, allied with their significant in vitro expansion capacity, their accessible isolation from multiple sources with few ethical issues associated (e.g. umbilical cord and adipose tissue (AT)), and their good safety and efficacy profiles from a variety of pre-clinical studies, encouraged their increased use in human clinical trials, particularly between 2004 and 2011[373]. However, despite the large number of clinical trials and contrary to expectations, the lack of statistically significant results in terms of efficacy and their discrepancy with the results of pre-clinical assays hampered the advancement of MSC-based therapies as marketed CGT[373,374]. It

was only in 2018 that the European Medicines Agency (EMA) approved Alofisel, an allogenic MSC-based therapy for complex perianal fistulae in Crohn's disease[375].

The success of Alofisel, contrasting with the underwhelming results of previous human clinical trials, can be explained by a paradigm shift in the mechanism of action of MSC. Focus was changed from their tissue regeneration potential to their immunomodulatory action, leveraging their complex secretome and opening the door for the first statistically significant results in human clinical trials using MSC[376,377]. Because of this, and despite their initial disappointing results, MSC are again being used in a great number of clinical studies, the great majority of them in phase I and II (a search in clinicaltrials.gov in July 2022 for the term "Mesenchymal" yielded 1,720 studies). The high number of ongoing early phase clinical trials suggests there is a great untapped potential for more MSC-based CGT to be developed and approved.

Considering the vast therapeutic potential of MSC, from GVHD to spinal cord injury, the establishment of a robust cGMP compliant manufacturing process that minimizes variability and facilitates the approval of new CGT, ensuring a quick translation from bench-to-bedside, should be a priority[122,371,372,376,377]. Furthermore, because CGT usually have higher costs when compared with other classes of medicines, and to ensure commercial effectiveness, it is important to consider COG optimization in the early stages of process development with the aim of minimizing the cost per dose without compromising the product quality. In the specific case of allogeneic MSC-based products, because these medicines usually require large manufacturing scales, opportunities for economies of scale can be leveraged[285,364,378]. Indeed, the large-scale production of allogeneic MSC is not a straightforward process and the decisions regarding production platform design have a great impact in the robustness, validation, and commercial viability of the cell product.

One of the critical steps in MSC production is their storage and journey from bench-to-bedside[379]. The process used for storage and transportation must ensure the cell product is consistently GMP-compliant and safe, maintaining cell viability and potency during the time window that separates the release of the product from a CCMP facility to the clinical trial center or therapeutic facility[377,380,381].

Cryopreservation is currently regarded as an indispensable step of CGT production, being a feasible strategy to allow for an MSC-based product as an off-the-shelf product that can meet economical, logistical, and regulatory requirements. Cells can be stored in controlled conditions for extended periods and be shipped in a frozen state to healthcare centers where they can be thawed and quickly administered to patients[381–383]. However, cryopreservation and thawing procedures are known to induce cellular injuries that negatively affect the stability and therapeutic efficacy of MSC-based products, being possibly responsible, at least partially, for early disappointing clinical results[382,384].

Although cryopreservation is currently considered the gold standard in MSC manufacturing, finding alternative strategies that can replace and/or complement this process (serving as transportation solutions between the production and the healthcare providing facilities) has been the focus of several studies. Lyophilization, or freeze-drying has been investigated as a possible strategy to store cells at ambient temperature by rapidly freezing and dehydrating cells while using a protective compound such as the sugar trehalose[385]. This method was efficiently demonstrated in preserving placental tissue at room temperature (RT), suggesting it can be a viable alternative for the preservation and storage of cellular products, including MSC, as it will simplify storage[255]. In the cases where an extended shelf-life is not required, the hypothermic storage (between 2 and 8°C) of cell products is perhaps a simpler solution as it relies only on storing and/or transporting cells in culture media designed specifically for this purpose. Multiple studies have showed the ability of research and clinical-grade media to maximize cell viability and function while storing them for periods between 1 and 7 days at temperatures around 4°C[253,386,387]. Another popular strategy that relies on hypothermic storage for safely storing and transporting cells is encapsulation in different polymers, both natural and synthetic, the most common of which being alginate[379].

Alginate is a natural polysaccharide that can be obtained from seaweed and jellified when cations are added, to generate a biocompatible hydrogel[388]. The advantages of alginate as a simple and cost-effective solution for protecting cell products during storage and transportation have been attributed to its ability to stabilize the membrane of cells in suspension and to protect them from osmotic shock and mechanical stress[379,389]. Alginate encapsulation has the potential to impact CGT manufacturing. Cells would be encapsulated in beads, stored at hypothermic temperatures in a non-proliferative stage, and then recovered by dissolving the gel and replacing the solutions with fresh culture media.

In this study we aim to attest the ability of alginate encapsulation to maintain cell viability, identity, and function in the context of MSC-based therapy manufacturing. For that, adipose tissue-derived MSC (MSC(AT)) were encapsulated and stored for a total of 12 days at hypothermic temperatures. To establish a xeno(geneic)-free condition, in line with CCMP requirements, MSC(AT) expanded in medium supplemented with human platelet lysate (HPL) were compared with cells expanded in medium supplemented with fetal bovine serum (FBS), the historical standard. To our knowledge, this is the first study to push MSC(AT) encapsulation to relevant time periods (i.e. 12 days) using a standardized, commercially available kit (BeadReady™) able to comply with CCMP conditions. Encapsulated MSC(AT) were extensively analyzed to determine if their identity and function were preserved for the tested conditions, in comparison to non-encapsulated cells.

III.3. Methods

III.3.1. *Human Tissues*

Adipose tissue (AT) samples were obtained through collaboration agreements secured by Institute for Bioengineering and Biosciences (iBB) at Instituto Superior Técnico (IST) with Clínica de Todos-os-Santos (Lisbon). Informed consent was obtained from healthy donors before harvesting of samples, in accordance with Directive 2004/23/EC of the European Parliament and of the Council of March 31st, 2004, regarding standards of quality and safety for the donation, procurement, testing, processing, preservation, storage and distribution of human tissues and cells, represented by the counterpart Portuguese Law 22/2007. Adipose tissue-derived mesenchymal stromal cells (MSC(AT)) isolation, characterization, and cryopreservation was performed following protocols previously established at the Stem Cell Engineering Research Group at iBB[329,390]. CB units were secured as described in Chapter II (II.3.1).

III.3.2. *MSC(AT) Expansion*

Cryopreserved MSC(AT) were thawed and seeded in low glucose DMEM (Thermo Fisher Scientific) supplemented with 10% (v/v) MSC-qualified fetal bovine serum (FBS) (Thermo Fisher Scientific) and 1% (v/v) Antibiotic-Antimycotic (A/A) (Thermo Fisher Scientific) (DMEM-FBS) at a cell density of 3 000 cells/cm2 on standard tissue culture plastic and transferred to an incubator at 37°C and 5% CO2 in a humidified atmosphere. DMEM-FBS expansion medium was changed every 3-4 days until cells reached between 70-80% confluence. Cells were detached from their culture surface with 0.05% (v/v) trypsin (Thermo Fisher Scientific) and 1 mM ethylenediaminetetraacetic acid (EDTA) (Sigma-Aldrich) in phosphate buffered saline (PBS) (Sigma-Aldrich). In order to establish a xenogeneic-free culture condition, detached cells were evenly split between the existing DMEM-FBS condition and low glucose DMEM supplemented with 5% (v/v) human platelet lysate (HPL) (UltraGRO™-PURE; kindly provided by AventaCell Biomedical Corp.) and 1% (v/v) A/A (DMEM-HPL). Adaptation to xeno-free conditions was completed after an additional DMEM-HPL passage for MSC(AT). Cell detachment under xeno-free conditions was performed using TrypLE (Thermo Fisher Scientific).

III.3.3. *MSC(AT) Encapsulation*

MSC(AT) encapsulation in alginate beads was performed following the instructions included in the BeadReady™ kit (kindly provided by Atelerix), provided by the manufacturer. Briefly, the procedure was separated into three sections, gelation, storage/transportation and release. For each single encapsulation, 6 x 10^6 cells were

suspended in their respective medium at twice the final encapsulation density and then carefully mixed with an alginate solution. Slowly, the mixture was dropwise transferred into a gelation solution, using a needle, in order to form uniform and spherical beads. After gelation stabilization, beads were washed and stored in their respective expansion medium in a tightly sealed tube, away from light, at a temperature between 10° and 20°C to mimic possible temperature oscillations during transportation. During encapsulation, medium samples were taken from each bead-containing tube, centrifuged and stored at -80°C for future metabolic analysis. Beads were dissociated 30 minutes after encapsulation (D0), and at day 5 (D5) and at day 12 (D12). Cell release was done by replacing expansion medium with the provided dissolution buffer. Afterwards, released cells were washed and resuspended in fresh expansion medium. Recovered MSC(AT) were quantified to determine bead recovery and their viability was also assessed.

III.3.4. *Glucose and Lactate Profiles*

Medium samples were thawed at room temperature (RT) and vortexed before being distributed on a 96-well culture plate in duplicates. Glucose and lactate concentrations were determined by membrane-bound immobilized enzyme quantification in a YSI 2500 Biochemistry Analyzer (YSI). First-order regressions were fitted to MSC(AT) glucose and lactate concentration profiles. MSC(AT) glucose consumption and lactate production rates were determined from regression slopes multiplied by the expansion medium volume (5.5 mL) in bead-containing tubes. MSC(AT) specific glucose consumption and lactate production rates were calculated by dividing glucose and lactate rates by the cell number at each encapsulation timepoint. Glucose consumption and lactate production rates for MSC(AT)-hematopoietic stem and progenitor cells (HSPC) co-culture and HSPC culture control (No FL) were calculated by dividing the difference in concentration at the beginning and at the end of the co-culture by the duration period of the hematopoietic support assay (7 days).

III.3.5. *MSC(AT) Immunophenotype*

Released and non-encapsulated MSC(AT) were sent in their respective expansion medium at 4°C to the Flow Cytometry Unit at Centro Hospitalar e Universitário de Coimbra, where their immunophenotype was analyzed by flow cytometry on a FACSCanto II cytometer (BD Biosciences), using the FACSDiva software (v8.02, BD Biosciences). For each condition, cells were resuspended in 100 µL PBS and stained for cell surface markers resorting to a stain-lyse-wash direct immunofluorescence technique. MSC(AT) were stained with the following antibodies: HLA-DR (L243) V450

(BD Biosciences), CD274 (29E.2A3) BV421 (BioLegend), CD108 (KS-2) BV421 (BD Biosciences), CD45 (2D1) V500-C (BD Biosciences), CD73 (AD2) FITC (BioLegend), CD44 (L178) FITC (BD Biosciences), CD105 (TEA3/17.1.1) PE (Beckman Coulter, USA), CD39 (TU66) PE (BD Biosciences), STRO-1 (STRO-1) PE (ExBio), CD54 (LB-2) PE (BD Biosciences), CD34 (8G12) PerCP-Cy5.5 (BD Biosciences), CD200 (OX-104) PerCP-Cy5.5 (BioLegend), CD146 (SHM-57) PerCP-Cy5.5 (BioLegend), ICOSL (2D3) PerCP-Cy5.5 (BioLegend), CD19 (J3-119) PE-Cy7 (Beckman Coulter), CD271 (ME20.4) PE-Cy7 (BioLegend), CD106 (STA) PE-Cy7 (BioLegend), CD90 (5E10) APC (BioLegend), CD142 (NY2) APC (BioLegend), CD14 (M**φ**P9) APC-H7 (BD Biosciences), B7-H4 (MIH43) APC Fire 750 (BioLegend), CD10 (HI10**α**) APC-H7 (BD Biosciences). MSC(AT) were surface stained for 10 minutes in the dark and at RT. Following this step, cells were incubated for 10 minutes in the dark at RT with 2ml of FACSLysing solution (BD Biosciences) and centrifuged, discarding the supernatant. Cell pellets were then washed with PBS and resuspended, ready to be acquired. Following acquisition, data analysis was performed using Infinicyt (Cytognos), version 2.0.

III.3.6. *MSC(AT) Multilineage Differentiation*

III.3.6.1. Adipogenic Differentiation

Released and non-encapsulated cells were plated at a density of 100 000 cells/cm2. After 24 hours, differentiation was induced with the StemPro™ Adipogenesis Differentiation Kit (Thermo Fisher Scientific). Complete differentiation medium supplemented with 1% (v/v) A/A was changed twice a week for 21 days. Cells were then washed with PBS, fixed with 4% (v/v) paraformaldehyde (Sigma Aldrich) for 30 minutes at RT and washed again with PBS. Fixed cells were initially incubated with a 60% isopropanol (Fisher Chemicals) solution for 5 minutes at RT. Then, cells were stained to determine their degree of adipogenesis with a mixture (3:2) of 0.3% (v/v) Oil Red O (Sigma Aldrich) in a 60% (v/v) isopropanol solution and water for 1 hour at RT. After incubation, cells were washed three times with distilled water and kept in PBS. Differentiation phenotype was observed under the microscope (Leica DMI3000 B, Germany) and images were taken.

III.3.6.2. Osteogenic Differentiation

MSC(AT) were seeded at a density of 100 000 cells/cm2 on a 24-well culture plate. Differentiation was also induced 24 hours later, by using StemPro™ Osteogenic Differentiation Kit (Thermo Fisher Scientific). Complete differentiation medium supplemented with 1% (v/v) A/A was changed twice a week for 21 days, after which cells were fixed as stated for the adipogenic differentiation protocol. To verify their

osteogenic differentiation, cells were subjected to both an alkaline phosphatase and to a Von Kossa stain. Firstly, fixed cells were incubated for 40 minutes at RT in a solution of Fast Violet (Sigma Aldrich) and Naphthol (Sigma Aldrich), being washed with distilled water afterwards. With the alkaline phosphatase stain completed, cells were then incubated for 30 minutes with silver nitrate (Sigma Aldrich), washed three times with distilled water and kept in PBS. Differentiation phenotype was observed under the microscope and images were taken.

III.3.6.3. Chondrogenic Differentiation

For the chondrogenic differentiation, released and non-encapsulated MSC(AT) (800 000 cells in each condition) were prepared for aggregation by the hanging drop method. After being centrifuged and having their supernatant discarded, cells were resuspended in 240 µL and droplets of 30 µL were placed on a Petri dish lid. After filling the bottom of the Petri dish with PBS, the droplet-containing lid was inverted onto its respective dish. Petri dishes were placed at 37°C for 24 hours for cell aggregates to form. Then, MSC(AT) aggregates were transferred onto Costar® ultra-low attachment plates (Corning) and differentiation was induced with the MesenCult™-ACF Chondrogenic Differentiation Kit. Complete chondrogenic differentiation medium supplemented with 1% (v/v) A/A was changed twice a week for 21 days. To assess chondrogenic differentiation, cells were incubated for 1 hour in an 1% (v/v) Alcian Blue (Sigma Aldrich) solution, washed three times with distilled water and kept in PBS. Cells were observed under the microscope and images were taken.

III.3.7. *Hematopoietic Support Assay*

III.3.7.1. MNC(CB) Isolation

MNC(CB) were isolated as described in Chapter II (II.3.2).

III.3.7.2. Generation of a Cryopreserved $CD34^+$ Pool from MNC(CB)

To generate a pool of CD34+ expressing cells for the entire study, six different donors of previously isolated MNC(CB) were thawed and pooled for CD34 enrichment through Magnetic Activated Cell Sorting (MACS) using the CD34 MicroBead Kit (Miltenyi Biotec) according to the manufacturer's instructions. CD34+ expression was confirmed by flow cytometry and a quality criterion of at least 70% CD34 expression was defined. Enriched cells were also subjected to a CFU assay and a complete immunophenotypic analysis before being refrozen in DMEM-FBS supplemented with 10% DMSO and stored in a liquid/vapor phase nitrogen tank.

III.3.7.3. MSC(AT) FL Preparation

Released and non-encapsulated MSC(AT) were seeded at a density of 100 000 cells/cm2 on 12-well plates and left to adhere overnight in an incubator. The day after, confluent feeder layers were selected for the hematopoietic support assay.

III.3.7.4. *Ex Vivo* Expansion of HSPC

For each expansion, a fraction of the pool of CB-derived CD34+-enriched cells was thawed and seeded at a density of 30 000 cells/mL, with the presence of an MSC(AT) feeder layer (co-culture) and without (no feeder layer control – No FL). HSPC were expanded for 7 days in StemSpan SFEM II (STEMCELL Technologies) (2 mL/well) supplemented with 1% (v/v) A/A and a cytokine cocktail consisting of stem cell factor (SCF), fms-like tyrosine kinase 3 ligand (Flt-3L), thrombopoietin (TPO) and basic fibroblast growth factor (bFGF) (PeproTech) with concentrations of 90, 77, 82 and 5 ng/mL, respectively. Cytokine concentrations used were previously optimized targeting maximization of the expansion of CB-derived CD34+-enriched cells in co-culture with MSC[109].

III.3.7.5. Proliferation Assay

Expanded HSPC were quantified as described in Chapter II (II.3.7).

III.3.7.6. CFU Assay

CFU assay was performed as described in Chapter II (II.3.8).

III.3.7.7. HSPC Immunophenotype

The immunophenotype of isolated and expanded HSPC was analyzed by flow cytometry. Briefly, cells were washed with PBS and viability was evaluated using a Far Red Fixable Dead Cell Stain Kit (Thermo Fisher Scientific). Afterwards, cells were surface stained using previously titrated CD45RA (HI100) FITC (BD Biosciences), CD90 (5E10) PE (BioLegend) and CD34 (8G12) PerCP-Cy5.5 (BD Biosciences). Stained cells were acquired on a FACSCalibur™ cytometer (BD Biosciences). Data was analyzed using FlowJo v10 software (FlowJo LLC).

III.3.8. *Statistical Analysis*

Data was analyzed using GraphPad Prism 8 software (Dotmatics). Results are presented as mean ± standard error of the mean (SEM). First-order regressions were made using the least squares regression fitting method. Goodness of fit was evaluated with the coefficient of determination (R2). For statistical hypothesis testing, a Shapiro-Wilk test was carried out to assess data normality. One-way analysis of variance (ANOVA) was used to detect significant differences and Tukey multiple comparison test was done to determine which specific groups had statistical significance.

III.4. Results

The feasibility of encapsulating mesenchymal stromal cells (MSC) as a means of storage and transportation for cell therapies was tested. Three independent donors of adipose

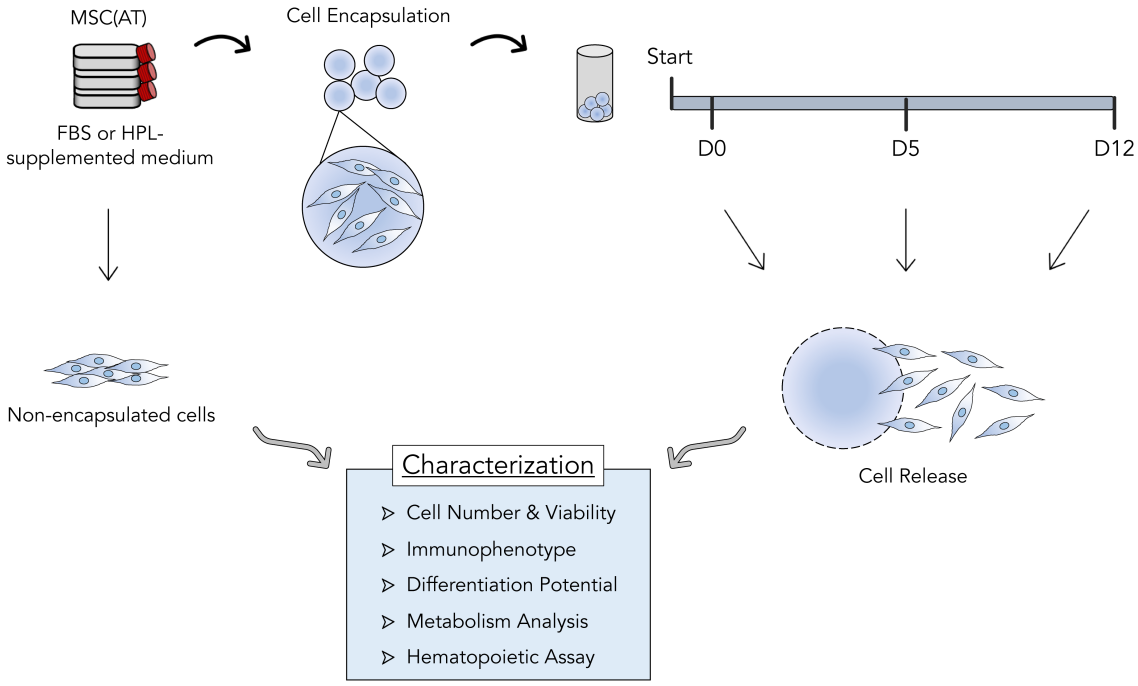

Figure III-1. *Study Design. Three different adipose tissue-derived mesenchymal stromal cell (MSC(AT)) donors were expanded in fetal bovine serum (FBS) or human platelet lysate (HPL)-supplemented expansion medium in standard tissue culture plastic. After reaching desired numbers, MSC(AT) were encapsulated in alginate beads and kept at temperatures between 10°C and 20°C. MSC(AT) were left encapsulated during three different time periods: 30 minutes (D0), 5 days (D5) and 12 days (D12). Cells were then released and subjected to different characterization assays and compared with non-encapsulated MSC(AT). Cell retainment and survival during encapsulation, MSC identity and functional immunophenotype, MSC tri-lineage differentiation potential, metabolic activity and hematopoietic support capacity were determined and compared between timepoints.*

tissue-derived MSC (MSC(AT) were expanded *in vitro* either in standard fetal bovine

serum (FBS)-supplemented medium or xeno-free, human platelet lysate (HPL)-supplemented medium. For each condition, cells were encapsulated in alginate beads using the BeadReady™ kit. Encapsulated cells were maintained in an environment simulating transportation and storage conditions during three different time periods (30 minutes (D0), 5 days (D5) and 12 days (D12)). When reaching their specific timepoints, encapsulated cells were released and compared to non-encapsulated cells in what concerns cell number, immunophenotype, metabolism, differentiation potential and hematopoietic support capacity (Fig. III-1).

III.4.1. *MSC(AT) were successfully encapsulated and able to withstand hypothermic temperatures for up to 12 days*

A commercially available encapsulation kit, BeadReady™, based on alginate beads, was tested using adipose tissue-derived mesenchymal stromal cells (MSC(AT)) as target cells. An initial timepoint of 30 minutes of encapsulation (D0) was defined to quantify the encapsulation efficiency (i.e. ratio between encapsulated cells at D0 and the initial cell number prior to encapsulation). MSC(AT) expanded in fetal bovine serum (FBS)-supplemented medium (MSC-FBS) reached a 71 ± 5% efficiency, whereas MSC(AT) expanded in human platelet lysate (HPL)-supplemented medium (MSC-HPL) achieved a 77 ± 5% encapsulation efficiency (Fig. III-2A). After closely following the encapsulation protocol, formed beads were stable throughout the duration of the study, with no unwanted bead loss being observed. As storage time increased, cell recovery decreased for both MSC-FBS and MSC-HPL, reaching 44 ± 2% and 50 ± 5% at D12, respectively.

Interestingly, while for MSC-FBS, cell recovery shows a gradual drop throughout the timepoints (D0 – 71 ± 5% vs. D5 – 56 ± 5% ($p>0.082$); D5 vs. D12 - 44 ± 2% ($p>0.194$); D0 vs. D12 ($p<0.01$)), MSC-HPL appear to show a more stable encapsulation profile with no detectable cell loss within the first five days (D0 - 77 ± 5% vs. D5 - 77 ± 6%; D5 vs. D12 - 50 ± 5% ($p<0.05$); D0 vs. D12 ($p<0.05$)). Nevertheless, from D5 to D12, MSC-HPL showed a sharper decline, reaching similar levels of cell recovery at D12 as for MSC-FBS.

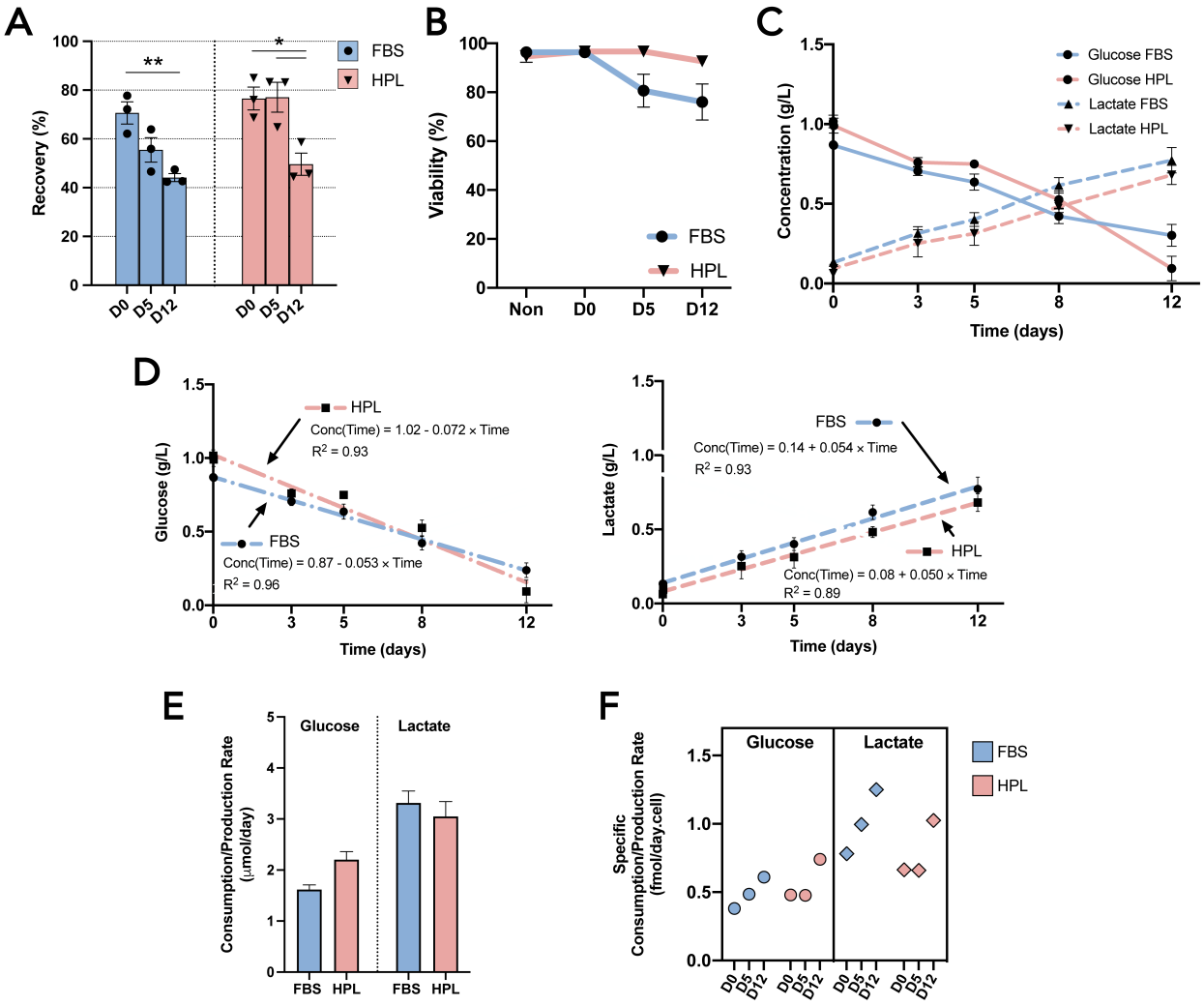

Figure III-2. *Cell encapsulation performance and MSC(AT) metabolic analysis. (A) – Cell recovery from alginate beads after 30 minutes (D0), 5 days (D5) and 12 days (D12) for MSC-FBS (blue) and MSC-HPL (red). (B) – Cell viability of MSC(AT) before encapsulation (Non) and after their release from encapsulation at D0, D5 and D12. (C) – Glucose and lactate concentration profiles. (D) – Glucose (left) and Lactate (right) profile regression modelling. Fitting of first-order regressions with presentation of equation and coefficient of determination (R^2). (E) – Molar glucose consumption and lactate production rates. (F) – Specific molar glucose consumption and lactate production rates at the various encapsulation timepoints. (Three MSC(AT) donors; mean ± SEM; *P < 0.05, **P < 0.01).*

Cell viability of encapsulated cells was also tracked throughout all timepoints (Fig. **III-**2B). Before encapsulation, a high viability was guaranteed (96 ± 0.3% for MSC-FBS and 95 ± 3% for MSC-HPL). Overall, recovered cells maintained their viability during the 12

days, although MSC-FBS did display a slight reduction trend to 76 ± 8% at D12, somewhat mimicking the trend observed for cell recovery.
These results show that MSC(AT) can be encapsulated and survive in hypothermic temperatures, albeit with some cell loss occurring over time and decrease in viability, namely when working with MSC-FBS.

III.4.2. *Encapsulated MSC(AT) demonstrated an active metabolism regardless of the expansion medium*

During encapsulation, adipose tissue-derived mesenchymal stromal cells (MSC(AT)) showed a coherent consumption of glucose and production of lactate between cell donors (Fig. III-2C). Neither biological variability, nor expansion medium choice (MSC(AT) expanded in fetal bovine serum (FBS)-supplemented medium (MSC-FBS) vs. MSC(AT) expanded in human platelet lysate (HPL)-supplemented medium (MSC-HPL)) were causes of different MSC(AT) metabolic profiles. Consumption of glucose and production of lactate displayed a mirrored behavior, with steady decreases and increases as the encapsulation time grew. By D12, glucose levels were residual, thus exhibiting signs of nutrient exhaustion.
To better assess the metabolism of MSC(AT) while encapsulated, metabolic profiles were subjected to regression analysis. Both glucose and lactate curves were successfully fit to individual linear functions with high correlation coefficients (R^2=[0.89-0.96]) (Fig. III-2D). Consequence of possessing linear regression functions, encapsulated MSC-FBS and MSC-HPL displayed constant glucose consumption and lactate production rates throughout the encapsulation (Fig. III-2E). Interestingly, MSC-HPL consumed 2.2 ± 0.2 µmol glucose/day, higher than MSC-FBS with 1.6 ± 0.1 µmol glucose/day. On the other hand, lactate production rates were very similar between MSC-FBS and MSC-HPL conditions.
For a better understanding of these metabolic rates at a cellular level, specific consumption and production rates were determined (Fig. III-2F). Since MSC(AT) had constant metabolic rates and cell recovery decreased over time, specific metabolic rates generally increased with encapsulation time. Specific glucose consumption rates from both MSC-FBS and MSC-HPL varied between 0.38 and 0.74 fmol/day.cell and specific lactate production rates between 0.65 and 1.25 fmol/day.cell. Apparent lactate/glucose yields ($Y_{lactate/glucose}$) reflect previously mentioned differences in glucose consumption between MSC-FBS and MSC-HPL, with values of 2.05 and 1.38, respectively.

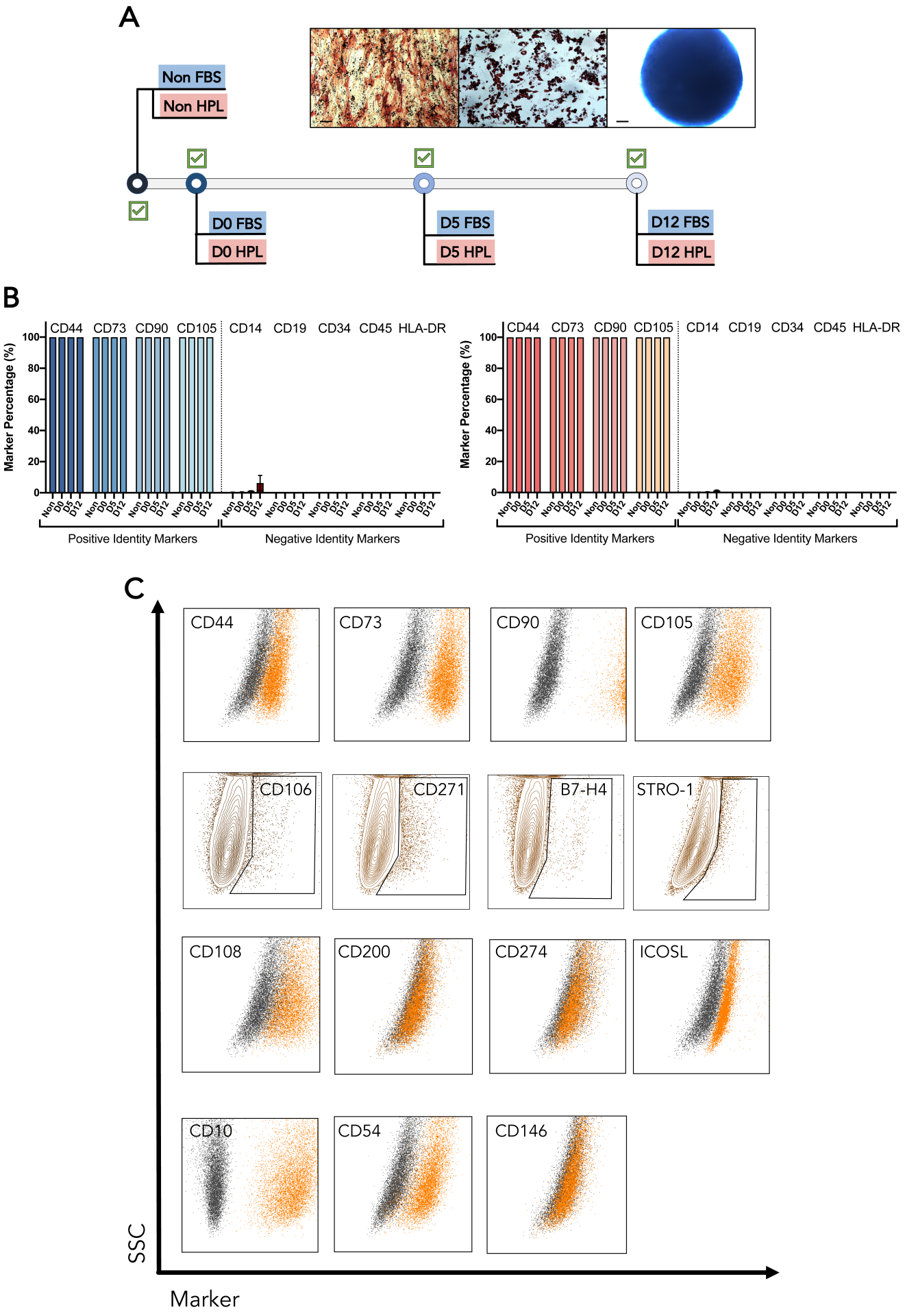
A
Non FBS
Non HPL
D0 FBS
D0 HPL
D5 FBS
D5 HPL
D12 FBS
D12 HPL
B
CD44 CD73 CD90 CD105 CD14 CD19 CD34 CD45 HLA-DR
Marker Percentage (%)
Positive Identity Markers
Negative Identity Markers
C
CD44
CD73
CD90
CD105
CD106
CD271
B7-H4
STRO-1
CD108
CD200
CD274
ICOSL
CD10
CD54
CD146
SSC
Marker

Figure III-3. *Differentiation potential and immunophenotype of MSC(AT) before and after encapsulation. (A) – Map of MSC(AT) tri-lineage differentiations showing successful differentiation in every timepoint. Representative image of osteogenic (left), adipogenic (center) and chondrogenic (right) stainings. (B) – Positive and negative identity marker expression for MSC-FBS (left) and MSC-HPL (right) (%). (C) - Representative MSC(AT) marker expression for a defined encapsulation timepoint. For homogeneous populations with no subpopulations identified, dotplots containing stained cells (orange) were overlaid with the unstained control (dark grey) (first, third and fourth row). Marker expression that led to MSC(AT) positive subpopulations were gated in contour plots (second row). Scale bar: 100 μm, Non – non-encapsulated; SSC – Side scatter; MFI – Median fluorescence intensity (Three MSC(AT) donors; mean ± SEM).*

III.4.3. *Upon encapsulation, released MSC(AT) maintained their identity, immunosuppressive potential and clonogenic capabilities as well as their differentiation potential*

After being encapsulated, recovered adipose tissue-derived mesenchymal stromal cells (MSC(AT)) preserved their ability to differentiate into osteogenic, chondrogenic and adipogenic lineages. Following a 21-day differentiation, every biological donor from MSC(AT) expanded in fetal bovine serum (FBS)-supplemented medium (MSC-FBS) and MSC(AT) expanded in human platelet lysate (HPL)-supplemented medium (MSC-HPL) was able to successfully originate cells from each one of the three lineages (Fig. **III-**3A). Thus, no changes in MSC(AT) differentiation potential were observed after encapsulation.

To uncover whether released MSC-FBS and MSC-HPL maintained their identity and function, their immunophenotype was extensively characterized by flow cytometry analysis. MSC identity markers (positive and negative) were tracked and did not change their expression throughout encapsulation (Fig. **III-**3B)[191,391]. Multiple MSC(AT) clonogenic and immunosuppression markers were also followed and showed different expression behavior (Fig. **III-**3C). Those that gave rise to positive subpopulations (e.g. B7-H4 – immunosuppression and CD271 – clonogenic), showed an increasing trend as encapsulation time grew for both MSC-FBS and MSC-HPL (Fig. **III-**4A). For markers where MSC(AT) displayed a homogeneous expression, median fluorescence intensity (MFI) analysis was done to detect variations in expression over time (Fig. **III-**4B). No significant differences in MFI were observed for these markers. Going further into MSC function, a small set of particular markers were also studied, namely motility-related CD10, trans-endothelium migration-related CD54 and hematopoietic support-related CD146 (Fig. **III-**4C). MFI tracking was able to discern an increase in CD146 expression as MSC(AT) reached D12 of encapsulation (Fig. **III-**4C). However, this MFI rise was not

enough to give rise to a positive population or subpopulation, with MSC-FBS and MSC-HPL maintaining their negative expression (Fig. III-3C).

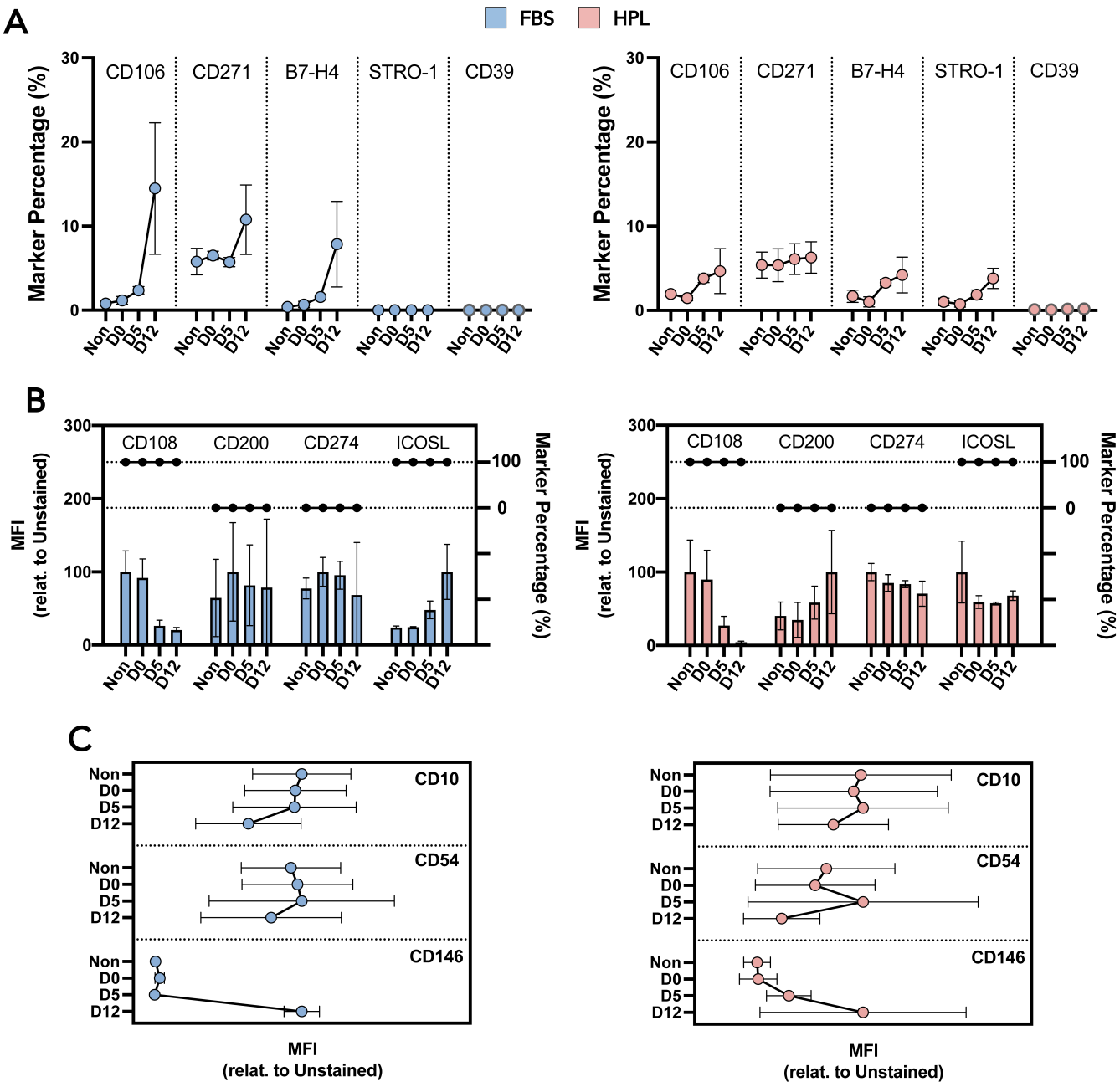

Figure III-4. Characterization of MSC(AT) immunosuppression potential and clonogenic ability. (A) – Subpopulation immunosuppressive and clonogenic marker expression for MSC-FBS (left) and MSC-HPL (right). (B) – Homogeneous immunosuppressive and clonogenic populations with marker percentage and median fluorescence intensity (MFI) levels, MSC-FBS (left) and MSC-HPL (right). Interconnected dots – marker percentage; bars - MFI (C) – MFI analysis for motility (CD10), translocation (CD54) and hematopoietic support-related (CD146) markers for MSC-FBS (left) and MSC-HPL (right). Non – non-encapsulated; (Three MSC(AT) donors; mean ± SEM).

MSC(AT) preserved their identity during encapsulation, as a homogeneous population for the set of markers analyzed. For MSC-FBS and MSC-HPL, numerous functional branches were explored and shown to be stable during storage at hypothermic temperatures.

III.4.4. *Encapsulation time did not impact the hematopoietic support capacity of MSC(AT)*

A hematopoietic support assay was proposed as a potency/functional assay for mesenchymal stromal cells (MSC) and was used to further evaluate the functionality of encapsulated cells (Fig. **III-**5A). Hematopoietic stem and progenitor cells (HSPC) from umbilical cord blood (CB) (HSPC(CB)), known for expressing CD34, were sorted and co-cultured with a feeder layer (FL) of MSC(AT). *In vitro* expansion of HSPC(CB) within this co-culture system was evaluated with MSC(AT) as feeder layers (MSC FL) from each encapsulation timepoint and MSC expansion medium. Each HSPC(CB) expansion had an internal control, where HSPC were cultured without an MSC FL.

Concerning the expansion fold change (FC) in total nucleated cells (TNC), no statistical differences were found between FL made by non-encapsulated MSC(AT) and encapsulated MSC(AT) (Fig. **III-**5B). Non-encapsulated MSC(AT) were able to support the expansion of HSPC(CB) up to a normalized 1.8-fold and 1.5-fold, for MSC-FBS and MSC-HPL respectively. This advantage in expanding HSPC with a FL co-culture was never lost, even though FL were prepared with MSC(AT) with increasingly longer encapsulation times. However, a slight decreasing trend appears to be present, apparently causing the FL advantage to shorten (Fig. **III-**5B).

Cell metabolism during HSPC(CB) expansion was also followed to detect any possible changes in MSC behavior due to encapsulation. Here, due to the nature of a co-culture, both MSC and HSPC contributed to the metabolic dynamics observed. In both profiles, glucose and lactate, co-culture led to more exhausted media due to its inherent higher cell number in culture than its control without FL (Fig. **III-**5C). Whether looking at glucose consumption or lactate production, co-culture of hematopoietic progenitors with MSC-FBS or MSC-HPL from the different encapsulation timepoints appeared to be very similar and did not seem to point to any metabolic changes. Quantification of metabolic rates confirmed that, metabolically, MSC(AT) FL established from previously encapsulated cells did not change their properties with the encapsulation process or encapsulation time (Fig. **III-**5D).

The impact of an MSC(AT) FL on the *ex-vivo* expansion of HSPC(CB) was further explored by identifying and quantifying different hematopoietic populations. Cell populations with ever increasing stemness were tracked ($CD34^+$, $CD34^+CD45RA^-$ and $CD34^+CD45RA^-CD90^+$) by immunophenotyping (Fig. **III-**6A).

Feeder layers formed by released MSC(AT), either MSC-FBS or MSC-FBS, had comparable impact on CD34 expression of expanded HSPC. Both types of FL caused decreasing trends as time of MSC encapsulation increased, with MSC-HPL FL, specifically, having an expression decline from close to 60% down to around 40% (Fig. III-6B). Interestingly, when looking to the expansion levels (FC), $CD34^+$ cells increased their numbers in a similar fashion between all conditions (encapsulation time and MSC expansion medium), namely around normalized 2.4-fold (Fig. III-6C).

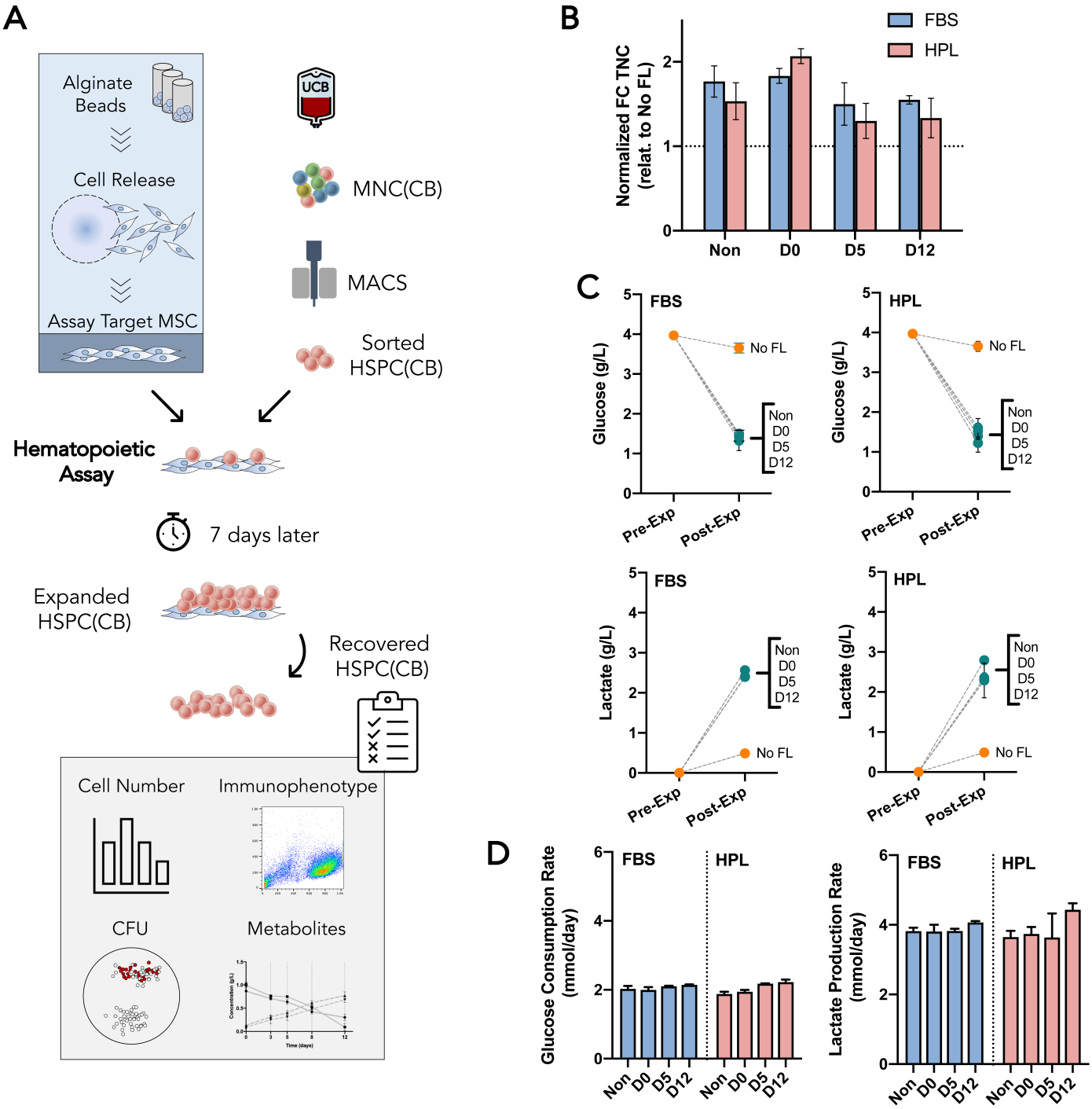

Figure III-5. *Hematopoietic support assay for MSC(AT) potency/function. (A) – Experimental layout. Non-encapsulated and released MSC(AT) are replated as a feeder layer to investigate their hematopoietic support capacity. Umbilical cord blood-derived hematopoietic stem and progenitor cells (HSPC(CB)) were isolated by magnetic activated cell sorting (MACS) and seeded onto the MSC(AT) feeder layer. After 7 days in a co-culture setting, expanded HSPC(CB) are harvested and analyzed concerning cell number, immunophenotype, metabolic activity and differentiation potential by colony forming unit (CFU) assay. (B) – Mean fold change (FC) in total nucleated cell (TNC) number after HSPC(CB) expansion normalized to the control condition (HSPC(CB) expanded without an MSC(AT) feeder layer; No FL). (C) – Glucose (top) and lactate (bottom) concentration profiles for co-cultures of HSPC(CB) and MSC-FBS (left) and MSC-HPL (right). (D) – Glucose consumption (left) and lactate production (right) rates during hematopoietic expansion. No FL – control condition without an MSC(AT) feeder layer; Non – non-encapsulated (Three MSC(AT) donors; mean ± SEM).*

Progenitor population $CD34^+CD45RA^-$ had post-expansion percentages with no considerable differences concerning increased MSC encapsulation time. On the other hand, expansion levels (FC) for $CD34^+CD45RA^-$ cells oscillated, with reduced levels for FL prepared with MSC(AT) encapsulated for longer periods. Concerning the more primitive HSPC population, $CD34^+CD45RA^-CD90^+$, with a percentage before expansion of around 7%, no obvious differences in post-expansion percentages were noticed. D12 for MSC-HPL seems to contribute towards a decreasing trend, reaching a positive percentage of 0.9% (Fig. **III-**6B). Overall, expansion FC followed suit, however D12 for MSC-HPL became the only condition with a significant decrease, being under the normalization line (Fig. **III-**6C).

To take advantage of the dynamics of CD34 expression, where the loss of CD34 during the expansion is gradual and continuous, median fluorescence intensity (MFI) of CD34-expressing cells at the end of each expansion was also followed (Fig. **III-**6D). No significant distinctions could be made between encapsulation conditions for both MSC-FBS and MSC-HPL.

The colony-forming unit (CFU) assay, which tests the myeloid differentiation potential of HSPC, was performed as part of the hematopoietic support assay. While cell culture without MSC FL typically originates an equal share of colony-forming unit granulocyte-macrophage (CFU-GM) and CFU-multilineage (CFU-Mix) for the expanded CB cells, the co-culture system increases the proportion of CFU-GM[109,124]. This difference was used to detect any loss of function by MSC(AT) during encapsulation. MSC-FBS were able to maintain this difference throughout the multiple encapsulation timepoints (Fig. **III-**6E). Coherent with the results concerning the percentage of $CD34^+$ and $CD34^+CD45RA^-CD90^+$ cells, D12 for MSC-HPL also shows a slight increase in the proportion of CFU-Mix.

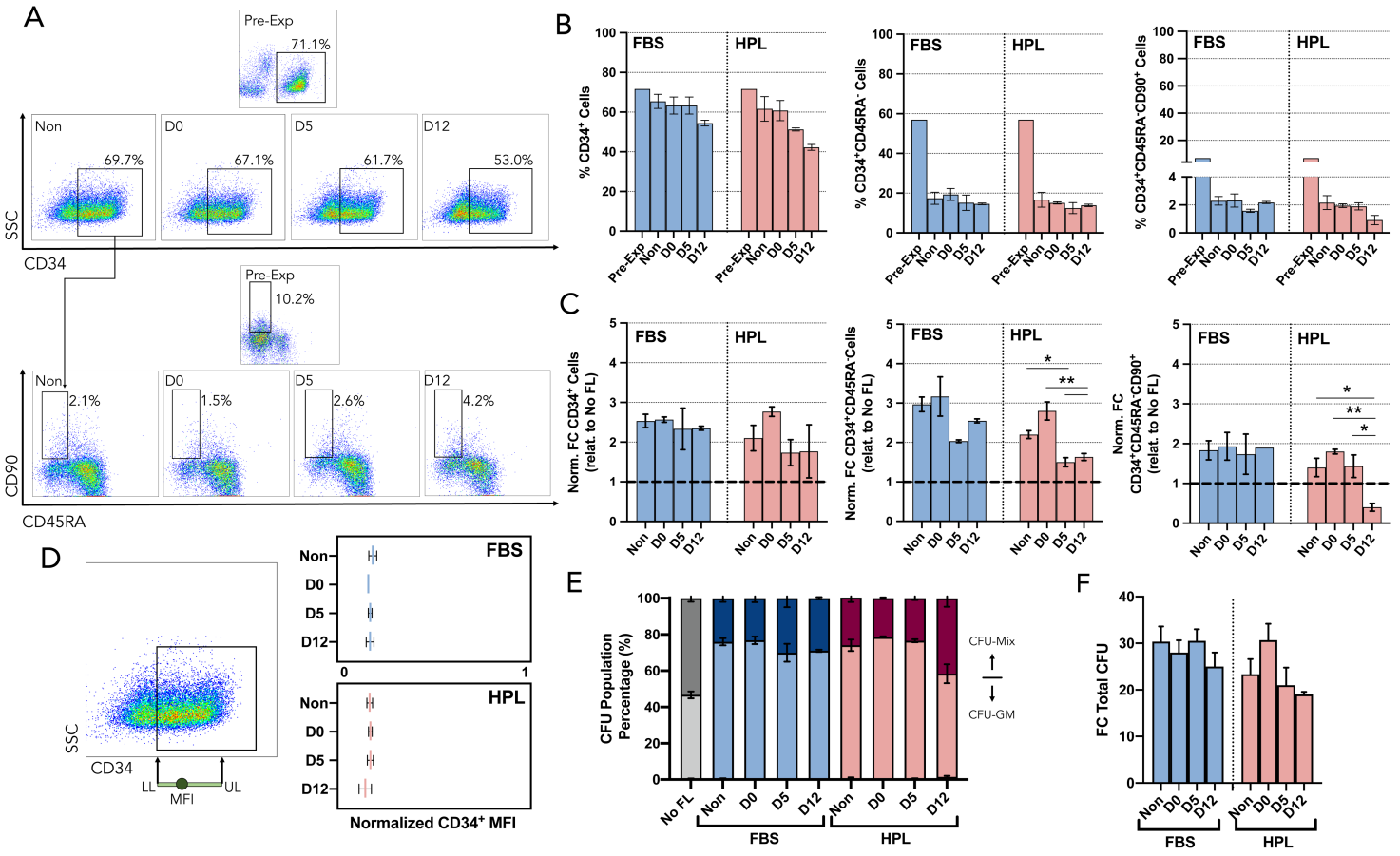

Figure III-6. *Immunophenotype and clonogenic potential (CFU) of hematopoietic stem/progenitor cells co-cultured with MSC(AT). (A) – Representative dotplots showing the gating strategy used for identification of different HSPC populations before expansion (Pre-Exp) and after expansion using released (D0, D5, D12) or non-encapsulated (Non) MSC(AT) as feeder layers. Live HSPC were gated on forward scatter (FSC) versus side scatter (SSC), followed by the use of a viability dye. Then, CD34 expression was identified (top) and, to explore the remaining populations, CD45RA and CD90 expression were also investigated (bottom). (B) – FC of normalized CD34⁺ (relative to the control No FL) (left), CD34⁺CD45RA⁻ (center) and CD34⁺CD45RA⁻CD90⁺ (right). (C) – Percentage of CD34 expression (left), CD34⁺CD45RA⁻ (center) and CD34⁺CD45RA⁻CD90⁺ (right). (D) – Quantification of CD34 loss after expansion. Mean fluorescence intensity (MFI) of CD34⁺ expression was quantified and normalized by the width of the positive CD34 population. (E) – CFU population percentage. Neglectable burst-forming unit-erythroid (BFU-E) led to mainly two populations, colony forming-unit granulocyte (CFU-GM) and colony forming-unit multilineage (CFU-Mix). (F) – FC in total CFU number after HSPC expansion using FL from encapsulated and non-encapsulated MSC(AT), previously expanded in FBS or HPL supplemented medium. No FL - control condition without an MSC(AT) feeder layer; Non – non-encapsulated; SSC – Side scatter; LL – Lower limit; UL – Upper limit (Three MSC(AT) donors; mean ± SEM).*

Nevertheless, FC in total CFU number of expanded HSPC show that levels obtained by co-culturing them with encapsulated MSC(AT) were similar to co-culturing them with non-encapsulated MSC(AT) (Fig. III-6F).
Considering every MSC-related variable studied, encapsulated MSC(AT) demonstrated mostly preservation of identity and functionality for the different encapsulation periods tested (Fig. III-7).

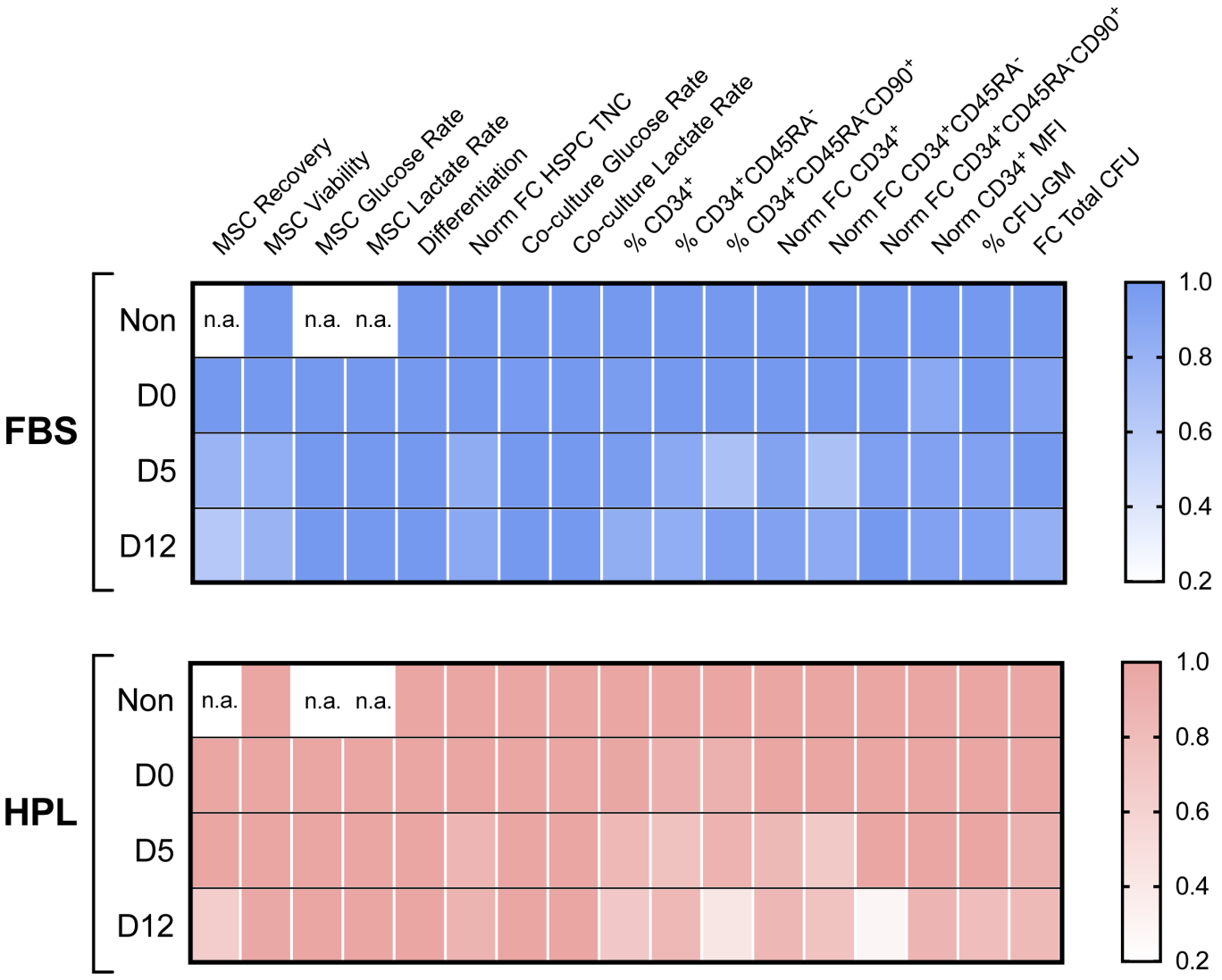

Figure III-7. *Heatmap score of MSC(AT) encapsulation. Key variables were put side-by-side to perform a comprehensive comparison between encapsulation timepoints for MSC-FBS (top) and MSC-HPL (bottom). Each variable was individually normalized by the value of non-encapsulated cells or D0, when non-encapsulated cells were not available. Differentiation was set to 1 for every timepoint, as every differentiation was successful. Non - non-encapsulated; Glu – Glucose; Lact – Lactate; Norm – Normalized; FC – Fold Change; MFI – Median Fluorescence Intensity; n.a. – not applicable (Three MSC(AT) donors; mean).*

III.5. Discussion

Cell and gene therapies (CGT) are becoming a new reality for treatment for multiple diseases, from cancer to auto-immune conditions[392]. With their approval gaining traction, tens of novel cell and cell-derived products may enter the market in the next years[393]. This paradigm shift, from traditional biopharmaceuticals to innovative CGT, has unlocked more powerful therapeutic means to tackle diseases. As we gain more specificity (e.g. CAR-T or CAR-NK targeting a particular tumor) or take advantage and augment existing cellular processes (e.g. mesenchymal stromal cells (MSC) for immunoregulation of auto-immune-derived wounds), the complexity involved in the manufacturing of these products has skyrocketed[122]. The existence of technical challenges in the development of functioning production processes for CGT have led to threats against their commercial viability[122]. Since the production cost has a direct influence on the price tag of the final approved therapy, CGT risk reaching unrealistic prices upon reaching the market.

Tackling these challenges has made production cost reduction a key priority for the field. Determining the cost of goods (COGs) for the entire manufacturing pipeline is an efficient way to map production costs and uncover optimization opportunities. Knowing this challenge exists for the entire production pipeline, with this study, we focused our ambition on impacting Product Storage and Distribution. Although the amount of COGs studies has been limited and the uniqueness of each CGT manufacture makes it hard to generalize, therapy distribution has been said to account for up to 20% of the total manufacturing cost[285]. The costly burden of these two process steps, Storage and Distribution, can be partially justified by the use of cryopreservation (i.e. preservation at ultra-low temperatures, below -130°C) as the standard storage strategy for cellular therapeutics.

Cell cryopreservation can be considered a double-edged sword. On one hand, it makes it possible to stop biological time for large periods, thereby extending the lifespan of cellular products and maintaining their properties in an unaltered state. On the other hand, cell recovery from thawing has been a longstanding issue when handling cells. Post-thaw damage to cells is multifaceted and its impact varies depending on the cell type. For MSC, cryopreservation has been thoroughly reviewed and multiple studies have shown negative effects on viability, amount of apoptosis, attachment and metabolism[394]. Furthermore, a growing concern in CGT is a cryo-stun effect after thawing. This effect appears to have a special relevance for MSC, since it is suspected to be a possible cause for the lack of success in their initial clinical trials[395]. Cryo-stun is a cell state where thawed cells display reduced potency or a dysfunctional phenotype. Differences between fresh and thawed MSC (e.g. cell growth, differentiation and bioactivity) have been reported and reviewed[384]. Most of these adverse effects due to

cryopreservation have been shown to be temporary and were recovered after being cultured *in vitro* (i.e. cryorecovery or revitalization)[384]. Nevertheless, these strategies require additional costly and time-consuming handling before infusion and may be unrealistic at a large scale.

Cell encapsulation proposed herein completely circumvents the challenges of cryopreservation by having working temperatures that overlap room temperature (RT) range (i.e. between 10°C and 20°C). This advantage can effectively eliminate an entire bioprocessing stage. By being currently available in the market and having an affordable price range, BeadReady™ contributes towards making this technology readily available for potential CTG developers. In addition, to facilitate full implementation by clinicians, a straightforward cell release step is available, involving a single solution exchange. Expensive and energy-consuming cryostorage equipment would no longer be necessary, along with qualified labor with certification for handling cryogenic gases. Although temperature-controlled containers with real-time temperature tracking would still be necessary to ensure the storage range is maintained, the distribution and supply chain model would change drastically, since only a handful of companies dominate the market of cryo-temperature distribution (e.g. Marken or Cryoport)[396]. The ability to ship and distribute at warmer temperatures would open up a significant range of previously ineligible companies as potential partners.

COVID-19 vaccines were just the latest example of the benefits of such a considerable shift. While first-to-market Pfizer required its vaccine to be distributed and stored at temperatures between -60°C and -80°C, demanding serious logistical maneuvering, the latter approval of a vaccine from Johnson & Johnson facilitated vaccine availability, needing only temperatures between 2°C and 8°C[397]. In **our** case, the difference in temperature ranges is even higher (from below -130°C to between 10°C and 20°C), having the potential to cause a very disruptive change in CGT logistics and supply chain. Indeed, we showed adipose tissue-derived MSC (MSC(AT)) were able to survive encapsulated up to 12 days. By being able to do so with an adherent cell type (which normally require surface adhesion and anchorage cues to survive), we unleash the potential of this method and this commercial kit for other non-suspension cells. Although we did observe a decline in the recovery percentage over time, values are similar to MSC thawing recovery by cryopreservation (around 75%)[398,399]. Importantly, cell viability was maintained over 70% throughout all timepoints and conditions. MSC(AT) were able to withstand warmer temperatures, showing few signs of deteriorating cellular health. Since cryo-temperatures were not present to halt cell metabolism, glucose consumption and lactate production were followed to determine the metabolic state of encapsulated MSC(AT) and their role in sustaining them over time. MSC(AT) expanded in fetal bovine serum (FBS)-supplemented medium (MSC-FBS) and MSC(AT) expanded in human platelet lysate (HPL)-supplemented medium (MSC-

HPL) appear to coalesce in their metabolic profiles during encapsulation, evidencing only slight distinctions in glucose consumption and lactate production behavior. Both specific glucose consumption and lactate production rates of encapsulated MSC(AT) determined in this study were consistently lower than previously reported values for non-encapsulated cells. Whether for umbilical cord tissue-derived MSC cultured in human serum-supplemented medium[400], bone marrow-derived MSC cultured in FBS-supplemented medium[401,402], MSC(AT) cultured in a commercially available xeno-free medium[403] or MSC(AT) cultured in HPL-supplemented medium in a bioreactor system[404], reported specific metabolic rates are always, at least, one order of magnitude higher. Of note, encapsulated MSC(AT) were still subjected to a degree of hypothermic temperatures (i.e. between 10°C and 20°C, lower than the physiological 37°C). The fact of being stored at such temperatures, combined with increased diffusion limitations present in alginate encapsulation may explain a slower metabolic state for encapsulated cells. A slower cell metabolism is typically associated with cell preservation, benefitting the use of alginate encapsulation for MSC storage and transportation. Interestingly, a degree of nutrient exhaustion was present at D12, coinciding with lower values of cell recovery. Unlike for MSC-FBS, where a downward trend already was in place, MSC-HPL had their cell recovery levels stable until D12. Running out of available glucose may have been responsible for the observed loss of cell recovery, especially for MSC-HPL. Nutrient limitations should be considered, especially when defining the storage or transportation duration. Storage medium changes or higher initial glucose concentrations could be considered to potentially prevent reaching undesired nutrient and metabolite levels.

It is worth mentioning that, to better mimic actual transport or storage and test this encapsulation in a less ideal scenario, our temperature control allowed for natural oscillations inside the recommended range. Although temperature-controlled containers exist, temperature variations at some point of the process are expected and must be considered for risk assessment. Since MSC(AT) had such a promising behavior with temperature oscillations, under the conditions of our study, we can expect cells to have improved phenotype and functionality in cases where temperature control is tighter.

The use of alginate as an encapsulation material has always shown promise for applications in cell therapy, though so far has not been translated to a clinical scenario. With efforts being made at creating high-scale production strategies with cGMP compliance[405], alginate encapsulation may finally push through as a viable option for CGT. Some groups have explored hypothermic storage using alginate encapsulation. Human umbilical vein endothelial cells (HUVEC) were shown to maintain around 70% viability after 7 days of encapsulation[406]. After 3 days, 85% of encapsulated MSC(AT) were recovered and were able to reattach to a culture surface[388]. Encapsulated human

limbus-derived MSC were able to sustain 5 days of hypothermic temperatures, with a recovery of close to 65% and a viability of 77%[407]. Of note, these encouraging results with limbus-derived MSC led to a participation in an ongoing clinical trial (Identifier: CTRI/2021/07/035034). Our alginate encapsulation strategy led to similar or better values of recovery and viability for those specific timepoints. To our knowledge, this is the first study demonstrating the feasibility of having MSC(AT) encapsulated under hypothermic conditions up to 12 days.

Focusing on tackling translational challenges of alginate encapsulation, we investigated the effect of alginate encapsulation on MSC(AT) with FBS supplementation, a standard for MSC culture, and also HPL supplementation, a xeno-free alternative, more amenable to clinical translation. Validation of HPL over FBS as a next-generation supplement to improve clinical production of therapeutic MSC has been pursued by several groups and has been extensively reviewed[408]. In addition to eliminating the risk of potential immunogenicity and transmission of zoonotic diseases associated with FBS, HPL was overwhelmingly shown to increase MSC proliferation, while maintaining their immunophenotypic identity and differentiation potential[408]. However, HPL has also been associated with reduced MSC immunomodulation, caused by an altered secretome and impaired inhibition of T- and NK-cell proliferation[409,410]. Additionally, the hematopoietic support capacity of MSC was demonstrated to be negatively affected by HPL supplementation, being unable to retain certain hematopoietic stem and progenitor cell (HSPC) populations[124]. In our study, cells maintained in HPL-containing medium had slightly better encapsulation recovery and viability over time compared to FBS-based medium, and comparable performance concerning the remaining assays. Cell encapsulation for MSC transportation and storage has been proven to be compatible with an animal component-free culture supplement, contributing towards a fully CCMP-compliant MSC manufacturing process and promoting its use in a clinical setting.

However, the use of cell encapsulation as a complete substitute for cryopreservation in any scenario may not be realistic. MSC-based therapies are typically allogeneic, which enable an off-the-shelf production model. Cell storage in such cases, largely exceeds our 12-day period, requiring cryopreservation. Our verified encapsulation model would not be exploitable in such circumstances. However, even if an allogeneic model is used in a particular therapy, the existence of the cryo-stun effect would require additional *in vitro* culture and subsequent transport to the therapeutic facility. Here, alginate encapsulation would be able to be complementary to cryopreservation instead of substituting it completely. Therefore, applicability of this specific cell encapsulation method has the potential to be widespread, being appropriate for both allogeneic and autologous scenarios.

When evaluating this commercially available alginate-based encapsulation kit, we sought to confirm whether MSC(AT) identity and function were preserved throughout their encapsulation. The need for reliable MSC functional or potency assays is a long-standing issue in the field[107,411]. Depending on the therapeutic goal, MSC therapies might require different readouts of potency. Taking this into consideration, the development of a set of assays, instead of relying on a single one, encompassing most of the therapeutic value of MSC (i.e., immunomodulation, tissue regeneration, homing, etc.) may be the future for MSC manufacturing. Such matrix of assays has been proposed and is still being refined[412,413]. In order to contribute to the efforts of establishing a potency matrix platform for clinical-grade MSC, we propose a novel hematopoietic support potency assay. MSC-HPSC co-culture is considered one of the main expansion platforms for clinical HSPC[414] and is currently in the clinical trial pipeline[218]. MSC also have a supportive role in hematopoietic cell co-transplants, assisting engraftment of transplanted HSPC and reducing conditioning-related bone marrow inflammation[415]. In this co-culture system, MSC feeder layers (FL) were shown to confer HSPC an advantage during their expansion, in comparison with systems that only use exogenous cytokines[109,416]. This hematopoietic support ability of MSC can be quantified and used as an indicator for MSC potency or function. Our group has an extensive background with this co-culture expansion system and has contributed towards its translation potential[109,124,204,301,324–327,417]. Our proposed hematopoietic support assay has the advantage of having multiple quantifiable readouts (e.g. HSPC expansion fold change, metabolite quantification, HSPC immunophenotype and percentages of colony-forming unit (CFU) populations) and an internal control (i.e. HSPC expansion only with exogenous cytokines). In our case, taking together all the assay readouts, MSC(AT) from both expansion media demonstrated that their encapsulation did not have an impact on their functional properties related with hematopoietic support. With this precedent, we consider the MSC potency matrix could only benefit from including the hematopoietic support assay in its ranks.

By unblocking access of Product Storage and Transportation to alginate encapsulation, we lay the ground for more ambitious goals. The development of an entire cell therapy manufacturing process using encapsulated cells may now be possible. This *all-in-one* strategy would allow MSC or other cell types to remain encapsulated from an initial manipulation step to the final infusion into the patient. Both cell manipulation and clinical administration of encapsulated cells have been widely explored for a great variety of applications. However, a bridge between these process units has been lacking. Concerning cell manipulation, 3D-expansion of MSC(AT) in alginate core-shell capsules has been shown to be possible, obtaining a modest 2.5-fold increase after 4 days[418]. Paracrine activity of MSC was also proven to be compatible with alginate encapsulation, with angiogenic and chemotactic factors being measured from

encapsulated MSC[419]. Genetic manipulation of MSC in alginate beads, to direct their phenotype to a more osteogenic or chondrogenic state as a cartilage or osteochondral tissue engineering approach, was likewise successfully demonstrated[420]. These examples validate the compatibility between alginate encapsulation and the different therapeutic avenues of MSC. In what concerns administration into patients, alginate has a substantial clinical safety record[421]. Alginate-based islet and **β**-cell encapsulation has had success in enabling *in vivo* glycemic control in Type 1 diabetes models, with several novel encapsulation systems currently in clinical trials[379,422]. Besides being safe and biocompatible, alginate encapsulation can also potentially address some of the challenges in MSC translation, namely lack of cell retention. *In vivo* presence of encapsulated immunomodulating MSC was substantially increased after intravenous injection in mice[423]. In a myocardial infarction mouse model, encapsulated MSC were detected in higher numbers after 7 days, reducing scar formation and demonstrating a superior angiogenesis when compared to free MSC[424]. Overall, our study has significantly contributed towards the feasibility of bridging cell manipulation and infusion using alginate encapsulation, making it possible for encapsulated cells to be temporarily stored and transported at convenient temperatures from their manufacturing and manipulation sites to their therapeutic administration.

IV. A Translational Toolbox for Tracking Hematopoietic Stem and Progenitor Cells in Cell Therapy Products

IV.1. Summary

With an increasing number of CGT reaching the market, therapy manufacturing quality must be assured. Cell potency or function are a direct measure of product quality and should be efficiently monitored. Assays to rigorously quantify potency in CGT are underdeveloped, putting therapy viability in jeopardy. The small number of existing assays that evaluate HSPC function, are limited to low dimensional cell features (e.g. surface marker expression). Consequently, such assays grant a very narrow understanding of the cell state and also are more susceptible to dissociations between assay readouts and actual cell potency due to *in vitro* culture artifacts. Highly dimensional techniques (i.e. transcriptomics and infrared spectroscopy) were evaluated as tools to better track HSPC after *ex vivo* expansion using different systems (i.e. static liquid culture, static MSC(M) co-culture and dynamic liquid culture). Current low dimensional functional assays were also compared with these novel techniques, to assess their possible replacement as HSPC function readouts. Transcriptomic profiling was able to differentiate expanded HSPC from their freshly isolated counterparts, and both techniques were able to distinguish each of the three expansion systems. Transcriptomic clusters showed a lower distance between MSC(M) co-culture and freshly isolated cells, with k-means distances of 126 for MSC(M) co-culture, 139 for static liquid culture and 145 for dynamic liquid culture. Comparison with transcriptomic data from publicly available HSPC expansion datasets demonstrated that transcriptomics can be used to thoroughly assess different expansion strategies. Manufacture of expanded HSPC products for CGT would significantly benefit from including transcriptomics and spectroscopy in their quality control guidelines. A more comprehensive view of cell machinery can also improve our understanding of the therapeutic mode of action, allowing more efficient monitoring of CGT product quality.

IV.2. Background

Cord blood (CB) has established itself as a main source of hematopoietic stem and progenitor cells (HSPC) for hematopoietic cell transplants (HCT) to treat a variety of hematological diseases[425]. Although its use has recently slightly declined[425], CB continues to be the most attractive source for an Advanced Therapy Medicinal Product (ATMP) production model. Since CB requires no invasive procedure to harvest and has desirable availability as a raw material, tissue procurement is facilitated[426]. However, an inherent limitation of CB is the lower population of native HSPC, with single CB units only being able to treat pediatric patients. *Ex vivo* expansion of HSPC has seen immense progress in becoming a viable solution for this drawback[414]. Different strategies have been successful in increasing HSPC number while maintaining their main function for

transplantation, being able to reconstitute an entire hematopoietic system long-term. Small molecules (e.g. UM171 or SR-1), exogenous cytokines (e.g. SCF or Flt-3L), induction of Notch signaling or co-cultures with feeder cells (e.g. endothelial cells or mesenchymal stromal cells (MSC)) have contributed to broaden the spectrum of options for *ex vivo* HSPC expansion[414]. Clinical application of *in vitro* expanded HSPC for HCT is within reach, as multiple expansion systems are advancing the clinical trial pipeline[427]. Our group has contributed significantly to the development and improvement of HSPC(CB) expansion through co-culture with MSC. By establishing serum-free co-culture systems[204,324], optimizing cytokine cocktails used in those systems[109,428] or investigating the impact of oxygen levels[417] and MSC sources[124] on HSPC expansion, we have continuously pursued a better translation of *ex vivo* HSPC(CB). Of note, co-culture with MSC has been the focus of three different clinical trials (*NCT00498316* - Phase I, DUCBT for myelodysplastic syndrome and leukemia; *NCT01624701* – Phase I/II, DUCBT for hematological malignancies; *NCT0309682* - Phase II, DUCBT for hematological malignancies)[427].

To date, non-manipulated or minimally manipulated HSPC isolated from whichever source must fulfill a stringent set of criteria to be selected for infusion into patients during HCT[90]. While selection of bone marrow (BM) and mobilized peripheral blood (mPB) donors mainly rely on HLA-matching, CB units must also reach cell dose targets to be selected. Yet, HSPC potency has been missing as a measure in current transplantation guidelines. While some CB banks have started to incorporate potency assays in their unit quality control, this practice is far from being standardized[429]. As manipulation of HSPC becomes an available clinical option through Advanced Therapy Medicinal Products (ATMP) (i.e. *ex vivo* expansion, genetic modification or improvement of homing capabilities), HSPC potency will gain an indisputable role in assuring cell product quality[430]. A survey conducted by the American Association of Blood Banks (AABB) – International Society for Cell and Gene Therapy (ISCT) Joint Working Group was able to tally HSPC potency assays currently performed in CB banks[431]. Of those who have a potency assay, 56% of CB banks mentioned the use of the colony-forming unit (CFU) assay for potency quantification. Semi-quantitative readouts of the CFU assay, where HSPC are cultured for two weeks in a methylcellulose-based medium to assess the formation of different myeloid colonies, are mainly based on manual colony classification. Quantification of 7AAD-viable $CD34^+$ cells was reported by 53% of CB banks, being a flow-based method. Levels of aldehyde dehydrogenase (ALDH) and actual engraftment in patients were also mentioned by a few CB banks (5% each).

With regulatory approval of expanded HSPC products in sight, ATMP quality control, especially through potency assessment, continues alarmingly underdeveloped[432]. In case of HSPC(CB), few potency assays currently exist and none is a front-runner to becoming a gold standard[431]. While the CFU assay determines HSPC differentiation

potential, which is essential for reconstitution of the hematopoietic system after transplantation, it takes significant time until readouts are available and colony classification can be subjective and prone to operator-derived variability. For viable $CD34^+$ cell quantification, although CD34 is the most notable marker for clinical HSPC[15] and its determination is fast and simple to perform, no direct HSPC functional property can be measured. Quantification of ALDH levels also benefit from the speed of a flow-based method and a correlation has been found with CFU readouts[433], but once more do not directly evaluate cellular function. These issues with potency testing add to worries that surrogate markers commonly associated with therapeutic function in freshly isolated cells may be not valid for expanded HSPC[173,434]. Thus, ideal tracking of HSPC potency remains elusive and must be pursued for future manufacture of expanded HSPC products[435].

In order to tackle the gap in monitoring HSPC potency, we explored three different expansion systems (i.e. static liquid culture with cytokines, static co-culture with MSC, dynamic liquid culture in a spinner flask) and expanded HSPC were subjected to total RNA-seq. We propose using transcriptomic data as a novel tool to track HSPC potency, potentially giving rise to a new surrogate assay. Transcriptomic profiles of expanded HSPC and non-expanded $CD34^+$ cells were determined and compared with publicly available datasets of other *ex vivo* expansion strategies.

IV.3. Methods

IV.3.1. *Human Tissues*

Femur BM samples were obtained through collaboration agreements between Institute for Bioengineering and Biosciences (iBB) at Instituto Superior Técnico (Lisbon) and Centro Clínico da GNR (Lisbon), respectively. BM samples were collected from healthy donors and with informed consent following the Directive 2004/23/EC of the European Parliament and of the Council of 31st of March 2004 on setting standards of quality and safety for the donation, procurement, testing, processing, preservation, storage and distribution of human tissues and cells, represented in the legal framework of Portuguese legislation by Law n°22/2007 of 29th of June. CB units were obtained as described in Chapter II (II.3.1).

IV.3.2. *CB Mononuclear Cell (MNC(CB)) Isolation*

MNC(CB) were isolated as described in Chapter II (II.3.2).

IV.3.3. *$CD34^+$-Enrichment from MNC(CB)*

$CD34^+$ enriched cells were sorted as described in Chapter II (II.3.3)

IV.3.4. *Bone Marrow-Derived MSC (MSC(M)) Feeder Layer (FL) Preparation*

Isolated MSC(M) from femur BM were obtained from the Stem Cell Engineering Research Lab (SCERG) cell bank at iBB, Instituto Superior Técnico, Lisbon. Cell isolation, expansion, characterization according to ISCT standards and preservation were performed through previously established protocols[329]. A single MSC donor was used to isolate HSPC variability in the study and mimic an allogeneic universal MSC donor. Cryopreserved MSC(M) were thawed and seeded at 3000 cells/cm^2 in DMEM supplemented with 5% (v/v) human platelet lysate (HPL) UltraGRO™ (kindly provided by AventaCell Biomedical Corp.) and 1% (v/v) A/A. After a revitalization passage, MSC(M) were passaged into 12-well plates. After reaching confluence, MSC(M) were growth arrested by Mitomycin C (Sigma) treatment. Cells were incubated with their culture medium supplemented with 0.5 µg/mL Mitomycin C for 2-3 hours. After treatment, inactivated FL were washed three times with culture medium to eliminate any residue of the treatment solution and stored in the incubator with fresh culture medium.

IV.3.5. *Ex Vivo Expansion of HSPC(CB)*

$CD34^+$-enriched cells were expanded using three different expansion systems, namely static liquid culture, static co-culture with MSC(M) and dynamic liquid culture in a StemSpan™ spinner flask (STEMCELL Technologies). Each expansion was performed using StemSpan™ SFEM II (STEMCELL Technologies) supplemented with 1% A/A and previously optimized cytokine cocktails (PeproTech)[109]. For expansions performed in static systems (i.e. liquid culture and co-culture with MSC(M)), HSPC(CB) were suspended in 2 mL of complete expansion medium (50 000 cells/mL) and seeded in 12-well plates at an initial concentration of 100 000 cells/well. In case of the static co-culture expansion, MSC(M) culture medium was removed from inactivated FL beforehand and HSPC(CB) were carefully seeded on top. For HSPC(CB) expansion in dynamic conditions, cells were suspended in 25 mL of complete expansion medium (50 000 cells/mL) and seeded into silicon-treated spinner flasks with continuous agitation set to 30 rpm. Sidearm caps were loosened to allow gas exchange during culture. HSPC(CB) were expanded over a 7-day period at 37°C and 5% CO_2 in a humidified atmosphere (Fig. 1). After HSPC(CB) expansion and cell recovery, conditioned medium samples were taken from each experimental condition. Medium samples were centrifuged at 360 g for 10 minutes and the respective supernatant was transferred to a new tube and stored at -80°C for future use.

IV.3.6. *Proliferation Assay*

For static expansion systems, after 7 days, adherent and non-adherent expanded HSPC were harvested using forced pipetting (with extra care for co-cultures to avoid lifting the MSC(M) feeder layer). For dynamic expansion, daily samples of 300 µL were taken from the spinner flask. When cell concentration was low, samples were centrifuged and resuspended in smaller volumes. Total nucleated cell (TNC) number was determined with the Trypan Blue (Thermo Fisher Scientific) exclusion method. Fold change (FC) in TNC was calculated by dividing the number of expanded cells by those initially seeded (i.e. 100 000 cells – static systems; 750 000 cells – dynamic system).

IV.3.7. *Glucose and Lactate Profiles*

Glucose and lactate concentrations were detected as described in Chapter III (III.3.4).

IV.3.8. *CFU Assay*

CFU assay was performed as described in Chapter II (II.3.8).

IV.3.9. *Cobblestone Area Forming-Cells (CAFC) Assay*

CAFC assay was performed as described in Chapter II (II.3.9).

IV.3.10. *HSPC Immunophenotype*

Immunophenotype of freshly isolated and expanded HSPC was done as described in Chapter III (III.3.7.7).

IV.3.11. *Quantification of Aldehyde Dehydrogenase (ALDH) Activity*

To detect more primitive HSPC, a flow cytometry-based assay to detect aldehyde dehydrogenase activity was used with both non-expanded and expanded HSPC(CB). Cells were subjected to an ALDEFLUOR™ Kit (STEMCELL Technologies) and steps were followed as described by the manufacturer. Before acquisition, cell samples were also co-stained with CD34 to assure detection of more primitive HSPC.

IV.3.12. *Telomere Length Assay*

Evaluation of possible telomere erosion was done using the Telomere PNA Kit (Agilent), which is based on detecting fluorescence resulting from *in situ* hybridization. A FITC-conjugated probe that recognizes telomere sequences allows for relative quantification of telomere length (RTL). Signal of tested HPSC(CB) is compared to the signal of a

tetraploid control cell line (i.e. 1301 - human T-cell leukemia cell line), resulting in a RTL percentage. Assay instructions were followed as defined by the manufacturer.

IV.3.13. *Fourier-Transform Infrared Spectroscopy (FTIR)*

Conditioned medium samples were thawed in ice while transported Laboratório de Engenharia e Saúde at Instituto Superior de Engenharia de Lisboa (ISEL) in Lisbon, Portugal. Thawed samples were vortexed and triplicates of 25 µL were diluted and transferred to a 96-well Si plate, where they were dehydrated for 2.5 hours in a desiccator under vacuum (Vaccubrand). Prepared samples were acquired using a Vertex 70 FTIR spectrometer (Bruker). With a resolution of 2 cm^{-1}, spectra were built in transmission mode by scanning between 400 cm^{-1} and 4000 cm^{-1}. Background signal was removed from sample spectra by subtracting a control well without sample. Principal Component Analysis (PCA) was performed using the PCAtools package in R.

IV.3.14. *Bulk Total RNA Sequencing*

Total RNA was isolated from non-expanded and expanded HSPC(CB) using the High Pure RNA Isolation Kit (Roche), as instructed by the manufacturer. RNA samples were sent to a sequencing facility of Novogene (Beijing) for library preparation and paired-end 150 base pairs (bp) sequencing on a Ilumina NovaSeq 6000 platform. After alignment, gene counts were normalized with the DESeq2 package and PCA was obtained as abovementioned. Data clustering was calculated using k-means, with the kmeans function from the stats package. Differentially expressed genes (DEG) were determined with the DESeq function. DEG were defined as having an adjusted p-value lower than 0.05 and FC between studied conditions higher than four ($log_2(FC) > 2$). Gene ontology (GO) enrichment analysis was done through the enrichGO function. All ontologies were selected from the org.Hs.eg.db package. When applied, gene sets of hematopoietic progenitor populations were obtained from deep transcriptomic diversity analysis of human blood progenitors[436]. Batch effect from multiple datasets was compensated with the ComBat-Seq algorithm. Publicly available datasets used in this study have the following GEO accession number: **Small Molecule** dataset - GSE57299, **Valproic Acid** dataset - GSE110968 and **Zwitterionic** dataset - GSE85800.

IV.3.15. *Statistical Analysis*

Experimental data was analyzed using GraphPad Prism 8 software. Values are presented as the estimated mean ± SEM. Data normality was determined using the Shapiro-Wilk test. Parametric ANOVA was performed to detect significant experimental group

differences. Tukey multiple comparison test was used to identify which individual groups had statistical significance.

IV.4. Results

An array of HSPC(CB) expansion systems with clinical relevance, namely static liquid monoculture (**LC_Stat**), static co-culture with MSC(M) (**CO_Stat**) and dynamic liquid monoculture (**LC_Dyn**), was used to evaluate the feasibility of integrating transcriptomics in controlling cell quality during manufacture (Fig. IV-1). Additionally, cell transcriptome profiling was explored as a novel surrogate of HSPC functionality and as a useful tool to equitably compare different expansion systems. To begin reaching this objective, expanded HSPC generated from abovementioned systems were exhaustively assessed using traditional and well-established proposed identity and functional assays.

IV.4.1. *Established identity and functional assays can differentially characterize expanded HSPC from different systems.*

With an expansion period set to 7 days, without any manipulation or intervention in between, LC_Stat, CO_Stat and LC_Dyn were compared side-by-side. HSPC expansion capacity was determined by quantifying proliferation through FC in TNC. While LC_Stat and CO_Stat showed similar FC in TNC (47 ± 1 vs. 39 ± 4), HSPC(CB) expansion in LC_Dyn led to significantly inferior FC, about one fourth of the other two systems (Fig. IV-2A). A brief insight into the metabolic flux during expansion, by measuring glucose and lactate levels, showed distinct profiles for each expansion system (Fig. IV-2B). LC_Dyn had the lowest consumption of glucose and production of lactate, coherent with the lower FC in TNC. LC_Stat and CO_Stat were also distinguishable, with CO_Stat having the highest nutrient consumption and metabolite production. Of note, none of the studied expansion systems reached nutrient exhaustion after 7 days.

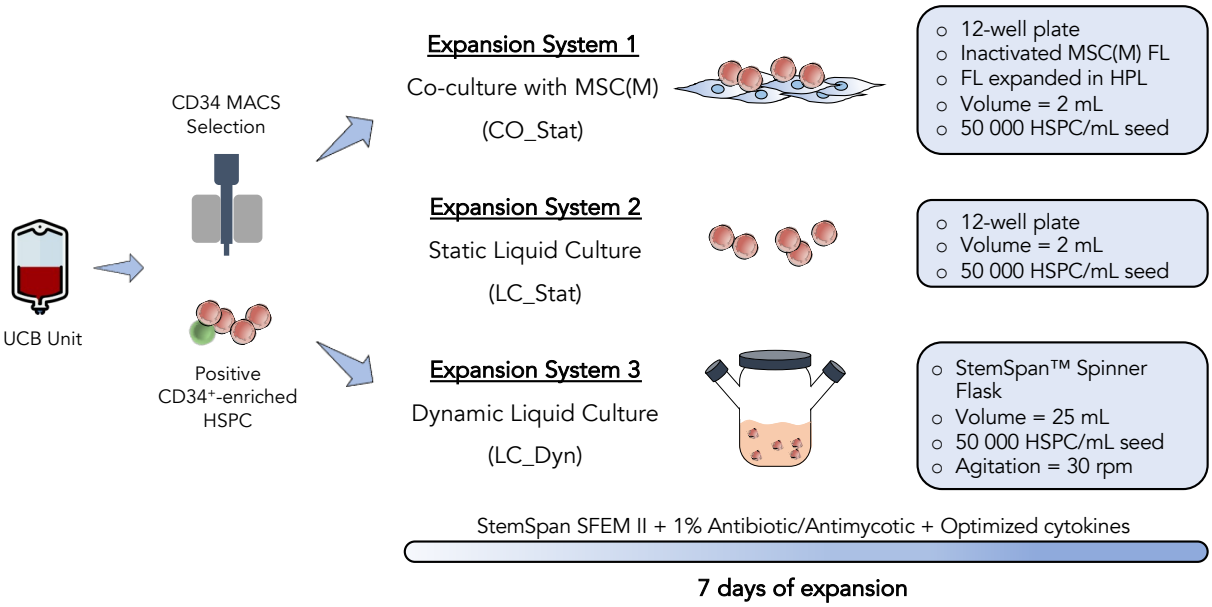

Figure IV-1. *Experimental design of studied expansion systems. Umbilical cord blood (CB) units were received after donor consent and mononuclear cells (MNC(CB)) were isolated before undergoing hematopoietic stem and progenitor cell (HSPC) enrichment. Magnetic activated cell sorting (MACS) through CD34 expression was performed, reaching an initial CD34⁺ percentage of 83 ± 4%. Enriched HSPC were used to seed three different expansion systems, namely co-culture with bone marrow-derived mesenchymal stromal cells (MSC(M)) **(CO_Stat)**, static liquid monoculture **(LC_Stat)** and dynamic liquid monoculture **(LC_Dyn)**. Initial HSPC concentration was 50 000 HSPC per mL of expansion medium. CO_Stat and LC_Stat were cultured in wells of a 12-well plate (2 mL each), while LC_Dyn was cultured in a StemSpan™ Spinner Flask (25 mL). Due to the different nature of each expansion system, CO_Stat had a growth inactivated MSC(M) feeder layer (FL) expanded in human platelet lysate (HPL)-supplemented culture medium previously prepared and LC_Dyn had a continuous agitation regimen of 30 rpm. HSPC expansion were performed in StemSpan SFEM II, supplemented with 1% (v/v) antibiotic/antimycotic and optimized exogenous cytokines during 7 days.*

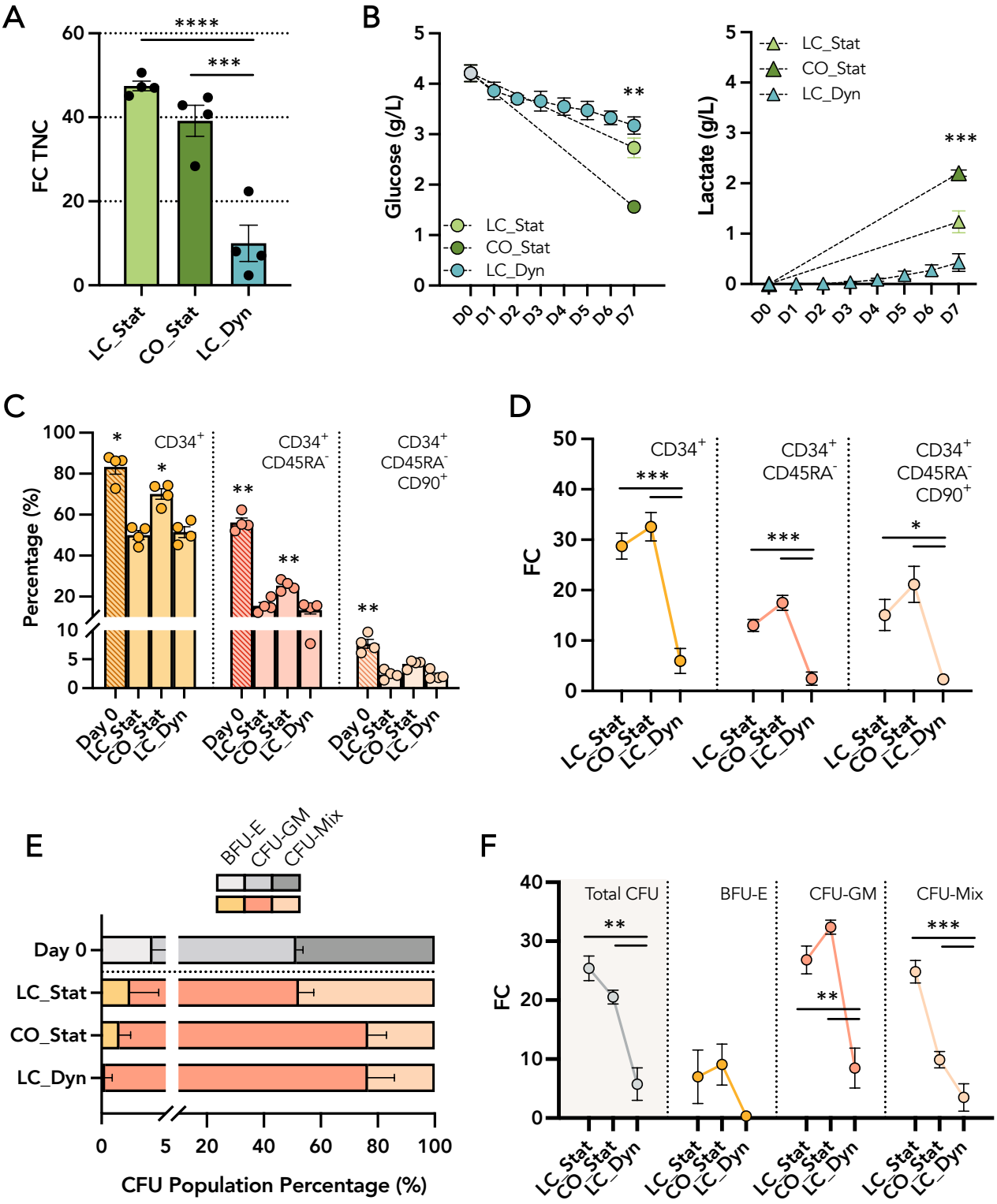
A
FC TNC
LC_Stat
CO_Stat
LC_Dyn
B
Glucose (g/L)
Lactate (g/L)
D0 D1 D2 D3 D4 D5 D6 D7
C
Percentage (%)
CD34+
CD34+ CD45RA-
CD34+ CD45RA- CD90+
Day 0
D
FC
E
BFU-E
CFU-GM
CFU-Mix
Day 0
CFU Population Percentage (%)
F
Total CFU
BFU-E
CFU-GM
CFU-Mix

*Figure IV-2. Characterization of expanded HSPC from three different expansion systems (i.e. CO_Stat, LC_Stat and LC_Dyn). **(A)** Fold change (FC) of total nucleated cell number (TNC) after a 7-day expansion. **(B)** Glucose (left) and lactate (right) profiles during expansion, measured in concentration (g/L). **(C)** Percentage of expression of several HSPC subpopulations (i.e. $CD34^+$, $CD34^+CD45RA^-$ and $CD34^+CD45RA^-CD90^+$) in the bulk expanded HSPC population and the initial CD34-enriched population (Day 0). **(D)** FC of each HSPC subpopulations after undergoing expansion with each different system. **(E)** Percentage distribution of multi-lineage colony-forming unit (CFU-Mix), burst-forming unit erythroid (BFU-E) and colony-forming unit granulocyte-macrophage (CFU-GM) colonies originated from colony-forming unit assays (CFU) of freshly isolated (Day 0) and expanded HSPC. **(F)** FC of CFU-Mix, BFU-E and CFU-GM colonies after expansion with CO_Stat, LC_Stat and LC_Dyn. Data was obtained from four different pools of CB units and values are represented by their mean ± standard error of the mean. * p-value < 0.05; ** p-value < 0.01; *** p-value < 0.001; **** p-value < 0.0001.*

Looking into specific subpopulations of HSPC with clinical relevance, $CD34^+$, $CD34^+CD45RA^-$ and $CD34^+CD45RA^-CD90^+$ cells were tracked by assessing population percentages and FC (Fig. IV-2C,D). HSPC(CB) enrichment before expansion led to an initial $CD34^+$ population with 83 ± 4% expression, whereas the expression of $CD34^+CD45RA^-$ and $CD34^+CD45RA^-CD90^+$ were 56 ± 2% and 8 ± 2%, respectively. CO_Stat was the best system at avoiding loss of CD34 expression during expansion, preserving 84% of CD34 expression. Here, LC_Stat and LC_Dyn exhibited lower levels of CD34 expression, resulting in a maintenance of only around 60% for both cases. Increased retention of relevant HSPC(CB) populations by CO_Stat was repeated for the remaining two subpopulations (i.e. $CD34^+CD45RA^-$ and $CD34^+CD45RA^-CD90^+$). Still, expanded HSPC(CB) from all systems were not able to completely retain hematopoietic subpopulations compared with Day 0. Marker loss for $CD34^+CD45RA^-$ and $CD34^+CD45RA^-CD90^+$ populations were at least half of the initial expression at Day 0 (for CO_Stat), being even higher for the other two. When evaluating the FC of each subpopulation, LC_Stat and CO_Stat always reached comparable values, although differences between the two systems, in case of $CD34^+CD45RA^-$ cells, were close to statistical significance (i.e. p-value = 0.06). In agreement with abovementioned results, LC_Dyn had the lowest FC for every subpopulation, reaching residual values for $CD34^+CD45RA^-$ and $CD34^+CD45RA^-CD90^+$ (i.e. 2 ± 1 for both).

Preservation of clonogenic capacity and differentiation potential in expanded HSPC(CB) was evaluated with the CFU assay. Freshly isolated CD34-enriched HSPC(CB) showed an equal distribution of CFU-GM and CFU-Mix colonies, with BFU-E colonies representing the remaining 4 ± 1% (Fig. IV-2E). Expanded cells from LC_Stat were able to more closely mimic the abovementioned CFU population distribution, albeit with a smaller percentage of BFU-E colonies (2 ± 1%). CO_Stat and LC_Dyn exhibited a

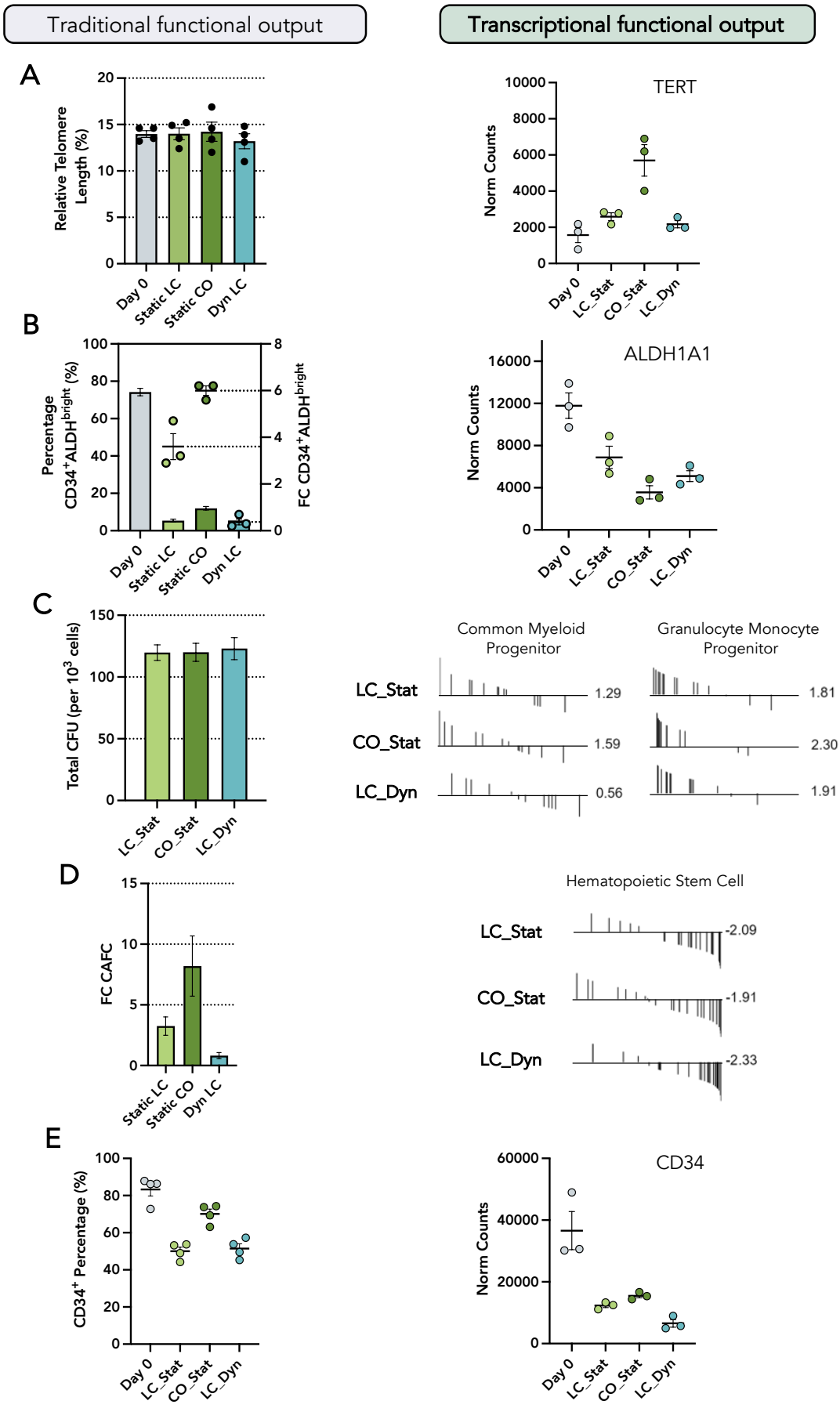
Traditional functional output
Transcriptional functional output
A
Relative Telomere Length (%)
Day 0
Static LC
Static CO
Dyn LC
TERT
Norm Counts
LC_Stat
CO_Stat
LC_Dyn
B
Percentage CD34+ALDHbright (%)
FC CD34+ALDHbright
ALDH1A1
C
Total CFU (per 10^3 cells)
Common Myeloid Progenitor
Granulocyte Monocyte Progenitor
1.29
1.59
0.56
1.81
2.30
1.91
D
FC CAFC
Hematopoietic Stem Cell
-2.09
-1.91
-2.33
E
CD34+ Percentage (%)
CD34

Figure IV-3. *Translation of functional outputs from traditional assays to transcriptomic alternatives.* ***(A)*** *Relative telomere length (left), in percentage, and normalized telomerase (TERT) transcript counts (right) of freshly isolated (Day 0) and expanded populations (i.e. LC_Stat, CO_Stat and LC_Dyn).* ***(B)*** *Expression of a $CD34^{+}ADLH^{bri}$ phenotype characteristic of more primitive HSPC, in percentage and FC (left), and normalized aldehyde dehydrogenase 1 family member A1 (ALDH1A1) transcript counts (right).* ***(C)*** *Total CFU count per 1000 seeded HSPC (left) and gene set enrichment analysis (GSEA) between each expansion system and Day 0 using common myeloid progenitor and granylocyte/monocyte progenitor gene sets (right).* ***(D)*** *Fold change (FC) of cobblestone area-forming cell (CAFC) colonies (left) and GSEA between each expansion system and Day 0 using a hematopoietic stem cell gene set (right).* ***(E)*** *Percentage of $CD34^{+}$ cells in Day 0 and expanded HSPC populations (left) and normalized CD34 transcript counts (right). For relative telomere length, total CFU/1000 cells, FC in CAFC colonies and CD34 expression, four different pools of CB units were used, while the remaining outputs were obtained from three pools. Values are shown by their mean ± standard error of the mean.*

considerable increase in the percentage of CFU-GM colonies at the expense of CFU-Mix and BFU-E. Remarkably, BFU-E colony potential disappeared when expanding HSPC(CB) in LC_Dyn. Overall, a positive FC in total CFU was observed for all tested expansion systems, reaching up to 25 (LC_Static). Again, LC_Static and CO_Static had similar behavior regarding FC of total CFU (25 ± 2 vs. 21 ± 1), as well as FC of individual colony types, except for CFU-Mix (Fig. IV-2F). Maintaining a trend of lesser capacity for promoting HSPC(CB) expansion, lower FC in CFU expansion, was revealed in general by LC_Dyn, compared to the other two systems. Interestingly, intrinsic capacity of forming CFU (#CFU/expanded HSPC) was similar between all three expansion systems (Fig. IV-3A).

Further surrogate assays regarding cell stemness, engraftment potential and long-term repopulation ability were also explored. Telomere length, a crucial measure of genomic stability which has to be preserved in a lifelong stem cell, was seen to be comparable between expanded HSPC, regardless of the expansion system, and freshly isolated HSPC(CB) (Fig. IV-3B). Increased presence of ALDH is associated with a more primitive phenotype in HSPC. Although highly detectable in non-manipulated HSPC(CB) (i.e. Day 0), expanded cells showed a significant decrease in ALDH expression. Still, CO_Stat displayed significantly higher levels of ALDH compared to LC_Stat and LC_Dyn, both in percentage and FC of $CD34^{+}ALDH^{bri}$ cells (Fig. IV-3C). Additionally, amount of CAFC was also quantified after expansion and compared to non-manipulated HSPC(CB). LC_Stat and CO_Stat outperformed LC_Dyn, leading to a higher FC in CAFC.

IV.4.2. *Individual HSPC(CB) potency assays can be replaced with transcriptomic output.*

Having obtained the transcriptome of HSPC(CB), functional assay readouts were equated to their transcriptional counterparts. Potency verification, according to existing surrogate assays for HSPC with multiple techniques, was tested herein with transcriptional readouts from RNA sequencing. TERT expression was evaluated as a substitute for telomere length quantification. Levels of TERT were alike across freshly isolated and expanded HSPC from LC_Stat, CO_Stat and LC_Dyn (Fig. IV-3A). As the transcript equivalent for aldehyde dehydrogenase in HSPC, ALDH1A1 isoform expression was investigated (Fig. IV-3B). A similar decrease of ALDH1A1 expression in expanded compared to freshly isolated HSPC was also observed. However, CO_Stat did not mirror levels of $CD34^{+}ALDH^{bri}$, exhibiting a similar transcript count as LC_Stat and LC_Dyn. Clonogenic potential of expanded HSPC was similar between all systems (Fig. IV-3C). Gene set enrichment analysis (GSEA) of myeloid gene sets (i.e. common myeloid progenitor and granulocyte/monocyte progenitor) was chosen as the transcriptomic equivalent. CO_Stat was in both cases more enriched than the remaining expansion systems, namely LC_Stat and LC_Dyn. As a surrogate assay for long-term hematopoietic reconstitution, a CAFC assay was performed, demonstrating that CO_Stat was able to form more CAFC colonies (Fig. IV-3D). Similarly to CFU, GSEA of a particular gene set (i.e. hematopoietic stem cell) was used to transfer the functional output to a transcriptomic perspective Coherently, although all expansion systems had negative scores due to the enrichment analysis being done against Day 0, CO_Stat obtained the highest enrichment score. Notably, CD34 expression was very highly correlated with its respective transcript (Fig. IV-3E). The trend of CD34 expression observed by flow cytometry was predominantly repeated when assessing transcript counts, except for a slight decrease from LC_Static to LC_Dyn.

IV.4.3. *HSPC(CB) expansion through different expansion systems leads to unique secretome signatures.*

Conditioned medium from LC_Stat, CO_Stat and LC_Dyn was analyzed by FTIR, a physical and unbiased analytical technique. Spectra capturing existing molecular vibrations were obtained and compared (Fig. IV-4A). As expected, a broad similarity between spectra was observed, since all samples were of comparable biological origin, namely secretomes of expanded hematopoietic cells. However, statistically significant differences between conditioned media from different expansion systems were detected. Although measured differences were not always shared between all

expansion systems, several wavelength ranges can be highlighted (e.g. 3650 – 3400 cm^{-1}; 3000 – 2750 cm^{-1}; 1750 – 1300 cm^{-1} or 850 – 650 cm^{-1}).

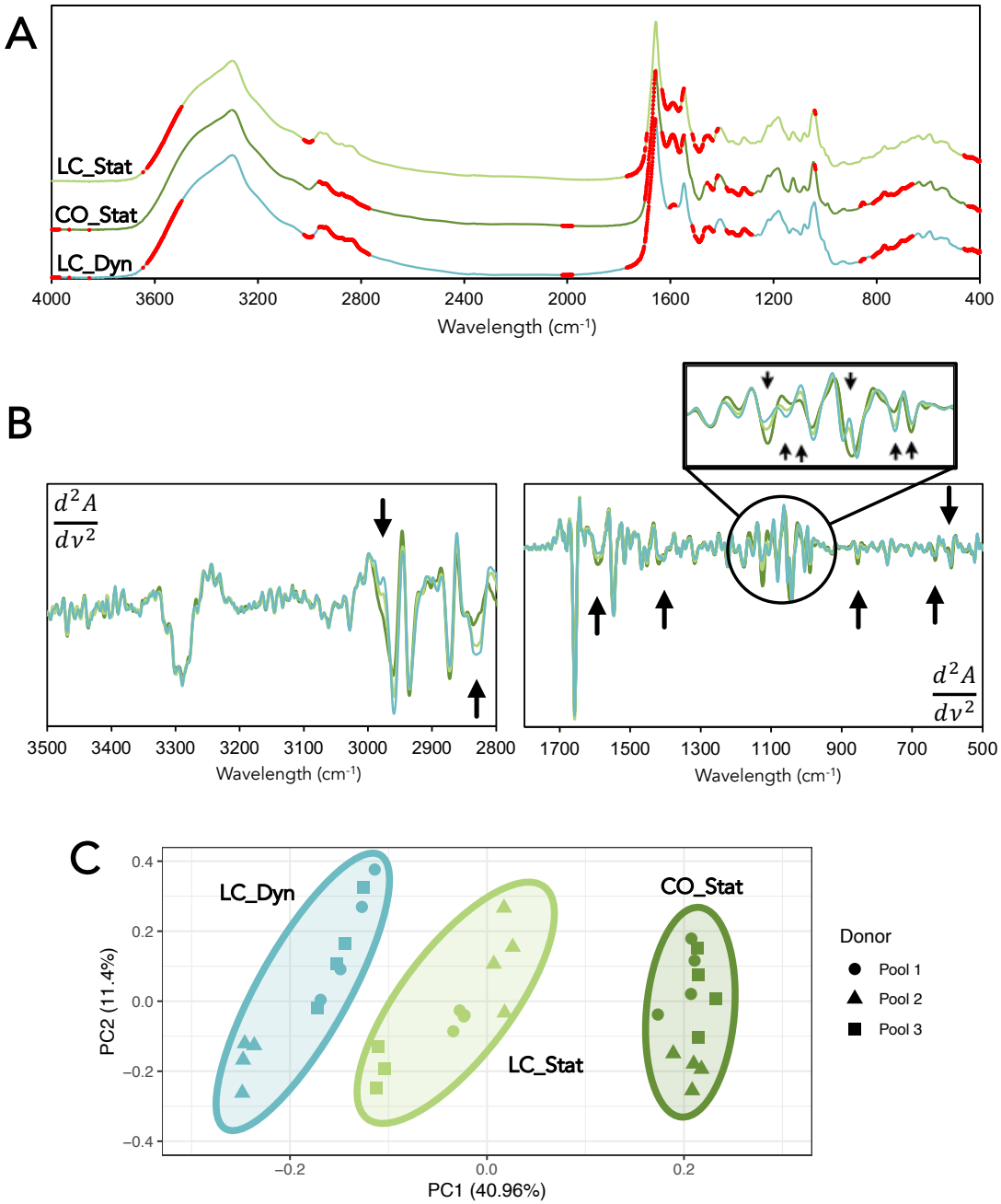

Figure IV-4. Fourier-transform infrared spectroscopy (FTIR) of expansion-derived conditioned media. **(A)** FTIR spectra obtained from samples of conditioned medium resulting from each expansion system, namely LC_Stat, CO_Stat and LC_Dyn. Red-marked wavelengths are statistically significant differences (p-value < 0.05) between each expansion system. **(B)** Second derivate spectra of biologically relevant wavelength ranges (500-1800 cm^{-1} and 2800-3500 cm^{-1}) of LC_Stat (light green), CO_Stat (dark green) and LC_Dyn (blue). Arrows highlight spectra differences. **(C)** Principal component analysis (PCA) of second derivative spectra and individual cluster identification. Bi-plot of principal component (PC) 1 and PC2. Each expansion system was represented by three different pools of CB units, with four technical replicates during spectrum acquisition.

To exclude non-relevant differences, spectra were analyzed in regions associated with vibration of biological molecules (i.e. 3500 – 2800 cm^{-1} – lipids; 1700 – 1450 cm^{-1} – proteins; 1200 – 500 cm^{-1} – carbohydrates, phospholipids and nucleic acid (fingerprint region)). Also, the second derivative was applied to intensify existing less obvious peak discrepancies (Fig. IV-4B). LC_Stat, CO_Stat and LC_Dyn showed distinct peaks in every biologically important region, namely 2970 cm^{-1} and 2825 cm^{-1} (C-H bonds in lipids), 1590 cm^{-1} and 1420 cm^{-1} (amide II bonds and carboxyl groups present in proteins) and also numerous peaks in the fingerprint region (highlighted in a close-up between 950 cm^{-1} and 1200 cm^{-1}) (Fig. IV-4B).
PCA of second derivative spectra was done to gain an overview of spectra differences for all three expansion systems and to evaluate whether HSPC(CB) expansion with these systems can be discriminated with FTIR. PCA of FTIR spectra showed clustering based on expansion system, mainly through PC1, accounting for 41% of variability (Fig. IV-4C). Clusters revealed independence from biological variability, which was also captured in the PCA by PC2 (11% variability). CO_Stat cluster displayed higher distance from the other two clusters, indicating increased dissimilarity compared to LC_Stat and LC_Dyn.

IV.4.4. *Distinct expansion systems produce cell products which are transcriptomically different and distant from freshly isolated cells.*

A global approach, taking advantage of transcriptomic multidimensionality, was taken to rigorously quantify overall differences between expansion systems and their relationship with the clinical reference for HCT, $CD34^+$-enriched HSPC(CB).
Samples clustered based on experimental condition rather than by biological donor variability, according to their correlation matrix (Fig. IV-5A). As expected, expanded cells in general were more correlated between each other than with non-expanded HSPC(CB) (i.e. Day 0). Again, when examining the entire transcriptome, LC_Stat and LC_Dyn were hierarchically closer to each other than to CO_Stat, when looking at the entire transcriptome. PCA confirmed cluster organization by k-means, with both PC1 and PC2 describing relevant variability, accounting for 55,7% and 14,3% respectively (Fig. IV-5B). However, between expansion systems, LC_Stat and CO_Stat were nearer compared to LC_Dyn (k-means distance: LC_Stat vs. CO_Stat - 29.7 and LC_Stat vs. LC_Dyn – 55.6), mainly due to PC2.

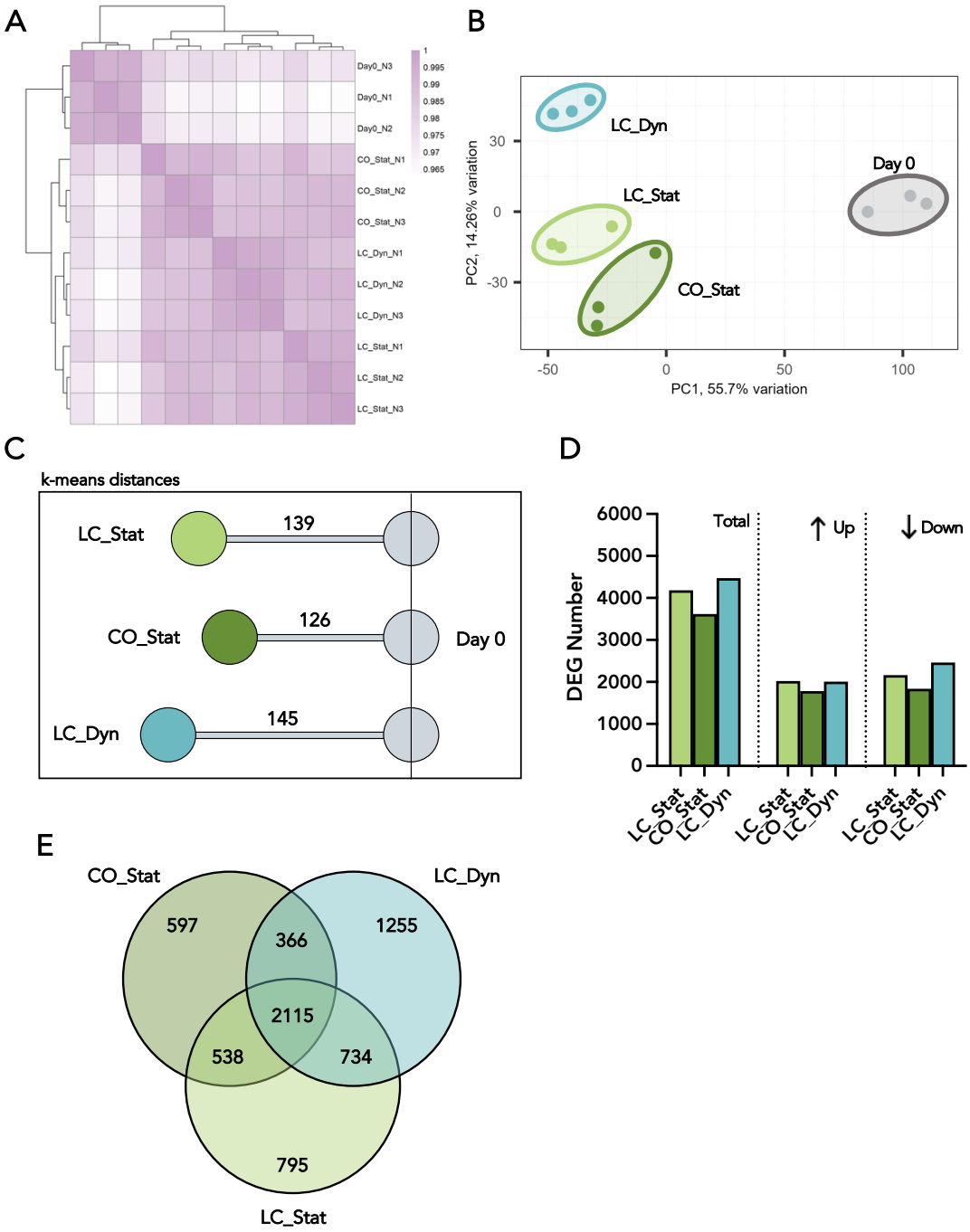

Figure IV-5. Transcriptomic characterization of expanded HSPC from different expansion systems (LC_Stat, CO_Stat and LC_Dyn). ***(A)*** *Correlation matrix with hierarchical dendrogram of sequenced samples, including freshly isolated (Day 0) and expanded HSPC using LC_Stat, CO_Stat and LC_Dyn.* ***(B)*** *Principal component analysis (PCA) and clustering by k-means. Bi-plot of principal component (PC) 1 and PC2.* ***(C)*** *K-means-derived cluster distances, namely of each expansion system from Day 0.* ***(D)*** *Number of differently expressed genes (DEG) of each expansion system compared to Day 0, shown by total genes, up-regulated genes and down-regulated genes.* ***(E)*** *Venn diagram of DEG, emphasizing the portion of DEG that are shared between the different expansion systems and which are uniquely expressed. Data was obtained from three different pools of CB units.*

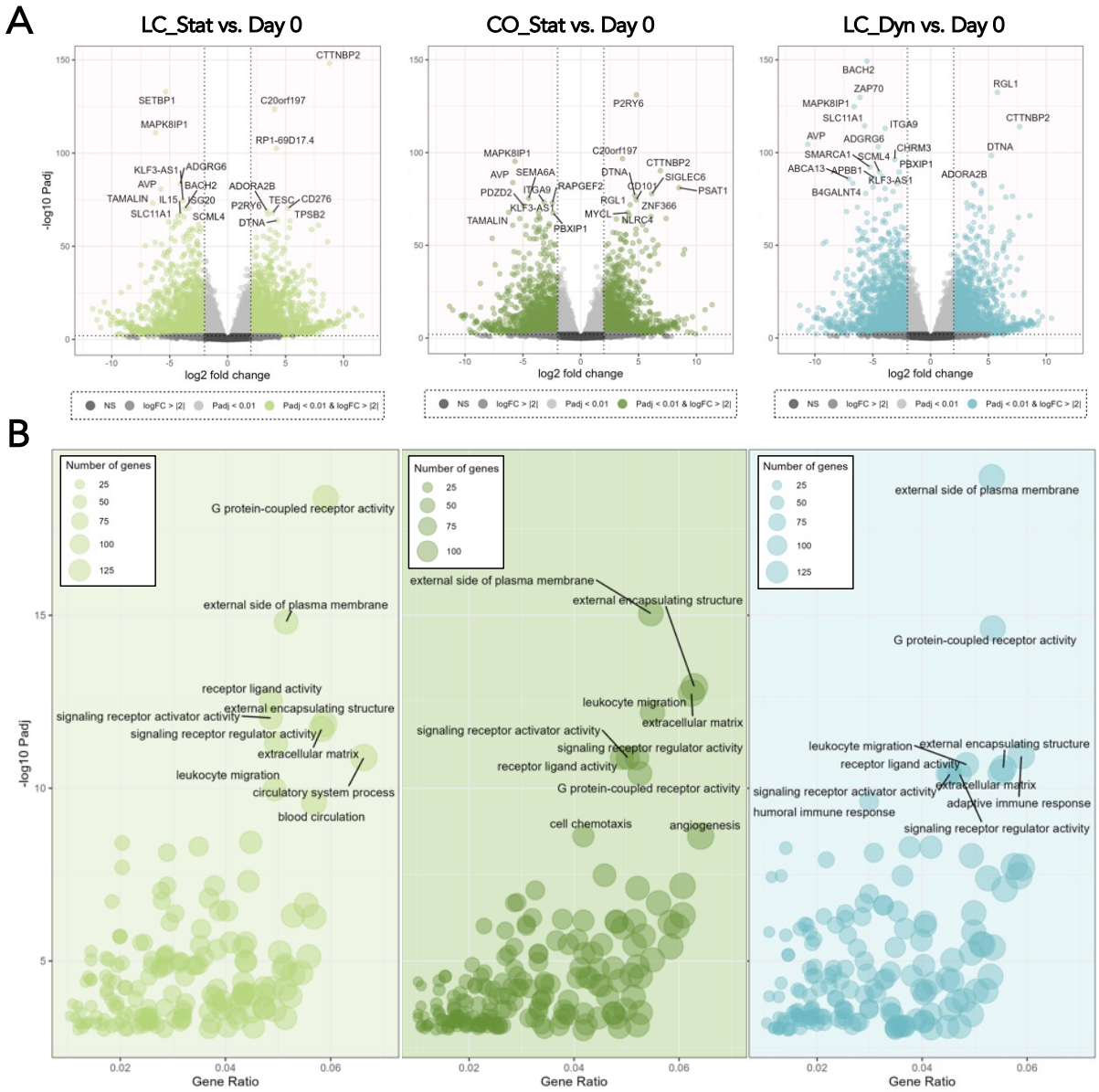

Figure IV-6. *Identification of differentially expressed genes (DEG) between each studied expansion system (LC_Stat, CO_Stat and LC_Dyn)* ***(A)*** *Volcano plots of up-regulated and down-regulated DEG of each expansion system. Top 20 genes were individually labelled.* ***(B)*** *Gene ontology (GO) enrichment analysis of identified DEG. Top 10 significant GO terms were individually labelled. Data was obtained from three different pools of CB units. Padj – adjusted p-value.*

Transcriptomic distances were also determined, namely between each expansion system and the defined reference (i.e. freshly isolated HSPC(CB)). PCA-derived k-means distances demonstrated that HSPC expanded with CO_Stat were transcriptomically closer to Day 0 (Fig. IV-5C). Differential gene expression analysis, based on Day 0, uncovered a total of 4182 significant genes for LC_Stat, 3618 for CO_Stat and 4470 for

LC_Dyn. Distribution of DEG was similar between up-regulated and down-regulated genes, mirroring the trend observed for k-means distances (Fig. IV-5D). Most DEG were shared between all three systems, with LC_Stat having the higher number of uniquely expressed DEG (Fig. IV-5E).

Taking a closer look into each group of DEG, even inside the most significantly expressed genes, there were DEG present in all systems (e.g. DTNA, CTTNBP2 or MAPK8IP1), DEG shared between only two systems (e.g. TAMALIN – LC_Stat and CO_Stat or RGL1 – CO_Stat and LC_Dyn) and uniquely expressed DEG (Fig. IV-6A). GO enrichment analysis exposed the most relevant terms in which DEG are represented (Fig. IV-6B). A clear majority of the most significant terms in all expansion systems were related with cell signaling, namely ligand-receptor interaction. To a lesser extent, terms connected with cell motility within the circulatory system, with specific mention to leukocytes, were also present.

IV.4.5. *Comparison between Studied Expansion Systems and Publicly Available Datasets.*

A transcriptome-based approach was taken to discern the potential of using this technology for HSPC expansion system comparison. Transcriptomic data from other clinically relevant expansion strategies were collected for this comparison. LC_Stat, CO_Stat and LC_Dyn were compared to HSPC expanded in zwitterionic hydrogels, valproic acid (VPA) or small molecules (i.e. StemRegenin-1 and UM171)[161,175,437]. Each dataset was chosen based on the relevance of the expansion approach, but also on the existence of a non-expanded population with similar immunophenotype as a reference. Initially, a side-by-side comparison resulted in a grouping of experimental conditions by research groups that generated each dataset. This was observed by correlation of entire transcriptomes (Fig. IV-7A), as well as by PCA (Fig. IV-7B). To overcome the existing batch effect associated with different workflows during RNA sequencing, including sequencing settings (e.g. coverage or individual read size), data harmonization algorithms were explored to isolate biologically-relevant variability. After implementing Combat-seq, to correct batch effect, the correlation matrix showed hierarchical organization similar to our study alone (Fig. IV-7C). Freshly isolated cells formed a group, even though originating from different research groups, and expanded HPSC were also more closely related. PCA confirmed improved resolution for relevant biological variability, with PC1 separating expanded from non-expanded HSPC (Fig. IV-7D). While PC2 still exposed vulnerability towards a batch effect, it was no longer the primary source of variability. Similar distances between expanded and freshly isolated HSPC(CB) were visible between the multiple expansion systems, except when cells were expanded in a zwitterionic hydrogel (i.e. ZW_Exp_1 and ZW_Exp_2 vs. ZW_Day0_1 and

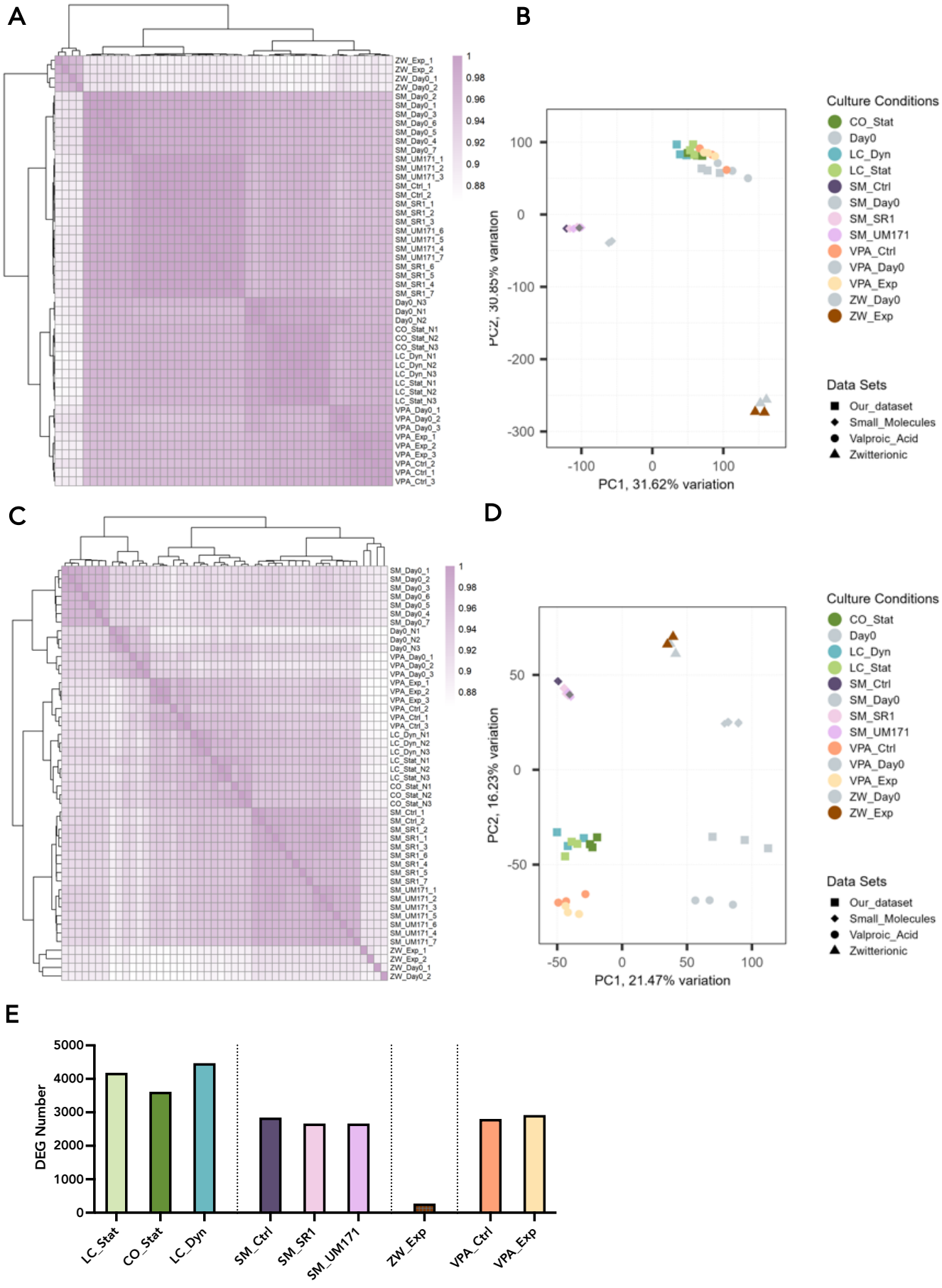
A
B
C
D
E
PC1, 31.62% variation
PC2, 30.85% variation
PC1, 21.47% variation
PC2, 16.23% variation
Culture Conditions
CO_Stat
Day0
LC_Dyn
LC_Stat
SM_Ctrl
SM_Day0
SM_SR1
SM_UM171
VPA_Ctrl
VPA_Day0
VPA_Exp
ZW_Day0
ZW_Exp
Data Sets
Our_dataset
Small_Molecules
Valproic_Acid
Zwitterionic
DEG Number
5000
4000
3000
2000
1000
0
LC_Stat
CO_Stat
LC_Dyn
SM_Ctrl
SM_SR1
SM_UM171
ZW_Exp
VPA_Ctrl
VPA_Exp

Figure IV-7. *Expansion system comparison by transcriptomic profiling using studied expansion systems (LC_Stat, CO_Stat and LC_Dyn) and other clinically relevant systems with publicly available datasets (**Small_Molecule** – non-expanded HSPC (SM_Day0), cytokine only (SM_Ctrl), StemRegenin-1 (SM_SR1) and UM171 (SM_UM171); **Valproic_Acid** – non-expanded HSPC (VPA_Day0), cytokine only (VPA_Ctrl) and valproic acid (VPA_Exp); **Zwitterionic** – non-expanded HSPC (ZW_Day0), zwitterionic hydrogel (ZW_Exp)).* ***(A)*** *Correlation matrix with hierarchical dendrogram of joined datasets without batch effect correction.* ***(B)*** *Principal component analysis (PCA) of joined datasets without batch effect correction. Bi-plot of principal component (PC) 1 and PC2.* ***(C)*** *Correlation matrix with hierarchical dendrogram with batch effect correction using a harmonization algorithm, ComBat-seq.* ***(D)*** *PCA with batch effect correction using a harmonization algorithm, ComBat-seq. Bi-plot of PC1 and PC2.* ***(E)*** *Total number of differentially expressed genes (DEG) between joined datasets.* ***Small Molecule*** *dataset - GSE57299,* ***Valproic Acid*** *dataset - GSE110968 and* ***Zwitterionic*** *dataset - GSE85800.*

ZW_Day0_2). Interestingly, almost no difference was observed between expanded and non-expanded cells in that particular dataset. Quantification of transcriptomic differences as a comparison tool was pursued through DEG determination, with each strategy using its own freshly isolated samples as an internal control (Fig. IV-7E).

IV.5. Discussion

Approvals for cell and gene therapies (CGT) are estimated to reach 64 by 2030 only in the US market[438]. Concerning CGT based on *ex vivo* expanded HSPC, Omisirge or omidubicel (HSPC expanded with nicotinamide) produced by Gamida Cell has just recently received FDA-approval (April 2023) for treatment of hematological diseases[170]. This breakthrough highlights the importance and urgency for potency tracking of CGT and development of robust quality control during manufacturing. Such complex products require much more stringent overwatch, with existing assays being insufficient for such a daunting task that can have considerable negative impact on patients if not assured[435]. This issue has long been identified and guidelines for development of novel potency assays have been shared by Cord Blood Advisory Group of the National Marrow Donor Program[439].

Here, we demonstrated characterization of expanded HSPC(CB) from three different systems to simulate control of product quality using an extended number of traditional and recognized assays that assess cell fitness, identity and function (direct or through surrogate assays). Overall, LC_Stat and CO_Stat behavior corroborated our far-reaching experience with these two systems[109,126,440]. Of note, CO_Stat expansion fold was not superior to LC_Stat, as has been accustomed. This unusual result may be attributed to

the utilization of HPL-supplemented culture medium for the expansion of MSC(M), an approach recently adopted in recent studies to improve process translation. So far, impact of HPL supplementation on MSC hematopoietic support capacity has been controversial. In a systematic study of the impact of MSC source and MSC culture medium during HSPC co-culture expansion, HPL-supplementation during FL preparation led to a decrease of expanded HSPC FC compared with FBS-supplementation[124]. Contrasting with this study, recent use of co-culture expansion as a potency assay for MSC, after undergoing alginate bead encapsulation, showed no adverse effect on the hematopoietic support capability of MSC, when FL were prepared with HPL-supplementation[441]. A more in-depth study is required to determine if the transition from FBS- to HPL-supplementation has a detrimental effect on MSC function, specifically their hematopoietic support capacity.

In contrast to LC_Stat and CO_Stat, LC_Dyn had unexpected disappointing performance. Dynamic cultures of HSPC were breakthroughs of past decades, demonstrating that HSPC expansion *in vitro* could transition to more scalable platforms, such as spinner flasks and stirred tank bioreactors[442,443]. This expansion system was included in this study to determine if it could capitalize on advances made in promoting HSPC expansion (e.g. development of tailored serum-free expansion media or optimization of cytokine concentrations), since dynamic expansion has not been pursued by many as an attractive and competitive alternative expansion system. Unfortunately, with an increased shear stress environment, LC_Dyn led to reduced HSPC expansion.

For such a characterization of expanded HSPC(CB), required equipment and specialized reagents necessary at a clinical-grade level would, at least, include a cell counter, a metabolite analyzer, a flow cytometer, methylcellulose-based assays, a CFU colony counter, patent-protected telomere length and aldehyde dehydrogenase quantification kits and supportive cell lines for CAFC assays. Significant investment would be involved in securing such non-complementing equipment and guaranteeing their maintenance, contributing towards increasing the final price tag of such a therapy. Worsening the situation, highly specialized operators would be required for each equipment to perform labor-intensive tasks. Included in our panel of assays are also colony forming assays (i.e. CFU and CAFC) which have previously mentioned limitations, namely their long duration. Extensive assay duration also disqualifies the use of xenotransplantation into immune-deficient mouse models as a readout of engraftment and hematopoietic reconstitution potential. To address these issues and focus on HSPC function, we initially harnessed the potential of transcriptomics to concentrate readouts from very different assays into a single one with fast workflow. Comparing functional assay outputs using traditional and transcriptional approaches led to very consistent results. Replacing all these different techniques with RNA sequencing would significantly impact CGT cost of

goods, by obtaining the same information of cell quality and function using a much lesser amount of means and resources. RNA sequencing has become a transversal technique for most differential gene expression and related studies, being a target of investment and innovation to continuously improve its workflow but also reduce cost[444,445]. Having cell function evaluated with RNA sequencing would only benefit from such advancements.

Of consideration, chosen transcriptional equivalents to traditional functional outputs may be improved to further capture HSPC functionality. Although telomerase expression (TERT) is responsible for elongation of telomeres, it is not a direct measure of telomere length. Nevertheless, increased telomerase expression has been associated with a HSPC phenotype and its quantification has been used to assess HSPC health, age and self-renewal potential[446,447]. For ALDH quantification, isoform ALDH1A1 has been described as the relevant transcript responsible for its expression in HSPC[448]. Having used bulk sequencing, we cannot infer the percentage of positive cells, but we can evaluate relative transcript quantity. Contrasting with these previous functional assays, CFU are a direct measure of HSPC clonogenic and differentiation potential into the myeloid lineage. When translating CFU to transcriptional output, our proposed conversion only transmits information on myeloid progenitor enrichment and does not quantify actual differentiation. However, CFU are not compatible with potency assay goals for expanded HSPC, which makes myeloid progenitor enrichment a feasible alternative. Similar to ALDH quantification, CD34 expression determination through transcript quantification cannot infer single cell expression. However, it is simultaneously proportional to percentage of positive cells and cell antigen density, incorporating both positive population determination and median fluorescence intensity (MFI) analysis from flow cytometry. To circumvent this particular drawback of bulk transcriptomics, namely the inability to determine single cell immunophenotype (specially for extensive hematopoietic surface marker panels), a digital cytometry algorithm (i.e. CIBERSORTx) has been developed[449]. This algorithm enables the identification of complex co-expression patterns of identity markers (e.g. cultured HSC – $CD34^{+}CD45RA^{-}CD90^{+}CD133^{+}ITGA3^{+}$) and allows for the inference of expanded cell subpopulations based on the analysis of bulk data. Thus, HSPC transcriptomes were demonstrated to be able to provide functional insight of expanded populations based on the rationale of traditional functional assays.

After adapting existing functional assays using RNA sequencing, a novel way to track expanded HSPC quality during manufacturing was also explored. FTIR-derived spectra analysis of conditioned medium was able to correctly distinguish all three expansion systems. Taking advantage of such a physical technique has considerable benefits, such as its unbiased nature, sensitivity to changes, label-free mode of analysis and non-destructive measurement[450]. Additionally, FTIR could be compatible with real-time

monitoring of HSPC expansion, providing continuous spectra that could follow expansion dynamics. Our initial attempt used conditioned medium, which is much simpler to sample and process. However, cell-derived spectra would also be worth evaluating, since tracking conditioned medium changes is limited to secretome-based fluctuations. It would also permit acquiring spectra from non-expanded cells (i.e. Day 0), providing an important reference. Cell-based FTIR analysis has been pursued for other applications, namely following chondrogenic differentiation in MSC, being able to distinguish chondrocyte-induced cells from undifferentiated MSC[451].

Genuine value of transcriptomic profiling relies in its multidimensionality, allowing a systemic comparison of individual cell states (i.e. systems modeling)[107]. While we have previously sought to compare *ex vivo* expansion of HSPC(CB), our battery of traditional analytical techniques was limited to the expression of identity surface markers, myeloid differentiation potential and *in* vitro expansion capacity[109]. By examining the entire transcriptome, expanded HSPC can be pinpointed in their manufacturing design space. Quality of expanded HSPC can be assured by tracking their transcriptomic signature, defined for the optimal product, after each expansion. Furthermore, when combined with a reference population, transcriptomic distances from ideal targets can be calculated, exposing potential shortcomings of a particular expansion system. CO_Stat was shown to best preserve HSPC phenotype (i.e. freshly enriched $CD34^+$ cells) at a global level after undergoing expansion. Even when filtering for genes contributing towards higher variability between experimental conditions, CO_Stat remained more similar. Most DEG between expanded and freshly isolated HSPC are shared between at least two systems, indicating that a considerable fraction of variability is due to pervasive and inevitable differentiation of stem and progenitor populations. This is to be expected, since most expansion systems share experimental settings (e.g. cytokine cocktail or expansion medium). Still, cell transcriptome is sensitive enough to also detect impact from innovations of different expansion systems, such as incorporation of shear stress (LC_Dyn) or a supportive cell type (CO_Stat). Therefore, we propose transcriptomic profiling as an efficient tool for accurately detecting expanded population differences compared to a chosen reference population.

Recognizing the significant potential of HSPC transcriptomics in improving production of expanded HSPC-derived therapies, we went further and used this tool to simultaneously evaluate multiple expansion systems beyond this study that have translational potential. This approach would allow a fair evaluation of expansion systems (e.g. screening of expansion strategies) to assist decision makers in selecting their therapeutic portfolio. However, integration of available datasets was hindered by a considerable batch effect. Such batch effects would not be an issue for the abovementioned purpose, since RNA sequencing would be performed in a single run after in-house screening of expansion systems. Nevertheless, an attempt was made to

bypass the batch effect by applying a harmonization algorithm (i.e. Combat-Seq)[452]. Transcriptomic compatibility is a recognized issue in the bioinformatic field, which can arise from existing variability in library preparation protocols and sequencing definitions, or from sequencing performed at different timeperiods[453]. Batch effect is present in both bulk and single cell transcriptomics and remains relevant, even with advances in machine learning and artificial intelligence[454]. Coherent with the batch corrected PCA, expansion strategies using small molecules and VPA had inferior DEG number than LC_Stat, CO_Stat and LC_Dyn. As described in their respective studies, these strategies are able to better promote HSPC while avoiding differentiation[175,437].

In this study we explored two different ways of tapping transcriptomic data to evaluate expanded HSPC. Tracking of individual expansion systems and differentiating between them was shown to be possible, having the potential of being used to control manufacturing quality of expanded HSPC products. In addition to a novel label-free technique (i.e. FTIR spectroscopy), such quality tracking may be significantly enhanced. Either continuous (with FTIR-based measurements of conditioned medium or expanded cells) or end-point (with RNA sequencing of expanded HSPC) quality control could be integrated into the manufacturing process. On the other hand, transcriptomic distances from a selected functional reference were determined to assess HSPC potency. For HCT using CB, freshly isolated HSPC are the current clinical reference. In fact, the initial goal of *ex vivo* expansion of HSPC was to increase cell number whilst conserving their more primitive phenotype. However, a different reference may be selected as we advance our knowledge on hematopoietic engraftment, short and long-term reconstitution. If wanting to focus on pure engraftment potency, transcriptomic reference could change to sorted short-term or long-term HSC. If aiming to produce a lymphoid product to apply as DLI, the reference population could change to progenitor or differentiated T cells. More complex references may be used, choosing a fine-tuned mixture of different hematopoietic populations, since similar importance has been attributed to lymphoid progenitor populations that accelerate immune reconstitution and HSC that ensure long-term graft success. If necessary, the reference may also be a smaller gene set, linked to a particular therapeutic action. For example, a GVHD-triggering gene set might be employed to assure that manufactured expanded HSPC will not trigger such a complex post-HCT complication[455].

From the different OMICS-approaches, transcriptomics possesses interesting benefits. Since it provides information of transcript and not protein levels (as in the case of proteomics), it can predict future behavior that has not yet translated to real-time protein expression and cellular phenotype changes[456]. Having such predictive power in the manufacturing process is a very valuable tool, helping to avoid failures in therapy batch production and assuring near-future functional phenotype.

V. Final Remarks and Future Directions

Hoping to shine light on the potential of CB as a versatile source of HSPC, several different approaches were taken to improve *ex vivo* expansion of HSPC(CB). While the technology for therapeutic application of HSPC(CB) already exists, as evidenced by the recent approval of Omisirge, manufacturing of these products is far from optimized. Aligning with an inexperienced field of CGT production that has been transitioning from knowledge obtained from conventional pharmaceuticals, production improvement of expanded HSPC products is greatly warranted. Each chapter will hopefully become another brick in the wall of consecutive advancements in making *ex vivo* HSPC expansion more efficient, sustainable and cost-effective.

In Chapter II, we had aimed at addressing three different goals. Initially, with expansion strategies reaching or advancing through the clinical trial pipeline, we recognized a window of opportunity where performed optimizations could be implemented without losing their applicability and sharing the same fate as previous studies. We were successful in optimizing each of the studied expansion systems, leading to improved expanded HSPC products with higher expansion yields while potentially maintaining the quality necessary for expanded HSPC to produce their expected therapeutic value (i.e. reconstitute the entire hematopoietic system), characterized herein by their $CD34^+$ expression and multilineage potential. Thus, we have produced enduring optimizations that directly influence clinically important HSPC expansion platforms or may even guide novel HSPC expansion strategies in the future. Secondly, as these strategies are simultaneously progressing towards regulatory approval, we had also ambitioned establishing optimization as a tool to perform a rational and comprehensive evaluation between different approaches. By doing so, differences between CS_HSPC and CS_HSPC/MSC were emphasized in an unbiased manner. Our study can influence decision-making and risk analysis of both systems as expansion platforms undergoing regulatory funneling to reach commercial approval. Finally, by increasing process knowledge on cytokine supplementation, we have demonstrated the variability of important production variables (e.g. FC in TNC), contributing towards the implementation of a healthy manufacturing process for CB-derived *ex vivo* expanded HSPC. Moreover, we have promoted the framework behind our study and its results to be used for other potential stem cell-based products outside its original scope, in terms of development, manufacturing and economic perspectives.

In Chapter III, we focused our attention on the supportive stromal cells present in our co-culture system. When producing an expanded HSPC(CB) product based on co-culture expansion, MSC manufacturing will also be integrated into the pipeline, being also targeted for process improvement. MSC(AT) were successfully demonstrated to be compatible with cell encapsulation at hypothermic temperatures (10°-20°C). Maintenance of identity markers was ensured, while MSC(AT) multilayered functionality

was proven to be maintained throughout encapsulation. Differentiation, expression of immunomodulatory molecules and hematopoietic support abilities were all individually confirmed. Translation of clinical-grade MSC(AT) to this novel product storage and transportation model appears to be within reach. Xeno-free processing of MSC(AT) was directly compared with traditional FBS-based handling. HPL supplementation, which by itself improves MSC proliferation *in vitro*, did not negatively impact cell behavior during our encapsulation study, making it a relevant candidate for FBS substitution for cGMP-compliant MSC logistics and supply chain. As a model, cell encapsulation will potentially have a disruptive impact on CGT as it does not require cryo-range temperatures (below -130°C). Alginate encapsulation also has the potential to be complementary to cryopreservation, being appropriate for both allogeneic and autologous scenarios. Optimization opportunities exist (e.g. improving initial encapsulation efficiency) and should be pursued to further enhance encapsulation potential.

In Chapter III, we faced the significant gap of HSPC(CB) function tracking through potency assays. Identifying cells as complex systems, we proposed going from a low to a high dimensionality perspective, especially when the therapeutic mode of action is not thoroughly understood. Transcriptomic data and conventional potency assays were mostly coherent regarding their readouts of HSPC function. A global view of expanded HSPC(CB) from different expansion strategies was uncovered, providing more resolution of their differences compared to freshly isolated $CD34^+$-enriched cells. This strategy was extrapolated to other expansion systems, through publicly available transcriptomic datasets. Although partially hindered by variability in library preparation and sequencing definitions, correction of the existing batch effect was attempted. Successful harmonization algorithms that allow compatibility between different datasets are needed. FTIR spectra of expansion-derived conditioned medium were proven to distinguish different expansion systems, being independent of the existing biological variability from CB donors. These powerful techniques demonstrated their potential for CGT manufacture monitoring and quality control, especially for expanded HSPC.

The goals reached during the abovementioned approaches can be built upon to enable a continuous improvement framework. Heavily influenced by QbD, adopted techniques are in line with manufacturing guidelines for CGT.

Tailored cytokine optimization should be pursued for the whole environment of existing expansion strategies, potentially providing increased HSPC yields. With expensive clinical grade reagents, such optimizations are critical for uncovering cost-effectiveness measures that do not affect product quality. This workflow, using experimental design, can also be transferred to other optimization opportunities. With the growing influence of small molecules on HSPC expansion protocols, used concentrations are an attractive opportunity for potential optimization. Chosen response variables may also be updated as more functional targets are uncovered in HSPC biology. Eventually, by determining

enough mathematical behavior equations, subpopulation distribution in expanded HSPC may be simply modulated by automized changes to cytokine or small molecule concentrations. This would give manufacturers extreme versatility when producing hematopoietic products derived from HSPC.

After successful cell encapsulation at hypothermic temperatures of supportive MSC, HSPC could also be evaluated using the same approach. With adherent MSC performing well during encapsulation, non-adherent HSPC are expected to adapt even better, possibly overcoming MSC encapsulation duration. With both cell types adapting to cell encapsulation, an all-in-one strategy as discussed previously could also be applied to co-culture expansion of HSPC. Although bead release would be necessary before patient infusion, co-culture might even be enhanced due to the 3D milieu inside the beads. Such encapsulation would be compatible with scalable vessels, such as the packed-bed, fluidized-bed or stirred tank bioreactors. Their relative lightweight allows for bioreactor packing without increasing too much pressure on the lower layers of the vessel, while also allowing for fluidization without a demanding flow rate. Alternatively, encapsulated cells are also protected from shear stress that can be very harmful towards cells in stirred tank bioreactors. Bioreactor sampling and recovery would be facilitated by the relatively simple bead dissociation that does not require any downstream separation technique. These projections of alginate bead potential for *in situ* HSPC expansion (using a co-culture or other simpler systems) might be envisioned to be performed during distribution. By using environment-controlled containers, manipulation might be done simultaneously with their distribution, shortening the total bench-to-bedside duration.

Use of transcriptomics has increased exponentially in cell biology, but application of FTIR has been reduced. Transcriptome profiling has considerable untapped potential as a quality indicator, since it gives a glimpse of the cell machinery at a given timepoint. As costs for sequencing decrease, generalized use is expected. Single-cell transcriptomics will provide even more detail, being especially important for heterogeneous therapeutic populations, such as HSPC. Ideally, other OMICS approaches should partner with transcriptomics, getting a more complete cell characterization, including function. On the other hand, FTIR also demonstrated interesting sensitivity towards measuring biological differences. Transitioning from conditioned media to actual cells could be the next step. In this case, FTIR could become similar to transcriptomics, giving rise to global perspectives of cell behavior. As a physical technique, FTIR is unbiased and can yield results from samples in a non-destructive manner. However, its main shortcoming is related with its difficulty in associating spectrum shapes or peaks with complex biological phenomena. Still, potential of FTIR for quality tracking during manufacture of CGT is evident.

All strategies explored to improve production of *ex vivo* expanded HSPC served their purpose but can be taken further when necessary. Manufacturing of expanded HSPC(CB) is very compatible with QbD and continuous improvement through optimization.

VI. Publications and Communications

Publications in Peer-Reviewed International Scientific Journals

Branco A, Bucar S, Moura-Sampaio J, Lilaia C, Cabral JMS, Fernandes-Platzgummer A, Lobato da Silva C. Tailored Cytokine Optimization for ex vivo Culture Platforms Targeting the Expansion of Human Hematopoietic Stem/Progenitor Cells. *Frontiers in Bioengineering and Biotechnology*. 8, 1–21 (2020). https://doi.org/10.3389/fbioe.2020.573282

Bucar S, Branco ADM, Mata MF, Milhano JC, Caramalho Í, Cabral JMS, Fernandes-Platzgummer A, Lobato da Silva C. Influence of the mesenchymal stromal cell source on the hematopoietic supportive capacity of umbilical cord blood-derived $CD34^+$-enriched cells. *Stem Cell Research & Therapy*. 12, 1–16 (2021). https://doi.org/10.1186/s13287-021-02474-8

Branco A, Tiago AL, , Laranjeira P, Carreira MC, Milhano JC, dos Santos F, Cabral JMS, Paiva P, Lobato da Silva C, Fernandes-Platzgummer A. Hypothermic Preservation of Adipose-Derived Mesenchymal Stromal Cells as a Viable Solution for the Storage and Distribution of Cell Therapy Products. *Bioengineering*. 9, 805 (2022). https://doi.org/10.3390/ bioengineering9120805

Book Chapters

*de Almeida Fuzeta M, *Branco A, Fernandes-Platzgummer A, Lobato da Silva C, Cabral JMS. Addressing the Manufacturing Challenges of Cell-based Therapies. In *Advances in Biochemical Engineering/Biotechnology, Springer: Cham, Germany,* 171, 225-278 (2019). ISBN 978-3-030-40463-5
*These authors contributed equally.

Poster Communications in Conferences

Branco A, Bucar S, Lilaia C, Cabral JMS, Fernandes-Platzgummer A, Lobato da Silva C. Cytokine Optimization for *Ex Vivo* Expansion of Hematopoietic Stem/Progenitor Cells in a Mesenchymal Stem/Stromal Cell Co-Culture System. *6th ENBENG IEEE Portuguese Meeting in Bioengineering 2019*. Lisbon, Portugal, February 2019

Branco A, Bucar S, Lilaia C, Cabral JMS, Fernandes-Platzgummer A, Lobato da Silva C. Cytokine Optimization for *Ex Vivo* Expansion of Hematopoietic Stem/Progenitor Cells in a Mesenchymal Stem/Stromal Cell Co-Culture System. *11th International Meeting of the Portuguese Society for Stem Cells and Cell Therapies*. Lisbon, Portugal, October 2019

Branco A, Bucar S, Lilaia C, Cabral JMS, Fernandes-Platzgummer A, Lobato da Silva C. Cytokine Optimization for *Ex Vivo* Expansion of Hematopoietic Stem/Progenitor Cells in a Mesenchymal Stem/Stromal Cell Co-Culture System. *3rd Stem Cell Community Day 2019*. Lisbon, Portugal, November 2019

VII. References

1. Fleischer, S., Tavakol, D. N. & Vunjak-Novakovic, G. From Arteries to Capillaries: Approaches to Engineering Human Vasculature. *Adv. Funct. Mater.* **30**, 1910811 (2020).
2. Keohane, E., Otto, C. & Walenga, J. *Rodak's Hematology*. (Elsevier, 2020). doi:10.1016/C2013-0-19483-4
3. Sender, R. & Milo, R. The distribution of cellular turnover in the human body. *Nat. Med.* **27**, 45–48 (2021).
4. Riera Romo, M., Pérez-Martínez, D. & Castillo Ferrer, C. Innate immunity in vertebrates: an overview. *Immunology* **148**, 125–139 (2016).
5. Paolini, R., Bernardini, G., Molfetta, R. & Santoni, A. NK cells and interferons. *Cytokine Growth Factor Rev.* **26**, 113–120 (2015).
6. Iwasaki, A. & Medzhitov, R. Control of adaptive immunity by the innate immune system. *Nat. Immunol.* **16**, 343–353 (2015).
7. Jackson, K. J. L., Kidd, M. J., Wang, Y. & Collins, A. M. The Shape of the Lymphocyte Receptor Repertoire: Lessons from the B Cell Receptor. *Front. Immunol.* **4**, 1–12 (2013).
8. Chapin, J. C. & Hajjar, K. A. Fibrinolysis and the control of blood coagulation. *Blood Rev.* **29**, 17–24 (2015).
9. Zhang, Y., Gao, S., Xia, J. & Liu, F. Hematopoietic Hierarchy – An Updated Roadmap. *Trends Cell Biol.* **28**, 976–986 (2018).
10. Tomellini, E. *et al.* Integrin-α3 Is a Functional Marker of Ex Vivo Expanded Human Long-Term Hematopoietic Stem Cells. *Cell Rep.* **28**, 1063-1073.e5 (2019).
11. Catlin, S. N., Busque, L., Gale, R. E., Guttorp, P. & Abkowitz, J. L. The replication rate of human hematopoietic stem cells in vivo. *Blood* **117**, 4460–4466 (2011).
12. Lee-Six, H. *et al.* Population dynamics of normal human blood inferred from somatic mutations. *Nature* **561**, 473–478 (2018).
13. Doulatov, S., Notta, F., Laurenti, E. & Dick, J. E. Hematopoiesis: A human perspective. *Cell Stem Cell* **10**, 120–136 (2012).
14. Hughes, M. R. *et al.* A sticky wicket: Defining molecular functions for CD34 in hematopoietic cells. *Exp. Hematol.* **86**, 1–14 (2020).
15. AbuSamra, D. B. *et al.* Not just a marker: CD34 on human hematopoietic stem/progenitor cells dominates vascular selectin binding along with CD44. *Blood Adv.* **1**, 2799–2816 (2017).
16. Laurenti, E. & Göttgens, B. From haematopoietic stem cells to complex differentiation landscapes. *Nature* **553**, 418–426 (2018).
17. Velten, L. *et al.* Human haematopoietic stem cell lineage commitment is a continuous process. *Nat. Cell Biol.* **19**, 271–281 (2017).
18. Carrelha, J. *et al.* Hierarchically related lineage-restricted fates of multipotent haematopoietic stem cells. *Nature* **554**, 106–111 (2018).
19. Hirschi, K. K. Hemogenic endothelium during development and beyond. *Blood* **119**, 4823–4827 (2012).
20. Barone, C., Orsenigo, R., Meneveri, R., Brunelli, S. & Azzoni, E. One Size Does Not Fit All: Heterogeneity in Developmental Hematopoiesis. *Cells* **11**, (2022).
21. Tober, J. *et al.* The megakaryocyte lineage originates from hemangioblast precursors and is an integral component both of primitive and of definitive hematopoiesis. *Blood* **109**, 1433–1441 (2007).
22. Frame, J. M., McGrath, K. E. & Palis, J. Erythro-myeloid progenitors: "Definitive" hematopoiesis in the conceptus prior to the emergence of hematopoietic stem cells. *Blood Cells, Mol. Dis.* **51**, 220–225 (2013).
23. Guibentif, C. *et al.* Single-Cell Analysis Identifies Distinct Stages of Human Endothelial-to-Hematopoietic Transition. *Cell Rep.* **19**, 10–19 (2017).

24. Ivanovs, A., Rybtsov, S., Anderson, R. A. & Medvinsky, A. Vast Self-Renewal Potential of Human AGM Region HSCs Dramatically Declines in the Umbilical Cord Blood. *Stem Cell Reports* **15**, 811–816 (2020).
25. Lewis, K., Yoshimoto, M. & Takebe, T. Fetal liver hematopoiesis: from development to delivery. *Stem Cell Res. Ther.* **12**, 139 (2021).
26. Ema, H. & Nakauchi, H. Expansion of hematopoietic stem cells in the developing liver of a mouse embryo. *Blood* **95**, 2284–2288 (2000).
27. Khan, J. A. *et al.* Fetal liver hematopoietic stem cell niches associate with portal vessels. *Science (80-.).* **351**, 176–180 (2016).
28. Chou, S. & Lodish, H. F. Fetal liver hepatic progenitors are supportive stromal cells for hematopoietic stem cells. *Proc. Natl. Acad. Sci.* **107**, 7799–7804 (2010).
29. Lee, Y., Leslie, J., Yang, Y. & Ding, L. Hepatic stellate and endothelial cells maintain hematopoietic stem cells in the developing liver. *J. Exp. Med.* **218**, (2021).
30. Popescu, D.-M. *et al.* Decoding human fetal liver haematopoiesis. *Nature* **574**, 365–371 (2019).
31. Bertrand, J. Y. *et al.* Fetal spleen stroma drives macrophage commitment. *Development* **133**, 3619–3628 (2006).
32. Lewis, S. M., Williams, A. & Eisenbarth, S. C. Structure and function of the immune system in the spleen. *Sci. Immunol.* **4**, 1–55 (2019).
33. Coşkun, S. *et al.* Development of the Fetal Bone Marrow Niche and Regulation of HSC Quiescence and Homing Ability by Emerging Osteolineage Cells. *Cell Rep.* **9**, 581–590 (2014).
34. Robin, C. *et al.* Human Placenta Is a Potent Hematopoietic Niche Containing Hematopoietic Stem and Progenitor Cells throughout Development. *Cell Stem Cell* **5**, 385–395 (2009).
35. Bowie, M. B. *et al.* Hematopoietic stem cells proliferate until after birth and show a reversible phase-specific engraftment defect. *J. Clin. Invest.* **116**, 2808–2816 (2006).
36. Li, Y. *et al.* Single-Cell Analysis of Neonatal HSC Ontogeny Reveals Gradual and Uncoordinated Transcriptional Reprogramming that Begins before Birth. *Cell Stem Cell* **27**, 732-747.e7 (2020).
37. Gao, X., Xu, C., Asada, N. & Frenette, P. S. The hematopoietic stem cell niche: from embryo to adult. *Development* **145**, (2018).
38. Wei, Q. & Frenette, P. S. Niches for Hematopoietic Stem Cells and Their Progeny. *Immunity* **48**, 632–648 (2018).
39. Kunisaki, Y. *et al.* Arteriolar niches maintain haematopoietic stem cell quiescence. *Nature* **502**, 637–643 (2013).
40. Frisch, B. J. The hematopoietic stem cell niche: What's so special about bone? *Bone* **119**, 8–12 (2019).
41. Cao, H. *et al.* Osteopontin is An Important Regulative Component of the Fetal Bone Marrow Hematopoietic Stem Cell Niche. *Cells* **8**, 985 (2019).
42. Comazzetto, S., Shen, B. & Morrison, S. J. Niches that regulate stem cells and hematopoiesis in adult bone marrow. *Dev. Cell* **56**, 1848–1860 (2021).
43. Zhao, M. *et al.* Megakaryocytes maintain homeostatic quiescence and promote post-injury regeneration of hematopoietic stem cells. *Nat. Med.* **20**, 1321–1326 (2014).
44. Bruns, I. *et al.* Megakaryocytes regulate hematopoietic stem cell quiescence through CXCL4 secretion. *Nat. Med.* **20**, 1315–1320 (2014).
45. Pinho, S. & Frenette, P. S. Haematopoietic stem cell activity and interactions with the niche. *Nat. Rev. Mol. Cell Biol.* **20**, 303–320 (2019).
46. Morrison, S. J. & Scadden, D. T. The bone marrow niche for haematopoietic stem cells.

Nature **505**, 327–334 (2014).
47. Main, J. M. & Prehn, R. T. Successful Skin Homografts After the Administration of High Dosage X Radiation and Homologous Bone Marrow. *J. Natl. Cancer Inst.* **15**, 1023–1029 (1955).
48. Barnes, D. W. H., Corp, M. J., Loutit, J. F. & Neal, F. E. Treatment of Murine Leukaemia With X Rays and Homologous Bone Marrow. *Br. Med. J.* **2**, 626–627 (1956).
49. Thomas, E. D., Lochte, H. L., Cannon, J. H., Sahler, O. D. & Ferrebee, J. W. SUPRALETHAL WHOLE BODY IRRADIATION AND ISOLOGOUS MARROW TRANSPLANTATION IN MAN*†. *J. Clin. Invest.* **38**, 1709–1716 (1959).
50. Gibson, T. & Medawar, P. B. The Fate of Skin Homografts in Man. *J. Anat.* **77**, 299–310 (1943).
51. Billingham, R. E., Brent, L. & Medawar, P. B. 'Activity Acquired Tolerance' of Foreign Cells. *Nature* **172**, 603–606 (1953).
52. Billingham, R. E. & Brent, L. Quantitative Studies on Tissue Transplantation Immunity. IV. Induction of Tolerance in Newborn Mice and Studies on the Phenomenon of Runt Disease. *Philos. Trans. R. Soc. London. Ser. B, Biol. Sci.* **242**, 439–477 (1959).
53. Dausset, J. Iso-Leuco-Anticorps. *Acta Haematol.* **20**, 156–166 (1958).
54. Gatti, R. A., Meuwissen, H. J., Allen, H. D., Hong, R. & Good, R. A. Immunological Reconstitution of Sex-Linked Lymphopenic Immunological Deficiency. *Lancet* **II**, 1366–1369 (1968).
55. Kawai, T. *et al.* HLA-Mismatched Renal Transplantation without Maintenance Immunosuppression. *N. Engl. J. Med.* **358**, 353–361 (2008).
56. Gentzkow, G. D. *et al.* Use of Dermagraft, a Cultured Human Dermis, to Treat Diabetic Foot Ulcers. *Diabetes Care* **19**, 350–354 (1996).
57. Falanga, V. *et al.* Rapid Healing of Venous Ulcers and Lack of Clinical Rejection With an Allogeneic Cultured Human Skin Equivalent. *Arch. Dermatol.* **134**, 293–300 (1998).
58. Cuono, C., Langdon, R. & Mcguire, J. Use of Cultured Epidermal Autografts and Dermal Allografts as Skin Replacement After Burn Injury. *Lancet* **327**, 1123–1124 (1986).
59. Boyce, S. T. *et al.* Randomized , Paired-Site Comparison of Autologous Engineered Skin Substitutes and Split-Thickness Skin Graft for Closure of Extensive , Full-Thickness Burns. *J. Burn Care Res.* **38**, 61–70 (2017).
60. Locatelli, F. *et al.* Outcome of children with acute leukemia given HLA-haploidentical HSCT after ab T-cell and B-cell depletion. **130**, 677–686 (2019).
61. Brentjens, R. J. *et al.* Eradication of Systemic B-cell Tumors by Genetically Targeted Human T Lymphocytes Co-stimulated by CD80 and Interleukin-15. *Nat. Med.* **9**, 279–286 (2003).
62. Niederwieser, D. *et al.* One and a half million hematopoietic stem cell transplants: continuous and differential improvement in worldwide access with the use of non-identical family donors. *Haematologica* **107**, 1045–1053 (2021).
63. Biasco, L. *et al.* In Vivo Tracking of Human Hematopoiesis Reveals Patterns of Clonal Dynamics during Early and Steady-State Reconstitution Phases. *Cell Stem Cell* **19**, 107–119 (2016).
64. Li, Z. *et al.* Immune-Mediated Complications after Hematopoietic Stem Cell Transplantation. *Biol. Blood Marrow Transplant.* **22**, 1368–1375 (2016).
65. Fleischhauer, K. *et al.* Effect of T-cell-epitope matching at HLA-DPB1 in recipients of unrelated-donor haemopoietic-cell transplantation: a retrospective study. *Lancet Oncol.* **13**, 366–374 (2012).
66. Meurer, T. *et al.* Permissive HLA-DPB1 mismatches in HCT depend on immunopeptidome divergence and editing by HLA-DM. *Blood* **137**, 923–928 (2021).

67. Martin, P. J. *et al.* Genome-wide minor histocompatibility matching as related to the risk of graft-versus-host disease. *Blood* **129**, 791–798 (2017).
68. Nie, D. *et al.* Targeted minor histocompatibility antigen typing to estimate graft-versus-host disease after allogeneic haematopoietic stem cell transplantation. *Bone Marrow Transplant.* **56**, 3024–3028 (2021).
69. Gyurkocza, B. & Sandmaier, B. M. Conditioning regimens for hematopoietic cell transplantation: One size does not fit all. *Blood* **124**, 344–353 (2014).
70. Jethava, Y. S. *et al.* Conditioning regimens for allogeneic hematopoietic stem cell transplants in acute myeloid leukemia. *Bone Marrow Transplant.* **52**, 1504–1511 (2017).
71. D'Souza, A. *et al.* Current Use of and Trends in Hematopoietic Cell Transplantation in the United States. *Biol. Blood Marrow Transplant.* **26**, e177–e182 (2020).
72. Huang, X. & Broxmeyer, H. E. Progress towards improving homing and engraftment of hematopoietic stem cells for clinical transplantation. *Curr. Opin. Hematol.* **26**, 266–272 (2019).
73. Fabrizio, V., Armeson, K., Warneke, S., Jaroscak, J. J. & Hudspeth, M. Trends in Cell Dose Requests for a NMDP Bone Marrow Collection Center. *Biol. Blood Marrow Transplant.* **23**, S408 (2017).
74. Greenbaum, A. M. & Link, D. C. Mechanisms of G-CSF-mediated hematopoietic stem and progenitor mobilization. *Leukemia* **25**, 211–217 (2011).
75. Bilgin, Y. M. & de Greef, G. E. Plerixafor for stem cell mobilization. *Curr. Opin. Hematol.* **23**, 67–71 (2016).
76. Sheridan, W. P. *et al.* Effect of peripheral-blood progenitor cells mobilised by filgrastim (G-CSF) on platelet recovery after high-dose chemotherapy. *Lancet* **339**, 640–644 (1992).
77. Broxmeyer, H. E. *et al.* Human umbilical cord blood as a potential source of transplantable hematopoietic stem/progenitor cells. *Proc. Natl. Acad. Sci.* **86**, 3828–3832 (1989).
78. Kindwall-Keller, T. L. & Ballen, K. K. Alternative Donor Graft Sources for Adults with Hematologic Malignancies: A Donor for All Patients in 2017! *Oncologist* **22**, 1125–1134 (2017).
79. Kraft, D. L. *et al.* The MarrowMiner: A Novel Minimally Invasive and Effective Device for the Harvest of Bone Marrow. *Biol. Blood Marrow Transplant.* **26**, 219–229 (2020).
80. Prokopishyn, N. L. *et al.* The Concentration of Total Nucleated Cells in Harvested Bone Marrow for Transplantation Has Decreased over Time. *Biol. Blood Marrow Transplant.* **25**, 1325–1330 (2019).
81. Velardi, E. *et al.* The role of the thymus in allogeneic bone marrow transplantation and the recovery of the peripheral T-cell compartment. *Semin. Immunopathol.* **43**, 101–117 (2021).
82. Anasetti, C. *et al.* Peripheral-Blood Stem Cells versus Bone Marrow from Unrelated Donors. *N. Engl. J. Med.* **367**, 1487–1496 (2012).
83. Srinivasan, A. *et al.* Outcome of Haploidentical Peripheral Blood Allografts Using Post-Transplantation Cyclophosphamide Compared to Matched Sibling and Unrelated Donor Bone Marrow Allografts in Pediatric Patients with Hematologic Malignancies: A Single-Center Analysis. *Transplant. Cell. Ther.* **28**, 158.e1-158.e9 (2022).
84. Auletta, J. J., Kou, J. & Shaw, B. E. Current use and outcome of hematopoietic stem cell transplantation: CIBMTR US summary slides. (2021).
85. Greil, C. *et al.* Stem cell mobilization in poor mobilizers with multiple myeloma or lymphoma before and after introduction of plerixafor: a single-center comparative analysis using a cost-efficient single fixed-dose schedule. *Leuk. Lymphoma* **59**, 1722–

1725 (2018).
86. Saraceni, F., Shem-Tov, N., Olivieri, A. & Nagler, A. Mobilized peripheral blood grafts include more than hematopoietic stem cells: the immunological perspective. *Bone Marrow Transplant.* **50**, 886–891 (2015).
87. Byrne, M., Savani, B. N., Mohty, M. & Nagler, A. Peripheral blood stem cell versus bone marrow transplantation: A perspective from the Acute Leukemia Working Party of the European Society for Blood and Marrow Transplantation. *Exp. Hematol.* **44**, 567–573 (2016).
88. Pastore, D. *et al.* CD3+/Tregs Ratio in Donor Grafts Is Linked to Acute Graft-versus-Host Disease and Immunologic Recovery after Allogeneic Peripheral Blood Stem Cell Transplantation. *Biol. Blood Marrow Transplant.* **18**, 887–893 (2012).
89. Sanchez-Petitto, G. *et al.* Umbilical Cord Blood Transplantation: Connecting Its Origin to Its Future. *Stem Cells Transl. Med.* **12**, 55–71 (2023).
90. Dehn, J. *et al.* Selection of unrelated donors and cord blood units for hematopoietic cell transplantation: guidelines from the NMDP/CIBMTR. *Blood* **134**, 924–934 (2019).
91. Panch, S. R., Szymanski, J., Savani, B. N. & Stroncek, D. F. Sources of Hematopoietic Stem and Progenitor Cells and Methods to Optimize Yields for Clinical Cell Therapy. *Biol. Blood Marrow Transplant.* **23**, 1241–1249 (2017).
92. Talib, S. & Shepard, K. A. Unleashing the cure: Overcoming persistent obstacles in the translation and expanded use of hematopoietic stem cell-based therapies. *Stem Cells Transl. Med.* **9**, 420–426 (2020).
93. Wang, J. & Metheny, L. Umbilical cord blood derived cellular therapy: advances in clinical development. *Front. Oncol.* **13**, (2023).
94. Saiyin, T. *et al.* Clinical Outcomes of Umbilical Cord Blood Transplantation Using Ex Vivo Expansion: A Systematic Review and Meta-Analysis of Controlled Studies. *Transplant. Cell. Ther.* **29**, 129.e1-129.e9 (2023).
95. Shi, P. A., Luchsinger, L. L., Greally, J. M. & Delaney, C. S. Umbilical cord blood: an undervalued and underutilized resource in allogeneic hematopoietic stem cell transplant and novel cell therapy applications. *Curr. Opin. Hematol.* **29**, 317–326 (2022).
96. Gabelli, M., Veys, P. & Chiesa, R. Current status of umbilical cord blood transplantation in children. *Br. J. Haematol.* **190**, 650–683 (2020).
97. Amouzegar, A., Dey, B. R. & Spitzer, T. R. Peripheral Blood or Bone Marrow Stem Cells? Practical Considerations in Hematopoietic Stem Cell Transplantation. *Transfus. Med. Rev.* **33**, 43–50 (2019).
98. Tucci, F., Scaramuzza, S., Aiuti, A. & Mortellaro, A. Update on Clinical Ex Vivo Hematopoietic Stem Cell Gene Therapy for Inherited Monogenic Diseases. *Mol. Ther.* **29**, 489–504 (2021).
99. Ribeiro-filho, A. C., Levy, D., Ruiz, J. L. M., Mantovani, M. da C. & Bydlowski, S. P. Traditional and advanced cell cultures in hematopoietic stem cell studies. *Cells* **8**, 1–13 (2019).
100. Pellegrin, S., Severn, C. E. & Toye, A. M. Towards manufactured red blood cells for the treatment of inherited anemia. *Haematologica* **106**, 2304–2311 (2021).
101. Pineault, N. & Abu-Khader, A. Advances in umbilical cord blood stem cell expansion and clinical translation. *Exp. Hematol.* **43**, 498–513 (2015).
102. Lund, T. C., Boitano, A. E., Delaney, C. S., Shpall, E. J. & Wagner, J. E. Advances in umbilical cord blood manipulation—from niche to bedside. *Nat. Rev. Clin. Oncol.* **12**, 163–174 (2015).
103. Costa, M. H. G., de Soure, A. M., Cabral, J. M. S., Ferreira, F. C. & da Silva, C. L. Hematopoietic Niche - Exploring Biomimetic Cues to Improve the Functionality of

Hematopoietic Stem/Progenitor Cells. *Biotechnol. J.* **13**, 1700088 (2018).
104. Qiu, L. *et al.* Ex Vivo Expansion of CD34+ Umbilical Cord Blood Cells in a Defined Serum-Free Medium (QBSF-60) with Early Effect Cytokines. *J. Hematother. Stem Cell Res.* **8**, 609–618 (1999).
105. Allison, D. W., Leugers, S. L., Pronold, B. J., Zant, G. Van & Laurel, M. Improved Ex Vivo Expansion of Functional CD34 + Cells Using Stemline ™ II Hematopoietic Stem Cell Expansion Medium. *Cell Transm.* **20**, 20–23 (2004).
106. Sei, J. *et al.* StemPro™ HSC expansion medium (Prototype) supports superior expansion of human hematopoietic stem-progenitor cells. *Cytotherapy* **21**, S64–S65 (2019).
107. Lipsitz, Y. Y., Timmins, N. E. & Zandstra, P. W. Quality cell therapy manufacturing by design. *Nat. Biotechnol.* **34**, 393–400 (2016).
108. Pineault, N. *et al.* Individual and synergistic cytokine effects controlling the expansion of cord blood CD34+ cells and megakaryocyte progenitors in culture. *Cytotherapy* **13**, 467–480 (2011).
109. Branco, A. *et al.* Tailored Cytokine Optimization for ex vivo Culture Platforms Targeting the Expansion of Human Hematopoietic Stem/Progenitor Cells. *Front. Bioeng. Biotechnol.* **8**, 1–21 (2020).
110. Shpall, E. J. *et al.* Transplantation of ex vivo expanded cord blood. *Biol. Blood Marrow Transplant.* **8**, 368–376 (2002).
111. Dolgalev, I. & Tikhonova, A. N. Connecting the Dots: Resolving the Bone Marrow Niche Heterogeneity. *Front. Cell Dev. Biol.* **9**, 1–11 (2021).
112. Méndez-Ferrer, S. *et al.* Bone marrow niches in haematological malignancies. *Nat. Rev. Cancer* **20**, 285–298 (2020).
113. Seandel, M. *et al.* Generation of a functional and durable vascular niche by the adenoviral E4ORF1 gene. *Proc. Natl. Acad. Sci.* **105**, 19288–19293 (2008).
114. Butler, J. M. *et al.* Endothelial Cells Are Essential for the Self-Renewal and Repopulation of Notch-Dependent Hematopoietic Stem Cells. *Cell Stem Cell* **6**, 251–264 (2010).
115. Birbrair, A. & Frenette, P. S. Niche heterogeneity in the bone marrow. *Ann. N. Y. Acad. Sci.* **1370**, 82–96 (2016).
116. Li, H. *et al.* Arterial endothelium creates a permissive niche for expansion of human cord blood hematopoietic stem and progenitor cells. *Stem Cell Res. Ther.* **11**, 358 (2020).
117. Li, W., Johnson, S. A., Shelley, W. C. & Yoder, M. C. Hematopoietic stem cell repopulating ability can be maintained in vitro by some primary endothelial cells. *Exp. Hematol.* **32**, 1226–1237 (2004).
118. Rafii, S., Butler, J. M. & Ding, B.-S. Angiocrine functions of organ-specific endothelial cells. *Nature* **529**, 316–325 (2016).
119. Pittenger, M. F. *et al.* Mesenchymal stem cell perspective: cell biology to clinical progress. *npj Regen. Med.* **4**, (2019).
120. Olsen, T. R., Ng, K. S., Lock, L. T., Ahsan, T. & Rowley, J. A. Peak MSC-Are we there yet? *Front. Med.* **5**, (2018).
121. Pigeau, G. M., Csaszar, E. & Dulgar-Tulloch, A. Commercial Scale Manufacturing of Allogeneic Cell Therapy. *Front. Med.* **5**, 1–8 (2018).
122. de Almeida Fuzeta, M., de Matos Branco, A. D., Fernandes-Platzgummer, A., da Silva, C. L. & Cabral, J. M. S. Addressing the Manufacturing Challenges of Cell-Based Therapies. in *Advances in Biochemical Engineering/Biotechnology* **171**, 225–278 (Springer, Cham, 2019).
123. Klein, C. *et al.* Ex Vivo expansion of hematopoietic stem-and progenitor cells from cord blood in coculture with mesenchymal stroma cells from amnion, chorion, wharton's jelly, amniotic fluid, cord blood, and bone marrow. *Tissue Eng. - Part A* **19**, 2577–2585

(2013).
124. Bucar, S. *et al.* Influence of the mesenchymal stromal cell source on the hematopoietic supportive capacity of umbilical cord blood-derived CD34+-enriched cells. *Stem Cell Res. Ther.* **12**, 399 (2021).
125. Jing, D. *et al.* Hematopoietic stem cells in co-culture with mesenchymal stromal cells - modeling the niche compartments in vitro. *Haematologica* **95**, 542–550 (2010).
126. da Silva, C. L. *et al.* Dynamic cell-cell interactions between cord blood haematopoietic progenitors and the cellular niche are essential for the expansion of CD34 + , CD34 + CD38 − and early lymphoid CD7 + cells. *J. Tissue Eng. Regen. Med.* **4**, 149–158 (2010).
127. Walenda, T. *et al.* Synergistic effects of growth factors and mesenchymal stromal cells for expansion of hematopoietic stem and progenitor cells. *Exp. Hematol.* **39**, 617–628 (2011).
128. de Lima, M. *et al.* Cord-Blood Engraftment with Ex Vivo Mesenchymal-Cell Coculture. *N. Engl. J. Med.* **367**, 2305–2315 (2012).
129. Khoury, M. *et al.* Mesenchymal Stem Cells Secreting Angiopoietin-Like-5 Support Efficient Expansion of Human Hematopoietic Stem Cells Without Compromising Their Repopulating Potential. *Stem Cells Dev.* **20**, 1371–1381 (2011).
130. Nakahara, F. *et al.* Engineering a haematopoietic stem cell niche by revitalizing mesenchymal stromal cells. *Nat. Cell Biol.* **21**, 560–567 (2019).
131. Raposo, G. & Stahl, P. D. Extracellular vesicles: a new communication paradigm? *Nat. Rev. Mol. Cell Biol.* **20**, 509–510 (2019).
132. Xie, H. *et al.* Mesenchymal Stem Cell-Derived Microvesicles Support Ex Vivo Expansion of Cord Blood-Derived CD34 + Cells. *Stem Cells Int.* **2016**, 1–13 (2016).
133. Ghebes, C. A. *et al.* Extracellular Vesicles Derived From Adult and Fetal Bone Marrow Mesenchymal Stromal Cells Differentially Promote ex vivo Expansion of Hematopoietic Stem and Progenitor Cells. *Front. Bioeng. Biotechnol.* **9**, 1–14 (2021).
134. Blank, U. & Karlsson, S. TGF-β signaling in the control of hematopoietic stem cells. *Blood* **125**, 3542–3550 (2015).
135. Gautheron, F., Georgievski, A., Garrido, C. & Quéré, R. Bone marrow-derived extracellular vesicles carry the TGF-β signal transducer Smad2 to preserve hematopoietic stem cells in mice. *Cell Death Discov.* **9**, 117 (2023).
136. Morhayim, J. *et al.* Identification of osteolineage cell-derived extracellular vesicle cargo implicated in hematopoietic support. *FASEB J.* **34**, 5435–5452 (2020).
137. Niazi, V. *et al.* Hypoxia preconditioned mesenchymal stem cell-derived exosomes induce ex vivo expansion of umbilical cord blood hematopoietic stem cells CD133 + by stimulation of Notch signaling pathway. *Biotechnol. Prog.* **38**, 1–15 (2022).
138. Teng, F. & Fussenegger, M. Shedding Light on Extracellular Vesicle Biogenesis and Bioengineering. *Adv. Sci.* **8**, 2003505 (2021).
139. Ulpiano, C., da Silva, C. L. & Monteiro, G. A. Bioengineered Mesenchymal-Stromal-Cell-Derived Extracellular Vesicles as an Improved Drug Delivery System: Methods and Applications. *Biomedicines* **11**, 1231 (2023).
140. Peled, A. *et al.* The chemokine SDF-1 stimulates integrin-mediated arrest of CD34+ cells on vascular endothelium under shear flow. *J. Clin. Invest.* **104**, 1199–1211 (1999).
141. Varnum-Finney, B. *et al.* Immobilization of Notch ligand, Delta-1, is required for induction of notch signaling. *J. Cell Sci.* **113**, 4313–4318 (2000).
142. Delaney, C., Varnum-Finney, B., Aoyama, K., Brashem-Stein, C. & Bernstein, I. D. Dose-dependent effects of the Notch ligand Delta1 on ex vivo differentiation and in vivo marrow repopulating ability of cord blood cells. *Blood* **106**, 2693–2699 (2005).
143. Delaney, C. *et al.* Notch-mediated Expansion of Human Cord Blood Progenitor Cells

Capable of Rapid Myeloid Reconstitution. *Nat. Med.* **16**, 232–236 (2010).
144. Vanderbeck, A. & Maillard, I. Notch signaling at the crossroads of innate and adaptive immunity. *J. Leukoc. Biol.* **109**, 535–548 (2021).
145. Ng, H. L., Quail, E., Cruickshank, M. N. & Ulgiati, D. To Be, or Notch to Be: Mediating Cell Fate from Embryogenesis to Lymphopoiesis. *Biomolecules* **11**, 849 (2021).
146. Milano, F., Thur, L. A., Blake, J. & Delaney, C. Infusion of Non-HLA-Matched Off-the-Shelf Ex Vivo Expanded Cord Blood Progenitors in Patients Undergoing Cord Blood Transplantation: Result of a Phase II Clinical Trial. *Front. Cell Dev. Biol.* **10**, 1–7 (2022).
147. Delaney, C. *et al.* Infusion of a non-HLA-matched ex-vivo expanded cord blood progenitor cell product after intensive acute myeloid leukaemia chemotherapy: a phase 1 trial. *Lancet Haematol.* **3**, e330–e339 (2016).
148. Araki, D. *et al.* NOTCH-mediated ex vivo expansion of human hematopoietic stem and progenitor cells by culture under hypoxia. *Stem Cell Reports* **16**, 2336–2350 (2021).
149. Stiff, P. *et al.* Autologous transplantation of ex vivo expanded bone marrow cells grown from small aliquots after high-dose chemotherapy for breast cancer. *Blood* **95**, 2169–2174 (2000).
150. Jaroscak, J. *et al.* Augmentation of umbilical cord blood (UCB) transplantation with ex vivo–expanded UCB cells: results of a phase 1 trial using the AastromReplicell System. *Blood* **101**, 5061–5067 (2003).
151. Csaszar, E. *et al.* Rapid expansion of human hematopoietic stem cells by automated control of inhibitory feedback signaling. *Cell Stem Cell* **10**, 218–229 (2012).
152. Csaszar, E., Chen, K., Caldwell, J., Chan, W. & Zandstra, P. W. Real-time monitoring and control of soluble signaling factors enables enhanced progenitor cell outputs from human cord blood stem cell cultures. *Biotechnol. Bioeng.* **111**, 1258–1264 (2014).
153. Caldwell, J., Wang, W. & Zandstra, P. W. Proportional-Integral-Derivative (PID) Control of Secreted Factors for Blood Stem Cell Culture. *PLoS One* **10**, e0137392 (2015).
154. Jones, M., Cunningham, A., Frank, N. & Sethi, D. The monoculture of cord-blood-derived CD34+ cells by an automated, membrane-based dynamic perfusion system with a novel cytokine cocktail. *Stem Cell Reports* **17**, 2585–2594 (2022).
155. Ingavle, G., Vaidya, A. & Kale, V. Constructing Three-Dimensional Microenvironments Using Engineered Biomaterials for Hematopoietic Stem Cell Expansion. *Tissue Eng. Part B Rev.* **25**, 312–329 (2019).
156. Wasnik, S., Kantipudi, S., Kirkland, M. A. & Pande, G. Enhanced Ex Vivo Expansion of Human Hematopoietic Progenitors on Native and Spin Coated Acellular Matrices Prepared from Bone Marrow Stromal Cells. *Stem Cells Int.* **2016**, 1–13 (2016).
157. Prewitz, M. C. *et al.* Extracellular matrix deposition of bone marrow stroma enhanced by macromolecular crowding. *Biomaterials* **73**, 60–69 (2015).
158. Madl, C. M. & Heilshorn, S. C. Engineering Hydrogel Microenvironments to Recapitulate the Stem Cell Niche. *Annu. Rev. Biomed. Eng.* **20**, 21–47 (2018).
159. Raic, A., Rödling, L., Kalbacher, H. & Lee-Thedieck, C. Biomimetic macroporous PEG hydrogels as 3D scaffolds for the multiplication of human hematopoietic stem and progenitor cells. *Biomaterials* **35**, 929–940 (2014).
160. Xu, Y. *et al.* Efficient expansion of rare human circulating hematopoietic stem/progenitor cells in steady-state blood using a polypeptide-forming 3D culture. *Protein Cell* **13**, 808–824 (2022).
161. Bai, T. *et al.* Expansion of primitive human hematopoietic stem cells by culture in a zwitterionic hydrogel. *Nat. Med.* **25**, 1566–1575 (2019).
162. Kim, J. E., Lee, E. J., Wu, Y., Kang, Y. G. & Shin, J. The combined effects of hierarchical scaffolds and mechanical stimuli on ex vivo expansion of haematopoietic

stem/progenitor cells. *Artif. Cells, Nanomedicine, Biotechnol.* **47**, 585–592 (2019).
163. Mokhtari, S. *et al.* Evaluating Interaction of Cord Blood Hematopoietic Stem/Progenitor Cells with Functionally Integrated Three-Dimensional Microenvironments. *Stem Cells Transl. Med.* **7**, 271–282 (2018).
164. Bourgine, P. E. *et al.* In vitro biomimetic engineering of a human hematopoietic niche with functional properties. *Proc. Natl. Acad. Sci.* **115**, (2018).
165. Efe, J. A. & Ding, S. The evolving biology of small molecules: controlling cell fate and identity. *Philos. Trans. R. Soc. B Biol. Sci.* **366**, 2208–2221 (2011).
166. Peled, T. *et al.* Linear polyamine copper chelator tetraethylenepentamine augments long-term ex vivo expansion of cord blood-derived CD34+ cells and increases their engraftment potential in NOD/SCID mice. *Exp. Hematol.* **32**, 547–555 (2004).
167. Peled, T. *et al.* Chelatable cellular copper modulates differentiation and self-renewal of cord blood–derived hematopoietic progenitor cells. *Exp. Hematol.* **33**, 1092–1100 (2005).
168. Prus, E. & Fibach, E. The Effect of the Copper Chelator Tetraethylenepentamine on Reactive Oxygen Species Generation by Human Hematopoietic Progenitor Cells. *Stem Cells Dev.* **16**, 1053–1056 (2007).
169. Peled, T. *et al.* Nicotinamide, a SIRT1 inhibitor, inhibits differentiation and facilitates expansion of hematopoietic progenitor cells with enhanced bone marrow homing and engraftment. *Exp. Hematol.* **40**, 342-355.e1 (2012).
170. FDA approves cord-blood therapy. *Nat. Biotechnol.* **41**, 589–589 (2023).
171. Bug, G. *et al.* Valproic Acid Stimulates Proliferation and Self-renewal of Hematopoietic Stem Cells. *Cancer Res.* **65**, 2537–2541 (2005).
172. Zimran, E. *et al.* Expansion and preservation of the functional activity of adult hematopoietic stem cells cultured ex vivo with a histone deacetylase inhibitor. *Stem Cells Transl. Med.* **9**, 531–542 (2020).
173. Schaniel, C. *et al.* Evaluation of a clinical-grade, cryopreserved, ex vivo-expanded stem cell product from cryopreserved primary umbilical cord blood demonstrates multilineage hematopoietic engraftment in mouse xenografts. *Cytotherapy* **23**, 841–851 (2021).
174. Boitano, A. E. *et al.* Aryl Hydrocarbon Receptor Antagonists Promote the Expansion of Human Hematopoietic Stem Cells. *Science (80-.).* **329**, 1345–1348 (2010).
175. Fares, I. *et al.* Pyrimidoindole derivatives are agonists of human hematopoietic stem cell self-renewal. *Science (80-.).* **345**, 1509–1512 (2014).
176. Gao, Y. *et al.* Small-molecule inhibitors targeting INK4 protein p18INK4C enhance ex vivo expansion of haematopoietic stem cells. *Nat. Commun.* **6**, 6328 (2015).
177. Hua, P. *et al.* The BET inhibitor CPI203 promotes ex vivo expansion of cord blood long-term repopulating HSCs and megakaryocytes. *Blood* **136**, 2410–2415 (2020).
178. Wagner, J. E. *et al.* Phase I/II Trial of StemRegenin-1 Expanded Umbilical Cord Blood Hematopoietic Stem Cells Supports Testing as a Stand-Alone Graft. *Cell Stem Cell* **18**, 144–155 (2016).
179. Cohen, S. *et al.* Hematopoietic stem cell transplantation using single UM171-expanded cord blood: a single-arm, phase 1–2 safety and feasibility study. *Lancet Haematol.* **7**, e134–e145 (2020).
180. Bozhilov, Y. K., Hsu, I., Brown, E. J. & Wilkinson, A. C. In Vitro Human Haematopoietic Stem Cell Expansion and Differentiation. *Cells* **12**, 896 (2023).
181. Sakurai, M. *et al.* Chemically defined cytokine-free expansion of human haematopoietic stem cells. *Nature* **615**, 127–133 (2023).
182. Iglesias-Lopez, C., Agustí, A., Vallano, A. & Obach, M. Current landscape of clinical

development and approval of advanced therapies. *Mol. Ther. - Methods Clin. Dev.* **23**, 606–618 (2021).
183. European Medicines Agency. European Medicines Agency. (2023).
184. United States Food and Drug Administration. Approved Cellular and Gene Therapy Products. (2023).
185. Chabannon, C. *et al.* Hematopoietic Stem Cell Transplantation in its 60s - A Platform for Cellular Therapies. *Sci. Transl. Med.* **10**, 1–10 (2018).
186. Tanne, J. H. FDA approves $3.5m gene therapy for adults with haemophilia B. *BMJ* **379**, o2858 (2022).
187. Cell, G. Gamida Cell Conference Call. (2023). Available at: https://investors.gamida-cell.com/news-events/events-presentations/event-details/gamida-cell-conference-call-0.
188. Ko□rbling, M. & Anderlini, P. Peripheral blood stem cell versus bone marrow allotransplantation: does the source of hematopoietic stem cells matter? *Blood* **98**, 2900–2908 (2001).
189. Pittenger, M. F. *et al.* Multilineage Potential of Adult Human Mesenchymal Stem Cells. *Science (80-.).* **284**, 143–147 (1999).
190. Barker, J. N. *et al.* CD34+ cell content of 126 341 cord blood units in the US inventory: Implications for transplantation and banking. *Blood Adv.* **3**, 1267–1271 (2019).
191. Dominici, M. *et al.* Minimal criteria for defining multipotent mesenchymal stromal cells. The International Society for Cellular Therapy position statement. *Cytotherapy* **8**, 315–317 (2006).
192. Lennon, D. P. & Caplan, A. I. Isolation of rat marrow-derived mesenchymal stem cells. *Exp. Hematol.* **34**, 1606–1607 (2006).
193. Lu, L. L. *et al.* Isolation and characterization of human umbilical cord mesenchymal stem cells with hematopoiesis-supportive function and other potentials. *Haematologica* **91**, 1017–1026 (2006).
194. Nimura, A. *et al.* Increased proliferation of human synovial mesenchymal stem cells with autologous human serum: Comparisons with bone marrow mesenchymal stem cells and with fetal bovine serum. *Arthritis Rheum.* **58**, 501–510 (2008).
195. Oedayrajsingh-Varma, M. J. *et al.* Adipose tissue-derived mesenchymal stem cell yield and growth characteristics are affected by the tissue-harvesting procedure. *Cytotherapy* **8**, 166–177 (2006).
196. De Bruyn, C. *et al.* A Rapid, Simple, and Reproducible Method for the Isolation of Mesenchymal Stromal Cells from Wharton's Jelly Without Enzymatic Treatment. *Stem Cells Dev.* **20**, 547–557 (2010).
197. Ghorbani, A., Jalali, S. A. & Varedi, M. Isolation of adipose tissue mesenchymal stem cells without tissue destruction: A non-enzymatic method. *Tissue Cell* **46**, 54–58 (2014).
198. Zhang, S., Muneta, T., Morito, T., Mochizuki, T. & Sekiya, I. Autologous synovial fluid enhances migration of mesenchymal stem cells from synovium of osteoarthritis patients in tissue culture system. *J. Orthop. Res.* **26**, 1413–1418 (2008).
199. Aktas, M., Radke, T. F., Strauer, B. E., Wernet, P. & Kogler, G. Separation of adult bone marrow mononuclear cells using the automated closed separation system Sepax. *Cytotherapy* **10**, 203–211 (2008).
200. Eyrich, M. *et al.* Development and validation of a fully GMP-compliant production process of autologous, tumor-lysate-pulsed dendritic cells. *Cytotherapy* **16**, 946–964 (2014).
201. Kato, K. & Radbruch, A. Isolation and characterization of CD34+ hematopoietic stem cells from human peripheral blood by high-gradient magnetic cell sorting. *Cytometry* **14**, 384–392 (1993).

202. De Wynter, E. A. *et al.* Comparison of purity and enrichment of CD34+ cells from bone marrow, umbilical cord and peripheral blood (primed for apheresis) using five separation systems. *Stem Cells* **13**, 524–532 (1995).
203. Simmons, P. J. & Torok-Storb, B. Identification of stromal cell precursors in human bone marrow by a novel monoclonal antibody, STRO-1. *Blood* **78**, 55–62 (1991).
204. Gonçalves, R., da Silva, C. L., Cabral, J. M. S., Zanjani, E. D. & Almeida-Porada, G. A Stro-1+ human universal stromal feeder layer to expand/maintain human bone marrow hematopoietic stem/progenitor cells in a serum-free culture system. *Exp. Hematol.* **34**, 1353–1359 (2006).
205. Leong, W., Nankervis, B. & Beltzer, J. Automation: what will the cell therapy laboratory of the future look like? *Cell Gene Ther. Insights* **4**, 679–694 (2019).
206. Sutermaster, B. A. & Darling, E. M. Considerations for high-yield, high-throughput cell enrichment: fluorescence versus magnetic sorting. *Sci. Rep.* **9**, 1–9 (2019).
207. Koehl, U. *et al.* IL-2 activated NK cell immunotherapy of three children after haploidentical stem cell transplantation. *Blood Cells, Mol. Dis.* **33**, 261–266 (2004).
208. Neurauter, A. A. *et al.* Cell isolation and expansion using dynabeads. in *Advances in Biochemical Engineering/Biotechnology* **106**, 41–73 (2007).
209. Rogers, S., Pritchard, R. & Zhukov, A. A faster GMP therapeutic cell sorter enabled by a new microfluidic technology: The inertial vortex sorter. *Cytotherapy* **20**, S70 (2018).
210. Feng, X. *et al.* Foxp1 is an essential transcriptional regulator for the generation of quiescent naive T cells during thymocyte development. *Blood* **115**, 510–518 (2010).
211. Kokaji, A. I. Method for the In Situ Formation of Bifunctional Immunological Complexes. 1–9 (2018).
212. Dai, X., Mei, Y., Nie, J. & Bai, Z. Scaling up the Manufacturing Process of Adoptive T Cell Immunotherapy. *Biotechnology Journal* **14**, 1800239 (2019).
213. McNaughton, B. H., Younger, J. G. & Ostruszka, L. J. Method and System for Buoyant Separation. 1–20 (2019).
214. Guruvenket, S., Rao, G. M., Komath, M. & Raichur, A. M. Plasma surface modification of polystyrene and polyethylene. *Appl. Surf. Sci.* **236**, 278–284 (2004).
215. Jung, S., Sen, A., Rosenberg, L. & Behie, L. A. Identification of growth and attachment factors for the serum-free isolation and expansion of human mesenchymal stromal cells. *Cytotherapy* **12**, 637–657 (2010).
216. Bryhan, D. Method for creating a cell growth surface on a polymeric substrate. 1–9 (2003).
217. Swistowski, A. *et al.* Xeno-free defined conditions for culture of human embryonic stem cells, neural stem cells and dopaminergic neurons derived from them. *PLoS One* **4**, (2009).
218. de Lima, M. *et al.* Cord-Blood Engraftment with Ex Vivo Mesenchymal-Cell Coculture. *N. Engl. J. Med.* **367**, 2305–2315 (2012).
219. Lee, D. W. *et al.* T cells expressing CD19 chimeric antigen receptors for acute lymphoblastic leukaemia in children and young adults: A phase 1 dose-escalation trial. *Lancet* **385**, 517–528 (2015).
220. Saint-Jean, M. *et al.* Adoptive Cell Therapy with Tumor-Infiltrating Lymphocytes in Advanced Melanoma Patients. *J. Immunol. Res.* **2018**, (2018).
221. Horwitz, M. E. *et al.* Umbilical cord blood expansion with nicotinamide provides long-term multilineage engraftment. *J. Clin. Invest.* **124**, 3121–3128 (2014).
222. Andrade-Zaldivar, H., Kalixto-Sánchez, M. A., Barba de la Rosa, A. P. & León-Rodriguez, A. Expansion of Human Hematopoietic Cells from Umbilical Cord Blood Using Roller Bottles in CO2 and CO2-Free Atmosphere. *Stem Cells Dev.* **20**, 593–598 (2011).

223. Wikström, K., Blomberg, P. & Islam, K. B. Clinical grade vector production: Analysis of yield, stability, and storage of GMP-produced retroviral vectors for gene therapy. *Biotechnol. Prog.* **20**, 1198–1203 (2004).
224. Wang, H., Kehoe, D., Murrell, J. & Jing, D. Structured Methodology for Process Development in Scalable Stirred Tank Bioreactors Platforms. in *Bioprocessing for Cell-based Therapies* (ed. Connon, C. J.) 35–64 (John Wiley & Sons Ltd., 2017).
225. Bayley, R. *et al.* The productivity limit of manufacturing blood cell therapy in scalable stirred bioreactors. *J. Tissue Eng. Regen. Med.* **12**, e368–e378 (2018).
226. Martin, Y., Eldardiri, M., Lawrence-Watt, D. J. & Sharpe, J. R. Microcarriers and Their Potential in Tissue Regeneration. *Tissue Eng. Part B Rev.* **17**, 71–80 (2010).
227. Chen, A. K. L., Reuveny, S. & Oh, S. K. W. Application of human mesenchymal and pluripotent stem cell microcarrier cultures in cellular therapy: Achievements and future direction. *Biotechnol. Adv.* **31**, 1032–1046 (2013).
228. dos Santos, F. *et al.* A Xenogeneic-Free Bioreactor System for the Clinical-Scale Expansion of Human Mesenchymal Stem / Stromal Cells. *Biotechnol. Bioeng.* **116**, 1116–1127 (2014).
229. Lawson, T. *et al.* Process development for expansion of human mesenchymal stromal cells in a 50L single-use stirred tank bioreactor. *Biochem. Eng. J.* **120**, 49–62 (2017).
230. Robb, K. P., Fitzgerald, J. C., Barry, F. & Viswanathan, S. Mesenchymal stromal cell therapy: progress in manufacturing and assessments of potency. *Cytotherapy* **21**, 289–306 (2019).
231. Tsai, A. C., Liu, Y. & Ma, T. Expansion of human mesenchymal stem cells in fibrous bed bioreactor. *Biochem. Eng. J.* **108**, 51–57 (2016).
232. Meissner, P., Schröder, B., Herfurth, C. & Biselli, M. Development of a fixed bed bioreactor for the expansion of human hematopoietic progenitor cells. *Cytotechnology* **30**, 227–234 (1999).
233. Haack-Sørensen, M. *et al.* Culture expansion of adipose derived stromal cells. A closed automated Quantum Cell Expansion System compared with manual flask-based culture. *J. Transl. Med.* **14**, 319 (2016).
234. Mizukami, A. *et al.* A Fully-Closed and Automated Hollow Fiber Bioreactor for Clinical-Grade Manufacturing of Human Mesenchymal Stem / Stromal Cells. *Stem Cell Rev. Reports* **14**, 141–143 (2018).
235. Tirughana, R. *et al.* GMP Production and Scale-Up of Adherent Neural Stem Cells with a Quantum Cell Expansion System. *Mol. Ther. Methods Clin. Dev.* **10**, 48–56 (2018).
236. Lechanteur, C. *et al.* Large-Scale Clinical Expansion of Mesenchymal Stem Cells in the GMP-Compliant, Closed Automated Quantum® Cell Expansion System: Comparison with Expansion in Traditional T-Flasks. *J. Stem Cell Res. Ther.* **4**, 1000222 (2014).
237. Lambrechts, T. *et al.* Large-scale progenitor cell expansion for multiple donors in a monitored hollow fibre bioreactor. *Cytotherapy* **18**, 1219–1233 (2016).
238. Junne, S. & Neubauer, P. How scalable and suitable are single-use bioreactors? *Curr. Opin. Biotechnol.* **53**, 240–247 (2018).
239. Hynes, R. O. Integrins : Bidirectional , Allosteric Signaling Machines. *Cell* **110**, 673–687 (2002).
240. Lei, Y. & Schaffer, D. V. A fully defined and scalable 3D culture system for human pluripotent stem cell expansion and differentiation. *Proc. Natl. Acad. Sci. U. S. A.* **110**, E5039–E5048 (2013).
241. Dos Santos, F. *et al.* A xenogeneic-free bioreactor system for the clinical-scale expansion of human mesenchymal stem/stromal cells. *Biotechnol. Bioeng.* **111**, 1116–1127 (2014).

242. Mariappan, I. *et al.* In vitro culture and expansion of human limbal epithelial cells. *Nat. Protoc.* **5**, 1470–1479 (2010).
243. Joen, V. T., Declercq, H. & Cornelissen, M. Expansion of human embryonic stem cells : a comparative study. *Cell Prolif.* **44**, 462–476 (2011).
244. Rowley, J., Abraham, E., Campbell, A., Brandwein, H. & Oh, S. Meeting Lot-Size Challenges of Manufacturing Adherent Cells for Therapy. *Bioprocess Int.* **10**, 16–22 (2012).
245. Rodrigues, A. L. *et al.* Dissolvable Microcarriers Allow Scalable Expansion And Harvesting Of Human Induced Pluripotent Stem Cells Under Xeno-Free Conditions. *Biotechnol. J.* **14**, 1800461 (2019).
246. Cunha, B. *et al.* Filtration methodologies for the clarification and concentration of human mesenchymal stem cells. *J. Memb. Sci.* **478**, 117–129 (2015).
247. Schnitzler, A. C. *et al.* Bioprocessing of human mesenchymal stem/stromal cells for therapeutic use: Current technologies and challenges. *Biochem. Eng. J.* **108**, 3–13 (2016).
248. Mehta, S., Herman, T., Ross, H., Iqbal, K. & McMahon, J. Methods and systems for manipulating particles using a fluidized bed. US 9.279,133 B2. (2016).
249. Cunha, B. *et al.* Exploring continuous and integrated strategies for the up- and downstream processing of human mesenchymal stem cells. *J. Biotechnol.* **213**, 97–108 (2015).
250. Wang, Z., Feke, D. & Belovich, J. Acoustic device and methods thereof for separation and concentration. US 8,889,388 B2. (2014).
251. Woods, E. J., Thirumala, S., Badhe-Buchanan, S. S., Clarke, D. & Mathew, A. J. Off the shelf cellular therapeutics: Factors to consider during cryopreservation and storage of human cells for clinical use. *Cytotherapy* **18**, 697–711 (2016).
252. Iyer, R. K., Bowles, P. A., Kim, H. & Dulgar-tulloch, A. Industrializing Autologous Adoptive Immunotherapies : Manufacturing Advances and Challenges. *Front. Med.* **5**, (2018).
253. Peltzer, J. *et al.* Mesenchymal Stromal Cells Based Therapy in Systemic Sclerosis: Rational and Challenges. *Front. Immunol.* **9**, (2018).
254. Coopman, K. & Medcalf, N. From production to patient: challenges and approaches for delivering cell therapies. in *StemBook* (2014). doi:10.3824/STEMBOOK.1.97.1
255. Dhall, S. *et al.* Properties of viable lyopreserved amnion are equivalent to viable cryopreserved amnion with the convenience of ambient storage. *PLoS One* **13**, 1–19 (2018).
256. U.S. Department of Health and Human Services Food and Drug Administration. *Guidance for Industry Guidance for Industry PAT - A Framework for Innovative Pharmaceutical*. (2004).
257. EMEA. *Mandate for Process Analytical Technology Team (EMEA/48327/2006 Mandate)*. *European Medicines Agency* (2006).
258. Claßen, J., Aupert, F., Reardon, K. F., Solle, D. & Scheper, T. Spectroscopic sensors for in-line bioprocess monitoring in research and pharmaceutical industrial application. *Anal. Bioanal. Chem.* **409**, 651–666 (2017).
259. O'Mara, P., Farrell, A., Bones, J. & Twomey, K. Staying alive! Sensors used for monitoring cell health in bioreactors. *Talanta* **176**, 130–139 (2018).
260. Haber, F. & Hlemensiewicz, Z. Über elektrische Phasengrenzkräfte. *Zeitschrift für Phys. Chemie* **67U**, 385–431 (1909).
261. Clark, L. C., Wolf, R., Granger, D. & Taylor, Z. Continuous Recording of Blood Oxygen Tensions by Polarography. *J. Appl. Physiol.* **6**, 189–193 (1953).

262. Biechele, P., Busse, C., Solle, D., Scheper, T. & Reardon, K. Sensor systems for bioprocess monitoring. *Eng. Life Sci.* **15**, 469–488 (2015).
263. Jeevarajan, A. S., Vani, S., Taylor, T. D. & Anderson, M. M. Continuous pH monitoring in a perfused bioreactor system using an optical pH sensor. *Biotechnol. Bioeng.* **78**, 467–472 (2002).
264. Ge, X. *et al.* Validation of an optical sensor-based high-throughput bioreactor system for mammalian cell culture. *J. Biotechnol.* **122**, 293–306 (2006).
265. Schirmaier, C. *et al.* Scale-up of adipose tissue-derived mesenchymal stem cell production in stirred single-use bioreactors under low-serum conditions. *Eng. Life Sci.* **14**, 292–303 (2014).
266. Hanson, M. A. *et al.* Comparisons of Optical pH and Dissolved Oxygen Sensors With Traditional Electrochemical Probes During Mammalian Cell Culture. *Biotechnol. Bioeng.* **97**, 833–841 (2007).
267. Lavine, B. K. Chemometrics. *Anal. Chem.* **72**, 91–98 (2000).
268. Arnold, S. A., Crowley, J., Woods, N., Harvey, L. M. & McNeil, B. In-situ near infrared spectroscopy to monitor key analytes in mammalian cell cultivation. *Biotechnol. Bioeng.* **84**, 13–19 (2003).
269. Salasznyk, R. M., Klees, R. F., Williams, W. A., Boskey, A. & Plopper, G. E. Focal adhesion kinase signaling pathways regulate the osteogenic differentiation of human mesenchymal stem cells. *Exp. Cell Res.* **313**, 22–37 (2007).
270. Rosa, F. *et al.* Monitoring the ex-vivo expansion of human mesenchymal stem/stromal cells in xeno-free microcarrier-based reactor systems by MIR spectroscopy. *Biotechnol. Prog.* **32**, 447–455 (2016).
271. Suhito, I. R., Han, Y., Min, J., Son, H. & Kim, T. H. In situ label-free monitoring of human adipose-derived mesenchymal stem cell differentiation into multiple lineages. *Biomaterials* **154**, 223–233 (2018).
272. Gomes, J., Chopda, V. & Rathore, A. S. Monitoring and Control of Bioreactor: Basic Concepts and Recent Advances. in *Bioprocessing Technology for Production of Biopharmaceuticals and Bioproducts* 201–237 (2018). doi:10.1002/9781119378341.ch6
273. Mercier, S. M. *et al.* Process analytical technology tools for perfusion cell culture. *Eng. Life Sci.* **16**, 25–35 (2016).
274. Courtès, F., Ebel, B., Guédon, E. & Marc, A. A dual near-infrared and dielectric spectroscopies strategy to monitor populations of Chinese hamster ovary cells in bioreactor. *Biotechnol. Lett.* **38**, 745–750 (2016).
275. Lambrechts, T. *et al.* Evaluation of a monitored multiplate bioreactor for large-scale expansion of human periosteum derived stem cells for bone tissue engineering applications. *Biochem. Eng. J.* **108**, 58–68 (2016).
276. Horiguchi, I. & Sakai, Y. Serum replacement with albumin-associated lipids prevents excess aggregation and enhances growth of induced pluripotent stem cells in suspension culture. *Biotechnol. Prog.* **32**, 1009–1016 (2016).
277. Dekker, L. & Polizzi, K. M. Sense and sensitivity in bioprocessing — detecting cellular metabolites with biosensors. *Curr. Opin. Chem. Biol.* **40**, 31–36 (2017).
278. Baradez, M.-O., Biziato, D., Hassan, E. & Marshall, D. Application of Raman Spectroscopy and Univariate Modelling As a Process Analytical Technology for Cell Therapy Bioprocessing. *Front. Med.* **5**, (2018).
279. Paton, J. Novartis' Kymriah Cancer Drug Priced at 320,000 Euros in Germany. *Bloomberg* (2018).
280. Hirschler, B. UK rejects Gilead's CAR-T cancer cell therapy as too expensive. *Reuters* (2018).

281. Liu, A. Beat you to it, Kymriah: Gilead strikes discount Yescarta deal with NHS in adults. *Fierce Pharma* (2018).
282. National Institute fo Health and Care Excellence. *Darvadstrocel for treating complex perianal fistulas in Crohn's disease*. (2019).
283. Panés, J. *et al.* Expanded allogeneic adipose-derived mesenchymal stem cells (Cx601) for complex perianal fistulas in Crohn's disease: a phase 3 randomised, double-blind controlled trial. *Lancet* **388**, 1281–1290 (2016).
284. Kirouac, D. C. & Zandstra, P. W. The Systematic Production of Cells for Cell Therapies. *Cell Stem Cell* **3**, 369–381 (2008).
285. Lipsitz, Y. Y. *et al.* A roadmap for cost-of-goods planning to guide economic production of cell therapy products. *Cytotherapy* **19**, 1383–1391 (2017).
286. Pereira Chilima, T. D., Moncaubeig, F. & Farid, S. S. Impact of allogeneic stem cell manufacturing decisions on cost of goods, process robustness and reimbursement. *Biochem. Eng. J.* **137**, 132–151 (2018).
287. Sousa Pinto, D. *et al.* Scalable Manufacturing of Human Mesenchymal Stromal Cells in the Vertical-Wheel™ Bioreactor System: An Experimental and Economic Approach. *Biotechnol. J.* 1800716 (2019). doi:10.1002/biot.201800716
288. Trainor, N., Pietak, A. & Smith, T. Rethinking clinical delivery of adult stem cell therapies. *Nat. Biotechnol.* **32**, 729–735 (2014).
289. Torikai, H. *et al.* A foundation for universal T-cell based immunotherapy: T cells engineered to express a CD19-specific chimeric-antigen-receptor and eliminate expression of endogenous TCR. *Blood* **119**, 5697–5705 (2012).
290. Jenkins, M. J. & Farid, S. S. Cost-effective bioprocess design for the manufacture of allogeneic CAR-T cell therapies using a decisional tool with multi-attribute decision-making analysis. *Biochem. Eng. J.* **137**, 192–204 (2018).
291. US Drug and Food Administration. *Pharmaceutical CGMPs for the 21s Century - A risk-based approach. FDA* (2004).
292. Rathore, A. S. & Winkle, H. Quality by design for biopharmaceuticals. *Nat. Biotechnol.* **27**, 26–34 (2009).
293. EMA & FDA. *Report from the EMA-FDA QbD pilot program (EMA/213746/2017).* (2017).
294. Senior, M. After Glybera's withdrawal, what's next for gene therapy? *Nat. Biotechnol.* **35**, 491–492 (2017).
295. Grover, N. Dendreon files for bankruptcy as cancer vaccine disappoints. *Reuters* (2014).
296. Martin-Moe, S. *et al.* A new roadmap for biopharmaceutical drug product development: Integrating development, validation, and quality by design. *J. Pharm. Sci.* **100**, 3031–3043 (2011).
297. Rathore, A. S. Roadmap for implementation of quality by design (QbD) for biotechnology products. *Trends Biotechnol.* **27**, 546–553 (2009).
298. Mandenius, C.-F. *et al.* Quality-by-Design for biotechnology-related pharmaceuticals. *Biotechnol. J.* **4**, 600–609 (2009).
299. Hunt, M. M., Meng, G., Rancourt, D. E., Gates, I. D. & Kallos, M. S. Factorial Experimental Design for the Culture of Human Embryonic Stem Cells as Aggregates in Stirred Suspension Bioreactors Reveals the Potential for Interaction Effects Between Bioprocess Parameters. *Tissue Eng. Part C Methods* **20**, 76–89 (2013).
300. Ratcliffe, E. *et al.* Application of response surface methodology to maximize the productivity of scalable automated human embryonic stem cell manufacture. *Regen. Med.* **8**, 39–48 (2013).
301. Andrade, P. Z., dos Santos, F., Almeida-Porada, G., da Silva, C. L. & Cabral, J. M. S.

Systematic delineation of optimal cytokine concentrations to expand hematopoietic stem/progenitor cells in co-culture with mesenchymal stem cells. *Mol. Biosyst.* **6**, 1207–1215 (2010).
302. Bravery, C. A. *et al.* Potency assay development for cellular therapy products: an ISCT∗ review of the requirements and experiences in the industry. *Cytotherapy* **15**, 9-19.e9 (2013).
303. Hough, R. *et al.* Recommendations for a standard UK approach to incorporating umbilical cord blood into clinical transplantation practice: An update on cord blood unit selection, donor selection algorithms and conditioning protocols. *Br. J. Haematol.* **172**, 360–370 (2016).
304. Woolfrey, A. *et al.* Cord-Blood Transplantation in Patients with Minimal Residual Disease. *N. Engl. J. Med.* **375**, 944–953 (2016).
305. Rocha, V. *et al.* Comparison of Outcomes of unrelated Bone Marrow and Umbilical cord blood Transplants in Children With Acute Leukemia. *Blood* **97**, 2962–2971 (2001).
306. Rocha, V. *et al.* Transplants of Umbilical-Cord Blood or Bone Marrow from Unrelated Donors in Adults with Acute Leukemia. *N. Engl. J. Med.* **351**, 2276–2285 (2004).
307. Wagner, J. E. *et al.* One-unit versus two-unit cord-blood transplantation for hematologic cancers. *N. Engl. J. Med.* **371**, 1685–1694 (2014).
308. Kelly, S. S., Sola, C. B. S., de Lima, M. & Shpall, E. J. Ex vivo expansion of cord blood. *Bone Marrow Transplant.* **44**, 673–681 (2009).
309. Maung, K. K. & Horwitz, M. E. Current and future perspectives on allogeneic transplantation using ex vivo expansion or manipulation of umbilical cord blood cells. *Int. J. Hematol.* **110**, 50–58 (2019).
310. Wagner, J. E. *et al.* Phase I/II Trial of StemRegenin-1 Expanded Umbilical Cord Blood Hematopoietic Stem Cells Supports Testing as a Stand-Alone Graft. *Cell Stem Cell* **18**, 144–155 (2016).
311. Ohmizono, Y. *et al.* Thrombopoietin Augments Ex Vivo Expansion of Human Cord Blood-Derived Heamatopoietic Progenitors in Combination With Stem Cell Factor and Flt3 Ligand. *Leukemia* **11**, 524–530 (1997).
312. Levac, K., Karanu, F. & Bhatia, M. Identification of Growth Factor Conditions That Reduce Ex Vivo Cord Blood Progenitor Expansion But Do Not Alter Human Repopulating Cell Function in Vivo. *Haematologica* **90**, 166–172 (2005).
313. Conneally, E., Cashman, J., Petzer, A. & Eaves, C. Expansion in vitro of transplantable human cord blood stem cells demonstrated using a quantitative assay of their lympho-myeloid repopulating activity in nonobese diabetic-scid/scid mice. *Proc. Natl. Acad. Sci. U. S. A.* **94**, 9836–9841 (1997).
314. Çelebi, B., Mantovani, D. & Pineault, N. Insulin-like growth factor binding protein-2 and neurotrophin 3 synergize together to promote the expansion of hematopoietic cells ex vivo. *Cytokine* **58**, 327–331 (2012).
315. Audet, J., Miller, C. L., Eaves, C. J. & Piret, J. M. Common and distinct features of cytokine effects on hematopoietic stem and progenitor cells revealed by dose-response surface analysis. *Biotechnol. Bioeng.* **80**, 393–404 (2002).
316. Zandstra, P. W., Conneally, E., Petzer, A. L., Piret, J. M. & Eaves, C. J. Cytokine manipulation of primitive human hematopoietic cell self-renewal. *Proc. Natl. Acad. Sci. U. S. A.* **94**, 4698–4703 (1997).
317. Aijaz, A. *et al.* Biomanufacturing for clinically advanced cell therapies. *Nat. Biomed. Eng.* **2**, 362–376 (2018).
318. Yoshida, T. & Takagi, M. Cell processing engineering for ex vivo expansion of hematopoietic cells: A review. *Biochem. Eng. J.* **20**, 99–106 (2004).

319. Petzer, A. L., Zandstra, P. W., Piret, J. M. & Eaves, C. J. Differential Cytokine Effects on Primitive (CD34+CD38 -) Human Hematopoietic Cells: Novel Responses to Flt3-Ligand and Thrombopoietin. *J. Exp. Med.* **183**, 2551–2558 (1996).
320. Zandstra, P. W., Petzer, A. L., Eaves, C. J. & Piret, J. M. Cellular determinants affecting the rate of cytokine depletion in cultures of human hematopoietic cells. *Biotechnol. Bioeng.* **54**, 58–66 (1997).
321. Zandstra, P. W., Conneally, E., Piret, J. M. & Eaves, C. J. Ontogeny-associated changes in the cytokine responses of primitive human haemopoietic cells. *Br. J. Haematol.* **101**, 770–778 (1998).
322. Ueda, T., Yasukawa, K. & Nakahata, T. Expansion of human NOD/SCID-repopulating cells by stem cell factor, Flk2/Flt3 ligand, thrombopoietin, IL-6, and soluble IL-6 receptor. *J. Clin. Invest.* **105**, 1013–1021 (2000).
323. Kiernan, J. *et al.* Clinical Studies of Ex Vivo Expansion to Accelerate Engraftment After Umbilical Cord Blood Transplantation: A Systematic Review. *Transfus. Med. Rev.* **31**, 173–182 (2017).
324. da Silva, C. L. *et al.* A human stromal-based serum-free culture system supports the ex vivo expansion/maintenance of bone marrow and cord blood hematopoietic stem/progenitor cells. *Exp. Hematol.* **33**, 828–835 (2005).
325. da Silva, C. L. *et al.* Differences amid bone marrow and cord blood hematopoietic stem/progenitor cell division kinetics. *J. Cell. Physiol.* **220**, 102–111 (2009).
326. da Silva, C. L. *et al.* Dynamic cell-cell interactions between cord blood haematopoietic progenitors and the cellular niche are essential for the expansion of CD34+, CD34+CD38− and early lymphoid CD7+ cells. *J. Tissue Eng. Regen. Med.* **4**, 149–158 (2010).
327. Andrade, P. Z., da Silva, C. L., dos Santos, F., Almeida-Porada, G. & Cabral, J. M. S. Initial CD34 + cell-enrichment of cord blood determines hematopoietic stem/progenitor cell yield upon ex vivo expansion. *J. Cell. Biochem.* **112**, 1822–1831 (2011).
328. Andrade, P. Z. *et al.* Ex vivo expansion of cord blood haematopoietic stem/progenitor cells under physiological oxygen tensions: clear-cut effects on cell proliferation, differentiation and metabolism. *J. Tissue Eng. Regen. Med.* **9**, 1172–1181 (2015).
329. dos Santos, F. *et al.* Ex vivo expansion of human mesenchymal stem cells: A more effective cell proliferation kinetics and metabolism under hypoxia. *J. Cell. Physiol.* **223**, n/a-n/a (2009).
330. Denning-Kendall, P., Singha, S., Bradley, B. & Hows, J. Cobblestone Area-Forming Cells in Human Cord Blood Are Heterogeneous and Differ from Long-Term Culture-Initiating Cells. *Stem Cells* **21**, 694–701 (2003).
331. Box, G. E. P., Hunter, J. S. & Hunter, W. J. *Statistics for Experimenters: Design, Innovation, and Discovery*. (John Wiley & Sons, 1978).
332. Cortin, V. *et al.* Efficient in vitro megakaryocyte maturation using cytokine cocktails optimized by statistical experimental design. *Exp. Hematol.* **33**, 1182–1191 (2005).
333. Lim, M., Panoskaltsis, N., Ye, H. & Mantalaris, A. Optimization of in vitro erythropoiesis from CD34+ cord blood cells using design of experiments (DOE). *Biochem. Eng. J.* **55**, 154–161 (2011).
334. Tursky, M. L., Collier, F. M., Ward, A. C. & Kirkland, M. A. Systematic investigation of oxygen and growth factors in clinically valid ex vivo expansion of cord blood CD34+ hematopoietic progenitor cells. *Cytotherapy* **14**, 679–685 (2012).
335. de Lima, M. *et al.* Transplantation of ex vivo expanded cord blood cells using the copper chelator tetraethylenepentamine: A phase I/II clinical trial. *Bone Marrow*

Transplant. **41**, 771–778 (2008).
336. Amsellem, S. *et al.* Ex vivo expansion of human hematopoietic stem cells by direct delivery of the HOXB4 homeoprotein. *Nat. Med.* **9**, 1423–1427 (2003).
337. Gilmore, G. L., DePasquale, D. K., Lister, J. & Shadduck, R. K. Ex vivo expansion of human umbilical cord blood and peripheral blood CD34+ hematopoietic stem cells. *Exp. Hematol.* **28**, 1297–1305 (2000).
338. Kögler, G. *et al.* Simultaneous cord blood transplantation of ex vivo expanded together with non-expanded cells for high risk leukemia. *Bone Marrow Transplant.* **24**, 397–403 (1999).
339. Tiwari, A. *et al.* Ex vivo expansion of haematopoietic stem/progenitor cells from human umbilical cord blood on acellular scaffolds prepared from MS-5 stromal cell line. *J. Tissue Eng. Regen. Med.* **7**, 871–883 (2013).
340. Bari, S. *et al.* Ex Vivo Expansion of CD34+CD90+CD49f+ Hematopoietic Stem and Progenitor Cells from Non-Enriched Umbilical Cord Blood with Azole Compounds. *Stem Cells Transl. Med.* **7**, 376–393 (2018).
341. Zonari, E. *et al.* Efficient Ex Vivo Engineering and Expansion of Highly Purified Human Hematopoietic Stem and Progenitor Cell Populations for Gene Therapy. *Stem Cell Reports* **8**, 977–990 (2017).
342. Calvanese, V. *et al.* MLLT3 governs human haematopoietic stem-cell self-renewal and engraftment. *Nature* (2019). doi:10.1038/s41586-019-1790-2
343. Csaszar, E., Cohen, S. & Zandstra, P. W. Blood stem cell products: Toward sustainable benchmarks for clinical translation. *BioEssays* **35**, 201–210 (2013).
344. Wodnar-Filipowicz, A. *et al.* Levels of soluble stem cell factor in serum of patients with aplastic anemia. *Blood* **81**, 3259–3264 (1993).
345. Huchet, A. *et al.* Plasma Flt-3 ligand concentration correlated with radiation-induced bone marrow damage during local fractionated radiotherapy. *Int. J. Radiat. Oncol. Biol. Phys.* **57**, 508–515 (2003).
346. Zhang, J., Wu, Q. & Zheng, Y. Persistent elevated bone marrow plasma levels of thrombopoietin in patients with aplastic anemia. *Cytokine* **85**, 11–13 (2016).
347. Purton, L. E. & Scadden, D. T. Limiting Factors in Murine Hematopoietic Stem Cell Assays. *Cell Stem Cell* **1**, 263–270 (2007).
348. Powell, K. *et al.* Variability in subjective review of umbilical cord blood colony forming unit assay. *Cytom. Part B - Clin. Cytom.* **90**, 517–524 (2016).
349. Alakel, N. *et al.* Direct contact with mesenchymal stromal cells affects migratory behavior and gene expression profile of CD133+ hematopoietic stem cells during ex vivo expansion. *Exp. Hematol.* **37**, 504–513 (2009).
350. Kirouac, D. C. & Zandstra, P. W. Understanding cellular networks to improve hematopoietic stem cell expansion cultures. *Curr. Opin. Biotechnol.* **17**, 538–547 (2006).
351. Wagner, W. *et al.* Molecular and Secretory Profiles of Human Mesenchymal Stromal Cells and Their Abilities to Maintain Primitive Hematopoietic Progenitors. *Stem Cells* **25**, 2638–2647 (2007).
352. Méndez-Ferrer, S. *et al.* Mesenchymal and haematopoietic stem cells form a unique bone marrow niche. *Nature* **466**, 829–834 (2010).
353. Naldini, L. Gene therapy returns to centre stage. *Nature* **526**, 351–360 (2015).
354. Dunbar, C. E. *et al.* Gene therapy comes of age. *Science (80-.).* **359**, (2018).
355. Hoggatt, J. Gene Therapy for "Bubble Boy" Disease. *Cell* **166**, 263 (2016).
356. Singh, J. & Zúñiga-Pflücker, J. C. Producing proT cells to promote immunotherapies. *Int. Immunol.* **53**, 1–30 (2018).
357. Frias, A. M. *et al.* Generation of functional natural killer and dendritic cells in a human

stromal-based serum-free culture system designed for cord blood expansion. *Exp. Hematol.* **36**, 61–68 (2008).
358. Singh, J. *et al.* Generation and function of progenitor t cells from stemregenin-1-expanded CD34+ human hematopoietic progenitor cells. *Blood Adv.* **3**, 2934–2948 (2019).
359. Darvish, M. *et al.* Umbilical cord blood mesenchymal stem cells application in hematopoietic stem cells expansion on nanofiber three-dimensional scaffold. *J. Cell. Biochem.* **120**, 12018–12026 (2019).
360. Fajardo-Orduña, G. R. *et al.* Human mesenchymal stem/stromal cells from umbilical cord blood and placenta exhibit similar capacities to promote expansion of hematopoietic progenitor cells in vitro. *Stem Cells Int.* **2017**, (2017).
361. Perdomo-Arciniegas, A. M. & Vernot, J. P. Co-culture of hematopoietic stem cells with mesenchymal stem cells increases VCAM-1-dependent migration of primitive hematopoietic stem cells. *Int. J. Hematol.* **94**, 525–532 (2011).
362. Dodson, B. P. & Levine, A. D. Challenges in the translation and commercialization of cell therapies. *BMC Biotechnol.* **15**, 1–15 (2015).
363. Mizukami, A. *et al.* Technologies for large-scale umbilical cord-derived MSC expansion: Experimental performance and cost of goods analysis. *Biochem. Eng. J.* **135**, 36–48 (2018).
364. Chilima, T. D. P., Moncaubeig, F. & Farid, S. S. Impact of allogeneic stem cell manufacturing decisions on cost of goods, process robustness and reimbursement. *Biochem. Eng. J.* **137**, 132–151 (2018).
365. Pinto, D. de S. *et al.* Scalable Manufacturing of Human Mesenchymal Stromal Cells in the Vertical-Wheel Bioreactor System: An Experimental and Economic Approach. *Biotechnol. J.* **14**, 1–9 (2019).
366. Toms, D., Deardon, R. & Ungrin, M. Climbing the mountain: Experimental design for the efficient optimization of stem cell bioprocessing. *J. Biol. Eng.* **11**, 1–10 (2017).
367. Barbosa, H. S. C., Fernandes, T. G., Dias, T. P., Diogo, M. M. & Cabral, J. M. S. New insights into the mechanisms of embryonic stem cell self-renewal under Hypoxia: A multifactorial analysis approach. *PLoS One* **7**, (2012).
368. Dias, T. P., Fernandes, T. G., Diogo, M. M. & Cabral, J. M. S. Multifactorial modeling reveals a dominant role of wnt signaling in lineage commitment of human pluripotent stem cells. *Bioengineering* **6**, (2019).
369. Levin, A., Sharma, V., Hook, L. & García-Gareta, E. The importance of factorial design in tissue engineering and biomaterials science: Optimisation of cell seeding efficiency on dermal scaffolds as a case study. *J. Tissue Eng.* **9**, (2018).
370. Branco, M. A. *et al.* Transcriptomic analysis of 3D Cardiac Differentiation of Human Induced Pluripotent Stem Cells Reveals Faster Cardiomyocyte Maturation Compared to 2D Culture. *Sci. Rep.* **9**, 1–13 (2019).
371. Aijaz, A. *et al.* Biomanufacturing for clinically advanced cell therapies. *Nat. Biomed. Eng.* **2**, 362–376 (2018).
372. Wang, L. L. *et al.* Cell therapies in the clinic. *Bioeng. Transl. Med.* **6**, e10214 (2021).
373. Hoogduijn, M. J. & Lombardo, E. Mesenchymal Stromal Cells Anno 2019: Dawn of the Therapeutic Era? Concise Review. *Stem Cells Transl. Med.* **8**, 1126–1134 (2019).
374. Kabat, M., Bobkov, I., Kumar, S. & Grumet, M. Trends in mesenchymal stem cell clinical trials 2004-2018: Is efficacy optimal in a narrow dose range? *Stem Cells Transl. Med.* **9**, 17–27 (2020).
375. Committee for Medicinal Products for Human Use. *Alofisel Assessment Report.* (2017).
376. Galipeau, J. & Sensébé, L. Mesenchymal Stromal Cells: Clinical Challenges and

Therapeutic Opportunities. *Cell Stem Cell* **22**, 824–833 (2018).
377. Celikkan, F. T. *et al.* Optimizing the transport and storage conditions of current Good Manufacturing Practice –grade human umbilical cord mesenchymal stromal cells for transplantation (HUC-HEART Trial). *Cytotherapy* **21**, 64–75 (2019).
378. ten Ham, R. M. T. *et al.* What does cell therapy manufacturing cost? A framework and methodology to facilitate academic and other small-scale cell therapy manufacturing costings. *Cytotherapy* **22**, 388–397 (2020).
379. Swioklo, S. & Connon, C. J. Keeping cells in their place: the future of stem cell encapsulation. *Expert Opin. Biol. Ther.* **16**, 1181–1183 (2016).
380. Ścieżyńska, A. *et al.* Influence of Hypothermic Storage Fluids on Mesenchymal Stem Cell Stability: A Comprehensive Review and Personal Experience. *Cells* **10**, 1043 (2021).
381. Meneghel, J., Kilbride, P. & Morris, G. J. Cryopreservation as a Key Element in the Successful Delivery of Cell-Based Therapies—A Review. *Front. Med.* **7**, (2020).
382. Cottle, C. *et al.* Impact of Cryopreservation and Freeze-Thawing on Therapeutic Properties of Mesenchymal Stromal/Stem Cells and Other Common Cellular Therapeutics. *Curr. Stem Cell Reports* **8**, 72–92 (2022).
383. Pakzad, M. *et al.* A Roadmap for the Production of a GMP-Compatible Cell Bank of Allogeneic Bone Marrow-Derived Clonal Mesenchymal Stromal Cells for Cell Therapy Applications. *Stem Cell Rev. Reports* **18**, 2279–2295 (2022).
384. Moll, G. *et al.* Cryopreserved or Fresh Mesenchymal Stromal Cells: Only a Matter of Taste or Key to Unleash the Full Clinical Potential of MSC Therapy? in *Advances in Experimental Medicine and Biology* **951**, 77–98 (2016).
385. Bissoyi, A. *et al.* Recent Advances and Future Direction in Lyophilisation and Desiccation of Mesenchymal Stem Cells. *Stem Cells Int.* **2016**, 1–9 (2016).
386. Petrenko, Y. *et al.* Clinically Relevant Solution for the Hypothermic Storage and Transportation of Human Multipotent Mesenchymal Stromal Cells. *Stem Cells Int.* **2019**, 1–11 (2019).
387. Freitas-Ribeiro, S. *et al.* Strategies for the hypothermic preservation of cell sheets of human adipose stem cells. *PLoS One* **14**, e0222597 (2019).
388. Swioklo, S., Constantinescu, A. & Connon, C. J. Alginate-Encapsulation for the Improved Hypothermic Preservation of Human Adipose-Derived Stem Cells. *Stem Cells Transl. Med.* **5**, 339–349 (2016).
389. Al-Jaibaji, O., Swioklo, S., Shortt, A., Figueiredo, F. C. & Connon, C. J. Hypothermically stored adipose-derived mesenchymal stromal cell alginate bandages facilitate use of paracrine molecules for corneal wound healing. *Int. J. Mol. Sci.* **21**, 1–22 (2020).
390. Moreira, F. *et al.* Successful Use of Human AB Serum to Support the Expansion of Adipose Tissue-Derived Mesenchymal Stem/Stromal Cell in a Microcarrier-Based Platform. *Front. Bioeng. Biotechnol.* **8**, 1–9 (2020).
391. Conget, P. a & Minguell, J. J. Phenotypical and functional properties of human bone marrow mesenchymal progenitor cells. *J. Cell. Physiol.* **181**, 67–73 (1999).
392. Shahryari, A. *et al.* Development and clinical translation of approved gene therapy products for genetic disorders. *Front. Genet.* **10**, (2019).
393. Quinn, C., Young, C., Thomas, J. & Trusheim, M. Estimating the Clinical Pipeline of Cell and Gene Therapies and Their Potential Economic Impact on the US Healthcare System. *Value Heal.* **22**, 621–626 (2019).
394. Bahsoun, S., Coopman, K. & Akam, E. C. The impact of cryopreservation on bone marrow-derived mesenchymal stem cells: A systematic review. *J. Transl. Med.* **17**, (2019).
395. Galipeau, J. Concerns arising from MSC retrieval from cryostorage and effect on

immune suppressive function and pharmaceutical usage in clinical trials. *ISBT Sci. Ser.* **8**, 100–101 (2013).
396. Rahul, R., Comeyne, L. & Agarwal, A. Distribution and Supply Chain Models in the Cell & Gene Therapy Landscape. *Deloitte* **1**, 1–33 (2021).
397. James, E. R. Disrupting vaccine logistics. *Int. Health* **13**, 211–214 (2021).
398. Bárcia, R. N. *et al.* Umbilical cord tissue–derived mesenchymal stromal cells maintain immunomodulatory and angiogenic potencies after cryopreservation and subsequent thawing. *Cytotherapy* **19**, 360–370 (2017).
399. Lechanteur, C., Briquet, A., Bettonville, V., Baudoux, E. & Beguin, Y. MSC manufacturing for academic clinical trials: From a clinical-grade to a full gmp-compliant process. *Cells* **10**, 1–19 (2021).
400. Lavrentieva, A., Majore, I., Kasper, C. & Hass, R. Effects of hypoxic culture conditions on umbilical cord-derived human mesenchymal stem cells. *Cell Commun. Signal.* **8**, 1–9 (2010).
401. Dos Santos, F. *et al.* Ex vivo expansion of human mesenchymal stem cells: A more effective cell proliferation kinetics and metabolism under hypoxia. *J. Cell. Physiol.* **223**, 27–35 (2010).
402. Hanga, M. P. *et al.* Expansion of bone marrow-derived human mesenchymal stem/stromal cells (hMSCs) using a two-phase liquid/liquid system. *J. Chem. Technol. Biotechnol.* **92**, 1577–1589 (2017).
403. Carmelo, J. G., Fernandes-Platzgummer, A., Diogo, M. M., Silva, C. L. & Cabral, J. M. S. A xeno-free microcarrier-based stirred culture system for the scalable expansion of human mesenchymal stem/stromal cells isolated from bone marrow and adipose tissue. *Biotechnol. J* **10**, 1235–1247 (2015).
404. de Sousa Pinto, D. *et al.* Scalable Manufacturing of Human Mesenchymal Stromal Cells in the Vertical-Wheel Bioreactor System: An Experimental and Economic Approach. *Biotechnol. J.* **14**, (2019).
405. Swioklo, S., Ding, P., Pacek, A. W. & Connon, C. J. Process parameters for the high-scale production of alginate-encapsulated stem cells for storage and distribution throughout the cell therapy supply chain. *Process Biochem.* **59**, 289–296 (2017).
406. Zhang, X., Cao, Y. & Zhao, G. Hypothermic Storage of Human Umbilical Vein Endothelial Cells and Their Hydrogel Constructs. *Biopreserv. Biobank.* **18**, 305–310 (2020).
407. Damala, M. *et al.* Encapsulation of human limbus-derived stromal/mesenchymal stem cells for biological preservation and transportation in extreme Indian conditions for clinical use. *Sci. Rep.* **9**, 16950 (2019).
408. Guiotto, M., Raffoul, W., Hart, A. M., Riehle, M. O. & Di Summa, P. G. Human platelet lysate to substitute fetal bovine serum in hMSC expansion for translational applications: A systematic review. *J. Transl. Med.* **18**, 1–14 (2020).
409. Oikonomopoulos, A. *et al.* Optimization of human mesenchymal stem cell manufacturing: The effects of animal/xeno-free media. *Sci. Rep.* **5**, 1–11 (2015).
410. Abdelrazik, H., Spaggiari, G. M., Chiossone, L. & Moretta, L. Mesenchymal stem cells expanded in human platelet lysate display a decreased inhibitory capacity on T- and NK-cell proliferation and function. *Eur. J. Immunol.* **41**, 3281–3290 (2011).
411. Levy, O. *et al.* Shattering barriers toward clinically meaningful MSC therapies. *Sci. Adv.* **6**, 1–19 (2020).
412. Galipeau, J. *et al.* International Society for Cellular Therapy perspective on immune functional assays for mesenchymal stromal cells as potency release criterion for advanced phase clinical trials. *Cytotherapy* **18**, 151–159 (2016).

413. Chinnadurai, R. *et al.* Potency Analysis of Mesenchymal Stromal Cells Using a Combinatorial Assay Matrix Approach. *Cell Rep.* **22**, 2504–2517 (2018).
414. Wilkinson, A. C., Igarashi, K. J. & Nakauchi, H. Haematopoietic stem cell self-renewal in vivo and ex vivo. *Nat. Rev. Genet.* **21**, 541–554 (2020).
415. Crippa, S., Santi, L., Bosotti, R., Porro, G. & Bernardo, M. E. Bone marrow-derived mesenchymal stromal cells: A novel target to optimize hematopoietic stem cell transplantation protocols in hematological malignancies and rare genetic disorders. *J. Clin. Med.* **9**, (2020).
416. McNiece, I. K., Harrington, J., Turney, J., Kellner, J. & Shpall, E. J. Ex vivo expansion of cord blood mononuclear cells on mesenchymal stem cells. *Cytotherapy* **6**, 311–317 (2004).
417. Andrade, P. Z. *et al.* Ex vivo expansion of cord blood haematopoietic stem/progenitor cells under physiological oxygen tensions: clear-cut effects on cell proliferation, differentiation and metabolism. *J. Tissue Eng. Regen. Med.* **9**, 1172–1181 (2015).
418. Nebel, S. *et al.* Alginate Core–Shell Capsules for 3D Cultivation of Adipose-Derived Mesenchymal Stem Cells. *Bioengineering* **9**, 1–15 (2022).
419. Costa, M. H. G., McDevitt, T. C., Cabral, J. M. S., da Silva, C. L. & Ferreira, F. C. Tridimensional configurations of human mesenchymal stem/stromal cells to enhance cell paracrine potential towards wound healing processes. *J. Biotechnol.* **262**, 28–39 (2017).
420. Gonzalez-Fernandez, T., Tierney, E. G., Cunniffe, G. M., O'Brien, F. J. & Kelly, D. J. Gene Delivery of TGF-β3 and BMP2 in an MSC-Laden Alginate Hydrogel for Articular Cartilage and Endochondral Bone Tissue Engineering. *Tissue Eng. Part A* **22**, 776–787 (2016).
421. Neves, M. I., Moroni, L. & Barrias, C. C. Modulating Alginate Hydrogels for Improved Biological Performance as Cellular 3D Microenvironments. *Front. Bioeng. Biotechnol.* **8**, 1–16 (2020).
422. Desai, T. & Shea, L. D. Advances in islet encapsulation technologies. *Nat. Rev. Drug Discov.* **16**, 338–350 (2017).
423. Mao, A. S. *et al.* Programmable microencapsulation for enhanced mesenchymal stem cell persistence and immunomodulation. *Proc. Natl. Acad. Sci. U. S. A.* **116**, 15392–15397 (2019).
424. Levit, R. D. *et al.* Cellular encapsulation enhances cardiac repair. *J. Am. Heart Assoc.* **2**, 1–11 (2013).
425. Dessels, C., Alessandrini, M. & Pepper, M. S. Factors Influencing the Umbilical Cord Blood Stem Cell Industry: An Evolving Treatment Landscape. *Stem Cells Transl. Med.* **7**, 643–650 (2018).
426. Gupta, A. O. & Wagner, J. E. Umbilical Cord Blood Transplants: Current Status and Evolving Therapies. *Front. Pediatr.* **8**, 1–11 (2020).
427. Sun, Z., Yao, B., Xie, H. & Su, X. C. Clinical Progress and Preclinical Insights Into Umbilical Cord Blood Transplantation Improvement. *Stem Cells Transl. Med.* **11**, 912–926 (2022).
428. Andrade, P. Z., dos Santos, F., Almeida-Porada, G., Lobato da Silva, C. & S. Cabral, J. M. Systematic delineation of optimal cytokine concentrations to expand hematopoietic stem/progenitor cells in co-culture with mesenchymal stem cells. *Mol. Biosyst.* **6**, 1207 (2010).
429. Barker, J. N. *et al.* Optimal Practices in Unrelated Donor Cord Blood Transplantation for Hematologic Malignancies. *Biol. Blood Marrow Transplant.* **23**, 882–896 (2017).
430. Lipsitz, Y. Y., Timmins, N. E. & Zandstra, P. W. Quality cell therapy manufacturing by

design. *Nat. Biotechnol.* **34**, 393–400 (2016).
431. Reich-Slotky, R. *et al.* Cryopreserved hematopoietic stem/progenitor cells stability program-development, current status and recommendations: A brief report from the AABB-ISCT joint working group cellular therapy product stability project team. *Cytotherapy* **24**, 473–481 (2022).
432. Basu, J. & Ludlow, J. W. Cell-based therapeutic products: potency assay development and application. *Regen. Med.* **9**, 497–512 (2014).
433. Shoulars, K. *et al.* Development and validation of a rapid, aldehyde dehydrogenase bright-based cord blood potency assay. *Blood* **127**, 2346–54 (2016).
434. Csaszar, E., Cohen, S. & Zandstra, P. W. Blood stem cell products: Toward sustainable benchmarks for clinical translation. *BioEssays* **35**, 201–210 (2013).
435. Bravery, C. A. *et al.* Potency assay development for cellular therapy products: an ISCT∗ review of the requirements and experiences in the industry. *Cytotherapy* **15**, 9-19.e9 (2013).
436. Chen, L. *et al.* Transcriptional diversity during lineage commitment of human blood progenitors. *Science (80-.).* **345**, (2014).
437. Papa, L. *et al.* Ex vivo human HSC expansion requires coordination of cellular reprogramming with mitochondrial remodeling and p53 activation. *Blood Adv.* **2**, 2766–2779 (2018).
438. Young, C. M., Quinn, C. & Trusheim, M. R. Durable cell and gene therapy potential patient and financial impact: US projections of product approvals, patients treated, and product revenues. *Drug Discov. Today* **27**, 17–30 (2022).
439. Spellman, S. *et al.* Guidelines for the development and validation of new potency assays for the evaluation of umbilical cord blood. *Cytotherapy* **13**, 848–855 (2011).
440. Andrade, P. Z., Santos, F. dos, Cabral, J. M. S. & da Silva, C. L. Stem cell bioengineering strategies to widen the therapeutic applications of haematopoietic stem/progenitor cells from umbilical cord blood. *J. Tissue Eng. Regen. Med.* **9**, 988–1003 (2015).
441. Branco, A. *et al.* Hypothermic Preservation of Adipose-Derived Mesenchymal Stromal Cells as a Viable Solution for the Storage and Distribution of Cell Therapy Products. *Bioengineering* **9**, 805 (2022).
442. Zandstra, P. W., Eaves, C. J. & Piret, J. M. Expansion of Hematopoietic Progenitor Cell Populations in Stirred Suspension Bioreactors of Normal Human Bone Marrow Cells. *Nat. Biotechnol.* **12**, 909–914 (1994).
443. Collins, P. C., Nielsen, L. K., Patel, S. D., Papoutsakis, E. T. & Miller, W. M. Characterization of Hematopoietic Cell Expansion, Oxygen Uptake, and Glycolysis in a Controlled, Stirred-Tank Bioreactor System. *Biotechnol. Prog.* **14**, 466–472 (1998).
444. Stark, R., Grzelak, M. & Hadfield, J. RNA sequencing: the teenage years. *Nat. Rev. Genet.* **20**, 631–656 (2019).
445. Hong, M. *et al.* RNA sequencing: new technologies and applications in cancer research. *J. Hematol. Oncol.* **13**, 1–16 (2020).
446. Morrison, S. J., Prowse, K. R., Ho, P. & Weissman, I. L. Telomerase Activity in Hematopoietic Cells Is Associated with Self-Renewal Potential. *Immunity* **5**, 207–216 (1996).
447. Brazvan, B. *et al.* Telomerase activity and telomere on stem progeny senescence. *Biomed. Pharmacother.* **102**, 9–17 (2018).
448. Gasparetto, M. & Smith, C. A. ALDHs in normal and malignant hematopoietic cells: Potential new avenues for treatment of AML and other blood cancers. *Chem. Biol. Interact.* **276**, 46–51 (2017).

449. Newman, A. M. *et al.* Determining cell type abundance and expression from bulk tissues with digital cytometry. *Nat. Biotechnol.* **37**, 773–782 (2019).
450. Talari, A. C. S., Martinez, M. A. G., Movasaghi, Z., Rehman, S. & Rehman, I. U. Advances in Fourier transform infrared (FTIR) spectroscopy of biological tissues. *Appl. Spectrosc. Rev.* **52**, 456–506 (2017).
451. Chonanant, C. *et al.* Characterisation of chondrogenic differentiation of human mesenchymal stem cells using synchrotron FTIR microspectroscopy. *Analyst* **136**, 2542–2551 (2011).
452. Zhang, Y., Parmigiani, G. & Johnson, W. E. ComBat-seq: batch effect adjustment for RNA-seq count data. *NAR Genomics Bioinforma.* **2**, 1–10 (2020).
453. Borisov, N. & Buzdin, A. Transcriptomic Harmonization as the Way for Suppressing Cross-Platform Bias and Batch Effect. *Biomedicines* **10**, 2318 (2022).
454. Goh, W. W. Bin, Yong, C. H. & Wong, L. Are batch effects still relevant in the age of big data? *Trends Biotechnol.* **40**, 1029–1040 (2022).
455. Latis, E. *et al.* Cellular and molecular profiling of T-cell subsets at the onset of human acute GVHD. *Blood Adv.* **4**, 3927–3942 (2020).
456. Unwin, R. D. & Whetton, A. D. Systematic Proteome and Transcriptome Analysis of Stem Cell Populations. *Cell Cycle* **5**, 1587–1591 (2006).

VIII. Appendix

VIII.1. Tailored Cytokine Optimization for Ex Vivo Culture Platforms Targeting the Expansion of Human Hematopoietic Stem/Progenitor Cells (supplementary information of Chapter II)

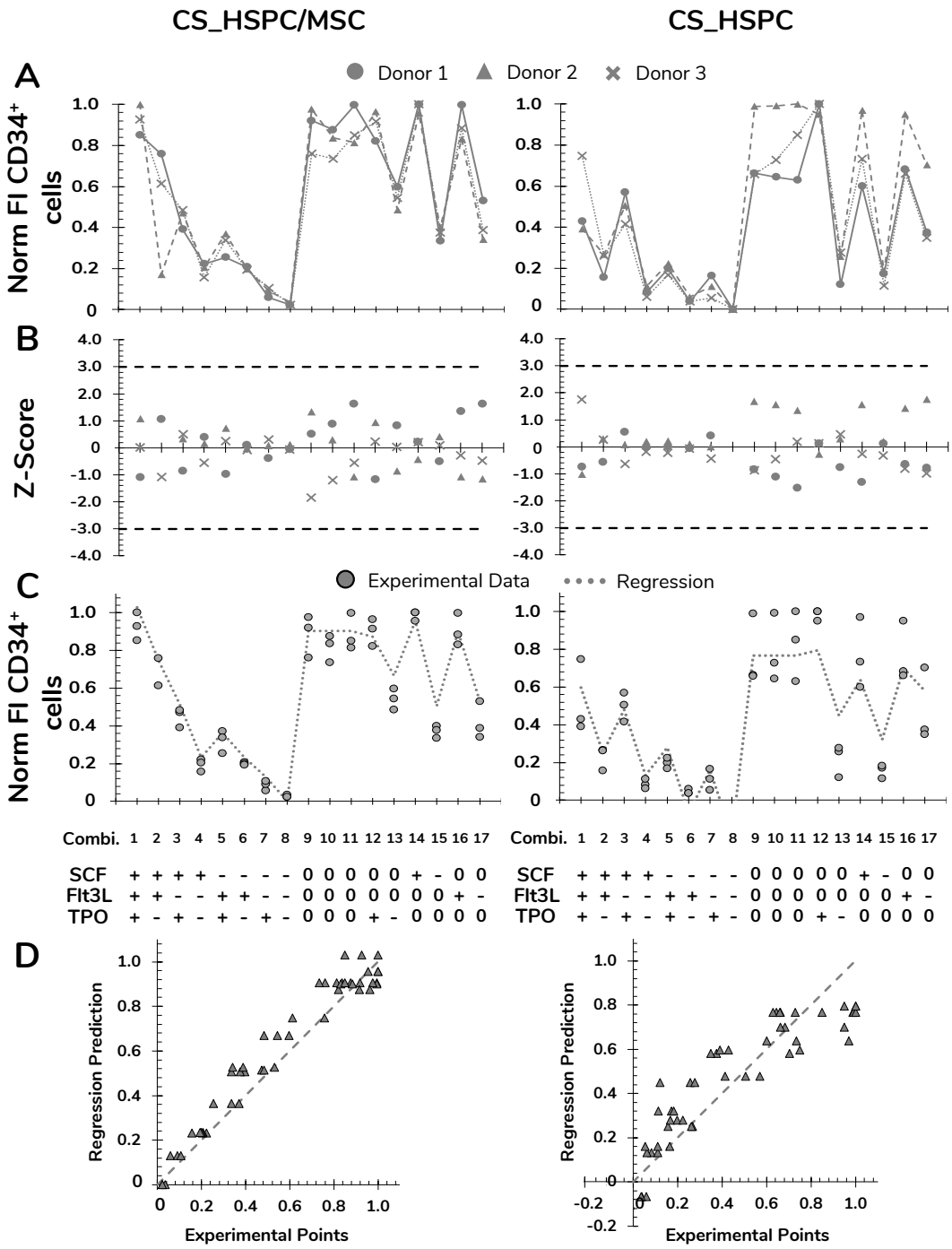

Figure VIII-1. *Preparation and polishing of experimental data with assessment of regression quality for FI CD34⁺ cells for both expansion systems, HSPC suspension culture (CS_HSPC) and HSPC co-cultured with MSC(M) (CS_HSPC/MSC).* ***(A)*** *Data from cells retrieved from every UCB donor was normalized revealing coinciding reaction patterns, highlighting variability exclusively due to different cytokine combinations.* ***(B)*** *Outlier screening was performed through Z-score determination. Data points with absolute score values higher than 3 were labelled outliers and were consequently removed from their data set before proceeding to the regression determination.* ***(C)*** *After regression determination, experimental data points were compared with calculated regression.* ***(D)*** *Deviations between data points and regressions were visualized. Norm – normalized.*

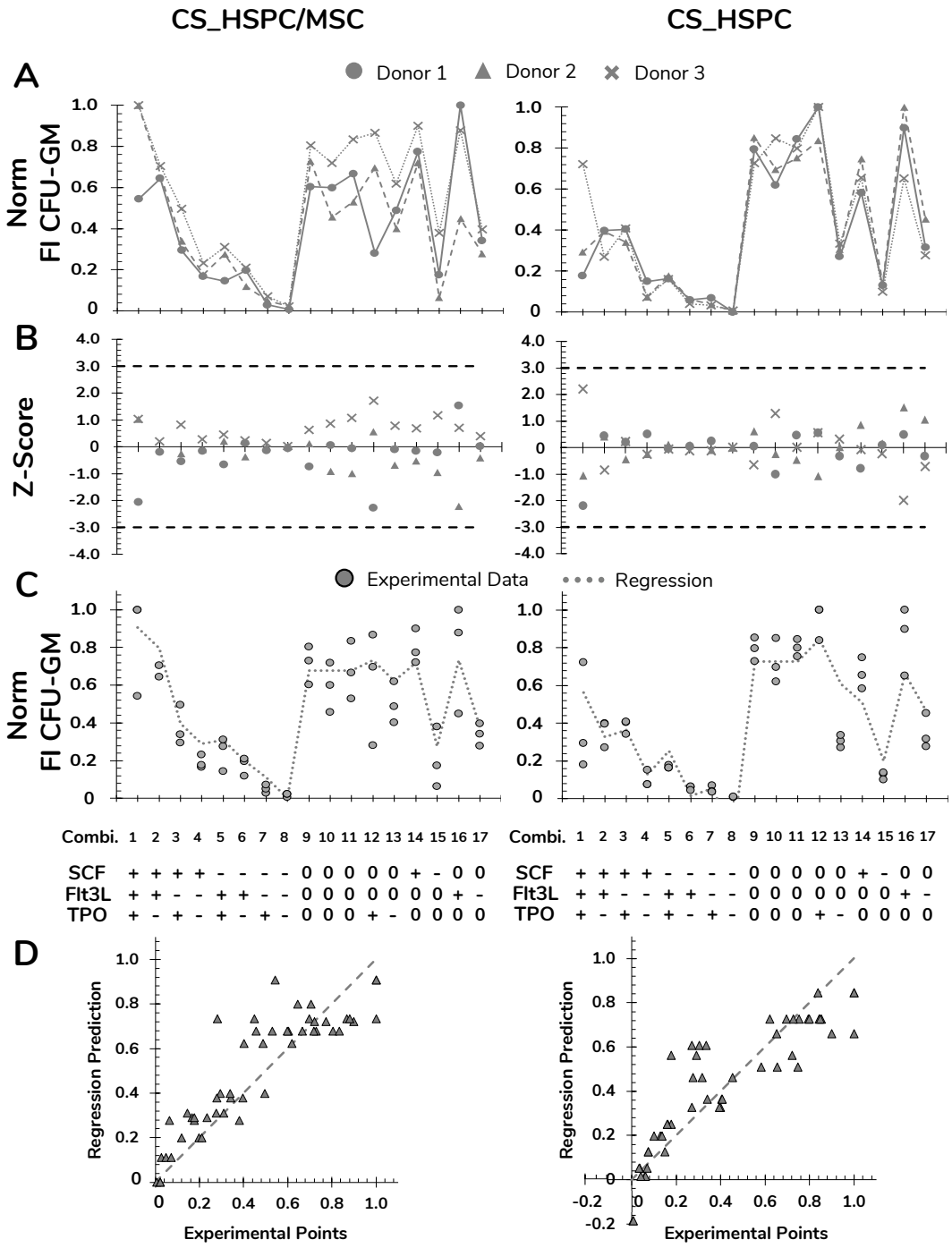

Figure VIII-2. Preparation and polishing of experimental data with assessment of regression quality for FI CFU-GM for both expansion systems, HSPC suspension culture (CS_HSPC) and HSPC co-cultured with MSC(M) (CS_HSPC/MSC). (A) Data from cells retrieved from every UCB donor was normalized revealing coinciding reaction patterns, highlighting variability exclusively due to different cytokine combinations. (B) Outlier screening was performed through Z-score determination. Data points with absolute score values higher than 3 were labelled outliers and were consequently removed from their data set before proceeding to the regression determination. (C) After regression determination, experimental data points were compared with calculated regression. (D) Deviations between data points and regressions were visualized. Norm – normalized.

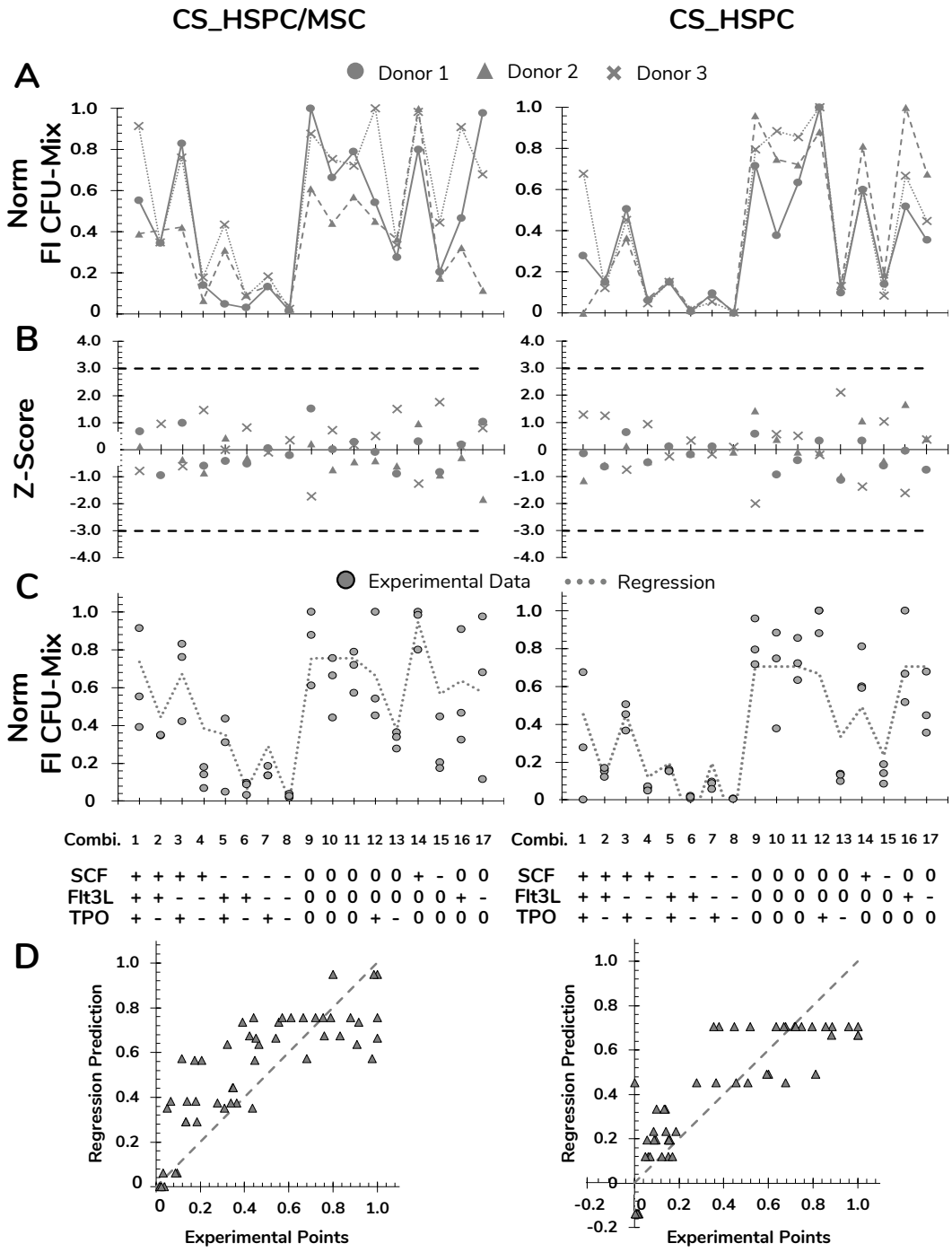

Figure VIII-3. *Preparation and polishing of experimental data with assessment of regression quality for FI CFU-Mix for both expansion systems, HSPC suspension culture (CS_HSPC) and HSPC co-cultured with MSC(M) (CS_HSPC/MSC).* ***(A)*** *Data from cells retrieved from every UCB donor was normalized revealing coinciding reaction patterns, highlighting variability exclusively due to different cytokine combinations.* ***(B)*** *Outlier screening was performed through Z-score determination. Data points with absolute score values higher than 3 were labelled outliers and were consequently removed from their data set before proceeding to the regression determination.* ***(C)*** *After regression determination, experimental data points were compared with calculated regression.* ***(D)*** *Deviations between data points and regressions were visualized. Norm – normalized.*